A MAGNETIC STUDY OF TERTIARY IGNEOUS ROCKS FROM GREENLAND, BAFFIN ISLAND AND ICELAND

LEO GEIR KRISTJANSSON

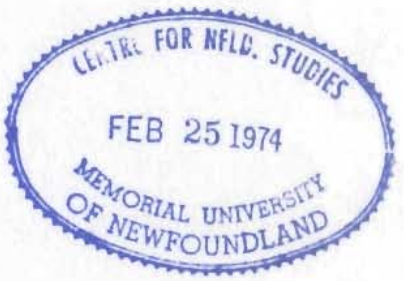
CENTRE FOR NFLD. STUDIES
FEB 25 1974
MEMORIAL UNIVERSITY
OF NEWFOUNDLAND

A MAGNETIC STUDY OF TERTIARY IGNEOUS ROCKS FROM GREENLAND, BAFFIN ISLAND AND ICELAND

by

© Leo Geir Kristjansson (M.Sc.)

Submitted in partial fulfilment of the
requirements for the degree of Doctor of Philosophy,
Memorial University of Newfoundland

December 1972

TABLE OF CONTENTS

ABSTRACT

This work describes paleomagnetic measurements carried out by the author on rock samples from Tertiary basalt areas in southern Disko Island (West Greenland), Cape Dyer (Baffin Island) and Iceland.

In the Disko collection, the stable remanence direction of samples from 45 felsparphyric lava flows in three separate profiles was measured and shown to be that of the primary remanence in the flows. A mean ancient pole position at 62°N, 169°W was derived from 37 of these flows. A relatively large secondary component of remanence was shown to be viscous remanence acquired *in situ* during the present geomagnetic epoch. Correlations between these magnetizations and other magnetic characteristics of the flows were studied.

The magnetic properties of several intrusive basalt units, a breccia, and local sediments, all from Disko Island, were also investigated. All formations were found to be reversely magnetized, but differences in these properties between and within the units were shown to be due to variations in oxidation state and in the rate of initial cooling.

Similar studies were carried out on samples from 6 olivine basalt flows in Cape Dyer. Their remanence was very stable and of normal polarity; secondary magnetization components are small except in three samples from one flow, which are reversely magnetized and appear to have suffered remagnetization *in situ*. A mean pole position of 83°N, 55°W was derived from five of the Cape Dyer flows.

Various magnetic properties of a number of rock samples from Iceland and from the Precambrian basement on the Baffin Bay coast

were investigated, to aid in the geological interpretation of magnetic anomalies found in these areas.

Two rock magnetic instruments, a thermomagnetic balance and a ballistic magnetometer, were designed, built and used during the present study and are described in detail.

ACKNOWLEDGEMENTS

The writer wishes to thank the following:

His supervisor, Dr. E. R. Deutsch of the Department of Physics, Memorial University, for supervision and encouragement throughout the course of this work.

Dr. S. W. Breckon and other faculty members of the Department of Physics for making available various research facilities, and for much instruction and assistance.

Faculty members of the Department of Geology for instruction and discussion; particularly Dr. J. S. Sutton and Dr. D. F. Strong for providing and inspecting rock samples.

Technical staff of the Departments of Physics and Technical Services, for invaluable assistance with instrumental work. Particular thanks are due to Mr. W. J. Drodge for his enthusiastic participation in both field and laboratory stages of the work.

Mr. R. P. Kennedy for skillful assistance on the 1970 collecting trip to the Baffin Bay coast.

Graduate students in Geophysics, especially Mr. K. V. Rao, Mr. A. P. Annan and Mr. R. Pätzold, for much help with laboratory equipment and computations, as well as for many happy hours of discussions and other cooperation.

Dr. B. T. May and Mr. C. R. Somayajulu for carrying out field and laboratory work on the Cape Dyer basalts.

The Science Fund of Iceland (Vísindasjódur), Memorial University, and the North Atlantic Treaty Organization, for financial support to

the writer; and the National Research Council of Canada for supporting this research under Grant A - 1946 to Dr. E. R. Deutsch.

The Science Institure of the University of Iceland for allowing the author to complete this thesis during his stay there.

Staff of the Science Institute, the National Energy Authority of Iceland, the Greenland Geological Survey, the Arctic Station in Godhavn, the Federal Electric Company of New Jersey, the University of Newcastle upon Tyne, Dalhousie University and other institutions who provided logistic and instrumental assistance for the present study.

Mr. W. Higgins, Mr. R. Breckon, Mr. R. Alexander, Mr. R. Tucker, Miss K. Thorsteinsdottir, Mrs. P. Bennett and others for helping in the preparation of this thesis.

Finally, the author wishes to thank his wife and family for their inestimable help and their patience for the duration of this work.

CHAPTER 1 INTRODUCTION

1.1 Geological background. Purpose of the present study

In recent years, geological and geophysical research has brought about a major change in man's understanding of geological processes. Previously, the earth's continents were thought to be stationary features, capable of only minor vertical movements. Now they are thought to be moving, along with parts of the ocean bottom, relative to each other with speeds measurable in centimeters per year. The earth's crust and the uppermost part of its mantle are envisaged as being composed of many semi-rigid "plates" whose interactions may be a decisive factor in many smaller-scale processes previously explained by other mechanisms.

These processes, among which are seismicity, volcanism and metallogenesis, are now better understood than before, and earth scientists are attempting to use them in re-interpreting and reconstructing the behavior and history of the upper layers of the earth.

Much of the impetus for these changes in geological approach has come from research in oceanic and coastal areas. This includes notably the application of various seismic and magnetic research techniques.

The present study is concerned with the magnetic properties and paleomagnetism of volcanic rock in two areas in the northern Atlantic Ocean. These areas are the southern Baffin Bay and Iceland,

both of which have been active centers of volcanism during the most recent epochs of the earth's history. In current terminology, they may represent "hot spots" of the earth's mantle, where the driving forces behind continental motions are concentrated.

In Baffin Bay, the activity is believed to have peaked between 80 and 40 million years ago; in Iceland, which is situated on the Mid-Atlantic ridge system, this activity has produced accessible rocks from between 20 million years ago and the present.

The results of the present study throw some light on the geological history and processes operating in these two areas. They also yield information on the behavior of the geomagnetic field in Tertiary times; on the causes of local anomalies in the present magnetic field; and on processes of magnetization in igneous rocks, as well as on the effects of metamorphism upon this magnetization.

Following the introductory chapters (1 and 2) on the concepts and methods used in this study, a separate chapter describes each of

(i) the results of magnetic measurements and observations on related basalt samples from Disko Island, West Greenland (Chapter 3);

(ii) results of similar measurements on basalt samples from the Tertiary areas of Baffin Island (Chapter 4);

(iii) the application of these results, as well as of other results from Baffin Bay and Iceland obtained by the author, to the problem of magnetic anomaly interpretation in these and

similar areas (Chapter 5).

A final chapter (6) summarizes the results and conclusions that may be drawn from them.

1.2 Magnetism: basic concepts and definitions

1.2.1 Coordinate systems. Magnetic fields and moments are vector quantities. The geomagnetic field at a point on the earth's surface (Fig. 1-1a) is usually either described in Cartesian coordinates or in spherical polar coordinates. In the former, the x-axis points towards geographic north, and the y-axis east, both in the horizontal plane, and the z-axis points vertically down. In polar coordinates, the inclination I of a vector is the angle between it and the horizontal plane, and is positive if the vector points down. Its declination D is the angle, in the horizontal plane, between north and the projection of the vector on the horizontal plane, measured clockwise. Mathematically,

$$I = \arctan\left(Z/(X^2 + Y^2)^{\frac{1}{2}}\right) \quad \text{and} \quad D = \arctan(Y/X) \qquad (1.1)$$

where X, Y and Z are the Cartesian components of the vector.

In the present work, this coordinate system is also used to express the direction in which a cylindrical rock core is drilled. Similar coordinate systems are then established with respect to the core itself for reference during measurements (Fig. 1-1b), and magnetization directions are converted from one system to the other by

calculation or graphical means. In the latter systems, z is along the core, and y is in the horizontal plane when the core is in situ. Analogous systems are used in the case of hand samples.

1.2.2 Magnetism. Except on the molecular scale, classical concepts are sufficient in describing and analysing most rock magnetic and geomagnetic phenomena. The Gaussian or electromagnetic c.g.s. system of units is employed in most of the literature on the subject, and will be used here. The magnetic field vectors $\vec{H}$ discussed will be mostly either uniform or dipole-type fields, and only dipole moments ($\vec{M}$) of rock samples have been measured in this study. Magnetic fields are measured in units of one Oersted (Oe), which in air is almost exactly equivalent to a magnetic flux density of one Gauss (G). A Gauss is equal to 10^{-4} Tesla in M.K.S. units, and one gamma (γ) is 10^{-5} Gauss (accuracy $\sim 1^{o}$).

The magnetization or specific moment in a body ($\vec{M}$/volume = $\vec{J}_t$), is also measured in units of one Gauss. Except where stated, the symbol $\vec{J}$ will in this work be reserved for remanent magnetization, i.e. magnetization which persists to some extent in the absence of an external field. Induced magnetization is one which is at any instant parallel to the external field (in isotropic materials), and it is proportional to it for sufficiently low field strengths. Therefore, the total vector magnetization in a body is equal to $\vec{J} + K\vec{H}$, where K is the volume susceptibility measured in Gauss/Oersted. The magnitude of $\vec{H}$ will be called F in this work, to avoid confusion with H, the horizontal component of the geomagnetic field. In some cases, it is

appropriate to divide $\vec{J}$ and K by the density of the body.

In highly magnetic materials, the concept of magnetic domains is a very useful one in understanding many of their intrinsic magnetic properties. Each magnetic crystal contains a large number of small volumes, domains, in each of which the net magnetization of all crystal lattice units is nearly parallel. The number and size of domain depends largely on energy minimization requirements. In response to an applied field, the walls separating the domains move laterally, reversibly for low fields but irreversibly for high fields (hysteresis effect). At still higher applied fields, the magnetization direction in the domains rotates towards the direction of the applied field, until a saturated state is reached.

The effective magnetic susceptibility K_g measured for a body depends upon its shape and on the direction of magnetic field with respect to the shape. In general, $K_g = K/(1 + KN)$, where N is a directionally dependent self-demagnetizing factor for the body. This is important in considering the magnetic properties of highly magnetic minerals and will be discussed further in section 2.6.2, but is generally a minor correction only in the case of whole-rock susceptibility (where KN is usually $\leq 10^{-2}$).

1.3 Rock magnetism

1.3.1 Ferrimagnetism in rocks. The only type of magnetic behavior dealt with to any extent in the present study is ferrimagnetism

(Néel 1955), residing in the spinel-type crystal lattices of titaniferous magnetites and some of their oxidation products. These magnetites are present in most igneous and metamorphic rocks, typically in concentrations of order 0.2 - 5% by volume. The grain size of these minerals is usually between 10^{-3} - 1 mm., i.e. 1-1000 microns (μ). The bulk composition of unoxidised titanomagnetite is $xFe_2TiO_4(1-x)Fe_3O_4$, where $0 \leq x \leq 1$, i.e., it is a solid solution of ülvöspinel, Fe_2TiO_4, and magnetite, Fe_3O_4 (Fig. 1-2a). These minerals are completely miscible only at temperatures above 600°C.

The magnetic properties of the ferrimagnetic minerals are due to quantum mechanical exchange interactions between iron-group atoms creating an intermolecular magnetic field. The energy associated with this field, called the exchange energy, then creates conditions favorable for a spontaneous alignment of atomic magnetic moments. In spinels, the iron atoms are in the form of both ferrous and ferric ions, distributed on two interlocking lattices called A and B. Under saturation conditions at 0°K, all A atoms are magnetized opposite to the B atoms, the net magnetic moment per molecule depending on x as shown by the solid lines of Fig. 1-2c.

Compared to the iron atoms, those of titanium and oxygen in the lattice are essentially non-magnetic. Therefore, the replacement of Fe by O and Ti in the lattice reduces not only the net moment as shown in Fig. 1-2c, but also the strength of the interaction between the remaining iron atoms. A good measure of this interaction is the temperature, known as the Curie point (T_c), above which thermal

agitation energy in the crystal lattice exceeds the exchange energy. A plot of the Curie point versus x for synthetic titanomagnetite is shown in Fig. 1-2b.

The composition of the pure iron-titanium oxides may be plotted on a triangle diagram as in Fig. 1-2a, the corner points being wüstite, FeO; rutile, TiO_2; and hematite, Fe_2O_3. The last-named mineral is rhombohedral, but there exists also a cation-deficient spinel of the same net composition; this is maghemite, which is a low-temperature oxidation product of magnetite. Oxidation of titanomagnetite grains at high temperatures, on the other hand, causes their net composition to move towards the right in the diagram and slightly upwards. During this oxidation, ilmenite ($FeTiO_3$) and later hematite, rutile and pseudobrookite (Fe_2TiO_5) precipitate out of the grains, forming characteristic exsolution textures. This exsolution may take place along the edges of the grains, in lamellae along specific crystal planes, or in euhedral regions and blebs. This process tends to leave other regions of increasingly pure magnetite in the grain, therefore increasing the Curie point. This also reduces the effective grain size of the magnetic mineral and, for reasons to be discussed later, increases its magnetic stability of the grains. The agents and circumstances causing such high-temperature oxidation in volcanic rocks are not certain, but may include magmatic gases, or atmosphere and ground-water oxygen (Ade-Hall *et al*, 1968a). Wilson and co-workers (1968) have used optical observations of these oxides to clarify many aspects of rock magnetism, though not all their conclusions agree with laboratory oxidation tests (Wasilewski, 1968).

1.3.2 The remanence of igneous rocks. The remanent magnetization in igneous rocks has been found to be mostly due to that of the titanomagnetites in these rocks. The magnetization may have many different origins, depending on the nature and history of the titanomagnetites.

The most important type of remanence in the present context is thermoremanent magnetization (TRM), the theory of which was developed by Néel (1949, 1955) for both single-domain and multi-domain grains. In his models, the concept of "blocking temperature", T_b, of a grain is important; in a narrow range of temperatures ΔT_b around T_b, the magnetic characteristics of the grain change very considerably. At $T > T_b$ the grain is essentially paramagnetic and its moment is partly aligned with any external magnetic field. On cooling through the ΔT_b-interval, the coercivity H_c of the grain, and hence the relaxation time for a change of remanence in external fields $H_{ex} < H_c$, increases enormously. A magnetization acquired in cooling through a ΔT_b-interval near, say, 500°C. and H_{ex} = 0.5 Oe, may be stable to external fields of that order of magnitude at 20°C. through millions of years.

In fresh volcanic rocks, the moment of TRM thus acquired in a given field (say of order 1 Oe) is commonly much higher than the induced moment, due to the same field, at room temperature. The ratio of these two moments is called the Koenigsberger ratio (Q), and is often of the order of ten in Cenozoic basalts. Its magnitude in general increases with decreasing magnetite grain size, increasing coercivity, and decreasing age.

The high-temperature oxidation processes mentioned in the previous section are therefore very important to the success of paleomagnetic research, as they cause large increases in the intensity and stability of remanence of the titanomagnetites. It is also important that, in most cases, they appear to occur during the initial cooling of the volcanic rock units, thus allowing a definite correlation of the remanence direction and intensity with the geological event of emplacement.

A rock sample almost always contains a wide range of effective titanomagnetite grain sizes, and therefore a range of blocking temperatures often spanning a greater than 400°C interval. It was shown experimentally by Thellier and others (see Nagata 1961, and Dunlop and West 1969) that a magnetization "frozen in" at one temperature would be "randomized" or released by reheating the rock in zero field to the same temperature. This result has been widely used in paleomagnetic work, in the technique of thermal demagnetization. By progressive heating of a rock in zero field, it is the lowest-coercivity and least stable components of remanence that are randomized first. These components are often secondary in origin, i.e. they are a partial thermoremanence (PTRM) caused upon cooling of the rock unit after a minor reheating some time after its formation.

A serious drawback with the thermal demagnetization method is that chemical changes may occur in the rock during the heating, irreversibly altering its magnetic properties.

Under special conditions of rock composition and cooling history, the remanence acquired by it may be in the opposite direction to the applied field. Several theoretical mechanisms have been proposed to account for such self-reversals, and they have been studied in synthetic materials in the laboratory. However, all evidence points to them being a very rare occurrence in natural magnetic minerals. This will be discussed further in Chapter 4.

A remanence may be acquired by a rock, if chemical changes take place in it in the presence of a steady external field at a temperature below the T_c of a magnetic mineral formed by the chemical changes. Here the transition of quasi-paramagnetic to single-domain behavior occurs at a critical grain size; in other aspects such as its response to demagnetization, this chemical remanence (CRM) is very similar to TRM. Grommé *et al.* (1969) concluded, on the basis of their observations in Hawaiian lava lakes, that the remanence of basalts may often reside in titanomagnetite grains which have exsolved into pure magnetite (the carrier of remanence) and other minerals at temperatures below the T_c of magnetite. Such remanence would therefore be CRM.

A third important type of remanence in naturally occurring titanomagnetite is the so-called viscous remanent magnetization (VRM). It is acquired, with a time constant that may be of the order of minutes to thousands of years, by a rock on being in a steady magnetic field. No chemical or temperature changes need be involved; due to thermal agitation, domain walls are continuously moving back and forth across energy barriers, and the presence of the external field introduces a

directional bias into the sense of wall displacement. When the time of application of the field is short, this type of remanence is the same as the ordinary remanent magnetization (IRM) as known from the shape of hysteresis loops.

These concepts suggest another way of randomizing low-coercivity components of magnetization in a rock, in order to isolate the higher-H_c components which are likely to be of primary origin. Surrounding the rock with a rapidly varying field whose amplitude is gradually decreased to zero will achieve this selective randomization; this is the basis of alternating-field (AF) demagnetization (Thellier and Rimbert 1954), which is now the standard procedure in the magnetic treatment of igneous rocks. Several precautions must be taken in this treatment to ensure a smooth reduction of the alternating field and the absence of a steady field, to avoid the buildup of anhysteretic remanence (ARM).

1.4 The geomagnetic field and its history

1.4.1 The present field and its origin. The geomagnetic field is described in several excellent textbooks; a brief summary of some of its properties is given here, mostly after Irving (1964) and Stacey (1969).

The present geomagnetic field resembles to a first approximation that of a geocentric dipole, of moment $8 \cdot 10^{25}$ Gauss·cm^3. The field at the earth's surface is about 0.65 Oe at the magnetic poles, and about 0.35 Oe at the magnetic equator. The inclination of a geocentric axial

field to the horizontal is $I = \pm \text{ arc tg } (2 \text{ tg } \lambda)$ where λ is the latitude, and its declination is either 0° or 180°.

On the dipole field there are superposed higher-order magnetic fields whose magnitude at the earth's surface averages about 0.06 Oe.

Research on the behavior of the geomagnetic field, both by direct observations during the last 400 years, and by research on the paleomagnetism of older lava flows, human artifacts and sediments from the past several thousand years, have shown that considerable variations are taking place in the magnitude and direction of both the dipole and the non-dipole fields. Thus the dipole field, which is inclined by 11° from the rotation axis, appears from the direct observations to be moving westwards by a fraction of a degree a year, and its magnitude to be decreasing by some 5% per century. From the paleo- (or archeo-) magnetic observations, these rates of change themselves are known to be quite variable.

The non-dipole field shows even less permanency; in addition to many of its features drifting westwards at rates of around 0.2° a year, some of these features are changing their form with time constants of order hundreds of years (Yukutake 1967).

The above variations, termed the geomagnetic secular variation, show that the geomagnetic field is most probably due to irregular motions within the earth, specifically in its fluid outer core. The ultimate origin of these motions is not clear, but they could be thermal convection currents or stirring of the fluid core by precessional

torques.

Magneto-hydrodynamic processes, involving interactions of the fluid motions with ambient magnetic fields to create toroidal electric fields and currents (e.g. Bullard and Gellman 1954; Elsasser 1956), in turn creating the observed poloidal-type main geomagnetic field, are now favored by most scientists as the most likely explanation of the main field (the "dynamo" theory).

In all suggested mechanisms, the axial rotation of the earth plays a dominant role, and it is therefore expected that the average geomagnetic field over a sufficiently long period during any part of geologic time averages to an axial dipole. The length of such a period, judging from the time scales of the various components of the geomagnetic secular variation in historic times (see above), appears to be several thousand years. Hide (1967), however, has suggested that asymmetries in the field could persist for much longer periods; this and other aspects of the paleo-secular variation will be discussed further in Chapters 3 and 4.

1.4.2 Pole positions. The most widely used material for paleomagnetic research is probably lava flows. Calculations, as well as observations on historic flows, indicate that such bodies will normally have cooled through their blocking temperature intervals in times of the order of 1-10 years, which is much shorter than the time scales of the secular variation. Each such unit may therefore be looked upon as giving a "spot reading" of the geomagnetic field.

A series of lava flows is usually assumed to give one independent spot reading for each flow; unfortunately, however, the length of the time between two lava flows is known only in very few instances. If the length of the time interval is similar to, or shorter than, that of the major component of the secular variation, the mean remanence directions of different flows will not be independent. If, further, the whole series being studied represents only a small number of such independent directions, the mean field calculated from the spot readings will most likely not be the correct average local field. This may well be a major cause of the scatter in published average pole positions for a particular epoch and particular continent, as in the case of the North American Lower Tertiary (Sect. 4.4).

The procedures and assumptions involved in obtaining pole positions from intrusives and from sedimentary rock units are broadly similar to those for lava flows.

One major result of paleomagnetism has been to provide convincing evidence showing that the mean magnetic pole, and by implication the rotation pole of the earth, has moved with respect to the continents during geologic time (e.g. summary in Irving 1964; Deutsch 1969). As seen from results on European rocks, the pole has moved generally northwards from near Japan since Triassic time (about 200 million years (m.y.) ago); but as seen from North America, the pole has moved from central Siberia. The different polar wandering paths, as seen from the various continents, and sometimes from various regions within the same continent, have been interpreted as being due to continental displace-

ments during geologic time. This view is now supported by much other geologic and geophysical research data.

1.4.3 Geomagnetic reversals. It was discovered through paleomagnetic work on lava flows, notably by Hospers (1954), that the geomagnetic field may have reversed its polarity a large number of times during geologic history. This has been confirmed by further research on many types of igneous and sedimentary rocks. As mentioned in Section 1.3.2 there are known instances of rock types which acquire a "self-reversed" remanence, but these are rare, and usually there occur at any collection site rocks with such a wide range of compositions that consistency arguments can be invoked to show without doubt that their magnetization is in the general direction and sense of the paleofield. The above presupposes that the available samples have been subjected to magnetic cleaning and other tests to correlate the age of their magnetic remanence with some other definable event in the history of the rock unit.

In a few instances it has been possible to follow the path of a local paleomagnetic field vector during a reversal of the field. It appears (Dagley and Wilson 1971) that the dipole field intensity weakens during a reversal, to a few tenths of its previous value, and that the thus weakened dipole rotates through 180^{o} of arc. The reversal process may take several times 10^{3} years, but there are reports (Ade-Hall and Lawley 1971) of paleomagnetic measurements suggesting that the geomagnetic field apparently has sometimes begun a reversal but returned to its original direction.

According to recent theoretical research on the properties of the geomagnetic dynamo (see Cox 1970) a possible explanation for field reversals is that the fluid motions in the core may become unable to maintain a dipole field when they pass through configurations of too high symmetry. Soon thereafter, they will begin to amplify the residual decaying field, whose polarity may or may not have changed by then.

For several years, paleomagnetic results were interpreted as indicating that Upper Cenozoic geomagnetic polarity epochs had been 0.5 - 2 m.y. long each. However, more recent research (see review by Watkins, 1972) has shown that a large number of short epochs or "events" has occurred in this time and that the average length of each epoch or event may hence be as short as 0.1 m.y. This discovery has considerably impaired the potential of magnetic reversal mapping as a tool in stratigraphic correlation and age dating of Upper Cenozoic strata, since the length of the average epoch is now inside the resolution limits for K-Ar dating of rocks more than a few m.y. old. In spite of major research efforts to delineate reversal zone boundaries in volcanics, sediments and oceanic magnetic anomalies, they are at present only known with reasonable certainty for the last 1.5 m.y. of geologic time.

For the period between 1.5 and 10 m.y. ago, only qualitative data on reversal frequencies are available. These have been extrapolated to 70 m.y. ago (Heirtzler *et al.* 1968) from ocean magnetic anomalies by assuming constant rates of sea-floor spreading and a geographical permanence of the spreading axes; investigations of

sediment thickness in the North Atlantic, however, indicate a change in the spreading rate there about 10 m.y. ago (Talwani *et al.* 1971).

As far as known, normal and reversed epochs are probably distributed in equal total lengths on the geologic time scale, although there is some evidence for the existence of two long magnetic intervals of predominantly reverse sense, having considerable stratigraphic significance. One of these was the Kiaman reverse interval (McMahon and Strangway 1968), perhaps 50 m.y. long in Carboniferous-Permian time. The other occurred during the building up of the basalt lava pile in the Brito-Arctic province, some time between 70 and 30 m.y. ago, and is therefore of direct relevance to the present study (Sect. 3.8.3).

CHAPTER 2 EQUIPMENT AND METHODS

2.1 Sampling of rocks

Oriented hand samples were collected at all Cape Dyer flows except flow 6, and at six flows in Disko. In the Cape Dyer flows, a horizontal bearing line was drawn on a flat face of a rock at an outcrop, and oriented by means of a sun compass before the rock was broken off. The tilt of the face was measured with a Brunton compass inclinometer. These samples were set in plaster of paris in the laboratory, in their original attitude, and the line transferred to the top of the sample, which was then drilled with a vertically mounted bit. Subsequently, the orientation mark was transferred to the side of the drill core.

In the Disko hand samples the horizontal line was oriented by a geographical sighting device or a Brunton compass, and the inclination measured with a "devil" level. These samples were set in plaster with the marked face being horizontal, eliminating the errors involved in transferring the line to the top of the sample. With this method, the transformation of magnetic vectors from the core coordinate system to geographic coordinates (Fig. 1-1) was more involved than in the above method: these transformations were carried out with a magnetic card programme for a desk calculator (developed by K. V. Rao and G. Haardeng-Pedersen) and checked with a Wulff equal-angle stereographic net.

Oriented core samples were obtained with portable gasoline-powered drills in flow 6 at Cape Dyer, at most of the Disko sites, and at various sites in Iceland. These were oriented in declination by geographic and sun sightings, using alternatively a standard Brunton magnetic compass and a military sun compass (Larochelle 1964). These devices were set on a levelled platform attached to the end of a tube that fitted into the drill holes. Through a slot in the tube, a mark was made on the side of the core where it was cut by the xz-plane (Fig. 1-1b), and the inclination of the tube was measured with the Brunton compass.

The bearings of geographic objects were obtained from topographic maps, and the azimuth of the sun from ephemeris tables, local time being known to within one minute. In Disko, duplicate sightings (two objects, or object and sun) were made for about 20 cores, and always agreed to 2° or better (see Sect. 3.2 for discussion of declination errors in samples oriented by magnetic bearing only).

The total error in the geographic declination and inclination of a magnetic vector obtained from a specimen depends in a complex way on the inaccuracies in sample orientation, drilling and transferring of orientation marks. Sample orientation errors, for instance, depend in turn on the length of core or the flatness of hand sample faces, on the availability of sighting objects, map and compass errors etc. In the results presented below, the average total orientation error in cylindrical specimens is believed to be about 4° of arc.

This error is much larger than the repeatability error in magnetometer measurements of remanence (Section 2.3), but similar to observed within-flow dispersions of stable paleofield directions. These dispersions are therefore likely to be largely due to orientation errors, but to some extent they must be due to natural effects such as inhomogeneous magnetization, magnetic disturbances at the time of cooling of lava flows, and stable secondary components of remanence. The average total orientation error, however, is much less than the between-flow dispersion of directions (see Section 3.8.2) found in the basalt flows of Disko.

In all lava profiles the flows were numbered in ascending order, and oriented samples in the order of collection. Thus, GL 8-1 is the first sample collected from the eighth lava from bottom of profile GL. The samples collected usually spanned at least four meters horizontally, and 2-5 m vertically. The average length of a core drilled in the field was about 4 cm.

A large number of unoriented samples, both hand samples and cores, was obtained from Baffin Bay and Iceland. Some were collected from outcrops, in which case their up-direction was often marked with an arrow so that the magnetic polarity of the sample could be found. Other samples were collected by the author from detritus, from large-diameter drill cores, or other occurrences, and many samples were kindly given to him by friends and colleagues. These were used for various supplementary studies of magnetic properties.

2.2 Preparation of specimens

For magnetic measurements with spinner magnetometer, susceptibility bridge and ballistic magnetometer, cylindrical specimens were cut from core samples drilled in the field or in the laboratory, by an oil-cooled rock saw. The diameters of the former were 2.20 cm., or less in the case of irregular cores; those of the latter were 2.25-2.28 cm. Cores drilled in Iceland had diameters of 2.4-2.5 cm. The lengths of any cylinders cut from these cores were usually between 1.9 and 2.4 cm., less frequently as short as 1.5 cm. or as long as 2.9 cm. The length is of minor consequence in any of the measurements described here. Basalt outcrops tend to contain cracks, and a significant proportion (roughly a fourth) of the cores drilled in outcrops broke during drilling or extraction. These were often abandoned, but some were recovered and glued together, without loss in orientation accuracy.

The dimensions of the cores were measured with callipers; with a mean error of 0.15 mm. each in length and diameter (mainly caused by the irregular shape of some cores) the mean error in volume is ± 2%. This error enters into all remanence intensity and saturation magnetization calculations. Pore volume in porous and vesicular rock was not measured.

Fragile samples and samples too small for drilling (e.g. interbasaltic sediments, and the Baffin Island basalt listed in Table 4.10) were mounted in plaster of paris, plasticine clay or "Geomount" plastic, all of which have negligible magnetization. Artificial remanence of

sand and drill chips (Section 5.7) was measured on samples of about 4 gm., mounted in plaster of paris or in "Ceramacast" high-temperature cement matrix. The solid-rock volume of these samples was estimated by weighing them and dividing by an assumed density in the range 2.5-3.0 g/cc.

Because different modes of sampling were employed, and because different measuring instruments may require different preparations of the rock material, the words "specimen" and "sample" cannot be defined unambiguously in the present series of measurements. However, in the case of solid rocks, "specimen" will generally refer to a cylinder, cut from a drill core.

2.3 Magnetic remanence measurements

All remanence measurements carried out at Memorial University by the writer were made with a Princeton Applied Research spinner magnetometer (type SM 1). In this instrument, the cylindrical specimen is held in a close-fitting perspex holder, in turn fitting closely into the spinner specimen cup. This cup is mounted on a rigid vertical shaft which is rotated at a steady speed of 105 c.p.s. during the measurement.

The rotating horizontal component of the specimen magnetic moment M creates an alternating e.m.f. in two coaxial vertical pick-up coils near the specimen. This e.m.f. is amplified and fed into a phase-sensitive detector which also received a reference signal from the

rotating shaft. For rotation about any axis, two orthogonal components of specimen moment are displayed on a digital voltmeter, calibrated to read directly in Gauss·cm^3.

By spinning the specimen six times in different orientations, four readings of each component of M along x, y and z (Fig. 1-1b) are obtained. These readings are averaged to reduce the effect of inhomogeneous magnetization in the specimen and the effect of centering errors. The averaging, and the subsequent transformation of the component values into values of d, i and M was done with the aid of a desk calculator.

Each measurement (six spins) took about five minutes; unoriented specimens, or others from which only rough measurements were needed, were only spun in two or three orientations. The earth's magnetic field at the specimen cup was nulled by means of three orthogonal sets of Helmholtz coils, to minimize the acquisition of VRM by the specimen during measurement.

Calibrations of the equipment to $\pm$ 0.3° in phase angle were carried out on most days on which measurements were made, using a short magnetic needle, set in a perspex cube to fit the specimen cup. The moment of this needle was monitored over a period of ten months, and found to fluctuate by up to 2% from an average value. This fluctuation may be due to effects of the room temperature changes on the needle moment, and has not been used to correct the results of intensity measurements in this work.

The repeatability of single measurements with the spinner magnetometer has been tested on two specimens by Rao (1970). Each specimen was measured ten times and removed from the holder between runs. Rao obtains standard deviations of 0.3-0.6° in declination, 0.2-0.4° in inclination and 0.5% in intensity. Similar repeatability have been obtained by the writer: a) 12 magnetically stable Cape Dyer basalt specimens were measured twice, with an average interval of a month between measurements. The mean change in magnetic direction was found to be 0.7°, and in intensity 0.8%; b) a stable Disko specimen was measured six times within an hour, giving a standard deviation of 0.15° in inclination i (mean i = 49.3°), 0.7° in declination, and 0.3% in intensity. The declination variation is mostly due to the difficulty in aligning the scribe or ink line on the specimen with the slot in the holder. All the above variations appear to be random.

Reference will be made to measurements carried out by the writer at Newcastle upon Tyne and Reykjavik, using astatic magnetometers (as described in Collinson *et al.*, 1967). These instruments, which were calibrated regularly with small solenoid coils, were less accurate than the spinner magnetometer, but were faster to operate.

2.4 Microscope observations

2.4.1 Preparation of thin and polished sections. Thin sections of rocks for microscope observation were prepared by standard methods, using a Mottacutta rock saw and grinding wheel, followed by fine grinding with wet 600 grade carborundum powder on a glass plate.

Lakeside 70 cement and "Caedax" resin were used for mounting.

Polished sections were prepared by hand. Following coarse grinding on a carborundum-impregnated wheel and fine grinding on wet 400 and 600 grade carborundum paper, the sections were polished with diamond paste. The paste and lubricating oil were spread on nylon cloth, which was stretched on flat brass discs. Three stages of polishing were carried out, using successively 6 μ, 1 μ, and 0.25 μ diamonds. The final polishing employed 0.05 μ (gamma grade) alumina powder and water on satin cloth. The sections were cleaned in an ultrasonic bath between stages. The above polishing procedure was very satisfactory in that scratches in the rock surface could be completely removed, but some surface relief on a length scale of order 1 mm. remained, reducing the focusing ability in some sections.

An area of 2-4 cm^2 was polished in most cases. Samples smaller than this, and powders, were mounted in "Geomount" plastic before polishing. A magnetite colloid, prepared by standard methods, was used to aid in the identification of minerals under the microscope.

2.4.2 Microscope. A Zeiss Universal Standard polarizing microscope was employed. Magnifications of 40x and 80x were used for observing thin sections, and 80x and 160x, 400x and 1000x for observing polished sections. The 1000x magnification was achieved with an oil immersion objective. Mean grain sizes were estimated with the aid of a square-grid graticule in one eyepiece; it must be remembered that the average grain size of spherical grains as seen in a plane section is

about 0.6 of their actual mean size. Opaque grain concentrations were measured with the same graticule, or by point-counting using cross-wires in one eyepiece.

The microphotographs shown in plates 5-8 were taken through the above microscope.

2.5 Demagnetization of rock specimens

2.5.1 AF demagnetization. Alternating field (AF) demagnetization is now standard technique in the magnetic "cleaning" of rocks for paleomagnetic research. Many of the techniques involved are described in the book edited by Collinson *et al.* (1967).

In the present study, AF demagnetization was carried out with the equipment described by Pearce (1967). The specimen, which for improved accuracy can be kept in the magnetometer specimen holder, is rotated by a three-axis tumbler centrally between two demagnetizing coils. The rotation speed of the axis rotated directly by the drive motor was 210 r.p.m. throughout this study.

The demagnetizing coils are connected to an adjustable mains (60 Hz, 220 V) transformer, and tuned to 60 Hz with series condensers. For constant coil separation, the amplitude of the alternating field is proportional to the coil current, which was measured with a battery-operated voltmeter across a series resistor.

The current is increased to a set maximum and reduced again to

zero by means of a liquid rheostat containing a copper sulfate solution. The reduction is very nearly linear with time, and in a typical run the drop to zero took about 80-100 seconds.

The alternating field strength was measured by the writer at a laboratory on campus using a search coil and an oscilloscope. When the equipment had been moved to the Geomagnetic Research Laboratory, it was re-calibrated using a Bell, Inc., Hall-effect Gaussmeter. The systematic difference between the two calibrations was about 3%.

The demagnetization equipment is surrounded by three orthogonal sets of Helmholtz coils of mean diameter 1.0 m., to compensate the earth's magnetic field and thus prevent the buildup of anhysteretic remanence. The compensation is probably only good to about 100 gamma, because of field gradients (especially in the laboratory on campus), natural magnetic disturbances and thermal drift in coil resistances, the coils being connected to adjustable constant-voltage power supplies. Fields were measured with a Schonstedt HSM-1 fluxgate magnetometer.

2.5.2 Thermal demagnetization. All thermal demagnetization treatment, and most other heating experiments (e.g. artificial TRM) described in this work, employed the non-magnetic electric furnace described by Somayajulu (1969).

All heatings were carried out in air, a heating-cooling cycle taking one to two hours. Temperatures were measured by means of a platinum/platinum-rhodium thermocouple and a potentiometer, which was calibrated by Mr. A. McCloy and found to depart by less than 3°C. from

correct readings. The furnace is surrounded by Parry coils of average dimensions 1.8 m.; for field nulling, see Section 2.5.1.

2.6 Susceptibility measurements

2.6.1 Equipment. A Scintrex SM-4 susceptibility bridge was used for measuring rock susceptibility. This bridge is of the Carey-Foster mutual inductance type; an oscillator feeds a 1000 Hz sine wave current (with a few percent harmonic distortion) into one of two co-axial cylindrical coils. The voltage induced in the other coil then depends on the magnetic susceptibility of materials present; this voltage may be compensated by changing the resistance of another arm of the bridge. Balance is achieved when the sound in a pair of head-phones connected across the bridge is minimum.

In measurement, the bridge is first balanced without any sample in the coils. A calibrated sample provided by the manufacturer is then inserted, and the difference in resistances needed for balancing is noted. This procedure is repeated with the core sample, which has to be at least 9 cm. long, and its susceptibility is obtained by direct proportions.

An absolute accuracy of 5% is claimed for this instrument, but according to a telephone conversation with a manufacturer's agent this accuracy is only achieved over a limited range of susceptibilities (between about $0.1 \cdot 10^{-3}$ and $3 \cdot 10^{-3}$ Gauss/Oe).

Because most of the cores obtained from Greenland were much

shorter than 9 cm., a conversion function was obtained, allowing measurement of cores 1.5-3 cm. long. This was done by measuring the susceptibility of 9-cm. cores drilled from 12 hand samples of basalt, cutting these into shorter sections and placing each short section in turn into a specified position in the bridge coils. The ratio of balancing resistances for the long and short cores was plotted as a function of short-core length, and used for converting all subsequent resistance readings for short cores into long-core readings. This graph showed scatter by up to 10% from a median curve, probably because of an inhomogeneous distribution of susceptibility in the long cores, and because of irregularities in the shape of the short cores.

In susceptibility measurements with this bridge, random errors in measurements are mainly due to errors in core diameter values, and are negligible compared to the calibration errors and inhomogeneity effect already mentioned. In addition, a systematic error of up to 5% may be caused by variations in susceptibility along the length of the calibrated sample. Further, the measured susceptibility of volcanic rocks depends on the r.m.s. amplitude of the applied field, here 1 Oe, and to some extent on sample remanence and other variables (Strangway 1967).

Reference will be made to some measurements of susceptibility made in Iceland also carried out with a 1000 Hz device (designed by the writer and Mr. Ö. Gardarsson). It was calibrated using core samples of basalt that had been measured on the transformer bridge constructed by H. C. Noltimier (Kristjansson 1967). Several short high-susceptibility

cores of gabbro were measured with both this bridge and the Scintrex bridge, giving agreement to ± 20% in susceptibility values in most cases. Anisotropy of susceptibility could be measured with the spinner magnetometer, but was found to be negligible in the basalt and gneiss investigated in this work (a few percent, probably due to sample shape and inhomogeneity effects rather than bulk anisotropy).

2.6.2 Magnetite content and susceptibility of rocks. On a classical continuum treatment, the susceptibility of a magnetite grain in a non-magnetic matrix should be $K_g = K_m/(1 + K_m N)$, where K_m is the susceptibility of an infinitely long rod of magnetite and N is the self-demagnetizing factor of the grain. If a rock contains non-interacting magnetite grains as its only magnetic mineral, and if the shape of the rock sample itself does not affect the measurement, then the whole-rock susceptibility is $K = VK_m/(1 + K_m \bar{N})$ for low volume fractions of magentite V, (say $V < 0.05$). $\bar{N}$ is the mean demagnetizing factor for the individual grains. K_m appears not to be known exactly, but from values quoted or obtained by Nagata (1961), Strangway (1967) and J.P. Hodych (pers. comm. 1971), it may be 1 Gauss/Oe within an accuracy of 50%. With this value of K_m, one is reaching the asymptotic limit of $K_g = 1/N$ in the formula for K_g above.

For spherical grains, N equals 4 Π / 3. For an assemblage of randomly oriented ellipsoidal grains, of fixed axial ratios, N is obtained from the relation

$$\frac{3}{1 + \bar{N}K_m} = \frac{1}{1 + N_1 K_m} + \frac{1}{1 + N_2 K_m} + \frac{1}{1 + N_3 K_m} \qquad (2.1)$$

where $N_{1,2,3}$ are the demagnetizing factors along the principal axes. Following Stacey (1962) one estimates that the average shape of a magnetite grain in a rock corresponds to an ellipsoid of revolution with an axial ratio of two (either prolate or oblate). Using two alternative values of K_m, the following values are therefore obtained for the expected susceptibility K of dispersed magnetite grains, normalized to unit concentration:

shape	K (K_m = 1)	K (K_m = ∞)
spherical	0.19	0.24
ellipsoidal 2:1	0.21	0.27.

For a rock containing less than, say, 5% of magnetite by volume, such that grain interactions are unimportant, we obtain $K \doteq K_g P/100$, where P = 100V is the volume percentage of magnetite and K_g is about 0.21 Gauss/Oe, assuming 2:1 ellipsoidal grains and K_m = 1 Gauss/Oe.

In the small grains of magnetite occurring in most igneous and metamorphic rocks, the above picture may be altered by the properties of magnetic domains (Sect. 1.2.2) in the grains. Since the value of the observed K_g may be largely governed by the facility with which domain walls are able to move under the application of external magnetic fields, one may expect susceptibility to be influenced by such factors as grain size, presence of lattice defects and stress.

The proportionality between magnetite content and susceptibility in artificially dispersed samples of pure magnetite has been investigated, e.g. by Parry (1965). He finds values of K_g in the range 0.16-0.24 G/Oe

for grain sizes 1.5-120 μ, with only a small increase in susceptibility with grain size. On the other hand, Shandley and Bacon (Strangway 1967) report an increase in susceptibility by over 150% in the range of grain sizes 5-40 μ.

These considerations, to be discussed in more detail in the following chapters, are only valid for applied field intensities much less than the internal magnetic fields in a magnetite domain. At these low applied fields, typically about 1 Oe in laboratory experiments, reversible translation of domain walls is the main contributor to the susceptibility. At higher fields, H, of the order of 100-1000 Oe, irreversible processes become more important and the differential susceptibility dJ_i/dH increases at first (Nagata 1961, Fig. 1-6; J_i is the induced magnetic moment per unit volume) but then decreases again as the domain walls move to the grain boundaries and the domain magnetic moments rotate towards the applied field direction. When the field is released, the rock susceptibility may have changed.

2.7 Ballistic magnetometer measurements

A ballistic magnetometer was constructed (Appendix 2.1) for further studies into the magnetization of Baffin Bay and Icelandic rocks. This type of instrument has been extensively used in rock magnetic research, both in nulled fields and in applied fields (Nagata 1961). For the suggestion to build this device, and for many design details, the writer is greatly indebted to Dr. J. P. Hodych.

The purpose of this magnetometer, which was operated in the field of a d.c. electromagnet at up to 2000 Oe, was to investigate the following aspects in the rocks under study:

2.7.1 Amount of magnetite. If a rock sample is known from thermomagnetic or other evidence to contain nearly pure magnetite (say $x < 0.12$, corresponding to $T_c > 500°C$) as the only magnetic constituent, the concentration of this magnetite in the rock may be found through measurements of its saturation magnetization J_{is}. It is known (Nagata 1961) that the value of this quantity for pure magnetite is 98 Gauss·cm^3/gm at 0°K and 93 Gauss·cm^3/gm at room temperature. J_{is} for titanomagnetites with $x \leq 0.12$ is proportional to 1-x within 7%, this error being the relative difference between the solid and broken curves in Fig. 1-2b (at 0°K). For these and higher values of x, the error can be allowed for if the Curie point, and hence the x of the magnetic phase, is known (Fig. 1-2b).

However, for $T_c < 500°C$, the room-temperature J_{is} may be much less than that at 0°K, as is illustrated in diagrams by Creer and Petersen (1969), Ozima and Larson (1970) and Grommé *et al.* (1969). In this case, estimates of magnetite content by room-temperature saturation magnetization measurements may yield seriously erroneous values. In some samples, this handicap may be overcome; heating in an oxidizing atmosphere to a sufficiently high temperature will cause ex-solution of the magnetite, so that measurement of J_{is} after heating will give a good value of their magnetite content after heating. For basalts, it appears from Fig. 3-15 that this temperature must be higher than 450°C. However

in some basalts, it is seen that on heating to above 500°C, the magnetic moment, and the susceptibility, at room temperature may drop considerably, indicating conversion of magnetite into hematite (Figs. 5-11, 3-15; Larson and Strangway 1969; Ozima and Larson 1970). The reduction in effective grain size through the exsolution (Strangway 1967) may cause some of the drop in susceptibility, though in the results obtained below, this appears to be a minor effect.

Another category of rock samples which may yield incorrect estimates of magnetite content from saturation magnetization experiments are highly oxidized rocks which contain maghemite or possibly other highly magnetic iron oxides. (Similarly, the presence of magnetic sulfides might interfere with measurements, but sulfides were not seen to occur in significant quantities in the present rock collection.)

Even with these limitations, the saturation magnetization method may give more reliable indications of magnetite content in a rock than does point-counting by microscope, especially in coarse-grained rock (see Section 5.4.).

2.7.2 Titanomagnetite composition. If the titanomagnetite content of a moderately oxidized high-T_c rock is known by microscope examination, and its pure-magnetite content is known from saturation magnetization measurements, the bulk value of x for the titanomagnetites may be obtained from these data.

2.7.3 Coercivity and other properties. The grain size, grain shape, presence of lattice defects, and grain (or lamellar) interactions

will affect the shape of high-field magnetization curves for rocks. The shape of such curves is to a first approximation characterized by a coercivity (Sect. 1.3.2) and by the ratio of saturation remanence to saturation magnetization. These two parameters, however, could not be measured with the present equipment for the following reasons: (a) the fact that saturation was not reached in most of the samples measured; (b) residual fields in the electromagnet; and, in some cases (c) insufficient sensitivity of the equipment. Instead, the field H' at which a certain fraction of J_{is} was reached, was estimated for most of the samples as shown below.

2.7.4 Results. Typical magnetization curves for gneiss and basalt, obtained with the ballistic meter, are shown in Fig. 2-2. It is seen that saturation has not been reached at the highest fields attainable (2000 Oe). Following Shapiro and Ivanov (1967) who worked on dynamic magnetization, it was assumed that saturation was being reached asymptotically by the formula

$$J_i = J_{is}(1 - e^{-H/H'}) \qquad (2.2)$$

where J_i is the specimen magnetization at a field H and J_{is} is its saturation magnetization. H' is that characteristic field at which $J_i = 0.63 \cdot J_{is}$.

To obtain J_{is} and H', formula (2.2) was fitted graphically to measurements of J_i at seven selected values of H (see Fig. 2-2), determined by intervals of 0.6 A in the magnet supply current. These values

of H were found to be reproducible to within 30 Oe (as measured with a Gauss-meter) over a period of several weeks.

H' was in many cases found to be about 1000 Oe, in which case J_i at the highest field was about 15% short of J_{is}. In many other samples, no reasonable values of J_{is} and H' could be found to fit (2.2) simultaneously; these appeared to be mainly rocks for which $J_i(H)$ was less than predicted by the formula at low H values. A similar effect is seen in Fig. 1-6 of Nagata (1961) and was discussed in Section 2.6.2. As seen on inspection of some of the curves in Fig. 2-2, a better approximation formula for these would have been

$$J_i = J_{is}(1 - e^{-(H-H_1)/H'}) \qquad (2.3)$$

H_1 being around 200 Oe. In such samples, however, J_{is} was estimated roughly by eye, with an estimated 5% error (beyond other errors discussed in Section 2.2 and Appendix 2.1) and the error in H', obtained as before as the field at which $J_i = 0.63 \cdot J_{is}$, may be about 100 Oe. These cases are distinguished by a $\sim$ sign in tables of results (e.g. Table 3.10).

A further example of the failure of formula (2.2) at low fields is that the initial susceptibility of any rock following it should be $(dJ_i/dH)_{H=0} = J_{is}/H'$, but actual initial susceptibility values for Baffin Bay gneiss were lower than this by factors of 1.2-2, and those for basalts by 1.9-2.6.

However, in many cases H' should be a useful parameter in in-

vestigating the state of the magnetic mineral in a rock; thus, increased lamellae development in a titanomagnetite grain may be expected to increase its domain wall energy density and its mean demagnetizing factor, thus increasing the difficulty with which it reaches saturation magnetization in an external field, i.e. increasing H'. Examples of this behavior are given below.

2.8 Thermomagnetic measurements

Valuable information about the nature and state of magnetic minerals in rocks can be obtained from observations of the change of their magnetic moment with temperature in strong external fields. Saturation fields are often employed in such measurements, but in the present work, only fields of up to 1300 Oe were available.

In the present study, the most important properties obtained from thermomagnetic measurements at high fields are: (i) the Curie point, providing an estimate of the parameter x of the magnetic spinel phase in the rocks (Fig. 1-2b) and of the state of titanomagnetite oxidation; (ii) changes taking place in these parameters with heating to various temperatures, especially irreversible changes.

The information obtained from this type of measurement cannot be obtained by other methods; thus, thermal demagnetization alone does not yield information on the irreversible chemical or physical changes that may take place in the rock on heating, affecting its magnetic properties. Indeed, thermomagnetic or high-temperature susceptibility

measurements are a necessary prerequisite to the proper planning and interpretation of thermal demagnetization experiments. Furthermore, the grain size of volcanic rocks is often so small that information on the nature and state of the magnetic minerals in these is difficult to obtain by chemical or x-ray methods.

The results from thermomagnetic measurements, generally being presented in the form of curves of magnetic moment against temperature, may depend considerably on the experimental conditions, and are therefore only useful for qualitative interpretation. First, the curve shape is influenced by the applied field strength: at low temperatures and low fields, a decrease in the parameter H' (Section 2.7.1) without a change in J_{is} will thus cause a "hump" (Ade-Hall *et al.* 1971) to occur in the thermomagnetic curve, as may be the case in Fig. 3-13 (right) and Fig. 4-9 (left), whereas such a hump would not occur in a saturation-field thermomagnetic curve. Second, the shape of a thermomagnetic curve depends greatly on the accessibility of air to the titanomagnetite grains during heating (Wasilewski 1969), and therefore on the atmosphere used in the experiment, on the size of sample used, and on the rate of heating. Third, in powdered or ground samples, the grain size of the powder, and the grinding method (Sakamoto *et al.* 1968) may cause significant changes in the curve shape.

A high Curie point in a fresh volcanic rock is often associated with a high oxidation state and a good remanence stability, but such correlations are not always valid. Thus, Watkins *et al.* (1970) have shown that T_c may vary over a range of 100°C in a single basalt pillow,

whereas in samples from a lava flow exhibiting a wide range of oxidation stages under the microscope, Wilson *et al.* (1968) found no significant variations in T_c.

2.9 Statistical treatment of remanence results

2.9.1 Intensities. The remanence intensity and susceptibility results found in any given strata usually have a range of values. This is mostly due to natural causes rather than errors of measurement. Tarling (1966) has shown, for many collections of Jurassic and Cenozoic basalts, that magnetic intensity and susceptibility results are better approximated by a lognormal than ordinary normal (Gaussian) distribution. In a lognormal distribution (Appendix 5.1) the logarithms of sample values are distributed normally about the geometric mean of these values; the standard deviation of the logarithms, to base e, is of the order of 2 in the collections described by Tarling (1966) and by Kristjansson (1970).

However, the arithmetic mean of the sample values is often physically a more significant property of the strata than is the geometric mean. Thus, in aeromagnetic anomaly interpretation over a body whose dimensions are much smaller than the survey height, the anomaly amplitude is largely determined by the magnetic moment $\vec{M} = (\overline{\vec{J}} + \overline{K\vec{H}})$ x vol., where $\overline{\vec{J}}$ and $\overline{K}$ are essentially arithmetic averages over the volume of the body, $\vec{J}$ being averaged as a vector quantity.

For small standard deviations, the difference between geometric

mean and arithmetic mean is small, and in collections of the size treated here, it is of a similar order of magnitude as the standard error in each mean. Therefore, and also because many of the acidic and metamorphic rocks treated in Chapter 5 were very weakly magnetized (below instrument noise levels), arithmetic averages will be used throughout in this work.

2.9.2 Remanence directions. Following Fisher (1953) it is assumed that the measured stable remanence of a lava flow or other rock formations consists of a "true" magnetization plus random noise or error vectors. These may have natural pre-sampling causes, or they may originate during collection, magnetic cleaning and measurement of the samples. The Cartesian components of the noise vectors are each assumed to be normally distributed about zero.

The most commonly used parameters in the statistical treatment of remanence directions include (Irving 1964):

R = the length of the resultant of N unit vectors

k = (N-1)/(N-R) = a precision parameter whose value increases sharply with increased alignment between the vector directions

α_{95} = arc cos $(1 - \frac{N-R}{R}((20)^{1/N-1} - 1))$ = the angular radius of a circular cone within which there is 95% probability of the true vector being positioned. The centre of this 95% confidence circle corresponds to the resultant of the N measured vectors

δ = arc cos (R/N) = dispersion angle of the N vectors; within a cone of angular radius δ around the resultant, 63% of the N vectors will be found.

Appendix 2.1 Description of ballistic magnetometer

This device is shown diagrammatically in Fig. 2-1 and is photographed in Plate 2. The rock specimen is inserted into a perspex tube of 2" external diameter, which is then closed with a stopper. Air, blown by the operator via flexible tubing to a hole in the tube wall and stopper, drives the specimen back or forth in the tube.

Two pick-up coils, 1500 turns each of 30 s.w.g. wire, were wound on the tube and connected to a Leeds and Northrup galvanometer of type 2239f, which has a current sensitivity of 0.00002 μA per mm deflection, an internal resistance of 7200 ohms, period 19 seconds, and damping constant 0.08 per period in open circuit.

A rock specimen with an axial component M_i of its total dipole moment $\vec{M}$, moving along the tube, will cause a change in flux through the coil windings. This causes an e.m.f. in the coils and in turn causes a flow of charge through the galvanometer. If the movement of the rock takes place in a very short time compared to the galvanometer period, it is easily shown that the ballistic deflection of the galvanometer is proportional to M_i. To avoid eddy currents caused by the movement of the galvanometer suspension, the specimen is made to break the galvanometer circuit by hitting a spring-loaded non-magnetic micro-

switch at one end of the tube. In the absence of such a switch, deflections would be damped to about a tenth of their open-circuit values.

The full-scale deflection of the galvanometer is 25 cm, and by calibration (see below) it was found that 1 cm deflection corresponds to about 0.03% magnetite by volume in an 8-cc rock specimen. For more highly magnetic rocks, attenuation resistors were inserted into the galvanometer circuit (Fig. 2-1a). The repeatability of a single reading was usually 0.2 cm in deflection from one minute to the next, due mostly to zero drift. For periods of weeks, the repeatability of an average of four readings was about 0.2 cm.

Sand, drill chips, small crushed rock samples, and magnetite for calibration purposes were put into vials of 23 mm external diameter. The vials could hold about 8 gm of basalt sand; the magnetite was mixed with an inert non-magnetic powder to fill up the vials.

Calibration of the ballistic magnetometer. Not all the core specimens measured in this instrument were of the same length. Especially for lengths of the order of the length of one coil (2 cm), one might expect to find the system response to be an appreciably non-linear function of specimen length.

This was investigated theoretically for needle-shaped specimens coaxial with the coils. With an assumed constant magnetic field along the axis, as was found by measurements to be very nearly the case, the flux through each coil due to an axial dipole is given by a simple expression (e.g. eq. 8-31 of Duckworth 1960). By numerically inte -

grating that expression over a finite needle length, approximating each coil as a simple solenoid of mean diameter 3.7 cm, it was found that the deflection D would be proportional to specimen length to within 2% for specimens of length 8-18 mm. For longer specimens, the saturation deflection calculated from the formula (2.2) should be multiplied by the following correction factors:

length, mm	19	20	21	22	23	24	25
multiply by	1.02	1.03	1.05	1.07	1.10	1.12	1.15

To calibrate the coils, two types of magnetite were used: (i) a coarse powder ($\sim$100 μ) of unknown origin, seen under the microscope to contain about 2% exsolution for which no correction was made; and (ii) a fine powder ($\lesssim$1 μ) of analytical grade. Two samples were made of each type, by mixing weighed amounts with a non-magnetic powder in vials having similar external dimensions as most of the core specimens.

The following calibration results were obtained, after the deflections D produced by each sample at seven field values had been extrapolated to saturation D_s by formula (2.2):

Magnetite weight, gm	type	D_s cm	atten. scale	atten. factor	D_s on scale 1, cm
0.23	fine	17.4±0.2	1	1	17.4±0.2
0.46	coarse	19.8±0.2	2	1.84	36.4±0.5
0.92	coarse	18.8±0.4	4	3.90	73.5±2
1.82	fine	9.3±0.2	15	15.6	145±4

The attenuation factors corresponding to the three attenuated scales

were obtained by careful measurement of the same specimen on two adjacent scales; these scales will be referred to in the tables of subsequent chapters.

On drawing the best straight line through the four points and the origin on a graph of D_s vs. magnetite content, no point was found to deviate from the line by more than a few per cent. From this data, the following sensitivity values for the magnetometer were found, assuming a density of 5.1±0.1 gm/cc for magnetite (Chemical Rubber Company 1962). A ballistic deflection of 1 cm corresponds to:

Atten. scale	weight of pure magnetite if saturated at 20°C, mg	magnetite vol., 10^{-3}cc	moment, $G \cdot cm^3$
1	12.6 ± 3%	2.5 ± 5%	1.16
2	23.1 ± 3%	4.6 ± 5%	2.14
4	49 ± 3%	9.6 ± 5%	4.55
15	196 ± 3%	38 ± 5%	18.8

Improved model of the ballistic magnetometer. In a new model of the ballistic magnetometer equipment, constructed by the writer in Iceland, the major improvement was that the equipment included a larger water-cooled electromagnet (Newport Instruments Ltd.), capable of reaching 3500-3600 Gauss in a 2¼" gap between flat 4" cylindrical poles.

The ballistic magnetometer itself consisted of a perspex tube of 25 mm internal diameter and 76 mm internal length, running across the pole gap (instead of along it as in the first model). The cylinder was flanked by two pairs of coils of 1800 turns each coil, mean diameter

30 mm. The differential induced voltage from the two pairs of coils, caused by the movement of a rock inside the tube, was fed into a low-resistance (31 ohm) ballistic galvanometer of 11 second period.

Calibration procedures for this magnetometer were similar to those for the previous model. Its sensitivity was also similar to that of the earlier model. Because of the high field intensities in the pole gap, saturation of the magnetic moment of the rock specimen was more complete than in the earlier model. No measurements relevant to the present studies were made with this instrument, except that the difference between the magnetization at 2000 Oe and 3500 Oe was measured for two rock specimens (basalt and gabbro). In both, the difference was found to be about 11% of the magnetization at the higher field, in agreement with formula (2.2), which predicts 10% at $H' = 1000$ Oe.

Appendix 2.2 Description of thermomagnetic balance

The instrument shown in Fig. 2-3 and Plate 1 was designed and built for measuring the temperature dependence of strong-field magnetization of rocks. This type of balance does not seem to have been described previously in the literature. It differs from commonly used balances by employing a long-period vertical pendulum (a) with the sample holder (c) at the top. This design requires less space, is more robust, and is simpler to construct than torsion or translation balances.

The detachable cup containing dry-powdered rock is located between the pole pieces (i) of an electromagnet (h) in the off-axis posi-

tion shown, which is that of the maximum field gradient. With a constant field, the force, F, on a sample tending to pull it towards the gap center is nearly proportional to its magnetic moment, M. The two small ferrite magnets (d), each of moment 45 ergs/Oe, are glued to the pendulum in opposition and so are almost unaffected by the leakage field from the electromagnet, whereas the non-uniform field from the nearby small coil (o) results in a new horizontal attracting force on the magnets. For a given coil current, this force will just compensate F. In this way the pendulum can be always maintained vertical, corresponding to "zero" deflection of a light spot on a vertical scale (q). The pendulum motion is damped with oil (f). When the sample is heated in the furnace surrounding it (j-n), its magnetic moment and hence the required compensating force, F_c, will change. Because the geometry of the apparatus remains fixed during an experiment, F_c is almost exactly proportional to the coil current, i, required to return the light spot to zero. Since F, and therefore F_c, is nearly proportional to M, i also will be nearly proportional to M, enabling one to measure M relatively in terms of i. The absolute value of M at room temperature, if required, is obtained by the ballistic magnetometer described in Appendix 2.1, which employs the same electromagnet.

The pendulum and cross bar are 1 mm quartz rods. The pendulum mirror (b) is located 2.5 m from the vertical scale. Using the commercially available electromagnet (Ealing, type A32-3121) described by Marcley (1961), with a current of 2.0 Amp, the field at the sample is about 850 Oe; here the field gradient has also a maximum value of about

100 Oe/cm. The current can be kept constant to 1% during an experiment, using e.g. a "Nobatron" d.c. power supply.

A 1- gram powder sample of Cape Dyer basalt, containing less than 1% magnetite, will cause a light spot deflection of about 15 cm in the above position, requiring a compensating current of some 300 mA in the coil (o) to bring the spot back to zero. This compensation can be made to 0.5%, the current being measured with a transistor AVO-meter. The a.c. furnace is wound with ten turns of 0.6 mm diameter alumel wire (j) and is supplied through a "Variac" transformer, using 35 volts (8 Amp) to attain 700°C.

The furnace has an inner brass tube for equalizing the temperature and is surrounded by an aluminum heat shield (not shown in Fig. 2.3), a few mm thick. The thermocouple (n) is platinum-platinum 10% rhodium. A full heating-cooling cycle to 600°C normally lasts one hour, with readings being taken about every five minutes. Heating is in air.

Friction at the pendulum supports would limit the accuracy of the balance when weakly magnetic rock is measured, but the Curie points of basaltic or iron-rich sedimentary rock powders can at present be found to ±15°C, repeatable to 5°C. In the rock magnetic literature at least three different conventions for determining Curie point from experimental curves are in use; the one to be employed in this work is to define Curie point where a straight-line extrapolation of the steepest part of the thermomagnetic curve crosses the temperature axis.

A duplicate instrument was assembled in Iceland, using the

Newport 4-inch electromagnet referred to in the preceding Appendix. Here the movement of the sample cup was not compensated, but the deflection of the light spot was read directly. Temperature measurements were made with a thermocouple and a calibrated "Scalamp" galvanometer.

CHAPTER 3 PALEOMAGNETISM OF DISKO ISLAND BASALTS

3.1 The Tertiary geology of West Greenland

In West Greenland, the largest areas of exposed volcanic rocks of Cretaceous to Tertiary age are found on the Svartenhuk peninsula, in Ubekendt Island, in Nugssuaq peninsula and on Disko Island (Fig. 3-1). No systematic stratigraphic mapping has yet been carried out here, but several limited aspects or regions have been described. The literature to 1968 is reviewed by Rosenkrantz and Pulvertaft (1969), and important geochemical work has since been published by Clarke (1970).

The West Greenland area appears to have been a sedimentary basin in the Lower Cretaceous to the Paleocene. Sedimentation in this fault-bounded basin, both of marine and non-marine origin, amounts locally to some 1.5 km thickness. The basin may have extended far beyond the present coastline of Greenland (Henderson 1969, 1971). The above age of the sediments has been inferred from fossil evidence, mainly in Nugssuaq. So far, only one radiometric dating has been carried out,on a lava flow from Ubekendt,and indicates an age of 64 million years (D. H. Tarling, pers. comm. 1971).

The uppermost sediments in Nugssuaq contain tuff beds, and they are overlain by olivine-rich basalt breccia and lava flows. These are of very primitive compositions, but on geochemical grounds Clarke (1968) believes that they are younger than the olivine basalts in Baffin Island. The olivine lava sequence is thickest in Ubekendt,

about 5 km, but thins to the north and south. Individual flows are usually less than 10 m thick.

Subsequently to the olivine lavas, large volumes of a more differentiated, felspar-porphyritic basalt type were erupted. These prevail in the northern and southern part of the Tertiary area, including Southern Disko. The main source area for these basalts may have been northwest of Disko, as is indicated by bedding in the breccia, and by the scarcity of dykes in the area studied here. The total thickness of felsparphyric lavas may be of the order of 3 km. The widespread presence of breccia at the base of the volcanics, of thickness up to 500 m locally, implies that eruptions took place in a shallow marine environment (Clarke 1968) although tuffs and other evidence of explosive activity are absent. The present altitude of breccia and marine sediment exposures indicates a subsequent uplift by several hundred meters.

Accompanying and subsequent to the volcanism in West Greenland, large tectonic displacements occurred within the area. These are manifested by faults, which generally have a downthrow on the west side. The total amount of throw is some hundreds of meters. Large blocks were also tilted by varying amounts, often $10\text{-}20^{\circ}$ or more. The tilt is in general to the west and increases in that direction. In the paleomagnetic collection localities described in the present work the tilt of the lava pile was measured from a distance by a Brunton compass. It is $0\text{-}2^{\circ}$ to the north and $< 1^{\circ}$ to east or west, and was not corrected for in the paleomagnetic measurements.

One "central volcano" of the type common in Iceland is found in West Greenland. Situated at the southern end of Ubekendt Island, it has been described by Drever and co-workers (Drever 1958). Ignimbrite horizons occur on Northern Disko (G. Henderson, pers. comm. 1970). Clarke (1968) has put forward an explanation of the sequence of subsidence, volcanism and tectonic displacements in West Greenland. In his view, these processes are connected with the splitting of Greenland from North America, by a process of sea-floor spreading. He suggests the presence of a "hot spot" in the mantle, situated, at the time, west of Ubekendt.

The origin of Baffin Bay, Davis Strait and the Labrador Sea by such a process of sea-floor spreading, appears now to be generally accepted. Using magnetic anomaly profiles and JOIDES drilling results in Labrador Sea, Laughton (1971) has timed the start of continental breakup at 82 m.y. ago, and its cessation at 47 m.y. ago. In the period 60 to 47 m.y. ago, there appears to have been active sea-floor spreading in both the Labrador Sea and in the North Atlantic. Other workers (Hood and Bower 1971; Pitman 1971; Le Pichon *et al.* 1971) have obtained slightly different ages from the magnetic anomalies; none have, however, been able to fit the subaereal volcanic activity in the Brito-Arctic Tertiary province into a correlated scheme of events. More research, especially radioactive dating, and geophysical research on the aseismic ridges in the North Atlantic is needed before this scheme can be worked out in detail.

Refraction seismic profiles in Baffin Bay (Ross and Manchester 1972; D. I. Ross, pers. comm. 1972) indicate a 3-4 km thick sedimentary cover in central Baffin Bay, and simultaneous magnetic profiles show very low amplitude (50 γ) anomalies, which cannot be used for dating purposes. Heat flow measurements, however (Pye and Hyndman 1972), indicate that Baffin Bay has been very inactive in spreading for at least the past 20 m.y., though earthquakes are known to be still occurring on a zone in its northern half, as well as in the Labrador Sea (Johnson *et al.*, 1969).

3.2 Disko Island Collection--Local Geology and Sampling

3.2.1 Basalt lava profiles. The three main collection profiles in Disko were named GL, GM and GK in the order of sampling (Fig. 3-2). The flows in each profile were numbered in ascending order.

Profile GL is the shoulder of the mountain Skarvefjeldet (Plate 3a), at 60°17'N, 53°27'W. The lava flows, from 200 m altitude and up, overlie a pillow-breccia without any intervening sediments, and the bottom flow (GL 1) may even grade into breccia south of the sampling sites. Very little sediment is seen between any of the flows; only between flows 1-2 and 9-10 did a few cm of fine red sediment occur. This will be described in section 3.12.3.

The boundaries between any two flows were marked by reddening and scoria-like textures where seen, but were in many places covered with talus. The central parts of the flows were fresh and non-vesicular

The last flow, GL 20, was sampled at an altitude of 730 m, above which the mountain levels off to a plateau covered with glacial and periglacial deposits. Since the average thickness of each of the sampled flows is about 25 m, and the plateau reaches to 130 m above the highest site, probably some 5 flows were missed. Their outlines can be discerned in air photographs.

No flows are believed to have been left out of the sequence where traversed, but an inaccessible flow was seen to peter out in nearby cliffs between flows 15 and 16, east of the sequence. Skarvefjeldet rises to the east of the sampling profile, but this rise is seen (from the sea and in aerial photographs) to be due to the presence of NE-trending faults. From the sea, on passing Skarvefjeldet, no more than 24 flows could be counted anywhere from the breccia up. At least three oriented cores were collected from each flow, and were numbered one to three. Extra cores, usually unoriented, were collected from some flows.

Profile GM is in the mountain Lyngmarksfjeldet (Plate 3b) at 60°16'N, 53°34'W. The breccia is much thinner here than at profile GL (Fig. 3-2) due to the presence of topography in the Precambrian basement, but conditions are otherwise similar to those at profile GL. A few cm of yellow sediment (see profile GK), are seen in places overlying the breccia, and 30-60 cm of fine bright-red sediments were seen between flows 11-12.

The flow above flow 6 was numbered 6A in the field, because of the uncertainty of a contact between them; subsequent paleomagnetic

results (Table 3.8) indicate that they are separate flows, but the numbering was not altered accordingly. A total of 17 flows were sampled in Lyngmarksfjeldet. The number of unexposed flows overlying the top of the profile (at 700 m altitude) is at least four, but this mountain is capped by a glacier that reaches to 1000 m altitude.

At least two oriented samples were collected from each flow in profile GM. Sample 14-2 and all samples from flows 3, 4, 15 and 16 are hand samples. Of these, the samples from the lower two flows were oriented by geographic sighting, but the rest by magnetic bearing only because of fog. The magnetic declination was known from geographic sightings with the Brunton compass in profile GL, and is $58^{o} \pm 4^{o}$ (s.d.) for class R samples (Sect. 3.4) and $54^{o} \pm 3^{o}$ (s.d.) for class N samples.

One specimen from each of the hand samples was used for initial AF demagnetization; sometimes extra specimens were drilled from these for other work and were labelled e.g. GM 4-1a.

Profile GK is in the mountain Marrait Qaqat (Plate 4a), at $69^{o}25'$N, $52^{o}47'$W. To the west of this profile is a major fault trending ENE and marked by dyke GD 4. East of this fault the breccia is largely replaced by thick sedimentary beds, which are of Cretacious and Tertiary age and of non-marine origin (Henderson 1969). These sediments consist mostly of unconsolidated yellow sand, with occasional thin ($\lesssim$1 m) layers of shale and thinner layers of limonitic sand and of lignite. The layers have been tilted towards the north.

The basalt lava profile overlies the sediments from an altitude of 450 m, reaching to 760 m altitude in Marrait Qaqat and 840 m in a nearby mountain. Layers of the yellow sediment, of the order of 1 m in thickness, were found between some of the flows in the profile.

3.2.2. Intrusives. Many basalt formations are seen to outcrop between sea level and lava profile GK. These are usually either shelf-like bodies tilting towards the north some 20^{o}, or very irregular outcrops. Their thickness is of the order of 5-20 m, and they are usually columnar; one was seen to have a glassy top. They are presumably all intrusive bodies, but may belong to more than one episode of volcanic activity. One of these sills (GD 2) was sampled at sea level and was found to be diabase; two at an altitude of 150-200 m (GD 3 and 3A); and two, which were at first thought to be lava flows and hence numbered GK 1 and 2, were sampled near the top of the sedimentary sequence. No attempt was made to study relations between these intrusives, which appear to be confused and possibly complicated by landslips.

Three samples were collected from each flow and two from each intrusive; these were drilled in the field, except for flow GK 10, where hand samples were collected. Flows 3, 6, 7 and 9 exhibit block-jointing ("kubbaberg") or columnar jointing, whereas flow 4 is a highly reddened and crumbly basalt. The top four flows are very thick, of the order of 50 meters each.

Two dykes were sampled: GD 1 is a 1.6 m thick felspar-porphyritic dyke, exposed at the river in Blaesedalen valley, below profile GL. It

cuts through rubbly breccia, which is also porphyritic. GD 4 is a 10-12 m thick non-porphyritic dyke exposed on a gravel beach 8 km southwest of profile GK, near the Sinigfik glacial river.

3.2.3 Breccia. Site GR 1 is near sea-level at the mouth of Rode Elv river in Blaesedalen. Pillows of the order of 0.5 m size were sampled. Site GR 2 is at about 100 m altitude on the way to the foot of profile GL, and site GR 3 is immediately below flow GL 1. They are situated in large pillow units (>5 m) within the breccia. Site GR 4 is immediately below flow GM 1. Site GR 5 is 4 km inland in Blaesedalen; here the breccia resembles weathered basalt, and the sample collected is faintly reddish. Site 6 is in Rode Elv river about 3 km inland; one piece from the edge of a 2 m pillow was collected. Site 7 is at the most easterly outlier of the breccia near profile GK. Pieces were collected from lumps in the breccia, 0.5 m or smaller.

3.2.4 Other basalt samples. Two hand samples AP 1 and 2 were collected from the lowest exposed lava in Apostelfjeldet west of profile GM. A few samples were collected from columnar exposures named GKS at about 100 m altitude on the east bank of the Sinigfik river north of GD 4. It is not known whether these exposures are sills or lavas. Sample GD 2A was collected 2 km west of GD 2. This is probably an outcrop of a single irregular sill which is seen at sea-level for at least 3 km in the area, and is over 20 m thick in places. Samples were collected at the same stratigraphic level as GK 3, in fine-grained dark basalt flow, about 0.5 km to the west and named LGK 3. All of

these samples were up-down oriented only. They were found to be reversely magnetized.

3.3 Petrology and appearance of the Disko basalts

Clarke (1968, abstract) states that "chemically, the basalts are regarded as members of a tholeiitic suite." Although he has only investigated Baffin and Svartenhuk basalts, his observations are probably also valid for the Disko basalts. He also points out various differences between the olivine flows and felsparphyric flows. In the field, these differences include that columnar jointing is more common in the latter; they are much thicker than the olivine flows and contain fewer vesicles and zeolites, the amygdale mineral being silica in the felsparphyric flows. In South Disko the average flow thickness is about 20 m, i.e. similar to Clarke's estimate for Svartenhuk (25 m), but columnar structures were only seen in profile GK. Clarke states that red bole is very common between Svartenhuk felsparphyric flows, but it was only seen at a few contacts in South Disko, the flow contacts being generally obscured by scree.

Among chemical differences between Clarke's samples of olivine-rich and felsparphyric basalts note that the former contain 3.3-5.6% normative magnetite and 1.1-2.3% ilmenite, whereas the latter contain on the average 6.3% and 4.4% of these minerals respectively. This is consistent with susceptibility differences between Cape Dyer and Disko flows, to be described below.

From inspection of hand samples and cores from Disko basalts, the concentration of felspar phenocrysts is highly variable from one flow to another. Since these phenocrysts are generally formed prior to eruption, a study of their abundance in individual flows may aid in stratigraphic correlation, as has been done in Iceland by Walker (1966). A brown weathering layer occurred on many of the samples; it appeared to be less than 2 mm thick and was cut off all specimens used for magnetic measurements.

On inspection of the same samples, zeolites were recorded in eight out of the thirty-seven flows of profiles GL and GM; since samples were mostly collected from the massive central parts of the flows, this is clearly a minimum estimate for the incidence of zeolites in the basalts. Empty vesicles occurred in many of these flows, and zeolites and vesicles were also recorded in some GK-flows, breccia samples and intrusive samples. The zeolites were not identified.

The densities of seven basalt cores from the flows sampled in Disko were found to be between 2.85-3.0 g/cc, with an average of about 2.95 g/cc. The densities of two intrusive samples also averaged 2.95 g/cc, and those of two breccia cores were 2.8 g/cc. Crumbly flow tops and highly altered samples, as from flow GK 4, have a lower density, around 2.5 g/cc.

Nine thin sections from Disko basalts, made by the author and inspected by him and Mr. S. Steinthorsson of the University of Iceland, are described in Appendix 3.1. It is seen that felspar and clinopyroxene

(augite) are the major constituents of the rock, with minor magnetite and olivine. The groundmass often has a granular texture. Very little alteration is seen in the felspars, but in two of the sections as well as in several hand samples, alteration of olivine to brownish minerals has occurred.

3.4 Disko basalts; the natural remanence of -1 samples

The paleomagnetic sampling in Disko was carried out in late July and early August of 1970. All core samples were taken to St. John's by air, cut into specimens, and the NRM of one specimen from each flow was measured in early September. These specimens were taken from the first core drilled at each site, and which will hereafter be referred to as -1 cores. Hand samples (Section 2.1) arrived by ship, and were cored and measured similarly in early December.

Both normal and reverse NRM polarities were found. In order to qualitatively test the stability of these remanences, the -1 specimens were stored in the laboratory, i.e. in the earth's field, in inverted positions for 4-6 weeks. Their NRM was then remeasured.

It was found that in all the reversely magnetized specimens the remanence intensity was either the same as before or had increased slightly. In the normally magnetized ones, the intensity had decreased considerably, and directional changes sometimes exceeding 10^{o} had occurred.

The simplest interpretation of this phenomenon is that a viscous

component of magnetization, in the direction of the earth's present field in Disko, had been present in varying amounts, before the sampling. During transportation and storage, this component decayed, and during storage, VRM components in the opposite (downward) sense were also introduced (Fig. 3-21).

This stability test is only a qualitative one, since the ambient magnetic field during transport was highly variable, and the ambient field during storage was not quite antiparallel to the presumed VRM components in each sample. Further, because the VRM components are not quite parallel to other magnetization components in each core, the changes during storage should be treated as vectors, but below, only intensity changes will be used in calculations (Section 5.2.1) as a first approximation.

It was inferred from the storage test that the VRM was much less stable than other, probably older, components of remanence in the basalts. It was decided to AF demagnetize all -1 specimens progressively in steps of 50 peak Oe in order to eliminate the VRM, and to test the stability of the older components.

In those specimens which had reverse NRM polarity, only minor directional changes occurred on demagnetization. The AF treatment of any specimen was stopped when two successive steps yielded the same direction to within 5^{o} or so. These were usually the 50 and 100 Oe, or 100 and 150 Oe steps. A maximum in the magnetic intensity, J_{max}, usually occurred at 50 or 100 Oe in the specimens from GL and GM (Table 3.1).

In normally magnetized specimens, the polarity changed below 100 Oe field, and their intensity reached a maximum at 100 to 150 Oe. At higher fields, small random changes in direction were seen in some specimens. These may be due to imperfections in the demagnetizing process, or to VRM building up in the specimens between treatment and measurement (Sect. 3.12.2).

Six selected specimens were later AF demagnetized to 600-800 peak Oe. Details are given in Table 3.5; see also Figs. 3-6 and 3-7. The last entry for each specimen in the Table is the average of two runs, because relatively large spurious components were noted in these. In their response to alternating fields and in other respects, the specimens of Figs. 3-6 and 3-7 are representative of three fairly well defined classes of magnetic behavior that occurred in the Disko Tertiary basalts:

Class N samples comprise about one-third of those from profiles GL and GM, and a few others. Their VRM at the time of measurement was larger than their more stable reverse remanence component; J_{max} is always less than $2 \cdot 10^{-3}$ Gauss.

Class R samples, occurring in almost all the flows and some of the sills, have a reverse NRM. J_{max} occurs at 50-100 Oe, and exceeds $2 \cdot 10^{-3}$ Gauss. J_{200}/J_{max} is usually more than 0.4, and VRM is small.

Class R' samples occur at many intrusive and breccia sites, and in flows where there is evidence of rapid cooling. NRM is reverse, J_{max} occurs at 0-50 Oe, and J_{200}/J_{max} is usually less than 0.4.

One difference between class N and class R samples is clearly shown in Fig. 3-3, where the primary remanence J_{max} is plotted against the mean VRM intensity $(-\Delta) = J_{max} - J_o$ for -1 samples from profiles GL and GM. Other important differences between the three classes of samples will be described below, but it should be stressed that all the Disko basalt samples collected and measured by the author possessed a magnetically stable reverse component of remanence. In this chapter (in contrast to the next chapter) reverse magnetization will therefore in tables and diagrams be referred to as being positive.

3.5 Systematic AF treatment of basalt specimens

Following an examination of the AF demagnetization results of the specimens from -1 samples, it was decided that 200 Oe AF treatment of the Disko basalt samples would give the most reliable paleo-field direction for these basalts. At lower fields, some viscous magnetization would still be present; at higher fields, spurious components might become noticeable in class R' and class N specimens.

After measurement of NRM, the remanence after 200 Oe treatment was measured in altogether three samples from each of the 20 lava flows of profile GL, and in two samples from each of the 17 flows of GM and the 8 flows of GK. Similarly, the remanence of one to three samples from each site in the breccia (seven sites) and intrusives (seven sites) was measured. Intensities of remanence and susceptibilities are given in Table 3.2, and directions after 200 Oe treatment in Table 3.7. One specimen was measured per sample, except in the case of a few poorly

stable ones (see Table 3.7). Intensity and susceptibility averages by profiles are given in Table 3.3.

At each site, the magnetic vectors from each sample were given unit weight and averaged by means of a desk calculator, using a magnetic-card programme devised by G. Haardeng-Pedersen and K. V. Rao. This programme also calculated certain statistical parameters for each average, as described in Section 2.9. However, as only two or three samples were averaged per site, these parameters are of little significance. Table 3.8 therefore only lists the average field direction from each site, and the quantity $\delta_w = \cos^{-1}(R/N)$, which for two vectors is equal to half the angle between them.

All site average paleomagnetic directions are plotted in Fig. 3-10 on a Wulff equal-angle stereographic projection, and their profile averages are given in Table 3.4. The r.m.s. value of the within-flow dispersion angle δ_w after 200 Oe treatment is 4.8^o. This parameter proved to be of similar magnitude, whether or not the samples measured from a flow had similar or widely different rock-magnetic properties. These results show that the stable reverse paleo-magnetic direction in each lava flow is primary, and that this component was acquired when the lava cooled from a molten state, during a time when the geomagnetic field in Disko had a reverse polarity.

3.6 Thermal demagnetization

Three specimens, one from a lava sample with normal NRM, one

from a lava sample with reverse NRM, and one from a reverse dyke, were heated stepwise and cooled in nulled ($\lesssim$ 100γ) fields. The results are shown in Table 3.6 and Fig. 3-8, and are seen to be quite similar in appearance to AF demagnetization results (Fig. 3-6). The rapid drop in remanence intensity of dyke sample GD 1-3 reflects the low Curie point of this rock unit (Section 3.11.4), but in all three samples a minor remanence fraction persists beyond the main strong-field Curie point (Table 3.9).

Similar results have been obtained in the case of Cape Dyer lavas (Section 4.6.1), and in other basalt material by Wilson and Smith (1968). The significance of this will be discussed in Section 4.6.1. As also found by Wilson and Smith, the viscous components of remanence in these specimens have been eliminated at a temperature of about 300°C. These results confirm the above interpretation of the origin of the stable and unstable remanence components in Disko basalts.

Three other specimens, GL 10-1A, GL 19-1A and GK 9-3A were also thermally demagnetized, following 100 Oe AF treatment to eliminate some of their viscous remanence. The results on their stability of remanence were similar to those in Fig. 3-8 but less reliable because of equipment trouble, and are omitted here.

3.7 Individual Disko paleofield directions

As seen from the previous section, all the oriented basalt samples from Disko Island have a stable reverse primary component of

remanence. This has several interesting implications.

(1) Most probably, all the extrusive volcanics of South Disko, between the easterly and westerly profiles samples and some distance beyond, were emplaced during a single reverse geomagnetic epoch. The intrusives sampled may also belong to this epoch, but with much less certainty. Low inclinations observed in the three lowest flows of profile GK may be due to a polarity transition or excursion.

(2) On the geomagnetic time scale of Heirtzler *et al.* (Naidu 1971) the average length of geomagnetic epochs in the Lower Tertiary appears to have been about 1 million years. Hence the volcanics in South Disko probably do not span more than 2 million years, but as remarked in Sect. 1.4.3, the validity of this time scale may be in doubt. A much lower limit can, however, be placed on the length of the interval of volcanism represented by the sampled sequence by the conspicuous lack of erosion, vegetation and aeolian sedimentation between the Disko flows. In eastern Iceland, the average thickness of an aeolian interbasaltic bed (excluding rhyolite ash) is of the order of 30 cm (Walker 1959) and represents 10000-15000 years, using data of Moorbath *et al.* (1968) and Dagley *et al.* (1967). The average time between two successive Disko flows may be one-fifth of this or less, i.e. the 20 flows of profile GL span of the order of 50000 years or less. Allowing for the eruption of breccia and of the unexposed flows above this profile, assuming the same rate of extrusion, the whole volcanic sequence at that profile may have erupted in less than 100000 years.

(3) Stratigraphic mapping by polarity reversal zones (e.g. Kristjansson 1968) obviously cannot be carried out in South Disko, and the reverse zone of volcanics is likely to persist inland for at least 50 km, if the source of those around Godhavn was to the northwest (Sect. 3.2). This agrees with magnetic anomaly evidence (Sect. 5.2.1).

(4) A lower bound on the time interval between successive lava flows is obtained by noting that in all profiles the differences in paleo-field directions between successive flows are similar to one another and to δ_k. These directions, therefore, do not trace out a sequential path (Fig. 3-9), indicating that the mean interval between two flows is at least half a period of the major component of geomagnetic secular variation. At the present time this half-period, estimated from archeomagnetism (Burlatskaya *et al.* 1968) may be about 1000 years. Therefore, the time spanned by the flows of profile GL, for instance, is at least 20000 years, on the reasonable assumption that the secular variation was broadly similar then and now.

(5) Even with the aid of field data on lava thickness, occurrences of sediments, and the relative felspar phenocryst content of the flows, no way has been found to correlate individual magnetic directions in GL flows with those in GM flows (Fig. 3-9). This is probably not to be expected, since the source of the volcanics was most likely to the north or north-west; thus each lava may have flowed from the source area in a stream of the order of 4 km width, overlapping with underlying lavas. This occurs commonly in the case of Quaternary and Recent lava flows, one of which is known to have travelled 100 km down a valley in

Iceland before solidifying. In Disko, it was also found impossible to trace any lava more than 1 km along the cliff face (Plate 3b), looking from sea-level towards the profiles with binoculars.

In any future attempt to carry out stratigraphic correlation in the West Greenland felsparphyric lavas by means of paleo-field directions, it is also necessary to collect more samples per lava than was done for this study. In the present collection, α_{95} for the GL flows is usually about 6-8^{o} with three samples per flow, which could be reduced to 3-4^{o} with six samples, or even with four samples using improved drilling and orientation techniques (cf. Wilson 1970).

(6) Paleomagnetism may be useful in the eastern part of Disko, in determining the relationships between various intrusions within the sediments (Fig. 3-1). Thus, intrusives GD 3 and GD 3A, which were sampled only a few hundred meters apart, have clearly different paleomagnetic directions (Table 3.8b). However, neither measurements of remanence nor of other magnetic properties (to be described below), seem capable of distinguishing unequivocally between samples from lava flows, intrusive or breccia in Disko.

3.8 Mean field directions and pole positions

3.8.1. Introduction. The error sources inherent in any attempt to obtain a significant mean paleomagnetic pole position from a limited number of observed field directions has already been discussed in Sect. 1.4.2; as stated by Wilson (1970, p. 9): "....the larger the number of

lavas sampled..., the more clearly it is seen that the ancient field has performed in very unsuspected ways, and the less confidence I personally have in reducing the data to a simple mean direction..."

In addition to the above sources of error, systematic errors of a few degrees in pole positions may be caused by using inappropriate models of the geomagnetic field for the averaging (Irving 1964, p. 49-51; Kristjansson 1967). Also, there is evidence that the Earth's magnetic field, at least in Upper Cenozoic times, has been an axial eccentric dipole (Wilson 1971), though this evidence is in some instances based on a biased selection of data. On the model of Wilson, a northwards displacement of an axial geomagnetic dipole by 300 km would reduce the inclination due to that dipole field by about 2^{o} at the present latitude of Disko. Other common error sources in paleomagnetism, including instability of the primary remanence, the presence of stable secondary components and tectonic disturbances after emplacement, do not seem to be present in the Disko lavas.

3.8.2. Results and discussion - Disko. The average paleomagnetic field for each of profiles GL and GM, with statistical parameters, is listed in Table 3.4. It is seen that the dispersion (δ) of directions in GM is larger, and that the mean field directions for the two profiles are about 8^{o} apart. F-ratio tests, using formulae quoted by Irving (1964) show that neither difference is significant at the 90% level. However, the application of statistics based on Fisherian distributions may not be appropriate here, since the directions obtained (Fig. 3-9) obviously occur mostly at a distance of about δ from the

profile means. Because the individual flow directions could not be correlated across the two profiles (Section 3.7) we must take the combined results of Table 3.4 to represent the best estimate of the mean paleomagnetic field for the South Disko felsparphyric flows. On the central dipole assumption, this field corresponds to a northern pole occurring at

62°N, 169° W, with 95% error oval semi-axes
of $\delta p = 8^{\circ}$ (along the meridian), $\delta m = 9^{\circ}$.

Fig. 3-10 shows this pole and the error oval. Also in Fig. 3-10 are shown the field directions of GL and GM combined, and directions for oriented samples from the GK-flows, the breccia and the intrusives. The mean field direction for the latter appears to be similar to that for GL and GM, but it has not been computed, for the following reasons:

(1) The three lowest flows of profile GK have shallow southerly remanence directions (Table 3.7).

(2) The age of the intrusives in relation to that of the flows is unknown; northerly remanence directions occur in some of them, and they may have been tilted to the north after emplacement.

(3) The breccia sites were spaced unevenly in the sampling area; also, some of the pillows sampled may have moved after their original cooling.

Sanver (1968) has presented a simple method of calculating the "true" between-site dispersion of paleomagnetic directions, from the

observed mean-square within-site dispersion $\overline{\delta_w^2}$ and between-site dispersion δ_k^2. His formula is $\delta_B = (\delta_K^2 - (B/N)\ \overline{\delta_w^2})^{\frac{1}{2}}$, where B and N are respectively the total number of sites and of samples. For GL and GM, δ_k is 19.0°, $(\overline{\delta_w^2})^{\frac{1}{2}}$ is 4.8°, B is 37 and N is 94. Hence δ_B is 18.7°, which is insignificantly different from δ_k, and is similar to δ-values from various other Tertiary strata (Kristjansson 1970, Creer and Sanver 1970).

3.8.3 The Disko pole and other Lower Tertiary poles. Along with the Disko paleomagnetic pole, a pole obtained by Tarling (1967) from 28 stable reversely magnetized lava flows from the Scoresbysund region of East Greenland is shown in Fig. 3-10. Their age (Tarling 1970) is about 58 m.y. It is seen to be not significantly different from the Disko pole. The α_{95} of the field was 15°, so δ^m = 23°, δp = 18°.

A pole position at 55°N, 153°W (i.e. south of Alaska; not shown in Fig. 3-10) has been obtained by Tarling (pers. comm. 1970) on six reverse olivine basalt flows from Ubekendt Ejland (Fig. 3-1), dated at about 64 m.y. The pole 95% confidence oval is 16° in size, so this pole position is not significantly different from the Disko pole.

A pole position has been obtained by Girdler (1961) from seven samples from the large Skaergaard intrusion in East Greenland. The pole is at 76°N, 116°E, but is of very low reliability because of the known anisotropy of susceptibility in the samples, and because no magnetic cleaning was carried out. The intrusion is dominantly of reverse polarity and is probably 50-60 m.y. old (R. Blank, pers. comm. 1972).

An unpublished pole position obtained by Ketelaar on 15 Trap Diabase (TD) dykes in SW-Greenland has been quoted by Tarling (1967). They are possibly Mesozoic (Allaart *et al.* 1969) in age. The pole position is at 68°N, 174°W, with a field $\alpha_{95} = 8°$, but details of polarity or of magnetic cleaning procedure were not given. Bullock (1967) gives results for two N and two R TD dykes.

Comparisons may also be made with European Lower Tertiary paleomagnetic pole positions. The most reliable of these is that obtained by Tarling (1970) from 253 Faeroese basalt lavas, mainly of reverse polarity, which have been dated at 52 m.y. Their mean pole position and error oval is shown in Fig. 3-10 and it appears to be significantly different from the Disko pole, possibly because of a different age or because of relative displacements (caused by the opening of the North Atlantic) after the eruption of the flows (Pitman and Talwani 1972).

The Faeroese pole, at 77°N, 161°E, is almost identical to a pole obtained by him from published paleomagnetic results on 16 British Tertiary formations (77°N, 171°E). Further British studies have yielded similar pole positions, e.g. 77°N, 149°W from 9 dykes in England and Wales (Dagley 1969); 81°N, 159°E from 34 formations in Scotland and N-Ireland (McMurry 1971); and 70°N, 163°E from 54 lavas (25 directions) in N-Ireland (Wilson 1970). Wilson states that with the exception of a few dykes, all British Tertiary formations studies so far have been reverse; their radiometric ages have been in the range 30-70 m.y.

Continental European paleomagnetic poles from the Lower Tertiary given in the literature tend to be based on too few rock units to be really significant. However, one may quote here the Eocene Lisbon pole, obtained from 12 normal flows (Watkins and Richardson 1968). Being at 69°N, 153°W (North Alaska) with a 10° error oval, it is not significantly different from the Disko pole, but Watkins and Richardson state that it may be affected by a post-Eocene rotation of the Iberian peninsula.

A pole by Vekua (1961) from 11 sites in Georgia (USSR) is at 75°, 123°W; these sites are of mixed polarities, and magnetic cleaning does not appear to have been carried out.

The above results indicate strongly that the lowest Tertiary paleomagnetic pole for Greenland and Europe was in the vicinity of the Bering Straits, rather than north of Siberia as deduced by Irving (1964) from then available data. However, it is possible that the Oligocene-Miocene pole for these areas was north of Siberia; this possibility is supported by e.g. the results of Watkins *et al.* (1968) from the Macaronesian insular region, by the writer's own results from NW-Iceland (Kristjansson 1968), by those by Dagley and Ade-Hall (1970) from Hungary, and by the results of Nairn and Vollstadt (1967) from Germany.

Some well-documented North American Oligocene-Miocene paleomagnetic pole positions (e.g. Gilliland *et al.* 1969; Grommé and McKee 1970; Watkins 1966; Grommé 1965), are also north of Siberia. However, a detailed analysis of these directions is outside of the scope of the present work.

Much paleoclimatic evidence is available from the Lower Tertiary of Alaska, Greenland, Siberia and Western Europe (Nairn 1961). The

global climate of the Lower Tertiary appears to have been much warmer than in the Pliocene and Pleistocene, and climatic zonation was less distinct. Hence, a comparison of the paleomagnetic pole position and the pole of climatic zones (both of which should approximate to the rotation pole of that period) may not be meaningful.

3.8.4 Paleomagnetism and rotation of Greenland. One possible use of magnetic data from rocks bordering Baffin Bay is paleogeographic, for example in a test of the proposed separation of Greenland from Canada (Wegener 1929). In planning future field work, the minimum sampling required for such a test may be roughly estimated.

For this purpose we assume that (1) the pole reported here for Disko Island (62°N, 169°W) is the "true" early Tertiary pole relative to present-day Greenland; (2) the Tertiary rocks on Baffin Bay become magnetized in a geocentric axial dipole field of either polarity; (3) after the rocks were magnetized, Greenland rotated away from Canada according to the model by Bullard *et al.* (1965); and (4) no other crustal displacements involving these rocks occurred. Rotating Greenland back to Canada (Fig. 3-11) shifts the Disko pole into a new position at about 67°N, 175°E, that should coincide with the hypothetical early Tertiary pole for Baffin Island. The angular distance p between the latter pole M_N and the original Disko pole M_0 then defines the limiting sensitivity of the test. For a specified rotation angle R, p depends only on the paleocolatitude θ of the rotation pivot and is given by Deutsch 1969): $1 - \cos p = \sin^2 \theta (1 - \cos R)$. In the Bullard model for Greenland, R = 18.0° and the pivot is at 70.5°N, 94°W. The

distance of the Disko pole from this pivot is $\theta = 29°$, giving $p = 9°$. Though small, p is more than twice the present great-circle distance between Cape Dyer and Disko.

One may judge the hypothetical poles for Greenland and Baffin Island to be distinct if their 95% error ovals do not intersect. For a maximum pole separation $p \sim 9°$, this means that the sum of the major semi-axes δm of the two ovals should not exceed about nine degrees; hence, on average, the oval dimensions should not be more than one-half those of the present oval for Disko ($\delta m = 9°$). We now assume for simplicity that the dispersion of the N remanence vectors averaged in calculating future pole positions will be the same as the dispersion we observed for Disko; then δm varies approximately as $N^{-\frac{1}{2}}$. A signficant test would thus require on average four times the present number of Disko flows (N = 37), i.e. 150 or so rock units, on each side of Baffin Bay. This minimum requirement is large, but probably can just be met. This test, however, as well as a similar test for the differential rotation of Greenland and Europe (Sect. 3.8.3), would still be only qualitative tests of the hypothesis of rotation of Greenland, since the rotations involved may have taken place in two or more stages with different rotation poles (Le Pichon *et al.* 1971).

We conclude that a paleomagnetic test of the opening of Baffin Bay is marginally feasible, provided the rocks on both sides are of the same age. The large rock collections needed to investigate these purely directional features of the early Tertiary field can probably yield more significant results on other characteristics of that field, such as its secular variation, strength and polarity.

3.9 Further observations and magnetic measurements on Disko N and R basalt samples

3.9.1 Introduction. It was stated above that the Disko samples could be divided into three distinct classes, according to their NRM polarity and behaviour during AF treatment. Out of the 137 samples listed in Table 3.2, 74 are of class R, 29 of class N, 26 of class R', and 8 are doubtful. Several experiments were done to elucidate the difference between these classes of magnetic behaviour, and are described below, as regards N and R class samples. R' class samples will be discussed in the next section.

3.9.2 Distribution of classes of magnetic behaviour. In the lava flows of all Disko profiles, both N and R class samples commonly appear in the same flow, and field notes show that an N and an R sample were sometimes collected within 1-2 meters of each other horizontally or vertically. In two flows, several samples were collected from vertical sections through the lower half of these flows (Section 3.12.1). It is seen that their magentic properties vary considerably and rather unsystematically through the flows.

All samples that were reddish in color belong to class R; this indicates that the differences between N and R samples are to some extent due to intra-flow differences in oxidation after extrusion, as the red color is due to hematite, limonite or goethite (oxidation products of iron-rich silicates). The red color, however, does not signify high NRM intensity, but only high stability and lack of VRM.

Because of the small within-flow δ (Sect. 3.8.2) and large between-flow δ, it is almost certain that this oxidation took place

during the initial cooling of the Disko flows and is not a secondary heating effect. The occurrence of such oxidation during cooling has been convincingly demonstrated by Grommé *et al.* (1969).

3.9.3 Microscope observations. Reflected-light microscope observations on polished sections from Disko class N and R basalts are described in Appendix 3.2. They include estimates of dominant grain sizes, concentration and oxidation class of the opaque minerals.

It is found that the opaque grains in class N and R samples are predominantly titanomagnetite with minor discrete ilmenite, together composing about 6-7% of the rock volume. No sulfides were seen in any section.

On a scale of one to six (e.g. Ade-Hall and Lawley 1970) it is found that the average oxidation class of the N samples is 1.5, whereas that of the R samples is 4. This is known (see Section 1.3) to be a consequence of deuteric oxidation of the lava at the time of initial cooling.

The average titanomagnetite grain size varies considerably between polished sections, but 20-50 μ grains appear to be most common. They are usually fairly equidimensional and euhedral to subhedral, indicating early and slow crystallization. No conspicuous grain size or shape differences were noted between N and R samples.

3.9.4 Thermomagnetic curves. Thermomagnetic curves were obtained from five class N and five R samples using the balance described in Appendix 2.1. The applied field was usually about 500 Oe. Typical curves are shown in Figs. 3-12 and 3-13, and all Curie points are listed

in Table 3.9 along with approximate values of the change in room-temperature strong-field moment in each sample on heating.

The systematic differences in the N and R curves are minor but significant. First, some of the class N curves show the presence of a component with a low Curie point, of about 250° - 300°C. On heating beyond 300°C, both the Curie point of this component and the room-temperature moment increase irreversibly. These features are present in the R samples to a much lesser degree. Secondly, the high Curie points of the N lava samples are 510°- 530°C, indicating that during the deuteric oxidation a titanomagnetite of x = 0.07 - 0.10 (Fig. 1-2b) was left in the lattice after exsolution. In R samples, the Curie points are 550°- 570°C, indicating x = 0.01 - 0.04.

These observations support the view that differences in remanence stability are linked with differences in the oxidation state of the titanomagnetites in these rocks. They should, however, not be taken to indicate a universal correlation between stability and Curie point in basalts: thermomagnetic curves from samples of e.g. intrusive GD 2, and of flow 6 in Cape Dyer (Sect. 4.6) have Curie points of only about 500°C, but their remanence is very stable and free from VRM. In many tens of basalt samples from Iceland measured by the writer, no distinct correlation between stability and T_c has been found; such correlations are probably affected by flow thickness, petrology and other variables.

3.9.5. Susceptibility of fresh samples. The very distinct grouping between class R and N samples in Fig. 3-3 becomes less distinct when either J_{max} or $J_{max} - J_o$ is plotted against initial volume susceptibility K (Fig. 3-4). It is therefore possible that the grouping of Fig. 3-3 is to some extent fortuitous; intermediate behavior will probably be present in flows that contain both classes of rock.

The negative correlation between J_{max} and K seen in Fig. 3-4b is similar to that found in an Icelandic lava flow by Wilson *et al.*, (1968); they also found a negative correlation between K and oxidation state within that flow. Keeping in mind that the opaque grain content of class N and R samples is similar (Sect. 3.9.3), it appears most probable that the main effect of increased oxidation is to reduce the effective grain size, and hence increase the coercivity and the remanence intensity. Deuteric oxidation will also reduce the susceptibility of the rock (after $T_c \sim 500°C$ is reached; see Fig. 3-15), partly by the reduction in grain size, but mostly because of conversion of magnetite to hematite and other essentially non-magnetic minerals. The presence of the latter effect was confirmed by observations of N and R polished sections before and after the application of a magnetite colloid, many of the oxidized titanomagnetite grains in class R samples proving to be insufficiently magnetic to attract any colloid.

Some of the scatter of the data points in Fig. 3-4b may be the results of variations in magnetite content between the various flows; these may be eliminated by plotting J_{max}/K against K, which was

indeed found to reduce the scatter. In the Cape Dyer flows (Chapter 4, Fig. 4-2) there is even a strong within-flow correlation between J_o (= J_{max}) and K. Another cause of this scatter may be time variations in the geomagnetic field strength during the building up of the lava pile in the two profiles.

The positive correlation between VRM intensity and K in Fig. 3-4a is probably partly due to variations in magnetite content. However, since the measured VRM values span a range of a factor of fifty or more, and the K values only range through a factor of five, most of the variations in VRM intensity are most probably due to oxidation effects on the coercivity of the magnetic grains.

3.9.6 Heating experiments. In an inert atmosphere, titanomagnetites with values of x up to about 0.08 are chemically stable at any temperature (Nagata 1961, Fig. 3-7). Wasilewski (1968) proposed that those with x up to 0.2 are chemically stable up to 600°C, though his considerations were not based on experiments directly applicable to this situation.

In the context of the Disko lavas, it is of interest to know whether class N rock (x = 0.07-0.10) can be converted into class R rock by moderate heating in air. To test this, the following experiments were done:

(1) Class N specimens from GL 15-1 and GM 3-1 were heated to 600°C during thermomagnetic runs. Their Curie points were found to increase only slightly, from 510° to 525°C and from 530° to 540°C respectively.

(2) A polished section of GM 15-2 was observed before and after heating to 600°C (Appendix 3.2). No increase in titanomagnetite oxidation was seen (cf. Wasilewski 1968, p. 142).

(3) After heating to 540° and 590°C during thermal demagmetization, a specimen from the N sample GM 4-1 showed an even greater tendency to pick up VRM than does fresh class N rock : on 15 minutes' storage in 0.5 Oe field immediately after cooling, this specimen picked up about $0.6 \cdot 10^{-3}$ Gauss. In that sample also, low-T_c components were absent from the thermomagnetic curve, and its room-temperature susceptibility did not change on heating to 600°C. In GL 19-1A, however, the susceptibility after heating to 600°C was considerably less than that for the fresh specimen (Fig. 3-15) in spite of an increase of susceptibility at lower temperatures due to exsolution of low-Curie-point components.

On this scant evidence it is concluded that heating to 600°C in air does change some magnetic properties of class N samples towards those of class R, but this effect may vary between individual samples. Heating to still higher temperatures may cause further changes in the same direction, as found by Strangway *et al.*, (1968), but above 600°C the heating also begins to affect the properties of class R samples (Fig. 3-15).

3.9.7 Remanence intensity differences. The negative correlation between primary remanence intensity J_{max} and susceptibility K in fresh Disko basalts may be summarized by stating that while the class N samples have a higher average K than R samples ($4.7 \cdot 10^{-3}$ G/Oe

for all samples from GL and GM), the former have a much lower J_{max} ($1.0 \cdot 10^{-3}$ vs. $4.5 \cdot 10^{-3}$ Gauss for the -1 samples from the same profiles). Since the average paleo-field strength F_p was the same for both classes, it follows that the Q- ratio J_{max}/KF_p is about seven times higher in the R samples.

This large difference may be due to a combination of two effects, both of which are in turn due to oxidation differences. First, the class R rock may have acquired a stronger remanence on original cooling; secondly, the remanence of the class N rock may have decayed faster through geologic time. A third effect, that of within-flow self-demagnetizing fields which would tend to produce the same negative correlation, is easily shown to be negligible (Wensink 1964).

In order to test the first two possibilities, six specimens from each of classes N and R were heated to 600°C in air and cooled in an applied field of 0.50 Oe. The artificial TRM intensity J_{th} acquired on cooling is plotted in Fig. 3-14a against the susceptibility K_t, measured after cooling. The slope of a line from the origin to any point, divided by the field strength of 0.50, is the Koenigsberger ratio Q_t as defined by Stacey (1967).

The figure shows that class R specimens have a higher average Q_t (= 9) than do class N specimens (Q_t = 7). The latter is similar to the value 7.2 found by Parry (1965) for dispersed magnetite of 1.5μ grain size. 6μ magnetite investigated by Parry had a Q_t of 2.0. and multidomain magnetite had a Q_t of o.5. Fig. 3.14a shows these results along with (see double circles) the class N and R average values of

K and J_{max} found during AF treatment of the natural remanence of -1 samples from GL and GM. The crosses in Fig. 3-14a illustrate results obtained for single specimens from high-T_c lava flows of Cape Dyer after similar heating; two specimens (flows 1 and 4) had Q_t values of about 16, but two others (flows 5 and 6) had Q_t values of 8. Basalt specimens from Iceland (Fig. 5-13) mostly have Q_t values between 10 and 35. $Q_n (=J_o/KF)$ for near-single-domain grains of titanomagnetite, such as are found in oceanic pillow basalt (Marshall and Cox 1971; Evans and Wayman 1971) may exceed 100.

One concludes that the Q_t in both N and R basalt in Disko is rather on the low side, and because of the positive correlation between Q_t and coercivity H_c found by Parry (1965) and others, it is likely that the primary remanence in both classes has decayed considerably since it originated. Because of the small difference in Q_t between the N and R samples of Fig. 3-14a, and because chemical changes may have taken place in these on heating, further evidence (e.g. from AF demagnetization of artificial TRM) is needed to decide whether the original remanence of class N decayed faster than that of class R.

Comparison of magnetic data from rocks and from experiments on dispersed magnetite is only a qualitative one, since each titanomagnetite grain may contain a large number of magnetically interacting lamellae (Dunlop and West 1969, p. 742), whereas interactions between the dispersed grains are likely to be negligible. Thus, Parry (1965) finds that the median destructive alternating field (m.d.f.) for his 1.5μ magnetite is about 380 Oe, similar to that of sample DY 1-5 which has more than twice the Q_t of Parry's magnetite. Further, the average

m.d.f. of the artificial TRM of four Quaternary basalt core samples from Stardalur, Iceland (200 Oe) is similar to that of Parry's 6μ magnetite (150 Oe), but their average Q_t is seven times higher.

The low Q_t values obtained from the above Disko basalts, and the common irreversibility of their strong-field thermomagnetic curves, appears to rule out the possibility of finding reliable values of paleo-field intensity for the time of their emplacement.

3.9.8 Ballistic magnetometer results - parameter H'.

Measurements of the parameter H' of formula (2.2), which expresses the difficulty of magnetically saturating a rock sample (Sect. 2.7.1) were carried out for 6 fresh N and R samples of basalt from Disko (Table 3.10). The values of H' for the three samples each of classes N and R average 770 Oe and 1010 Oe, respectively.

This difference is probably due to oxidation effects causing any or all of the following in the more highly exsolved R rock: reduced effective grain size, increased grain anisotropy, increased strain in the lattice, and increased self-demagnetizing fields. Judging from results of similar measurements of gneiss containing pure magnetite (Sect. 5.4), which also yield H' values of about 1000 Oe, the last-named effect may be the most important one, but the actual situation may be complicated and involve transition to single-domain lamellae (Strangway *et al.* 1968) and interactions between these.

3.10 Magnetite content and composition in the Disko flows

3.10.1 Introduction. Below, results from experiments described in Chapter 5 will be anticipated. These showed that in artificially prepared samples and in Precambrian metamorphic rocks containing pure magnetite as the only opaque mineral, there is a linear relation between magnetite content and susceptibility. This relation is in good agreement with theoretical considerations discussed in Sect. 2.6.2, and holds at least up to magnetite concentrations of 4% by volume, largely independent of grain size. The characteristic field H' may also be fairly constant at about 1000 Oe (Tables 3.10 and 5.5) for a wide range of grain sizes.

Because of the close association of iron and titanium minerals in basic igneous rocks, it is not possible to obtain reliable estimates of their pure-magnetite content by optical or chemical means. For this reason and because of the many error sources inherent in optical measurements (Sect. 5.4), it was decided to try to measure the magnetite content of some basic rocks by their saturation magnetization, using a ballistic magnetometer (Appendix 2.1).

A large number of basic rocks were measured this way. The results for some of the areas studied will be discussed separately, but all results from samples that had a single high (< 500°C) Curie point only (Sect. 2.7.1) are plotted against susceptibility (before saturation) in Fig. 3-16 (see legend). The straight line in that figure, drawn for rough comparison rather than being the exact mean of the results, represents a linear relation between the variables with a proportionality constant of $2.2 \cdot 10^{-3}$ G/Oe per volume percent

of magnetite. Among others, Wilson *et al.* (1968) and Ade-Hall *et al.* (1968a) have found , though not expressed explicitly, a similar linear relation between these variables in basalt. From Fig. 4a of the paper by Wilson *et al.*, which contains data on high-Curie-point rock only, a proportionality constant of approximately $2.1 \cdot 10^{-3}$ G/Oe per percent is obtained.

From the data used in obtaining Fig. 3-16 it appears that the points farthest away from the straight line on either side represent mostly highly oxidized rock samples, as inferred from their high (590° - 620°C) Curie points, low M'_o/M_o values (see legend, Table 3.9) and values of H' in excess of 1200 Oe. The approximate linear relation of Fig. 3-16 may therefore not apply strictly to such samples or to maghemite-rich, sulfide-rich, geothermally altered, weathered, or very fine-grained (< a few μ) rock, as well as to low-T_c rock.

3.10.2 Results from Disko lava flows. The saturation magnetization J_s in three R and three N lava samples was measured. These were chosen in such a way that the mean susceptibility of all six, $3.3 \cdot 10^{-3}$ G/Oe, is the same as that for all samples collected in profiles GL and GM. The results are shown in Fig. 3-14b. where J_s has been converted into equivalent content of pure magnetite by volume.

Although not all the data points may represent actual magnetite content of the samples used, because of the presence of low-T_c components (note systematic difference between the N and the

R data points), a linear relation of $2.1 \cdot 10^{-3}$ G/Oe per percent (broken line) fits them reasonably well. It is inferred from this result that the magnetite content of Disko flows is 1.5% by volume, but it may be as high as 1.8% if corrected for the presence of low-T_c titanomagnetite in the fresh samples used for the measurement, using data from Table 3.9 as a correction factor.

From thermodynamic considerations and microprobe measurements (Banerjee 1970), the x-value of unoxidized titanomagnetites in basic rocks appears to be generally between 0.6 and 0.7. With 6-7% opaque minerals in the GL and GM flows (Sect. 3.9.3), of which a tenth may be separate ilmenite, the pure-magnetite content of these rocks should be about $0.35 \cdot 0.9 \cdot 6.5 = 2.0$ to 2.1%. The difference betwwen this result and the value of 1.8% obtained above may be due to the further partial oxidation of titanomagnetite to non-magnetic minerals that has taken place in the class R samples. The value of x inferred from the low-Curie point component in some of the Disko samples (250° - 300°C) is however only 0.4 to 0.5, i.e. lower than that given by Banerjee. This will be discussed in Section 3.11.4 in the context of class R' samples.

3.11 Class R' basalt; further observations and measurements

3.11. 1 Introduction. Class R' of Disko basalt was earlier defined as including all samples with a reverse NRM and $J_{200}/J_o < 0.4$; its other distinguishing magnetic properties will be discussed below. This class includes all samples whose remanence was measured from: intrusive GD 1,3,4, and GK1; breccia sites

GR 1,2,3,6; flows GK 3,6,7,8,9, and a few samples from other sites. Field evidence indicates that at the R' sites the rock has cooled from a molten state more rapidly than in the flows of profiles GL and GM. This evidence includes the pillow structure of the breccia, the occurrence of columnar and block jointing in some of the intrusives and GK-flows, and glassy margins in others.

3.11.2 Remanence and susceptibility. Class R' samples, compared to those of classes N and R, show a tendency for high J_o ($> 6.10^{-3}$G) and low K ($<2.10^{-3}$G/Oe) values to occur; see Fig. 3-5, which includes mostly class R' samples, and Table 3.13.

The remanence intensity drops very rapidly on AF demagnetization (Figs. 3.6, 3.7). Thus, J_o usually exceeds J_{50}, in which cases J_{max} has been set equal to J_o (Table 3.1c). However, the direction of remanence in all R' samples has been found to be very stable (e.g. Table 3.5), and the within-site agreement between directions (Table 3.8) is fair to good. It is therefore concluded that these are primary remanence directions.

3.11.3 Microscope observations. The class R' samples are generally fine-grained or glassy rock, apart from the common occurrence of felspar phenocrysts. In some of the polished sections made from the R' samples, (Appendix 3.2) the titanomagnetites occurred in skeletal or dendritic clusters, and trains of octahedra (Plate 6a). This points to either rapid cooling through the crystallization temperature range at the time of the emplacement, or to the titano-

magnetites crystallizing in a highly viscous magma. Very little exsolution or silicate reddening is seen in the R' sections, indicating either a low oxygen fugacity in the temperature interval at which high-temperature oxidation could have taken place, or rapid cooling through this interval. Separate ilmenite grains were not seen in the most highly skeletal R' sections.

However, skeletal forms of the titanomagnetites are not observed in some of the class R' polished sections, nor in R'-type dykes from Iceland (Table 5.8) nor in the flow studied by Lawley and Ade-Hall (1971): in these the magnetite may have crystallized prior to emplacement. The small grain size, of the order of 10μ, in the breccia and intrusive polished sections makes it difficult to estimate their titanomagnetite content, but in three sections (Appendix 3.2) it appeared to be just over 4%.

It is concluded that the magnetic properties of R' samples, e.g. their high J_o, low K and low J_{200}/J_o values, are largely due to the effects of rapid cooling and low oxidation state. This is consistent with the results of other workers on the magnetic properties of ocean floor basalts (e.g. Irving 1970; Watkins *et al.* 1970) and will be further confirmed below.

The microscope observations may explain why two of the breccia sites, GR 5 and 7, have higher values of J_{200}/J_o than the others. GR 5 was seen to have suffered very extensive high temperature oxidation (even compared to class R basalt); and GR 7, where samples were collected from rock fragments and boulders in the breccia, contains a large number of exceedingly small (<1μ) opaque grains.

A similar situation may prevail in flow 3, Cape Dyer (Sect. 4.5.1) and in GR 1-3.

3.11.4 Thermomagnetic measurements. Curie points for some R' samples are given in Table 3.9 and typical thermomagnetic curves are shown in Figs.3-17 and 3-18. It is seen that these samples tend to have low Curie points, often with no detectable high-Curie-point components. Similar thermomagnetic curves have been observed in some Cape Dyer flows and in dykes, breccia and some flows from Iceland (Tables 4.8, 5.8).

Out of 26 low-T_c samples listed in these tables, 24 have Curie points between 160° and 320°C, and two between 320° and 500°C. This distribution is similar to the data of Grommé *et al.* (1969, Fig. 10) which also shows relatively few Curie points between 320° and 500°; most of the low Curie points obtained by then occurred in lava quenched from temperatures in the range 800°-1000°C.

The T_c range of 160°-320°C corresponds to an ulvöspinel molar fraction x in the range 0.6-0.4 (Fig. 1-2b), whereas Banerjee (1970) states that x in basalts should be in the range 0.6 to 0.7. Values of x above 0.6 were also obtained (Smith, 1967a), by microprobe, in ten out of fourteen Plio-Pleistocene rock samples from Iceland. Of these samples, eight had Curie points below 160°C.

The absence of Curie points below 160°C in the samples measured by the writer is therefore enigmatic. However, it may be caused by processes of ulvöspinel exsolution during solidification (Ade-Hall *et al.* 1965) or by other exsolution effects connected with the fact that these samples come from sites buried under 300-800m

of basalts. Ade-Hall *et al.* (1968b, 1970) have produced evidence indicating an increase in Curie point of basalts on deep burial over geological periods, whereas the samples of Smith (1967) were collected from exposures where such burial had not taken place. The chemical changes and heating accompanying the burial may not affect the stable remanence direction in these basalts (Ade-Hall *et al.* 1971).

The irreversible increase in T_c on heating in air (Figs. 3-17 and 3-18) appears to begin just below the actual Curie point. This increase does not occur in synthetic titanomagnetites in vacuum (Ozima and Ozima 1970) nor in some continental basalts (Creer *et al.* 1970), but it has been reported to occur in vacuum in oceanic basalts (Schaeffer and Schwarz 1970) and in subaerial basalts (Ade-Hall *et al.* 1965). The latter authors suggest that the source of oxidation may be water bound in interstitial glass; zeolites and adsorbed pore water could also be responsible. The oxidation takes place gradually, such that the new T_c is approximately equal to the ambient temperature on heating; it is always irreversible. Heating to 580°-600°C, however, generally does not produce a T_c of more than 510°-550°C on cooling (Tables 3.9 and 5.8).

At the applied fields used in these experiments, the room-temperature magnetization of the low-T_c samples sometimes increases by a factor between 1.5 and 3 after cooling from 570°-620°C (Figs. 3-17, 3-18; M'_o/M_o of Table 3.9b). This is partly due to the difference between the solid and broken curves in Fig. 1-2c, and partly to the fact that at room temperature the magnetization of the fresh samples is already much less than that at 0°K. At 500-1000 Oe,

the increase in room-temperature magnetization observed after cooling is probably counteracted by an increase in the characteristic field H' (see Sect. 3.11.5) and by further oxidation of titanomagnetite into essentially non-magnetic constituents.

These oxidation processes may depend critically on the accessibility of oxygen to the opaque grains during heating, as was brought out during calibration of the thermomagnetic balance: on heating a coarse-grained (100μ) magnetite powder to 580°C, no change in room-temperature moment was seen (i.e. $M'/M_o = 1$), whereas in fine-grained magnetite ($\leq$1 μ) M'_o/M_o was about 0.5. This view is supported by a negative correlation between grain size and M'_o/M_o observed in some of the low-Curie-point samples investigated in this work (Fig. 4-10b).

3.11.5 Ballistic magnetometer results after heating.

Results from ballistic measurements on three class R' specimens and on GR 7-3 (which has a high J_{200}/J_o, but low T_c) are shown in Table 3.10. The measurements did not fit formula (2.2) very well, so the saturation moments were estimated graphically. These moments cannot be interpreted in terms of magnetite content, as already explained. However, it is interesting that the value of H' is in all cases 600-700 Oe. This is lower than in class R and N basalts, and is consistent with the lack of exsolution in R' rocks; H' does not appear to be affected by the small grain size in GR 7-3.

On heating in air, one would expect both J_{is} and H' to increase, the latter to around 1000 Oe. This was found to occur in

GR 2-1 after heating to 600°C, but not in GD 1-2 (Table 3.10). In a polished section made from GD 1-2 after heating, no exsolution was seen at 1000x magnification. Only after heating that specimen to 700°C did abundant exsolution occur, along with the expected increase of H' to 1000 Oe; however, a reduction in H' occurred on heating of a low-T_c specimen from Cape Dyer (Sect. 4.6.2), for reasons that are not clear. Various experimenters (Wasilewski 1968; Ade-Hall *et al.* 1968b; Creer and Petersen 1970) have commented upon the fact that visible exsolution does not always accompany a rise in T_c on heating.

After heating to 600°C, the measured J_{is} of GR 2-1 and GD 1-2 indicate a pure magnetite content of 1.3% by volume. With a value of 4-4.5% titanomagnetite derived from microscope observations on these samples (Appendix 3.2) one obtains $x \doteq 1 - (1.3/4.3) = 0.7$. Their T_c, however, is 285°C, correspoonding to $x = 0.43$. This discrepancy may be partly due to ulvöspinel exsolution, burial effects, and magnetite destruction on heating (Sect. 3.11.4). The results fit well the relation of Fig. 3-16.

After further heating of GD 1-2 to 700°C, only a slight (5%) change is seen in its J_{is}, but its susceptibility and that of GR 2-1 dropped by about 30% from their 600°C values. This may be an oxidation effect (Sect. 2.7) related to very advanced exsolution and restriction of domain wall movements.

3.11.6 VRM and other observations. Viscous remanence buildup, as well as viscous decay of TRM, is important in oceanic basalts (Irving 1970; Marshall and Cox 1970), which in many aspects

resemble the class R' basalts described here. Because of the magnetic softness of the primary remanence in the R' rocks subjected to AF demagnetization (Table 3.5), the magnitude of the *in-situ* VRM could be estimated in only a few of these. It appeared to be on the average less than $0.5 \cdot 10^{-3}$ Gauss. However, the change in remanence in 12 class R' specimens on 4-6 weeks' storage in the earth's field averaged $0.35 \cdot 10^{-3}$ G in magnitude, only slightly less than for class N specimens after similar storage. Therefore, the average *in-situ* VRM in the former may have been larger than the estimated $0.5 \cdot 10^{-3}$ G of Table 5.2, a possibility also supported by the buildup of VRM in two fresh R' specimens stored after AF treatment in a constant field (Fig. 3-19).

In specimen GD 1-3, a VRM intensity of $0.3 \cdot 10^{-3}$ G was found to build up on 15 minutes' storage in the earth's field immediately following heating to 590°C (cf. Section 3.9.6).

3.11.7 Q-ratios; artificial TRM. The relatively high average J_o value ($9.6 \cdot 10^{-3}$ G) and low average K value ($2.1 \cdot 10^{-3}$ G/Oe) in class R' basalt leads to a high average Q_n ratio of about 8, if one uses the value of the present geomagnetic field in Disko (0.56 Oe). High Q_n values have also been noted in fresh submarine basalts by many workers, and in the subglacial basalt of Iceland (Kristjansson 1970). As already remarked, this property is probably mostly due to rapid cooling rather than the low oxidation state, since R'-type dykes in Iceland (Kristjansson 1970) of low oxidation state do not exhibit very high J_o-values.

The high J_o-values are most probably due to so-called pseudo-single-domain behaviour (p.s.d.). In the theoretical model (Stacey 1962) the number of domains in each grain is small, say less than 20, and their net magnetic moment for most configurations of the domains is a significant fraction of the grain saturation magnetic moment. They will therefore acquire large TRM intensities in applied fields of 0.1 Oe or less. This behaviour may be applicable to grain sizes of 2-10μ (Soffel 1971) and has been used successfully by Marshall and Cox (1971) in explaining the NRM intensity of pillow basalt. The smaller the grain size, the higher is the TRM for a given external field and a given concentration of magnetic mineral; the effective grain size may be much reduced by skeletal grain shape and lattice defects.

The low observed K-values quoted above are likely to be due to the low opaque content and high x-values of the titanomagnetites, rather than to grain size and the presence of defects. Similarly, the low values of H' and J_{200}/J_o in class R' indicate that crystal defects and grain shape are unimportant in determining the magnetic behaviour of these rocks at room temperature and at 50-2000 Oe; rather, the low values of these parameters and T_c are due to the lack of exsolution and weakness of the exchange interaction between iron atoms in class R' rock.

The Q_t-ratio of rock acquiring artificial TRM on cooling from about 600°C in air has been measured in two class R' specimens from Disko. The results are tabulated below along with results from one low-T_c specimen from Cape Dyer.

	K, 10^{-3}G/Oe	K_t, 10^{-3}G/Oe	J_{th}, 10^{-3}G	Q_t
GR 1-3A	0.8	2.9	37	25
GK 9-3A	2.1	3.1	17	11
DY 3-2-3	0.17	1.1	18	33

For legend refer to Fig. 5-13 which shows results from similar measurements on Icelandic basalts. Both these and the above specimens yield higher average Q_t values than found in class R and N specimens (Sect. 3.9.7).

3.12 Miscellaneous observations - Disko

3.12.1 Within-flow variations in magnetic properties. In two flows, GL 5 and GM 13, several samples were collected from near-vertical profiles through the middle portion of each flow. The top and bottom of GL 5, and the top of GM 13, were covered with talus. Table 3.11 lists the results on measurements on the NRM intensity J_o and the susceptibility K for these samples.

These results show readily that the magnetic behaviour may change from class N to R over a vertical distance of one meter or

less within the same flow. In several other flows, N and R samples were collected within a horizontal distance of a few meters or less from each other, e.g. 0.5 m in GM 3 and GM 8; 1-2 m in GL 6, GL 17 and GM 1; and 3 m in GM 16. In some properties, the distinction between N and R samples seems to be sharp (Fig. 3-3), but in others less so (Fig. 3-4). Field data indicate that the more stable class R rocks tend to occur at flow margins, as is frequently observed in basalt lavas (e.g. Ade-Hall 1969).

3.12.2 Controlled experiments on viscous magnetization.

3.12.2.1 VRM buildup. It was stated above that the soft, normal remanence component present in Disko basalts is probably viscous and was built up during the current (Brunhes) geomagnetic epoch. In order to confirm that such buildup can take place at the present temperature of the lave pile, five Disko specimens which had been demagnetized to 600-800 Oe (Table 3.5) were AF demagnetized at 100 Oe one week later, and their residual remanence J_{res} was measured immediately. They were subsequently all stored in the same attitude, their z-direction pointing down (Fig. 1-1) and their x-direction towards magnetic north.

Fig. 3-19 shows the change in the z-component of remanence of each sample as a function of time; this change is caused by the z-component of the geomagnetic field (0.50 Oe). Changes in the x-component of remanence (due to 0.19 Oe). were proportionately smaller, and those in the y-component were negligible. In the following table, J-values are given in 10^{-3}Gauss and K in 10^{-3}G/Oe.

J_{Vzo} is the z-component of the VRM acquired in 0.50 Oe in 74 days in each specimen (obtained by interpolation in the case of GK 9-1).

Specimen	Class	Δ =				
		J_{max}	$J_{max}-J_o$	K	J_{res}	J_{Vzo}
GL 5-2	R	5.9	0.4	3.4	1.0	0.20
GL 8-2	N	0.9	1.4	2.9	0.14	0.16
GL 10-1	R	4.0	0.4	3.3	0.56	0.27
GL 15-1	N	1.0	3.0	3.5	0.13	0.63
GK 9-1	R'	5.1	?	2.0	0.14	0.92

J_{Vzo} is seen to be a substantial fraction of the VRM intensity Δ inferred to reside in the samples prior to any treatment. It must be kept in mind, however, that the viscous properties of freshly AF-magnetized samples may be largely due to grains whose domain magnetization directions have been forcibly randomized, tending to move them away from crystalline easy axes. During the time interval (probably minutes to months) while the domain walls are seeking to move towards minimum energy positions, the domains must be very susceptible to the presence of external bias fields.

The large buildup of VRM in a specimen of class R' (GK 9-1) was especially unexpected, since their *in-situ* VRM was thought to be small (Section 3.11.6). To confirm that this behavior was not due to experimental accident, a previously untreated R' specimen from GD 1-1 was treated at 400 Oe and stored. The VRM buildup on 7 days storage (Fig. 3-19) is similar to that from the other specimens, but this experiment was terminated because of magnetometer breakdown.

The spurious remanence components found during AF demagnetization of these and other samples to high fields (Figs. 3-6 and 3-7) very likely are due to a similar rapid VRM buildup immediately after treatment, as their moments were often seen to change by several percent during spinning.

One N-class and one R-class specimen used for the above experiment were turned upside down upon its completion, and left for a further 35 days. In this time inverval, the VRM of both specimens was found to change sign and grow to about the same intensity as that of the respective specimens before they were inverted.

In this small number of specimens, no obvious correlations were seen between the rate of VRM buildup and other magnetic parameters. The VRM occurs in all three magnetic classes and in specimen GD 1-3 of class R', remanence intensities of $0.4 \cdot 10^{-3}$ G and $0.3 \cdot 10^{-3}$ G were found to build up on 15 minutes' storage after cooling in air from 540°C and 600°C respectively.

Because the specimens were not stored immediately following the high-field demagnetization, changes in the VRM acquired up to the final demagnetization step (where the field was only 100 peak Oe and

may therefore not have erased the VRM completely) could have interfered with the subsequent buildup process. For this reason and that of the forced randomizing mentioned above, the VRM buildup shown in Gif. 3-19 is not similar to the processes postulated by Néel (Negata 1961) and does not follow his logarithmic law of buildup with time.

3.12.2.2 Elimination of VRM by AF demagnetization. At the end of the storage period, four specimens were AF demagnetized, with the following results (fields quoted in peak Oersteds).

Sample	Class	Storage, days	Fraction of VRM remaining		
			25 Oe	50 Oe	100 Oe
GL 8-2	N	74	0.28	0.17	0.11
GL 10-1	R	74	0.68	0.61	0.54
GK 9-1	R'	105	0.14	0.04	-
GL 5-2	R	35	0.73	0.69	0.61

It is seen that the VRM is most resistant to demagnetization in the R samples. It was attempted to demagnetize these further at 200 Oe, but this produced spurious components of magnetization.

3.12.3. Interbasaltic sediments. Three samples of red interbasaltic beds were collected in Disko. Two of these, each a few cm thick, were found between flows GL 1 - GL 2 and GL 9 - GL 10, and a third in a scree below profile GM. Between GM 11 - GM 12 a bright red bed about 50 cm thick was seen, but only exposed in inaccessible cliffs. No other occurrences of these were seen, but the flow

boundaries were frequently obscured by talus.

In Ireland, such red beds are commonly observed between Tertiary lava flows, and are known to represent lateritized flow tops (Eyles 1952). In Iceland, red interbasaltic beds are also common, often exceeding 50 cm in thickness. They have not been studied in detail by any one scientist, but individual occurrences have been described in field reports. From these and rock magnetic evidence, Kristjansson (1967) considered them to be predominantly aeolian volcanic ash, each bed having been altered in a moist environment prior to eruption of the overlying flow.

Microscope examination of two Disko and several Icelandic polished sections from these beds shows that they are composed mostly of red amorphous material and white zeolitic minerals. They also contain dark spots (possibly carbon) and a few grains (< 0.1%) of highly oxidized titanomagnetites, which usually appear to be in the process of "dissolving" into red material. During this examination, rare intact pieces of basaltic ash were seen (Plate 8a), confirming that the beds are at least partly aeolian ash beds.

The Disko samples were very crumbly, but the random NRM moment (Section 5.8) of several pieces from one of these, set in plastic, was measured and AF-demagnetized. The results of intensity measurements on this and three Icelandic samples are shown in Fig. 3-20b. The NRM intensities of the latter were $(0.3, 2 \text{ and } 8)\cdot 10^{-3}$ Gauss, which is surprisingly high. The stability of the remanence is seen to vary from sample to sample.

The sediment thermomagnetic curves, for which Fig. 3-20a is

typical, (see also Table 3-12) show a characteristic straight-line drop in magnetization as a function of temperature; the Curie points of four samples measured by the author are 600-620°C, in some cases with a minor break in the curve at 570°C. The moment measured after the heating is usually less than that before the heating.

Curie points T_c of samples from 17 Icelandic sites of red sediments, measured by Wilson and Smith (1968), range between 550° and 620°C, and other instances of sediment Curie points in the range 590° - 620°C have been reviewed by Rao (1970). These are likely to be due to material of maghemite (γ - Fe_2O_3) composition, which in red sediments may be localized in the red material rather than in discrete magnetite grains. T_c of the sample Hamar (Table 3.12) after heating in air to 900°C, was found to be about 550°C, possibly indicating an oxidation of the maghemite to relatively non-magnetic hematite, leaving magnetite as the only magnetic mineral.

Two highly reddened Disko flow tops were also measured in the magnetic balance, giving T_c values of respectively 615°C and 605°C on heating. It is likely that the red material in these flow tops and in the sediments is similar, and that in both cases it originated by low-temperature oxidation of titanomagnetite (Section 1.3.1).

Other reddened lava samples giving high Curie point values include DY 4-4 and 4-6 (Table 4.8) although DY 5-1, also highly oxidized, gave a T_c of 555°C. A sample from 60 m depth in the Stardalur drill hole in Iceland, with very highly oxidized small titanomagnetite grains, also had a T_c near 620°C (Kristjansson and Buason 1970). Samples of Lower Teriary dykes, investigated by Larson and Strangway (1969) and

known to have undergone much low-temperature alterations, had similarly high T_c and straight-line thermomagnetic curves.

Implications of the thinness of the interbasaltic beds with respect to the local eruptive history were discussed in Section 3.7.

Appendix 3.1 Description of Thin Sections from Disko Basalts

GL 12-2 Felspar-porphyritic basalt; clear flow structure seen in felspar laths in groundmass. Groundmass granular mostly clinopyroxene (augite) and magnetite. Olivine rusty.

GL 19-1 Felspar-porphyritic basalt, a few felspar phenocrysts being seen in the thin section. Well crystallized (granular) groundmass with prominent felspar laths (30-100μ) and augite. No or very little alteration seen in felspars.

GL 20-2 Fine-grained felspar-porphyritic basalt, with at least several percent of opaque minerals.

GM 2-2 Sub-ophitic texture, with a few microphenocrysts of plagioclase. Considerable amounts of equidimensional granular opaque grains and euhedral clinopyroxene.

GM 4-2 Microphenocrysts of felspar (up to 500μ), in granular groundmass of augite, magnetite and felspar laths. Typical basalt with a low f_{O_2} and rapid cooling in evidence.

GM 12-2 Felspar-porphyritic basalt showing some weathering effects or other alteration in groundmass and in the two olivine crystals seen in the section. A few zeolites in vugs.

GK 5-2 Similar to GM 4-2, but with a more coarse groundmass. A large felspar phenocryst and an augite phenocryst. Groundmass granular clinopyroxene and magnetite. Considerable weathering.

GD 2-2 Diabase, rich in felspar; also clinopyroxene and opaques. Ophitic texture.

GR 1-2 Fine-grained olivine-plagioclase porphyritic basalt.

Appendix 3.2 Description of Polished Sections from Disko (400x and 1000x)

(1) Class N samples from profiles GL and GM

GL 4-1 Opaque grains rarely larger than 20μ, rounded or irregular in shape. No exsolution in opaques or reddening of silicates; oxidation class 1 (Ade-Hall and Lawley 1970). Ilmenite in discrete grains or grain parts about 10% of the opaques. Counted 300 points, giving 6-7% opaques by area in the section.

GL 7-1 Opaque grains commonly 20-200μ, often with pits. Exsolution seen in most grains at 1000x, but no reddening of silicates; oxidation class 2-2.5 Ilmenite 10%. Counted 250 points, giving 7% opaques.

GL 17-1A Opaque grain size very uniform, 20-50μ. Exsolution in titanomagnetites very variable; average oxidation class about 2. Ilmenite 10%. Counted 350 points, giving 7% opaques.

GM 4-1 Opaque grain size 10-30μ, but very small subgraphic titanomagnetites also occur in (?) olivine. Minor exsolution in some grains; some reddening of silicates; oxidation class 1-1.5. Ilmenite 10%. Counted 300 points in polished sections from both GM 4-1 and 4-1a, giving an average of 5% opaques.

GM 15-2 Opaque grain sizes in a wide range around 50μ. No exsolution, or reddening of silicates, but some alteration has taken place along cracks in the opaques. Oxidation class 1. Ilmenite 10%. A polished section was heated to 600°C in air, the silicates turning brown, but no exsolution was seen to have occurred.

(2) Class R samples from profiles GL and GM

GL 1-1 Opaque grain size 20-200μ; irregular outlines. Much exsolution of ilmenite and hematite seen in the titanomagnetites. Discrete ilmenite grains (generally small) also oxidized to steel-gray rutile and pseudobrookite. Silicates often reddish, especially around titanomagnetites. Oxidation class 4.

GL 13-1 Opaque grain sizes up to 200μ, many grains being subhedral. Minor exsolution, silicates sometimes brown; oxidation class 2. Separate ilmenite perhaps 20% of the opaques. Counted 350 points, giving 6-7% opaques.

GL 14-2 Very abundant grains of titanomagnetites with minor separate ilmenite; grain size 20-50μ. Much exsolution of ilmenite and hematite, reddening of silicates, mainly around the opaques; oxidation class 4-5. Counted 300 points, giving 6-7% opaques.

GM 10-1 Sample reddish in color. Opaque grain sizes both around 50μ and around 5μ. Very much exsolution of steel-gray pseudobrookite; also hematite and other iron minerals. Edges of many opaque grains altered, much reddening of silicates. Oxidation class 5-6. Point-counting difficult, but 300 points gave 7% unaltered opaques.

GM 11-1 Opaque grain size around 20μ. Very much exsolution and silicate reddening, cf. GL 14-2. Oxidation class 5. Some discrete ilmenite. Counted 250 points, giving some 7% opaques.

(3) Samples from profile GK, intrusives and breccia

GK 6-1 (R') Homogeneous isotropic titanomagnetite, subhedral to euhedral and not skeletal; grain size 10-40μ. Oxidation class 1. Separate ilmenite in lath-shaped grains perhaps 20% of the opaques.

GK 9-3 (R', 1 m from GK 9-1). Similar to GK 6-1, but less ilmenite. Oxidation class 1.

GK 8-2 (R') Mainly regular grains of size range 40-200μ. Regular exsolution lamellae in some grains; oxidation class 1-2. Ilmenite, as parts of these grains or separate, about 25% of the opaques. Counted 300 points, giving 6% opaques by area.

GD 1-3 (R') Titanomagnetites in dendritic clusters and strings; grain size about 5μ. No exsolution, oxidation class 1. No separate ilmenite. Counted 400 points, giving 4-4.5% opaques.

GD 3-2 (R') Regular opaque grains, 20-200μ. Minor exsolution; oxidation class 1-2. Ilmenite 15%. Counted 300 points, giving 4-4.5% opaques.

GR 2-2 (R') Dendritic titanomagnetite grains and clusters of octahedra, grain size 5-20μ. Similar to flow 3 of Cape Dyer. Oxidation class 1. Ilmenite may be present in fine laths. Counted 300 points, giving 4-4.5% opaques.

GR 5-1 (R) Grain sizes 10-100μ, with some tendency to skeletal shape. Much fine intergrowth and exsolution, much silicate reddening; oxidation class 5.

GR 7-3 (R'?) Considerable number of 10-μ subhedral grains of titanomagnetite, but also very abundant small ($\leq$ 1μ) grains. Oxidation class 1.

Appendix 3.3 Potassium-argon age of the flow GM 4

Of the available hand samples from Disko flows, only four appeared to be free enough of visible zeolites and other alteration effects to warrant further examination in view of obtaining radioactive datings from them. Thin sections were made from these four samples (GM 4-1, GM 4-2, GM 13-3E and GM 14-2) and kindly inspected in detail by Dr. D. F. Strong of the Department of Geology at Memorial University. To him, the sample GM 4-1 appeared to be very suitable for such dating. It contained less than 3% glass, partly devitrified and chloriticized, but there is evidence that some of this alteration is primary. The section otherwise consists of quite unaltered crystalline material, being largely felspar laths of average dimension around 50μ.

Subsequently, this sample was dated by the Geochron Laboratories Division of Krueger Enterprises Inc. in Cambridge (U.S.A.). The sample GM 4-2, collected 8-10 m away, was also sent to Geochron, but appeared less suitable for dating.

The analysis by Geochron is dated 9 June 1972, and was carried out in duplicate on whole rock crushed to 60-100 mesh. It yielded the following results:

Potassium content: 0.413 and 0.410 weight percent.

Argon content: Radioactively produced Ar^{40} was 0.002051 and 0.002146 ppm, respectively 14.4% and 17.6% of total Ar^{40} measured in the analysis.

Using the accepted constant $K^{40}/K = 1.22 \cdot 10^{-4}$ gm/gm, a mean K^{40} content of 0.502 ppm is obtained for the sample. Its age may then be computed from standard formulae (e.g., Stacey 1969), using the

decay constants of $4.72 \cdot 10^{-10}$/year and $0.585 \cdot 10^{-10}$/year for β decay and electron capture of K^{40} respectively.

From this data, Geochron obtain the age of the sample as

70.1 ± 4.3 million years,

the ± signifying their experimental uncertainty.

This result may be compared to various other data. First, Laughton (1971) and other investigators of magnetic anomalies in Baffin Bay and the Labrador Sea, time the start of continental breakup there at 8082 m.y. ago, which is consistent with this date, since Clarke (pers. comm. 1972) considers the South Disko volcanics to be among the youngest in West Greenland. Second, it may be compared to K-Ar dates of 58 ± 2 m.y. from Baffin Island (Clarke and Upton 1971) and one of 64 ± 7 m.y. from Ubekendt (D. H. Tarling, pers. comm. 1970). Both of the latter dates are obtained from olivine - rich flows, which are known to be much less resistant to weathering and other alteration effects than are the massive felsparphyric flows of Disko. Hence, those from the olivine flows are likely to be affected by argon loss, and the dates quoted must be looked upon as minimum ages. It should be recalled, however, that Clarke's (1968) conclusion that the Baffin lavas are older than the West Greenland lavas, rests on the tenuous assumption that these were erupted from a common magma source. Third, evidence on marine fossils in Nugssuaq (Rosenkrantz and Pulvertaft 1969) and their relations to European fossils, seems to place the beginning of volcanic activity in West Greenland in the Upper Danian, i.e., between 65 and 70 million years ago. This age is too low by 5-10 million years to be fully consistent with the Disko date, but the discrepancy is hardly a serious one.

CHAPTER 4 PALEOMAGNETISM OF CAPE DYER BASALTS

4.1 Geology of the Baffin Island Tertiary Volcanics

The Tertiary volcanic rocks of Baffin Island were first described by Kidd (1953) and later by Wilson and Clarke (1965), Clarke (1968, 1970) and Clarke and Upton (1971). These volcanics are breccia and lavas of very olivine-rich basalt, overlying the Precambrian basement either directly or with thin terrestrial sediments intervening. They occur on a strip of coast 90 km long by 10 km wide (Fig. 3-1) between Cape Dyer and Cape Searle. The exposures are not continuous, but consist of 20-30 isolated patches, evidently erosional remnants of a plateau.

The breccia is the basal member of the volcanics and was formed by eruptions in shallow-water environment. The volcanics appear to have flooded a topography in the basement, and their source was to the north-east, judging from bedding in the breccia. Lava flows are mainly thin (average 3.5 m), and almost no interbasaltic sediments are observed. The total thickness of the lava pile is of the order of 500 m or less in any exposure.

The age of the volcanics has been approximately determined as Paleocene from plant fossils and from a 58 m.y. potassium-argon date (results quoted by Clarke and Upton 1971). The latter may not be very reliable (see Appendix 3.3).

According to Clarke (1968) the olivine content in the olivine basalts of Baffin Island and of the Svartenhuk peninsula of West

Greenland may reach 40-50%. Other important minerals are plagioclase, 20-40%, and clinopyroxene, 20-40%. Opaque minerals are a minor constituent, usually 1% of the rock or less, though values of up to 3% occur in Svartenhuk picrites. Zeolites are rare and may be magmatic in origin.

Clarke (1968) suggests that the volcanics in Baffin Island, as well as those in West Greenland (Sect. 3.1) are related to the opening of Baffin Bay. The opening process caused crustal subsidence and sedimentation, culminating in volcanic eruptions. However, the locus of volcanic activity moved away from Baffin Island before other than primary olivine lavas were erupted; an uplift of 400-500 m occured subsequently.

4.2 Cape Dyer sampling; local geology and petrology

Thirty-eight oriented samples of basalt were collected by Dr. B. T. May and Mr. W. J. Drodge at M. U. N. in the summer of 1968 at Cape Dyer. This is the most southerly outlier of the Baffin Island volcanic area (Plate 4b). Five flows were sampled in a gully, from sea level to an altitude of some 500 m. Snow and inaccessibility prevented sampling of some intervening flows. Flow six was sampled on the plateau about three miles away, at an altitude of about 700 meters. Each lava was sampled horizontally over a distance of 10-15 m, and vertically over a distance of some 3 m. The thicknesses of each flow, relative positions of samples within each, and other field data, were not available.

Thin sections were made from one sample from each flow and examined by Mr. J. Cant and the writer (Appendix 4.1). Olivine was a major constituent in all samples; in some it has suffered iddingsization and/or serpentinization. Minor or no alteration is seen in the felspars. All flows, especially Flow 6, are porous or vesicular, with densities of 2.6 - 2.8 gm/cc (about 2.5 in flow 6). Zeolites occur in one or more samples from each flow except flow 3, and may reach 1 cm size.

4.3 Remanence measurements

The natural remanence of two specimens from each of the Cape Dyer samples (with some exceptions as noted in Table 4.2, also excepting the cores from flow 6, where one specimen was measured per sample) was measured. Table 4.2 shows the mean field direction obtained from each sample, as well as its mean remanence intensity and δ, half the angle between the specimen directions after demagnetization treatment.

In most of the samples, the difference between the NRM intensities of the two specimens was 10% or less. In some, however, the intensity was more than 30% higher in one specimen than in the other, including samples 2-4 (60%), 2-5 (100%), 3-1 (50%), 3-2 and 3-3 (40%), 3-4 (180%) and 4-6 (40%). These are mainly samples from the more highly viscous group of Sections 4.5.2. In sample 4-6 only, these differences also occur in J_{400} and in K; in 3-2, 3-3 and 3-4 they occur in J_{400} but not (< 20%) in K.

One specimen from each flow was AF-demagnetized progressively at fields up to 900 Oe, by Mr. C. R. Somayajulu. The results are given in Table 4.1a and Fig. 4.1. Other less detailed measurements to 400 Oe were also carried out (Table 4.1b). It is seen from the Table that, after elimination of minor viscous components at 25-50 Oe, the direction magnetization is exceedingly stable in all the specimens up to fields of 300-400 Oe. At higher fields, minor spurious components appear, indicated by random directional changes of a few degrees from step to step.

All samples except nos. 2, 3 and 4 from flow 3 were found to have steep positive inclinations, i.e., they were normally magnetized. In the normally magnetized samples, within-site agreement between directions was good except in flow 6. The declinations of that flow were scattered, which may be either due to natural causes or to errors in orientation in the field. This flow was not used in subsequent paleomagnetic work, but its remanence intensity and other properties have been included in the profile average. A few other samples were not used in the averaging of results; see Table 4.3.

From the results of the detailed AF demagnetization, it was decided to measure the remanence of all the remaining specimens after demagnetization at 400 Oe. (Because of the high directional stability of the pilot samples, however, it would probably have made no difference in overall results to measure the paleomagnetic direction after 100, 200 or 300 Oe). Table 4.2 gives the sample average directions, and Table 4.3 the site average directions and intensities. It is seen that only minor changes in mean direction and statistical parameters

have occurred during this treatment. The high stability of magnetization in most samples, both in intensity and in direction, is good evidence that the remanence of the Cape Dyer flows is primary, i.e., acquired during initial cooling. The problem of the three reversely magnetized samples of flow 3, hereafter referred to as the 3^- samples, will be discussed in Section 4.7.

Two distinct stability groups were found in flow 4. Samples 1, 2 and 3 had an average J_{400}/J_o of 0.11, compared with 0.60 for samples 4, 5 and 6. This difference was not reflected in the directional stability of these samples, nor in their susceptibility (Table 4.6). However, it may be caused by greater oxidation or by a greater proportion of small opaque grains in the latter samples, which had higher values of T_c and H' (Tables 4.8, 4.9).

4.4 Lower Tertiary and Cretaceous paleomagnetic poles for North America

4.4.1 Cape Dyer pole position. Fig. 4-3 shows the five flow mean directions, their 95% confidence circles and the overall mean direction for Cape Dyer, giving unit weight to each flow. The latter is

$$\bar{D} = 2.7^\circ \ , \ \bar{I} = +81.7^\circ, \text{ with } k = 155, \ \alpha_{95} = 6.2^\circ \ ,$$

where α_{95} is the radius of the 95% confidence circle. This direction differs by 1° of arc from the mean NRM direction. It is associated with normal polarity and corresponds to an ancient mean magnetic pole at 83°N, 55°W, with 95% confidence oval semi-axes of $\delta p = 11.5^\circ$, $\delta m = 12^\circ$ (see Sect. 1.4 and 3.8).

The occurrence of the very steep mean inclination (82°) for the Cape Dyer flows, as compared to that (67°) of the Disko flows and of other reversely magnetized Greenland Tertiary rocks, may have various explanations.

One possibility is that the geomagnetic dipole at the time was displaced southward in normal epochs, and north in reverse epochs. However, for this to explain fully the difference, very large displacements are needed. Thus, it is easily calculated with the formulas given by Wilson (1971) that such a displacement of the dipole by 300 km (as inferred by him from Upper Cenozoic rocks) would change the magnetic inclination in Cape Dyer and Disko by only 2° (Section 3.8.1).

The most likely explanation of the inclination difference is that the Cape Dyer field directions represent a large, but not exceptionally so, excursion of the geomagnetic dipole field from its average value. Thus, the angular difference between the Disko and Cape Dyer field directions is 18°, whereas the angular dispersion or circular standard deviation of the Disko GL and EM directions is 19°. If the Disko results had included transitional field directions, the standard deviation could have risen to around 23°, as in the large paleomagnetic surveys on Upper Cenozoic rocks listed by Kristjansson (1970).

In rocks from the lower Tertiary of Britain and Faeroes respectively, McMurry (1971) and Tarling (1970) find no significant difference between normal and reverse mean pole positions. Similarly, there is no such difference in the pole positions for the Oligocene Buck Hill formation of Texas (Gilliland *et al.*, 1969), nor in the Cretaceous results quoted above.

4.4.2 Discussion of other North American results. The published Paleocene-Eocene pole positions from North America are shown in Table 4.11 and Fig. 4-4. In some of these studies, unstable samples and sites occurred, but were excluded from analysis by the authors of these studies. All results are based on 8 or fewer rock units, which is probably the main cause of the large scatter in the mean poles. Both magnetic polarities occur. The results are still too few and scattered to permit comparison with the European and Greenlandic results given in the previous chapter, especially as regards their use in inferring the extent of continental drift since the Lower Tertiary.

Eight Cretaceous paleomagnetic pole positions from North America have been summarized by Hanna (1967, Fig. 10) and lie with one exception in the vicinity of the Bering Straits. Further published Cretaceous pole positions include one from the Mesaverde sediments (Kilbourne 1969) and additional results from one of the formations tabulated by Hanna (Larochelle 1969), which also fall in the vicinity of the Bering Straits. Watkins, *et al.*, (1970) report a paleomagnetic pole in the same area from 12 Cretaceous dykes in Jamaica.

It is concluded from these and the previously discussed European Lower Tertiary results, that the mean geomagnetic pole was near 60 - 70°N, 160 - 180°W for the whole of Cretaceous and Lower Tertiary time, as seen from both North America and Europe. The divergent low-latitude poles obtained from the Siletz River flows (Cox 1957), the California Fransiscan formation (see Hanna, 1967) and Jamaican dykes (Watkins *et al.*, 1970; Guja and Vincenz 1971) may

represent a semi-stable intermediate orientation of the geomagnetic dipole field.

4.5 Origin of the Magnetization

4.5.1 Susceptibility and the stable remanence. Polished sections from seven fresh samples were examined in reflected light at up to 1000x magnification (Appendix 4.2). The average diameter of the opaque grains as viewed was about 15 microns. However, skeletal grains of much smaller size (< 5μ) and exhibiting no obvious internal structure were common in some of the sections, mainly from flow 3; these came from samples where thermal demagnetization had indicated (Fig. 4-6) that part of the NRM is blocked at low temperature. Elsewhere, exsolution of ilmenite lamellae and other characteristic oxidation features of titanomagnetite were found, especially in the samples from flows 5 and 6 which had been shown (Figs. 4-1, 4-5) to be very stable to demagnetization. This is consistent with the evidence (Wilson *et al.*, 1968; Larson *et al.*, 1969b) for a strong positive correlation between advanced high-temperature oxidation state and high stability in basic lavas.

If the oxidation state is more important in determining NRM intensity than is the amount of magnetic material present, the remanence intensity and susceptibility should be inversely correlated (Wilson *et al.*, 1968; Section 3.9.5). This was tested for those Cape Dyer samples that had uniform intensity of magnetization, and where enough material was available for accurate susceptibility measurements

(legend to Table 4.6). Fig. 4-2 shows that both J_o and K vary considerably at each site but are positively correlated within each site. The simplest explanation is that at any Cape Dyer site the concentration of magnetic material varies from sample to sample, while the effects of variable oxidation state, tending to produce a negative J_o - K correlation, are unimportant (oxidation perhaps having approached a maximum in flows 1, 4, 5 and 6, and having been arrested by rapid cooling in flows 2 and 3). The effects of oxidation have been discussed in more detail in Sections 3.9 to 3.11. Readers should note, however, that J_o and K are not proportional to each other in Fig. 4-2; this may be due to oxidation or grain size effects.

The arithmetic mean values of NRM intensity and susceptibility for Cape Dyer, based on the flow averages in Table 4.3, are

$$\overline{J}_o = 4 \cdot 10^{-3} \text{ Gauss}, \quad \overline{K} = 0.6 \cdot 10^{-3} \text{ Gauss/Oe}.$$

This average excludes a few rejected or inhomogeneously magnetized samples (Table 4.2), as well as sample DY 5-1 which has a J_o of $59 \cdot 10^{-3}$ Gauss for unexplained reasons. For a present field of F = 0.6 Oe, the above mean values yield a mean Koenigsberger ratio of $\overline{J}_o / K F = 11$, which is of the usual order for stable Cenozoic basalts.

Some magnetic properties of eight other basalt samples from the Tertiary Baffin volcanics are given in Table 4.10. They were also found to possess a stable remanence, and were in other magnetic properties similar to the Cape Dyer samples.

Magnetic anomaly maps (Section 5.2.2) indicate that all major basalt outcrops in Baffin Island have a total magnetization which is

normal and considerably larger than that of the Precambrian formations in Baffin. With the above evidence of high Q-ratio and remanence stability, we may conclude that most or all of the Tertiary basalts in Baffin are normally magnetized. Adding the evident lack of inter-basaltic sedimentation, it is concluded that the basalts were mostly emplaced during one geomagnetic epoch.

4.5.2 Storage test for stability of remanence. To test the stability of remanence, the NRM of eighteen specimens was re-measured after undisturbed storage in the earth's field. The duration of storage averaged about four weeks.

This storage test is a qualitative one. The pre-storage measurement yields a vector sum of primary and viscous components of magnetization. During storage the viscous components are oriented at random angles to the earth's field and may be expected to change in magnitude and/or direction. The magnitude of the vector difference between the pre- and post- storage measurements, averaged for many specimens, gives a fair estimate of the magnitude of short-period viscous components in these rocks. In the results below, changes in angle and in intensity are listed separately, because these are calibrated independently in the spinner magnetometer.

These results showed that the specimens could be divided as follows into two groups, one with a much more noticeable tendency for viscous buildup:

(1) Low- VRM specimens:

Flow	Number of specimens	Total % change in intensity	Total change in angle, degree
1	3	1.4	2.3
4	4	5.0	2.1
5	3	2.6	1.3
6	2	0.3	2.6
Average		0.8	0.7

(2) Higher- VRM specimens:

Flow	Number of specimens	Total % change in intensity	Total change in angle, degree
2	2	7.0	2.2
3	4	14.0	3.8
Average		3.5	1.0

Even in the latter group, the changes are small. Since a VRM component amounting to 1% of the primary remanence and at right angles to it will deflect the total moment by 0.57°, it follows that the average change in VRM components in that group is $(3.5^2 + (1.0/0.57^2)^{\frac{1}{2}}$ = 4% of the primary RM. In the low-VRM group, the VRM is of similar order as instrumental error; see Section 2.3. In section 4.6.1 it will be seen that in group 2 are probably those samples which have a low Curie point and contain unexsolved titanomagnetites. This would correspond to the results from Disko. Of the four specimens from flow 4 included above, three have a low J_{400}/J_o ratio (Table 4.3, footnote b), but their viscous properties are not above average for that group.

On AF demagnetization, it appears (Table 4.1) that all VRM components in Cape Dyer rocks have been eliminated at 25-50 Oe peak field, compared to 100-150 Oe in Disko lava samples.

4.5.3 Stepwise thermal demagnetization. In a further stability test, 12 fresh specimens were thermally demagnetized in air in steps up to 630°C. Fig. 4-6 and Table 4.4 show typical results. The remanence intensity of all specimens fell to low values. Curve 5 (Fig. 4-5) is representative of the specimens both from flow 5 and flow 4 and has a characteristic single-component shape. The remanence is blocked mostly between 500° and 600°C. A high-temperature component also dominates the curves from flows 1 and 6.

In the specimens from flow 2 (curve 2) and flow 3 (Fig. 4-6), a significant fraction of the NRM is blocked at relatively low temperatures; this is borne out in the high-field thermomagnetic curves for these flows (Figs. 4-7, 4-8, 4-9) which we discuss later. The NRM intensity of the two anomalous specimens, plotted on the negative J-axis, decreases monotonically to zero with increasing temperature. Near 300° to 360°C., J becomes positive, corresponding to an apparently abrupt change of close to 180° in direction (not shown), from steep negative to steep positive inclination. The positive remanence thus isolated was weak and fluctuated in direction during measurement.

The remanence directions of the specimens with normal NRM, including those from flows 2 and 3, rarely changed by more than a few degrees during demagnetization, except for random changes after the final step. These findings confirm the result of the AF treatment,

showing that the main part of the remanence in the normal Cape Dyer samples is very stable. It is possible that although chemical changes occur in the specimens during heating, the new material retains the magnetic direction of the original material. This has been demonstrated by Wilson and Smith (1968) and would explain why significant fractions of the NRM remain in both the 3^+ samples and in other stable Cape Dyer samples beyond their strong-field Curie points (Tables 4.4, 4.8).

4.5.4 Artificial TRM. It is often of interest to know the strength of the paleomagnetic field H_p at the time of eruption of volcanic rocks. One method of obtaining H_p is to measure the NRM intensity of a rock, cool it in a known applied field from above its Curie point and measure the TRM acquired. There are several drawbacks, however: first, the rock may contain a large secondary component of magentization (VRM or CRM); secondly, changes may take place in the rock on heating; thirdly, the primary remanence may have decayed in time.

In order to be certain of the suitability of rock for paleointensity work, involved procedures are often needed. However, Ade-Hall *et al.*, (1968b) have found that for basaltic rock having a reversible thermomagnetic curve, chances are good that it is suitable for this analysis. Carmichael (1970) derived paleofield intensities from basalts on the further assumption that the change in saturation remanence on laboratory heating reflects essentially the creation or destruction of magnetic material.

In a simple test for the paleofield intensity H_p at Cape Dyer, 8 samples from flows 1, 4, 5 and 6 were cooled from 580°C in an applied field of 0.42 ± 0.01 Oe. All samples had been previously demagnetized to at least 400 Oe, to eliminate some of the remanence that was seen to persist in the samples used for thermal demagnetization. Samples from flows 2 and 3 were excluded from this study because of the presence of secondary components and because major changes took place on heating (Sections 4.5.2 and 4.6.1). The results in Table 4.7 indicate that at least for flows 1, 4 and 6 the value of H_p was about 0.4 Oe, but probably it was higher in the case of flow 5. Applying a correction derived from inferred changes in magnetite content, improves the internal consistency of the results in flows 1 and 4. This correction (Table 4.7) is different from that used by Carmichael (1970). The results are consistent with the slopes of the J_o -K curves of flows 1, 4 and 6 in Fig. 4-2 being about equal, while that for flow 5 is steeper.

4.6 Thermomagnetic and Ballistic Magnetometer Measurements.

4.6.1 Thermomagnetic results. To find out more about the magnetic minerals in the Cape Dyer flows, powdered samples from all flows were measured in the thermomagnetic balance (Appendix 2.2). Heating was carried out in air, in applied field of about 1000 Oe. Some typical curves are shown in Figs. 4-7, 4-8 and 4-9, and further Curie point data are given in Table 4.8.

Flows 1, 4, 5 and 6, which were seen to be more stable than

the others on storage test (Section 4.5.2) and thermal demagnetization (Fig. 4-6) were found to have single Curie points in the range 540°-580°C. Since the titanomagnetite grains in polished sections from these flows are also found to be exsolved (Appendix 4.2) it appears that the exsolution has left regions of nearly pure magnetite in these grains. Samples 4-4 and 4-6 were found to have a Curie point of < 580°C, and some drop in magnetic moment took place during heating. This behaviour is typical for highly oxidized magnetite (Sections 1.3.1, 3.10) and is consistent with the reddened appearance of the hand samples. However, reddish color does not always indicate an abnormally high T_c, e.g., in DY 5-1.

Thermomagnetic curves from the less stable flows 2 and 3 differed from the others in two major aspects. First, they all had Curie points in the range 230° - 320°C., corresponding to that of homogeneous titanomagnetite with x = 0.5 - 0.38 (Fig. 1-2b). Of the 9 samples measured (Table 4.8), more than 80% of the room-temperature magnetic moment resides in this component in seven samples; it is less in 2-6 (70%) and in 3-6 (40%). Secondly, on heating beyond this temperature, both Curie point and magnetic moment at room temperature increased steadily and irreversibly. This behavior has been noted by many workers, especially in oceanic basalts, and is due to exsolution of the titanomagnetite taking place. It has already been discussed in the case of Disko class R' rocks (Section 3.11.4) and the behavior noted here is similar: in both cases the original material wholly transforms into a material with high Curie point (Wilson and Smith 1968) until it reaches T_c = 500°-560°on heating to 560°-600°C.

There is, however, one interesting difference between the Disko class R' basalts and Icelandic low-Curie point basalts (Table 5.8) on one hand, and the Cape Dyer samples on the other. In the former, room-temperature magnetic moments do not increase by more than a factor of 2-2.5 on heating to about 600°C. In the Cape Dyer flow 3, this parameter may increase by a factor of 3-6. An increase of room-temperature saturation magnetization by a factor of ten has been found by Ozima *et al.*, (1968) in an oceanic basalt, and Ozima and Larson (1970, Fig. 10) demonstrate that such large increases are probably due to the presence of titanomagnetites with Curie point near room temperature.

It is not clear how the presence of these very low Curie points might affect the remanence of the flow 3 samples. In any event, in the case of flow 3, one would expect magnetite formed in its very fine-grained opaques by heating, to be very stable to AF demagnetization. This is borne out experimentally (Table 4.1a) for a 3^- specimen cooled from 600°C in an applied field. The magnitude of the field was not measured, but a duplicate specimen from the same sample cooled in 0.50 Oe field had a J_{th} of $18.2 \cdot 10^{-3}$ Gauss and its K_t was $1.1 \cdot 10^{-3}$ Gauss/Oe.

It is concluded that in all normally polarized Cape Dyer samples the remanence resides essentially in a single titanomagnetite component rather than two or more superposed ones. In different samples the Curie point of this remanence occurs in one of two widely different ranges, 230°-330°C and 540°-580°C., the higher range being associated with the more advanced oxidation state and higher stability.

Material in the lower range of T_c must contain a significant low-coercivity fraction available for buildup of VRM to explain the remanence changes observed in samples from flows 2 and 3 after storage. Apart from this VRM, the natural remanence even of the low-T_c samples is fairly stable and thermal demagnetization presumably further stabilizes it, along with the rise in T_c. The mean directions in Fig. 4-3 based on samples in both Curie point ranges, are broadly similar. These results are compatible with a primary origin for both the low-Curie point and high-Curie point remanence.

4.6.2 Ballistic magnetometer results. Table 4.9 gives ballistic magnetometer results for Cape Dyer. These show that the amount of pure magnetite in the samples is always less than 1%, in contrast to Disko rocks. The plot of magnetite percentage against susceptibility is similar to that in Disko rocks (Fig. 4-10a), with an average reciprocal slope of $2.1 \cdot 10^{-3}$ G/Oe per percent magnetite. The value of this parameter seems to be above average in samples 4-6 and 5-6, which are possibly more oxidized than others, and they also have relatively high values of H' (Table 4.9).

In order to estimate the titanomagnetite compositional parameter x in the Cape Dyer basalts, the average opaque content in three polished sections from flows 1, 4 and 5 (Appendix 4.2) was compared with the average magnetite content in specimens from the same samples. The values of these averages are respectively 0.8 and 0.34 Hence $x \doteqdot 1 - (0.34/0.8) = 0.6$, which is similar to the mean value obtained for the Disko basalts.

Of the two low-Curie-point specimens measured, the one from DY 3-6 gave a low value of H', as may be expected for unexsolved titanomagnetite. The value of H' in Dy 3-2 and its change on heating are more difficult to interpret, but they may be due to errors in measurement, since this specimen had a very weak moment before heating.

4.7 Anomalous polarity

What is the origin of the reverse NRM polarity in some samples from flow 3? As the directions of the normal and reverse sets of samples (Table 4.2) are nearly opposed and coexist in the same flow, they cannot both represent primary field directions. If one assumes from the previous discussion that the normal samples reflect a primary field of normal polarity, then the reverse polarities remain to be explained.

One possibility is that part of the flow became self-reversed in opposition to a normal geomagnetic field. Naturally occurring self-reversal in titanomagnetites has not been reported but would be difficult to verify if some irreproducible process (Verhoogen 1962) had been responsible. In Verhoogen's order-disorder mechanism, self-reversal could theoretically occur in quenched basalt if ordering of cations in the spinel were to result in a predominant tetrahedral (A-) sublattice magnetic moment Schult (1965) finds this model difficult to invoke, because of the requirement of quenching and because in experiments the octahedral (B-) sublattice moment always predominated at atmospheric temperatures. In an alternative mechanism (O'Reilly

and Banerjee 1966), highly oxidized, cation-deficient titanomagnetite produced at high temperatures in the magma would decompose into a magnetite-ilmenite intergrowth, resulting in a predominant A-sublattice moment and self-reversal. It is doubtful that this model would explain our results, as no pronounced exsolution lamellae or other indications of high-grade oxidation were found in the samples from flow 3. Moreover, one would have to explain why self-reversal did not occur also in the petrologically similar, but normally polarized, samples from that flow.

The thermomagnetic curves of the two sets (3^+, 3^-) show a difference that may be a clue to the actual origin of the reverse magnetization: the moment of all 3^+ samples (Fig. 4-9 left) rose distinctly and irreversibly on heating to 100°-150°C., whereas that of the 3^- samples did not rise (Fig. 4-9 right). These results are consistent with the hypothesis that the reverse samples, but not the normal ones, suffered secondary heating *in situ* to perhaps 250° at a time of reverse geomagnetic polarity and, on cooling, became remagnetized in the direction of the reverse field. This would imply that the anomalous samples have two components, both residing in originally the same mineral with $T_c \sim 300°C$: a predominant secondary remanence with reverse polarity, blocked below about 250°C is superposed on a weaker primary component of normal polarity blocked between T_c and 250°C.

The thermal demagnetization results (Fig. 4-6) support this interpretation. Assuming it to be correct one must ask, however, why those parts of flow 3 having normal NRM were not reheated as much as

the reversely polarized parts, if at all. The answer must await a more detailed magnetic study of Cape Dyer lavas in their geological setting. Geometrical relationships between successive flows may be critical, as is suggested by analogy in thermomagnetic curves we have obtained for basalt samples from lava-dyke contacts in Iceland (Section 5.5): these curves sometimes show systematic differences as a function of distance from the contact, and in one case (contact HG) we find the behaviour of Fig. 4-9 (right) near the dyke and that of Fig. 4-9 (left) farther away, as expected from the above interpretation at Cape Dyer.

4.8 Comparison Between Magnetic Properties of Disko and Cape Dyer flows

Although the iron content of the Cape Dyer olivine basalts and the South Disko felsparphyric basalts is fairly similar, averaging about 9 weight percent (Clarke 1970), the composition and the crystallization history of these rock types has caused them to have very different magnetic properties. In simple terms, the early-crystallizing olivine has in the olivine basalts taken up most of the iron as Fe^{II}, leaving only small amounts for crystallizing separately as titanomagnetite at 900°-1000°C. During the cooling of the thus formed mineral, oxygen fugacity has been high, causing extensive oxidation of the titanomagnetite, lamellae development and very high stability of the original remanence. In the anomalous flow 3 and to some extent in flow 2, cooling appears to have been unusually rapid, causing the observed fine-grained skeletal texture of unexsolved

low-Curie-point titanomagnetites. Such rapid cooling may indicate contact with water during eruption, though field data to test this possibility are lacking.

In the felspar-phyric flows, magmatic oxygen fugacity has been much higher than in the olivine basalt flows, causing the iron to precipitate early and partly as Fe^{III} in euhedral crystals of titanomagnetite at 1000°-1300°C. During subsequent cooling of the titanomagnetite, however, oxygen fugacity has been insufficient (especially in the central parts of the flows) to cause a complete exsolution in the titanomagnetites. The controlling influence of the oxidation conditions in the Disko flows is reflected in the negative correlation between primary remanence and susceptibility (Fig. 3-4). In rapidly cooled extrusives and intrusives, the fugacity was still lower, but differences between these rocks and the low-T_c samples in Cape Dyer, e.g., in remanence stability, may reflect grain size effects.

In both areas, however, the stable remanence component is most probably primary, though the mean field directions happen to be of opposite polarity.

Appendix 4.1 Description of Hand Samples and Thin Sections of Cape Dyer Flows

One thin section was made from each flow, except two from Flow 3. These were examined microscopically by the writer and Mr. J. Cant.

Flow 1: Porous fine-grained flow. Vesicles of up to 1 cm. size occur in most of the samples, all being filled with a whitish zeolite. Some iddingsization has taken place along the borders of olivine grains in sample 1-5.

Flow 2: Dark-green very olivine-rich flow. A few zeolites up to 5 mm. size occur in two hand samples, and much smaller zeolites in other samples. Considerable serpentinization has taken place in the olivine.

Flow 3: Similar to flow 1, except that no zeolites occur. Some serpentinité alteration in the olivine of sample 3-3, but not in sample 3-6. Abundant felspar laths.

Flow 4: Similar to flow 1, zeolites occurring in sample 4-4. It and sample 4-6 are reddish, possibly from the top of a flow. Some serpentinization of olivine, but no alteration in the felspars.

Flow 5: Pale gray rock, with a few empty vesicles. Zeolites occur in sample 5-1 which is deep red and probably from a flow margin.

Flow 6: Very vesicular flow; size of vesicles of order 3 mm. Abundant felspar needles seen in the samples with the naked eye, and in thin section. Thin zeolite crust in vesicles, which is unlikely to be secondary because of the altitude of the outcrop. Minor iddingsite in the olivine of sample 6-5.

Appendix 4.2 Description of Polished Sections from Cape Dyer (400x and 1000x)

DY 1-5 Average opaque grain size about 20μ. Gray fine-scale exsolution seen in most grains at 1000x. Reddening of silicates, mostly around the opaques. Oxidation class 4-5. Discrete ilmenite about 10%. Counted 10000 squares, giving 0.7% opaques.

DY 2-6 Most common opaque grain size is about 8-10μ, but both grains of up to 300μ and less than 5μ size occur. The latter are seen to be skeletal at 1000x. Minor exsolution; oxidation class 1-2. Counted 10000 squares, indicating 0.7% opaques. Testing with colloidal magnetite showed that many of the larger grains are non-magnetic, possibly chromite.

DY 3-1 Tiny grains, usually 5μ or less, in strings or in skeletal arrangement. Often in dark areas in the section. Rare grains of 10-20μ size. No exsolution; oxidation class 1(?). Impossible to estimate opaque content because of the small grain size.

DY 3-3 Very similar to DY 3-1; grain size even smaller.

DY 4-1 Similar to DY 2-6. Average opaque grain size 15μ. Ilmenite exsolution seen at 1000x. Alteration has taken place along cracks in the opaques. Oxidation class 2. Discrete ilmenite and a non-magnetic gray spinel, possibly chromite, makeup more than a half of the opaques. Counted 10000 squares, giving 0.8% opaques.

DY 5-3 Average grain size about 15μ. Exsolution common, much reddening of silicates; oxidation class 5. Minor discrete ilmenite. Counted 10000 squares, giving 1% opaques. Very porous rock.

DY 6-5 Average grain size about 40μ. Ilmenite exsolution common in the larger grains, both as lamellae and equidimensional areas. Strings of very small reflecting grains seen, but their structure could not be discerned. Oxidation class 3. Discrete ilmenite 5%. No estimate of the opaque content could be obtained because of the variable grain size and the presence of many vesicles.

CHAPTER 5 ROCK MAGNETISM AND MAGNETIC ANOMALIES IN BAFFIN BAY AND THE NORTH ATLANTIC

5.1 Introduction

As mentioned in Section 1.1, magnetic surveys over oceanic and coastal areas have in recent years yielded much information on the history of the oceans and continents.

It was postulated by Vine and Matthews (1963) that basalt emplaced at ocean ridge crests was continually being transported outwards by motions in the underlying mantle. The basalt emplaced during a particular geomagnetic epoch would acquire a remanence in the direction of the ambient field, and carry this remanence with it outwards. The polarity changes of the dipole field would thus create a series of strip-like portions of the ocean floor, symmetrical about the ridges and alternatively normally and reversely magnetized.

This prediction appears now to have been verified by magnetic surveys and ocean floor drilling in all oceans, and their ages are being mapped in detail. The paths of rotation pivots for the relative displacements of continental areas since the beginning of the present phase of continental drift are being traced out (Pitman and Talwani 1972). According to the most recent data (Pitman 1972), the South Atlantic Ocean began to open about 130 m.y. ago, and the North Atlantic about 80 m.y. ago.

The amplitude of oceanic magnetic anomalies is commonly of the order of 300-500γ in high latitudes. The anomaly following the mid-ocean rift valleys is generally positive and of twice this amplitude.

It is of considerable importance to the understanding of sea-floor spreading to know the nature of the causative bodies of these anomalies. In the earlier literature dealing with this subject, these bodies were loosely referred to as "dykes", and some workers attempted to infer various properties of these dykes from magnetic anomaly studies (e.g. Harrison 1968). They were generally assumed to reach down to a Curie point isotherm at 6-10 km below the ocean bottom.

Later work on dredged and drilled ocean-floor rock, particularly pillow basalt, have shown it to be very highly magnetic (Irving 1970; Carmichael 1970); NRM values are highest in the central rift valley of the ocean ridges, where they may exceed $50 \cdot 10^{-3}$ Gauss. Similar results have been obtained from a detailed analysis of magnetic survey profiles by Talwani *et al.*, (1971), implying that the thickness of the ocean-floor magnetic layer is of the order of 400 m. It is possible that the relatively high remanence intensity of the central rift valley basalts is partly due to a large geomagnetic dipole moment in the present geomagnetic epoch (Ade-Hall *et al.*, 1972) or to a progressive decay of remanence with time in the older oceanic basalt.

Preliminary results from Iceland (Kristjansson 1970) indicate that the remanence intensity of dykes is not much higher than that of local lava flows. Instead, rapidly cooled crystalline Pleistocene subglacial pillow lava and breccia are the most highly magnetic formations in the country, in agreement with the ocean floor findings.

Further to the studies described in Chapters 3 and 4 it was therefore decided to include here a study of various igneous rock types from Iceland. Their remanence intensity and susceptibility are the

main properties studied. The main objective is to throw some light on the causes of magnetic anomalies in oceanic and coastal areas, including Iceland and other parts of the Mid-Atlantic Ridge. Because many of the rock types studied from Iceland are likely to be present in Baffin Bay, though presently inaccessible, the results on these rocks may also be applied to Baffin Bay magnetic anomalies. Further, these results, some of which have been quoted in the previous chapters, may help in understanding the processes by which the exposed Baffin Bay rocks acquired their magnetization.

The geology and paleomagnetism of Iceland has been reviewed in the volume edited by Björnsson (1967). The island is mostly made up of basalt lava flows ranging in age from Miocene (20 m.y.) to Recent. They are mostly either flat-lying or dipping gently towards the central active volcanic zone.

At least 65 magnetic reversals have occurred during the emplacement of the presently exposed Tertiary lavas east of the central zone. The central or Neo-volcanic zone is largely Pleistocene to Recent volcanics, erupted subglacially and therefore much less regular or uniform than the Tertiary lavas. Intrusive bodies are common in all parts of the country. Most important of these are the so-called central volcano complexes, where large intrusions of both acid rocks and plutonic basic rocks occur. Magnetic anomalies are common over the central volcanoes, and also gravity and seismic velocity anomalies. The substructure of Iceland has been inferred from many types of evidence including seismic, gravity, magnetic, geological, geochemical and magnetotelluric. The results have still to be merged into a coherent

picture, but it is generally agreed that the basalt lava pile reaches to at least 2 km depth in most of the country. The nature and age of underlying material is unknown.

5.2 Magnetic Surveys in the Baffin Bay Tertiary Coastal Areas and Their Interpretation

Several magnetic surveys have been carried out in Baffin Bay and nearby regions (Hood *et al.*, 1967; Johnson *et al.*, 1969; Mayhew *et al.*, 1970; Haines *et al.*, 1970; Vogt, 1970; Geological Survey of Canada 1970; Part *et al.*, 1971; Laughton 1971; Hood and Bower 1971; Ross and Manchester 1972; Grant 1972). Attempts at interpreting anomalies found in these surveys have suffered from a lack about the nature and magnetic properties of the causative bodies, since they are often submarine, subglacial or otherwise unexplored. Examples of how much knowledge may provide constraints on the interpretation of magnetic surveys in the Baffin Bay area are discussed below. The presently available rock magnetic results from the area are somewhat fragmentary (see legend to Fig. 5-1) but they may serve as guidelines for future work on establishing the origin of the magnetic anomalies.

5.2.1 South Disko area.

As stated before, all samples collected in Disko Island by the writer possess a stable reverse remanence of presumed primary origin, and one may therefore expect a broad negative aeromagnetic anomaly to occur over Disko. Such appears to be the case in the results of Hood and Bower (1971), but in the magnetic maps of Haines *et al.*, (1970) a small positive anomaly in total field F occurs over the south coast. This anomaly may perhaps

be explained by the following results from profiles GL and GM (Chapter 3):

The NRM of one sample from each flow (total 37) was measured as soon as they arrived at Memorial University. They were then stored for a period of 4-6 weeks, remeasured and AF-demagnetized in steps of 50 Oe (Sect. 3.5). It was found that in all samples the remanence shifted towards the reverse sense on storage, and still further, up to a maximum value (Fig. 3-6) on AF treatment. The maximum usually occurred between 50 and 150 Oe. These results clearly indicate that on the primary remanence there was superimposed a very soft viscous remanence (VRM) due to the present geomagnetic field in Disko, and that this VRM was decaying during storage, and being replaced with one of the opposite polarity since the samples were stored upside down. By extrapolating the observed change in VRM back to the date of collecting (assuming simple exponential decay, though the changes involved are mostly small and the choice of method of extapolation makes little difference), we were able to estimate the average *in-situ* VRM and hence the *in-situ* NRM. It was assumed that the maximum J_{max} in each AF demagnetization curve (as in Fig. 3-6) represents the *in-situ* primary remanence J_p, i.e., that the intensity of this remanence is unaffected by AF treatment to 50-150 Oe. This assumption may cause small systematic errors, by underestimating both J_p and the viscous remanence, but the errors cancel in the NRM.

Volume susceptibility K of all samples was also measured. These measurements were used in Section 3.11.8 and Fig. 3-21 for estimating the average magnitudes of primary, secondary and induced

magnetization components in each class of magnetic behaviour. By grouping these values according to collection profiles, Table 5.1 then yields an estimate of the total *in-situ* intensity of magnetization J_t for each profile. Because the paleo- and present field directions are not far from the vertical, we have added all magnetization values as scalar quantities, with due regard to sign, but for improved accuracy in application to local magnetic surveys they may be multiplied by correction factors as indicated by Kristjansson (1970).

Table 5.1 shows that the flows of profiles GL and GM, although reversely magnetized to begin with, would cause a small positive anomaly in the local total-field geomagnetic intensity, as found by Haines *et al.*, (1970), if surrounded by effectively non-magnetic material. If surrounded by similar basalts of a normal primary magnetization, the net magnetization contrast would be twice the value of J_p in Table 5.1, i.e., about $6 \cdot 10^{-3}$ Gauss.

Because the primary remanence in the other basalt formations sampled in South Disko, especially those that appear to have cooled rapidly, was often very soft to AF treatment (cf. the large decreases of intensity in samples GR 2-1 and GK 9-1 of Figs. 3-6 and 3-7, though the remanence direction was stable), their *in-situ* VRM could not be estimated by extrapolation as above. From repeat measurements after storage, however, it appears that this VRM is small (Table 5.2). As the mean primary remanence intensity in these formations is much higher than that in profiles GL and GM, they could by themselves cause considerable negative anomalies.

The Tertiary areas in Greenland are partly made up of olivine-poor

basalts as decribed above and partly of olivine lavas as those in Cape Dyer (Chapter 4), both of which may locally overlie a variable thickness of breccia. The breccia in turn being partly made up of randomly magnetized material, it may prove very difficult to correlate local geology with details in the magnetic anomalies.

Two other results from South Disko may have some relevance here: First, we have measured the susceptibilities of three samples from the Cretacious-Tertiary sediments underlying the lavas of profile GK (Fig. 4-2) and found them to be essentially non-magnetic ($K \sim 0.01 \cdot 10^{-3}$ Gauss/Oe). Secondly, it is known that iron inclusions occur in the Disko basalts (Melson and Switzer 1966; Pauly 1969) and these may be highly magnetic: selected and cut pieces ($\sim$ 1 cc) from two samples of basalt, kindly sent by Mr. E. Fundal, were found to have remanence intensities of the order of $500 \cdot 10^{-3}$ Gauss. However, the iron inclusions are probably sufficiently rare so as not to contribute appreciably to local aeromagnetic anomalies.

5.2.2 Cape Dyer area. A map by Clarke (Clarke and Upton 1971) shows about twenty outcrops of Tertiary basalt between Cape Dyer and Cape Searle. Comparison with Geological Survey of Canada (1970) aeromagnetic total-intensity maps (one inch to one mile) show magnetic anomalies at most of the localities in Clarke's map. The anomalies are all positive and range from a few hundred to a few thousand gammas at 300 m flight altitude. Some major anomalies in the area do not correspond to outcrops marked by Clarke, but on inspection of air photos kindly lent by Dr. Clarke, the writer found

good evidence of basalt exposures at most of these. Some outcrops mapped by Clarke, do not produce noticeable anomalies, but these appear to be exposures of a few lavas only (e.g., the lone flow 6 at Cape Dyer). Some anomalies, of up to several hundred gammas amplitude, do not correspond to basalt outcrops, and will be discussed in Section 5.4.

5.3 Other Baffin Bay Coastal and Oceanic Magnetic Anomalies

Magnetic data on Precambrian rocks collected by Memorial University on the Baffin Bay coast are shown in Tables 5.3 - 5.6. In Fig. 5-1, which summarizes data available to the writer on the magnetism of Baffin Bay and nearby coastal rocks, each dot represents a site or sample average of NRM intensity, plotted without regard to sign, or of susceptibility. The lengths of the arrows indicate the magnitude of the present geomagnetic field, i.e. the distance that the susceptibility values should be moved along the axis to become values of induced magnetization in Gauss.

It may be assumed that the Baffin Bay coast Precambrian basement consists predominantly of metamorphic rock types (Allaart *et al.*, 1969) magnetic results for which are shown in the bottom lines of Fig. 5-1b. It may also be assumed, as has been demonstrated by Puranen *et al.*, (1968, Fig. 9), that the r.m.s. amplitude of magnetic anomalies observed over a region is directly related to the standard deviation of total-magnetization values in the underlying rocks. On comparing the gneiss values in Fig. 5-1b with the values for Tertiary basalts shown in Fig. 5-1, it is seen that magnetization contrasts occurring within

the basement are probably much smaller than within the basalts, and hence the former will, under similar conditions, produce smaller anomalies. This has been used by Park *et al.*, (1971) to map the extent of Tertiary volcanics off West Greenland. It must also be noted, however, that both in the metamorphic rock types and especially in the less common basic Precambrian rocks (Fig. 5-1b), magnetization values comparable to those in Tertiary basalts do occur. The average susceptibility of the gneiss samples in the figure is about 1.10^{-3} G/Oe.

In anomaly interpretation over the presumed submarine basalts underlying the central parts of Baffin Bay and Labrador Sea, it is important to know their average remanence, but this cannot be inferred directly from subaerial basalt results. It is known that rapid cooling, such as would take place in extrusive submarine basalts, generally tends to produce higher remanence intensities than are common in subaerial basalts. Some of the samples collected in Disko show evidence of rapid cooling (pillow and block-jointing structures; small skeletal homogeneous titanomagnetite grains in a glassy groundmass) and these tend to have remanence intensities a few times higher than the subaerial basalts of profiles GL and GM. Similar results have been obtained from the subglacial volcanics in Iceland (Kristjansson 1970). On the other hand, the magnetic effects of magmatic oxygen fugacity and of secondary alteration mechanisms in suboceanic basalts are not well known.

An empirical approach to the problem of estimating the average magnetization of submarine Baffin Bay basalts may, however, proceed as follows. First, it may be found from Tables 3.2, 4.3 and the other data making up Fig. 5-1a that the arithmetic mean remanent intensity

(without regard to sign) in South Disko, Ubekendt Island and Cape Dyer Tertiary basalts is everywhere of the order of $(3\text{-}5)\cdot10^{-3}$ Gauss. Secondly, the average NRM intensities of Teriary subaerial basalts in East Greenland (Tarling 1967) and in Iceland (Kristjansson 1970) are also of similar order. Thirdly, Irving (1970) has shown that the mean remanence of basalts dredged from the Mid-Atlantic away from the axial rift zone is of the order $(5\text{-}8)\cdot10^{-3}$ Gauss. Since the exposed Baffin Bay and North Atlantic subaerial rocks are so similar, one might, by analogy, expect the submarine Baffin Bay basalts to have an average remanence not very different from that of Mid-Atlantic rocks, i.e., $(5\text{-}8)\cdot10^{-3}$ Gauss, or slightly lower because of more advanced alteration.

Irving (1970) has proposed that the magnetic "smooth zones" bordering the North Atlantic are due to the presence of underlying diabase intrusives and subaerial basalts, emplaced in the initial (Mesozoic) stages of continental drift. The average remanence of these, according to Irving's estimates, would be of the order of $0.6\cdot10^{-3}$ Gauss. As this is much less than the average NRM intensity of the Tertiary rocks just mentioned, we conclude that any basic rocks underlying the smooth zone would resemble the Mesozoic volcanics tabulated by Irving, and not these Tertiary rocks.

Because of the high ($(2\text{-}5)\cdot10^{-3}$G/Oe) susceptibilities occurring in some of the Tertiary rocks, and the relative constancy of K up to 500°C typical in basalts (Pätzold 1972), considerable susceptibility contrasts, and therefore considerable (< 200γ) magnetic anomalies, would be expected over such Tertiary basalts near the ocean bottom. Therefore the above conclusion would hold even if the

smooth zones represented a long interval of low or constant geomagnetic dipole moment, and even if the smooth zones basement were buried under 1-2 km thickness of sediment (see also Fig. 5-2 and Section 5-8).

The various theories for the production of the smooth zones have been reviewed by Pitman and Talwani (1972).

5.4 The magnetization of gneiss

In Pre-Cambrian rocks, especially metamorphic rocks, one might expect to find magnetite which has been annealed with time, and should be pure and free of crystal defects. If the final metamorphism took place at low temperatures, one would also expect the magnetite to be free from titanium (Nagata 1961). Measurements on magnetite content and susceptibility have been carried out by various authors, including the following:

Reference	rock type	susceptibility measurement	magnetite estimate
Mooney and Bleifuss (1953)	Minnesota iron formation and volcanic rocks	*in-situ* and laboratory a-c bridge	chemical
Pomonarev and Glukhikh (1963)	Soviet ores	laboratory a-c bridge	chemical
Gaucher (1965)	Quebec magnetite serpentinite	laboratory	density (inaccurate)
Puranen *et al.*, (1968)	Finnish gabbroic and acid rocks	laboratory a-c bridge	saturation magnetization
Ghisler and Sharma (1969)	Fiskenaesset anorthosite and metam.	laboratory fluxgates	thin-section point counting

Authors of the first two and fourth references found a linear relation of susceptibility vs. magnetite volume content, P, for P<5%, being in all cases about $3.0 \cdot 10^{-3}$ G/Oe per % magnetite (compare section 2.6.2). In order to gain more knowledge of causes of local magnetic anomalies, it was decided to test this relation for some samples of Baffin Bay gneiss collected by Memorial University expeditions. Polished sections were made from 11 samples, and areal percentages of magnetite in parts of each section were measured, using a 20 x 20 square-grid eyepiece at 80x and 160x magnification. One section (metavolcanics from West Greenland) had too fine-grained magnetite for counting, but magnetite grain sizes were of the order of 100μ in the other samples. These results are shown in Table 5.4 and Fig. 5-3, along with results from the most magnetite-rich samples of Ghisler and Sharma (1969).

In Fig. 5.3, a straight line through the origin, fitted with least squares, gave a mean reciprocal slope of $2.8 \cdot 10^{-3}$ Gauss/Oe per percent. The possible error in this value, due both to random and systematic errors in the estimate of P, may be of the order of $\pm 0.5 \cdot 10^{-3}$, and there may be random and systematic errors in the susceptibility measurements (Sect. 2.6) giving a further error of $0.2 \cdot 10^{-3}$ G/Oe per percent of magnetite.

The error sources present in such observations of magnetite content include the following:

- foliation of minerals in the rock, seem to occur on a scale of millimeters in some of the samples measured.
- coarse grain size of the silicates, and inhomogeneities (on a scale of centimeters) in the rock.

- the occurrence of pores and holes, especially those in and around opaque grains (as in plate 8b).
- possible occurrences of ilmenite or other minerals misidentified as magnetite, or the occurrence of magnetite in grains too small to be identified at the ambient magnification.
- an inadequately small number of squares being counted, because of the low percentage of magnetite in the sections; 6000 squares at a magnification of 80x only cover an area of 0.2 cm^2.

In order to provide a check on the optical measurements, six saturation magnetization measurements were done, with the ballistic magnetometer (Table 5.5). Since Table 5.6 and Fig. 5.4 show that the magnetic properties of the gneiss reside almost exclusively in pure magnetite, the calculations of magnetite percentage do not have to be corrected for low Curie point components.

Fig. 5.5 shows that in addition to one almost non-magnetic sample, four are on a line through the origin with a reciprocal slope of just over $2.0 \cdot 10^{-3}$ G./Oe. The fifth, which is a very coarse-grained and foliated rock from Frobisher Bay, yields a ratio of 2.7 in the same units. Estimated errors in these slopes, due to systematic errors in magnetite determination, may be of the order of $0.2 \cdot 10^{-3}$ G/Oe per percent.

In summary: classical theoretical considerations (Sect. 2.6.2) and the laboratory tests of Parry (1965) indicate that a susceptibility value of about $2.0 \cdot 10^{-3}$ G/Oe should be obtained for each volume percent of pure magnetite, largely independently of magnetite grain size above 1.5μ diameter. The work of various earlier authors on natural Precambrian

samples yields a value of about 3.0; the present author's and Ghisler and Sharma's microscope work yields 2.8 for Precambrian rocks; and our ballistic magnetometer measurements on these and Tertiary basalts (Fig. 5.5b or Fig. 3.16) yield 2.2, in the same units. The differences in these results probably reflect the many errors which can enter into the measurements (as reviewed above).

The remanence of Baffin Bay gneiss samples is rather weak (Table 5.3, Fig. 5.1B), the Koenigsberger ratio Q_n being between 0.08 and 1 in most of those measured. In all the twenty oriented samples, the remanence was found to be of normal polarity, and was therefore probably mostly acquired in the earth's field during the current geomagnetic epoch (cf. Sections 3.4 and 3.12.2).

However, this remanence is not always unstable, as in some samples the median destructive alternating field exceeded 200 Oe (Fig. 5.5a). The Q-value of the TRM acquired on cooling from 600°C. in an applied field is also much higher than Q_n; in specimens from Greenland gneiss thus treated, Q_t was between 1 and 1.4; in one Frobisher Bay specimen, Q_t was 2.8; and in one Labrador specimen, Q_t was 6.5. Therefore, the magnetite in Precambrian gneiss is obviously not entirely multi-domain magnetite (see legend to Fig. 3.14a), and in the immediate neighbourhood of Tertiary intrusives, values of Q_n exceeding 1 may be expected to occur in the gneiss due to partial thermal remanence acquired on cooling.

In ballistic magnetometer experiments, it was anticipated that the characteristic field H' for gneiss would be much less than that for basalts containing exsolved titanomagnetites, because of the

smaller effective grain size and greater shape anisotrophy of the latter. However, in four of the six gneiss samples measured (Table 5.5), H' was between 900 and 1400 Oe, in one sample it was about 1800 Oe, and one sample was non-magnetic.

These results show that grain size and shape effects on certain magnetic properties of rocks (K, Q_t, hysteresis), are not always as important as one might expect from arguments presented in texts on the subject. It would appear more likely from the above results, including those from Disko and Cape Dyer, that in pure magnetite and exsolved titanomagnetite grains, grain size has a minor ($\lesssim$ 20%, see Fig. 3.1b) effect on K and H' for grain or lamellae sizes 1 cm. - 1μ, and that Q_t only varies by a factor of 20 or so in this size range (data of this section and Fig. 5.13). This may be partly due to lamellar interactions, opposing the magnetic effects of reduced grain size.

It is concluded that magnetic anomalies over gneiss in the Baffin Bay area are due to induced magnetizations in local magnetite concentrations, of the order of a few percent by volume. Thus a concentration of 2% magnetite in a gneiss formation would cause it to have an induced *in-situ* magnetization of about $3 \cdot 10^{-3}$ Gauss, which is similar to the remanence in many local Tertiary basalts. This result may explain the occurrence of many of the magnetic anomalies seen over the Precambrian regions in the published survey results and which, over land, often reach hundreds of gammas in amplitude. It also emphasizes the need for independent control, e.g., for seismic or gravity data, on interpretation of magnetic anomalies in regions of unexposed basement in the Baffin Bay area.

5.5 Magnetic effects of dyke intrusions on country rock.

In the interpretation of magnetic anomalies in Mesozoic and Cenozoic basalt areas, such as in the mid-ocean ridge areas, it is very important to know the magnetic effects of secondary heating of the country rock. The heat conducted away from cooling dykes (both purely intrusive dykes and lava feeders) on the surrounding rock is generally thought to be a major contributing cause of such secondary heating. The remanence of the dykes themselves, and the PTRM of the baked country rock, are thought to be significant contributors to the magnetic anomalies (Harrison 1968).

Serson *et al.*, (1968) have used secondary heating by dykes in a model of the geological structure of Iceland, in order to explain the fact that magnetic anomalies over Iceland do not possess the symmetry and linearity of mid-ocean ridge anomalies. They conclude that these features could be explained if the dykes constituted one-fifth by volume of the local crust, and if the intrusion had heated all the country rock by 100°C. through the main blocking temperature interval, 400-500°C. (Fig. 5.2), with subsequent cooling.

However, since the temperature gradient in Iceland is generally about 60° - 100°C. per km (Palmason 1970), a temperature of 400°C. is not reached until 4-7 km. depth below sea level. At higher levels, the concentration of dykes is also less than in Serson *et al.*'s model; according to Walker's (1959) East Iceland data, the proportion of dykes in the local crust is about 6% at sea level in the vicinity of the central volcanoes and 2% elsewhere, increasing by 4 percentage points

per km. depth. Hence, the major part of aeromagnetic anomalies in Iceland and similar areas will be caused by rock not fitting the model of Serson *et al.* (1968). These authors also did not take into account the chemical alteration which may have occurred in the rock below the 400°C. isotherm.

In an attempt to obtain more definite boundary conditions on this problem, oriented samples from seven lava-dyke contacts in Iceland were studied, and data on two others were kindly supplied by Dr. N. D. Watkins of Florida State University. Two to six samples were collected from each dyke, and three to eight samples from each flow, at increasing horizontal distances (0.2 - 10 meters) from the contact.

List of dyke-lava contacts

Contact	Locality	Altitude m	Thickness where sampled m
AG	Bolungavik	140	4.5
HG	Skutulsfjördur	2	9.5
MG	Skutulsfjördur	80	5.3
SG	Alftafjördur	20	3.0
JG	Hvalfjördur	50	1.6
RG	Hvalfjördur	150	2.8
KG	Kjos	30	2.5

The first four localities are in NW-Iceland (area B of Fig. 5.9), the others in SW-Iceland. The average thickness of the dykes

is similar to the East Iceland average of 4m (Walker 1959).

The susceptibility and natural remanence of all samples was measured, and several were AF or thermally demagnetized (to 200 Oe or 200°C). Strongfield curves were obtained for at least three samples from each lava flow, generally two of these being near ($\lesssim$ 1m) to the dyke and one or more being farther away.

Thermal conduction computations by Jaeger (1957), and Mundry (1968) indicate, that with reasonable values of the thermal properties of the dyke and lava, and an ambient lava temperature of 50°-100°C before the intrusion, the maximum temperature reached at distance of one-fifth of the dyke width from the contact is about 500°C. However, these workers only carried out calculations for the case of an instantaneous emplacement of the dyke, with a subsequent solidification of the dyke as a whole. It is easily seen that a sustained eruption of lava through the dyke will considerably increase the maximum temperatures reached at all distances from it, but on the other hand, gradual solidification of the dyke inwards from the contact after eruption will reduce these temperatures, compared to the case of the instantaneously solidifying dyke. The presence of ground water at the time of eruption will also reduce the temperatures outside the contact.

It may be assumed that secondary heating to over 500°C for a period of days or weeks will generally have a significant effect on the magnetic properties of a lava, such as the intensity and stability of NRM (Fig. 3.8), the susceptibility (Fig. 3.15) and the shape of the strong-field thermomagnetic curve (Fig. 3.18).

Results from measurements carried out partly at Memorial

University and partly at the University of Iceland, are shown schematically in Fig. 5.6 for five of the dyke contacts listed above. The remanence was in most cases found to be stable to within 10° in direction; remanence polarities for both the dyke and the lava in each case are shown in Fig. 5.6.

The results indicate a variable extent of the secondary heating zone around the dykes. This may be partly a reflection of the fact that lava-dyke contacts are seldom plane or distinct, and partly because of difficulties in interpreting the results, as even far from some of the dykes, considerable unsystematic lateral variations were seen to occur in the magnetic properties of the lava samples. (These variations were in many ways analagous to the differences between class N and R behavior in the Disko basalts, or to the vertical variations found in the detailed study of a single lava flow by Wilson *et al.* (1968)).

However, the results on the whole support the theoretical inference that major heating ($\leq 500°C$) due to an average dyke at depths of less than one km. from the surface would extend to less than one-fifth, or even as little as one-tenth, of the dyke thickness on either side of the dyke contact. The two dyke contacts JG and KG were not included in Fig. 5.6, because the remanence directions from the JG dyke samples were scattered, and the remanence intensity of the samples from the KG-flow was very low (of the order of $0.3 \cdot 10^{-3}$ Gauss). However, the data from these, as well as those from the two Eastern Iceland contacts supplied by Dr. Watkins (NRM and susceptibility data only) are consistent with the conclusion of the heating effects reaching less

than one-fifth dyke thickness from the dyke contact.

The above results must be looked upon as being preliminary: a further paleomagnetic study should be made of a larger number of contacts, with an interval of 10 cm. between samples near the dyke for the first half-thickness instead of 30-50 cm. as done here. The samples should be collected along a line strictly parallel to the surfaces of the flow, and several extra samples should be collected above or below the line in order to investigate vertical and lateral changes in magnetic properties in the flow prior to intrusion.

No studies of this kind could be made in the South Disko profiles. Only two dykes were seen to occur there, one (GD 1) being exposed in breccia, the other (GD 4) being on a large fault and exposed only on a gravel beach. However, dykes are known to be very numerous in Ubekendt Ejland (Drever 1958) and in Svartenhuk (Pulvertaft and Clarke 1966), and studies of the magnetic effects of dyke heating there could probably yield important information on local paleo-heat flow and eruptive processes as well as on the contribution of these dykes to magnetic anomalies in the area.

5.6 Magnetic anomalies over gabbroic rocks

Tertiary plutonic and hypabyssal rock types are known to occur in Greenland. Examples include gabbro and granophyre in the Ubekendt Ejland complex (Drever 1958), diabase in Svartenhuk (Pulvertaft and Clarke 1967), and at least two large gabbro intrusions in East Greenland. They also occur in minor intrusions in Iceland (see Walker 1966), and samples not thought to be transported by ice have been dredged from

the mid-Atlantic ridge (Irving and Park 1970; De Boer *et al.* 1970). Ultrabasic rocks and anorthosites also occur in some of these localities (Aumento *et al.* 1970) and in the Precambrian of Greenland and Baffin Bay.

In his aeromagnetic survey of Iceland, Sigurgeirsson (1970) has found large ($\sim$1000 γ) positive and negative anomalies in the vicinity of Tertiary volcanic centers. These anomalies are in some cases associated with gabbro outcrops.

In order to obtain an estimate of the magnetic properties of Tertiary gabbro, 21 unaltered samples were acquired from ten outcrops in Iceland (Fig. 5.9). Their NRM intensities and susceptibilities were measured in Iceland (Fig. 5.7) and yielded arithmetic average values of $(6\text{-}7)\cdot10^{-3}$ Gauss and $6\cdot10^{-3}$ Gauss/Oe respectively (Kristjansson 1970, Kristjansson and Buasson 1970). The latter value is similar to that quoted by Ostenso and Wold (1971) for continental gabbros, but both are a few times higher than average NRM intensity and susceptibility values for Tertiary Icelandic subaerial basalts, and about twice as high as the average J_{max} and K values in the flows of profiles GL and GM in Disko (Table 5.1).

It is therefore very likely that gabbroic rocks cause a significant part of the magnetic anomalies observed over volcanic centers in Iceland and other Tertiary volcanic areas. Only a few samples measured from Iceland were oriented, but in these the sense of magnetization agreed with that of the local magnetic anomalies. VRM in several samples investigated appeared to be small (Kristjansson 1970), as found also in class R samples from Disko.

Further investigations into the magnetic properties of these gabbros were carried out at Memorial University, yielding the following results.

Thermomagnetic curves, obtained for five samples, are nearly reversible (as in Fig. 5.4), each having a single high Curie point (Table 5.7) indicative of nearly pure magnetite being the major magnetic constituent.

Microscope investigations of six gabbro and one diabase polished sections showed grains of titanomagnetite of general size 0.1 - 5 mm., with minor discrete ilmenite. The oxidation index of the titanomagnetites was in all sections about 2-3, and low-temperature oxidation was not seen (Plate 7a).

The stability of NRM direction to AF demagnetization was found to be good (Fig. 5.8). That of intensity was variable but fairly characteristic of titanomagnetites. There was a positive correlation between NRM intensity and susceptibility (Fig. 5.7; correlation coefficient = +0.45); in this respect the gabbros are similar to the Cape Dyer basalts (Fig. 4.2), rather than the Disko basalts, which showed no or a small negative correlation between J_{max} and K (Figs. 3.4b and 3.5). There was also a positive correlation between J_{50}/J_o and J_o during AF demagnetization of specimens from 10 gabbro samples. This may indicate that the remanence intensity, especially the amount of its low-coercivity fraction, is partly controlled by oxidation effects (cf. Wilson *et al.* 1968).

Ballistic magnetometer results (Table 5.10) fit the relation between susceptibility and magnetite content found earlier in high-

Curie-point basalts and metamorphic rocks. In two gabbro samples and one diabase, the parameter H' was found to be about 1000 Oe, as in Disko class R basalts.

The above results indicate strongly that the NRM in Icelandic gabbro is mostly a stable primary remanence residing in deuterically exsolved titanomagnetite grains. This would make the gabbro excellent material for paleomagnetic work. The results also confirm the likelihood of gabbro being capable of causing magnetic anomalies of amplitude about 1000 gamma in the surveys of Sigurgeirsson (1970). The Koenigsberger ratio Q_n of the gabbro being about 2 on the average, positive anomalies will be larger than negative ones over gabbro occurrences. Because of the high density of gabbro (2.9 - 3.1 gm/cc in most of the 21 samples from Iceland), the magnetic anomalies are likely to be associated with positive gravity anomalies.

Out of eight samples of the basic hypabyssal rock types diabase and ankaramite obtained from Iceland, six had NRM intensities of $\leq 1 \cdot 10^{-3}$ Gauss, but two had respectively 3 and $4 \cdot 10^{-3}$ Gauss. A similar situation occurred in the only diabase outcrop sampled in South Disko, the sites GD 2 and GD 2A yielding NRM intensity values of $1.5 \cdot 10^{-3}$ G and $17 \cdot 10^{-3}$ G respectively. The above diabase samples all appear to be magnetically stable, but further sampling of local hypabyssal rock types is needed for making significant estimates of their average NRM and susceptibility values which determine their effect on magnetic anomaly patterns: see also the last paragraphs of Section 5.2.2.

It will be recalled, however, that the Precambrian diabase

dykes from which data were obtained for Fig. 5.1b, are mostly of average to high NRM intensity and susceptibility. Similarly, the ultrabasic and anorthosite samples of that figure were fairly magnetic. Kristjansson (1970) has suggested that gabbroic intrusions may cause some of the anomalies observed over mid-ocean ridges; however, dredged gabbro samples from these areas are still too few in number and of too uncertain origin for a test of this suggestion.

5.7 Magnetic anomalies over acid volcanics

The NRM intensity and susceptibility values for 30 samples of acid volcanic rocks from Iceland are given in Table 5.9. These are mostly from South-Western Iceland and of Plio-Pleistocene age. The remanence was measured with an astatic magnetometer; intensities are given in weight units because of the irregular shape and porosity of some of the specimens. The densities of samples HV 2A, SJ and HL 1 were found to be 2.5 g/cm^3, but that of the altered sample AK. was 2.15 g/cm^3.

It is seen that intensities and susceptibilities are generally very low, both averaging about $0.2 \cdot 10^{-3}$ e.m.u./g (roughly $0.5 \cdot 10^{-3}$ Gauss and Gauss/Oe respectively). The mean Königsberger Q ratio is therefore about 2; however, many of the samples gave almost no instrumental deflection and their Q-ratios are therefore not known with any accuracy.

The Curie points of three samples were measured in a strong ($\sim$1000 Oe) applied field. That of the acid tuff HV 3 was

about 620°C, with the room-temperature moment having dropped by about half after the experiment. The Curie point of HL 2 was 570°C; that of the granophyre HV 10 was 570°C (with another Curie point at just over 400°C during heating only).

Microscope observations were made on polished sections from the same samples and Mó 4A. In HV 3, there is a large number of small (1 μ) dark grains, apparently non-reflecting and amorphous. HV 10 has grains of similar appearance, but also a few large grains, pitted in appearance and resembling some of the magnetite grains in gneiss (Plate 8b). HL 2 contained a large number of unidentifiable small grains, but also magnetite with hematite exsolution and magnetite which is dissolving into the silicates, colouring them red. Mó 4A has a distribution of exceedingly fine grains smeared over the section, making it reddish in places.

The magnetite, seen in polished section and inferred to be in these acid rocks by the thermomagnetic results, is probably original. It is generally in small quantities, the mean susceptibility indicating 0.2% by volume (though the relationship of Section 3.10.1 may not be strictly applicable because of the exceedingly fine grain size in some samples). Since rhyolites solidify at much lower temperatures than basalts, and are relatively poorer in titanium, it is probable that their opaques are mostly pure magnetite-hematite minerals. This is borne out by the thermomagnetic curves, except that HV 10 has also a low Curie point which may be due to titanomagnetite.

Possibly because of the small grain size (end of Section 3.11.4), the room-temperature strong-field moments of HV 4A and HV 10 had dropped considerably after measurement; the magnetic balances used by the author are not sensitive enough to detect the presence of the resultant hematite. The Curie point of HV 4A is similar to that of red sediments (Section 3.12.3) indicating very advanced oxidation.

The fact that Icelandic acid rocks contain magnetite and its oxidation products is consistent with the occurrence of magnetite in metamorphic rocks in the Greenland-Baffin region; the mean susceptibilities are of a similar order of magnitude, but cannot be compared directly because the latter collection includes rocks of basic and intermediate composition (Table 5.3). The magnetite in the metamorphics may therefore be partly primary, though perhaps recrystallized into larger grains during the metamorphic events (cf. the low Königsberger ratio, usually between 0.08 and 1).

The low content of magnetic minerals in the acid rocks investigated here indicates that occurrences of acid rocks in Iceland and the Tertiary volcanoes of Greenland (Ubekendt) are not likely to create any magnetic field anomalies.

5.8 Magnetic Properties of Material Recovered by Deep Drilling

5.8.1 Introduction. Magnetic anomalies over Iceland (Serson *et al.*, 1968) are known to be much less regular than those over the Mid-Atlantic ridge crest to the southwest and north. In the geologic interpretation of these anomalies, it is therefore important to have available estimates of the magnetic properties of local rocks at depth, as well as surface outcrops.

The writer has obtained from the National Energy Authority (N.E.A.) 21 samples of drill chips recovered from four deep holes drilled by them in South-Western Iceland in search for geothermal power. Three core pieces were also obtained, but very few core drillings have been carried out in Iceland below 600 m depth. The drill chips are routinely collected by N.E.A. personnel from the bit cooling water during rotary cutting operations, and have been extensively used by them in stratigraphic correlation between drill holes.

The deepest hole drilled in Iceland to date is R4 in Reykjavik (Fig. 5-10), 2200 m in depth from the well head, and having a bottom temperature of 140°C. The deepest hole within the presently active volcanic zone is H8 at the geothermal field at Reykjanes (Fig. 5-10), 1754 m, where temperatures of 280°C were encountered. No drill holes in Iceland are believed to have reached the seismically defined "layer 3" (G. Palmason, pers. comm. 1970), which occurs at about 2.5 km depth on Reykjanes peninsula. No magnetic field measurements have been carried out in these holes below 400 m depth.

The size of individual drill chips is usually 0.05 - 2 mm.

Samples weighing about 20 gm each and composed of large numbers of chips were obtained from the two holes mentioned above, and also from two nearby but shallower holes. Descriptions of these (from N.E.A. reports) are given in Table 5.11. Measurements of susceptibility and artificial thermal remanence (TRM) were carried out on 4-gm specimens, and 1-gm specimens were used for microscope, ballistic magnetometer and thermomagnetic work. These specimens were portions of the above samples and themselves consisted of multiple chips.

5.8.2 The magnetic mineral in the drill chips. Strong-field thermomagnetic measurements were carried out in air on four drill chip specimens, using the equipment described by Deutsch *et al.*, (1971). Two thermomagnetic curves and Curie points are shown in Fig. 5-11; the other two Curie points were respectively 590°C and 600°C for a specimen each from 1230 m depth in hole R22 and from 900 m in H3.

These results are consistent with the presence of magnetite as the principal magnetic constituent of the rock. Since the Curie points were in three cases higher than that of pure magnetite, this phase in the fresh chips may be oxidized towards maghemite composition. After heating as in Fig. 5-11, the room-temperature moment of all four specimens dropped considerably, which could be explained by further oxidation of some of the magnetite to hematite during the experiment (Ozima and Larson 1970). No evidence for ferromagnetic contamination of the chips by the drilling equipment was found.

By microscope examination (to 1000 x) of polished sections of drill chips mounted in resin, it was ascertained that the opaque grains in these are mostly oxidized titanomagnetites, of size range 1 - 20 microns.

Ilmenite exsolution is common in these, indicating that they are a primary high-temperature constituent of the rock. In two sections from Reykjavik samples, the concentration of opaques varied greatly between chips, averaging 2-4 volume percent. In two Reykjanes samples, this value was of the order of 1%. Discrete ilmenite grains occur as a minor constituent; pyrite is less than 0.05% of the rock volume in these sections.

5.8.3. Susceptibility and magnetite content.

5.8.3.1. Rock density. Because of the very small and irregular dimensions of the drill chips, their density cannot be measured as a mass/volume ratio. The density values given for some samples in Table 5.11 are obtained by a pycnometric method that will yield a higher density value than would result from mass and volume measurements in the case of porous formations. From measurements on cores, the rock pore volume in tuffs and sediments in Iceland may be up to 30%. Hence, to avoid ambiguities, the results shown in Fig. 5-12 have been plotted in mass units. In Fig. 5-13 however, the ambiguity is partly eliminated by multiplying the results on both coordinate axes by the same estimated density value (always in the range 2.4 - 3.0 gm/cm^3).

5.8.3.2. Susceptibility: Reykjavik area. Initial susceptibility values for fresh drill chips are shown in Fig. 5-12 as dots or open circles connected by solid straight lines. Also shown are susceptibility values, not included in Table 5.11, from shallow depths at Reykjanes and Reykjavik drilling sites. For Reykjavik rock below 800 m depth in particular, the susceptibilities are in the range $(0.7 - 2).10^{-3}$ $Gauss \cdot cm^3/Oe \cdot gm$, corresponding to approximately $(1.8 - 5) \cdot 10^{-3}$ Gauss/Oe for the volume susceptibility of solid rock of the same composition, with

an arithmetic average value of about $3 \cdot 10^{-3}$ Gauss/Oe for the depth range 800 - 2200 m at Reykjavik. This value is higher than corresponding values for basalt from surface outcrops, which include $1.5 \cdot 10^{-3}$ G/Oe for Miocene flows in NW-Iceland; $2.4 \cdot 10^{-3}$ G/Oe for Plio-Pleistocene basalt in the Reykjavik area; and $1.3 \cdot 10^{-3}$ G/Oe for basalt within the Upper Pleistocene subglacial volcanics of SW-Iceland. Logarithmic averages of the same data are given in Kristjansson (1970).

According to Section 3.10 there is a fairly good linear relation between the susceptibility and magnetite content of volcanic and metamorphic rocks, provided they have a single, high (> 500°C) Curie point only. The proportionality constant is $(2.2 \pm 0.3) \cdot 10^{-3}$ G/Oe per volume percent of magnetite. Using this relation and correcting for the occurrence of low-Curie-point components in some of the surface rocks, one obtains an average magnetite content of 1.3% by volume in the drill chips from 800 - 2200 m depth in Reykjavik; 0.9 - 1.3% in Icelandic surface basalt; and 2.5 - 3% in gabbro from Iceland.

There is no obvious downward trend in susceptibility with increased depth below 800 m in the Reykjavik drill holes. This is consistent with the results of chemical analyses of drill chips from hole R4, carried out by G. E. Sigvaldason (pers. comm. 1971). In each of ten samples from depths of 900 - 2200 m, he finds a value of between 11-13 weight percent for (Fe_2O_3 + FeO).

5.8.3.3. Susceptibility: Reykjanes area. The susceptibility of drill chips from deep layers at Reykjanes is considerably lower than that in Reykjavik (Fig. 5-12). The arithmetic average solid-rock susceptibility of nine samples of chips and cores from 400-1500 m depth

here is $0.65 \cdot 10^{-3}$ Gauss/Oe, corresponding to a magnetite content of some 0.3% by volume. This low value is probably due to the low magnetite content of palagonite tuff (Kristjansson 1970), though it is also known that the high porosity of the Reykjanes volcanics greatly facilitates alteration of the rock by hot circulating ground water. This latter effect may be a major cause of a local magnetic low at the Reykjanes geothermal field.

According to N.E.A. logs for the Reykjanes drill holes, it appears that rather porous layers of tuffs, clastics and thin lava flows give way to a more uniform and massive series of lava flows below 1550 m depth. At these depths also, the TRM and susceptibility values (Fig. 5-12) of these rocks appear to be more similar to those of the Reykjavik deep rocks than of the overlying formations at Reykjanes. However, one cannot yet draw conclusions from these results on possible genetic or age relationships between the deep layers in the two areas. The highly magnetic shallow-level sample from Reykjanes (Fig. 5-12) may be from a pillow basalt or rapidly cooled dyke rock, but it does not seem feasible to identify such facies in the deep-level drill chips.

5.8.4 Artificial TRM and Q_t - ratios. Fig. 5-12 shows, as dots or open circles connected by broken lines, values of TRM intensity acquired by specimens of drill chips on cooling in air from 600°C in an applied magnetic field of 0.50 Oe. NRM values of some drill cores are shown as crosses. The TRM intensity values are in the range $(3\text{-}9) \cdot 10^{-3}$ Gauss$\cdot$cm^3/gm for the Reykjavik drill chips, corresponding to solid-rock volume intensities of $(8\text{-}24) \cdot 10^{-3}$ Gauss. The arithmetic

average for 12 samples from 800-2200 m depth is $14 \cdot 10^{-3}$ Gauss, comparable to $16 \cdot 10^{-3}$ Gauss similarly obtained from 21 typical surface basalt samples from SW-Iceland.

Thus, in artificial TRM as well as in susceptibility, the deep layers are similar to surface basalts and show no downward magnetic trend with increasing depth. Results from Reykjanes (Fig. 5-12) are again low down to below 1500 m, but are comparable to Reykjavik values at still larger depths.

In Fig. 5-13, TRM intensity values J_{th} are plotted against susceptibility for drill chips, surface basalts and basalts from shallow drill holes in SW-Iceland. It is seen that in all but one case, the Königsberger ratios $Q_t = J_{th}/K_tH$ are in the range 10 to 35, indicating a similar state of the magnetic mineral in all these rock types. The susceptibility values K_t of Fig. 5-13, which are measured after cooling, are usually lower than values of K for fresh material, by 10-40%.

Laboratory results on the acquisition of TRM in air by chips indicate that most ($\geq$ 70%) of the room-temperature intensity is blocked above 500°C. The stability of this artificial TRM (Fig. 5-14) is similar to that usually found in deuterically oxidized surface basalt. Values of high-temperature susceptibility, measured on a sample from 1683 m in hole R4, were higher, up to 540°C, than the room temperature susceptibility.

5.8.5 The natural remanence of drill chips. The most important magnetic properties of the deep layers under Iceland, both for stratigraphic work and magnetic anomaly interpretation, are their *in-situ*

NRM polarity and intensity. However, no definite information on this is yet available. The NRM intensity of the diabase core from 840 m depth in Reykjavik (Table 5-11) is $25 \cdot 10^{-3}$ Gauss, while that of two tuff core pieces from Reykjanes is only $0.2 \cdot 10^{-3}$ and $2.5 \cdot 10^{-3}$ Gauss. The NRM intensity of a normal-polarity basalt core from 430 m depth in the Krisuvik geothermal area was $0.5 \cdot 10^{-3}$ Gauss. The last-mentioned three cores have very low susceptibility, averaging $0.2 \cdot 10^{-3}$ Gauss/Oe.

Measurements were made of the NRM intensity of 50 single, large (0.01 - 0.03 gm) drill chips from 1500-2000 m depth in Reykjavik, using a P.A.R. spinner. Their average intensity was $(10\text{-}12) \cdot 10^{-3}$ Gauss, which may be considered as an upper limit to the possible *in-situ* NRM of rocks having this composition. However, it must be remembered that during the drilling, the rock in the vicinity of the drill bit has been simultaneously subjected to heating, to large shear stresses, and to stray magnetic fields. The measured NRM is therefore likely to be largely soft magnetization, similar to isothermal, piezomagnetic or dynamic (Shapiro and Ivanov 1967) remanence. This view is supported by results of AF demagnetization of the random moment of NRM in mounted 1-gm specimens of multiple drill chips (Fig. 5-14). The NRM is found to be much less stable, both in intensity and direction, than is TRM acquired on cooling from 600°C. Further, the drill chips are commonly thin and plate-like, in which case their individual NRM moments were found to be dominantly oriented at right angles to the plate plane.

5.8.6. Summary; application to magnetic anomalies. The magnetic mineral in samples of small rock chips recovered during deep

drilling in South-Western Iceland has been found by thermomagnetic and other methods to be magnetite. It seems to occur mostly in deuterically oxidized titanomagnetite grains in the rock, containing ilmenite exsolution features. Secondary sulfide alteration products are absent.

Measurements of susceptibility and artificial TRM intensity on 12 samples of these chips from depths between 800-2200 m in Reykjavik (Fig. 5-10) indicate that in this depth interval the amount and composition of magnetite is similar to that in oxidized surface basalts. The magnetite concentration in these samples has been estimated by a magnetic method to average about 1.3% by volume, and to show no downward trend with increased depth in the drill holes.

A lower magnetite content, averaging about 0.3%, has been similarly derived from 11 samples of chips and cores from a high-temperature geothermal area at Reykjanes, at 400-1500 m depth. Higher values were obtained in two samples from 1600-1750 m depth, indicating that the magnetic mineral in non-porous basalts may retain its identity through considerable rock alteration, even at temperatures of up to 300°C.

One may therefore expect magnetic anomalies observed over Iceland to be due to magnetization contrasts in a layer of $\geq$ 2 km thickness. This conclusion, being in contrast to views on the thickness of the crustal magnetic layer south of Iceland (Talwani *et al.*, 1971), may be a key to understanding the relatively irregular structure of magnetic anomalies over Iceland. It is supported by magnetic anomaly computations, using a realistic model of the lateral structure of the magnetic layer in Iceland and data from a large number of paleomagnetic sampling sites (L.Kristjansson, unpublished data 1972).

Appendix 5.1. The random magnetic moment of rock chips

The following results were obtained during research into the magnetic properties of small rock chips recovered during deep rotary drilling for geothermal power in Iceland. They are also of interest to considerations of depositional remanence in sediments, and to the interpretation of magnetic anomalies over detrital beds.

A5.1.1. Statistical considerations. Let us take a lump of solid rock such as basalt, having density ρ gm/cc, and mass m gm. Its remanent magnetic moment is $M = Jm/\rho$, where the remanence J(in Gauss) is assumed to be uniform in direction throughout the rock. Its susceptibility is not relevant here. We crush this sample into a large number N of small pieces, say 1,000-10,000 pieces per gm. They will be called "chips" here to avoid confusion with the "grains" of magnetic mineral in the rock, whose number is assumed to be much greater than N. The chips should have varying sizes, but no preferred shape orientation with respect to their remanence direction. We further assume that the chips do not interact magnetically, and that the crushing does not affect their magnetic properties.

Out of the N chips, only a number n will contain magnetic mineral, while the others will be non-magnetic portions of pheno-crysts, zeolites etc. We put all N chips into a vial and shake the vial thoroughly to randomize the directions of the individual chip momnets. We then measure 3 orthogonal components of the resultant total magnetic moment of the chips, taking care to avoid any viscous buildup of secondary magnetization. The chips are held tightly together during

the measurement, but are then taken out of the magnetometer, re-randomized, measured again, etc.

What distribution of resultant total moments of the sample is likely to be obtained? This question has been considered in different contexts, by e.g. Irving *et al.*, (1961) and by Nagata (1961), who considered respectively the statistics of equal chip moment magnitudes and of a Maxwellian distribution of these.

Let us consider a more general case, where the distribution of chip moment magnitudes is assumed to be a lognormal one. In a lognormal distribution, written here as

$$dn = f(v)dv = \frac{n}{v\sigma(2\pi)^{\frac{1}{2}}} e^{-\left[\frac{\log_e(v)}{2^{\frac{1}{2}}\sigma\log_e(v_m)}\right]^2} dv \qquad (A5.1)$$

the variable f is a Gaussian function of the logarithm of the variable v. The standard deviation of the log plot, σ , is related to the range of orders of magnitude in v spanned by the distribution; if 68% of the number n of magnetic chips have moment magnitudes within a range of p factors of ten (centered, in the log plot, on the geometrical mean v_m), then σ=1.15 p. Fig. 5-17 shows a lognormal distribution with σ = 1; a Maxwellian distribution resembles fairly closely a lognormal distribution with σ = 0.4 - 0.5.

Other useful properties of the lognormal distribution include:

(a) The arithmetic mean of v is

$$\bar{v} = \left[\int_0^\infty v \cdot f(v)dv\right] / n \qquad (A5.2)$$

$v \cdot f(v)$ is itself a lognormal distribution with a geometric mean at $v_{rms}=\bar{v}_m e^{\sigma^2}$ and having a logarithmic standard deviation of σ. It is easily found that $\bar{v} = v_m e^{\sigma^2/2}$.

(b) The root-mean square of v is

$$v_{rms} = \left[\int_0^\infty v^2 f(v)\,dv \right]^{\frac{1}{2}} / n^{\frac{1}{2}} \qquad \text{(A5.3)}$$

where $v^2 f(v)$ is a lognormal distribution centered on $v_h = v_m e^{2\sigma^2}$, again with a standard deviation of σ. Thus

$$v_{rms} = v_m e^{\sigma^2} = \bar{v} e^{\sigma^2/2} \qquad \text{(A5.4)}$$

(c) The distribution of components of chip moments along an arbitrary direction, say the coordinate axis x of a magnetometer sample holder, is

$$q(v_x)\,dv_x \simeq (n e^{\sigma^2}/2\bar{v}) \left\{ 1 - F\left[\log_e (v_x/\bar{v})^{1/\sigma} + 3\sigma/2 \right] \right\} dv_x \qquad \text{(A5.5)}$$

$$\text{where} \quad F(a) = (1/2\pi)^{\frac{1}{2}} \int_{-\infty}^{a} e^{-t^2/2}\,dt \qquad \text{(A5.6)}$$

From this expression or from general principles it may be shown that the r.m.s. value of v_x is

$$v_{xrms} = v_{rms}/3^{\frac{1}{2}} = v_m e^{\sigma^2}/3^{\frac{1}{2}} \qquad \text{(A5.7)}$$

Of course, the arithmetic mean of v_x is zero, since $q(v_x)$ is an even function of v_x.

According to the central limit theorem (e.g. Jenkins and

Watts 1968). the measured values of any component, say μ_x, of the net random moment μ of the chips should be normally distributed about zero with a standard deviation of

$$\mu_{xrms} = n^{\frac{1}{2}} \cdot v_{xrms} = (n/3)^{\frac{1}{2}} \cdot (\bar{v} e^{\sigma^2/2}) \doteq (3n)^{-\frac{1}{2}} \cdot (M e^{\sigma^2/2}) \qquad (A5.8)$$

since $M = \bar{v}n$. One sees from this formula that a lump crushed into finer and finer chips should yield random moments inversely proportional to the square root of the number n of magnetic chips. On the other hand, the random moment expected from an increase in the number of magnetic chips having a given size distribution is directly proportional to the square root of n.

If the remanence moments of individual chips are too small to be measured, an estimate of their remanence J can still be simply obtained by the following procedure:

(i) Obtain an estimate of μ_{rms} for the specimen by measuring the three components of μ several times.

(ii) Thoroughly demagnetize the specimen in an alternating field or by heating in a zero field.

(iii) Re-magnetize the chips by bringing them near a strong magnetic field.

(iv) Measure their new, field-aligned magnetic moment M', then again randomize their directions, as previously described.

(v) Measure several times the random moment of the chips, μ', with this new magnetization.

Then it is reasonable to assume that

$$J/J' = M/M' \doteq \mu_{rms}/\mu'_{rms} \qquad (A5.9)$$

provided the statistical distribution of chip moment magnitudes after step (iii) has a similar shape as f(v), i.e. is such that the ratio of mean and r.m.s. chip moment magnitudes is the same for the original and the new magnetization.

A5.1.2. Measurements. It is simple to test the conclusions derived from the central limit theorem, namely that the distribution of component magnitudes of the specimen net random moment should be Gaussian, and that the r.m.s. value of these magnitudes should increase proportionally to $\sqrt{n}$. Fig. 5-15 shows the observed frequency histogram of net moment components (x, y and z) in a specimen of chips from a drill hole in Reykjavik, SW-Iceland. These results were obtained by randomizing and remeasuring the specimen 30 times, using a spinner magnetometer. The distribution was found, by a χ^2 - test, to be not significantly different from a Gaussian one. The distribution of total-moment magnitudes is similarly a Maxwellian distribution to a good approximation.

Fig. 5-16 is a plot of component variance as a function of specimen mass for another sample of Reykjavik drill chips. Each point on the graph represents 36 measurements of component sizes, with 80% confidence bars as obtained from Fig. 3.10 of Jenkins and Watts (1968). The results show a good linear relation, as expected, between the square of the r.m.s. component, or total-moment value, and the number of chips in a specimen.

An attempt at obtaining the average original remanence of these chips from statistical considerations as described here did not yield results in agreement with results of measurements on individual

large chips; this was chiefly because the chips were often plate-shaped with the remanence being at right angles to the plate plane. This remanence is probably a piezomagnetic remanence acquired during the drilling process.

Finally, one may ask what is the minimum number of chips, n, needed in order that lognormal statistics may be applied to a real specimen of rock chips. Since the size of measured specimens may often be limited by experimental conditions, it is better to change the question and ask: what is the maximum value of σ for which the lognormal model can be applied, in a specimen with given n, say $n = 10^4$ chips. An estimate of this value of σ may be obtained by requiring that not more than half the value of the integral $\int_0^\infty v \cdot f(v)dv$ derives from those 2-5% of the chips which have the highest values of v. This is found to be equivalent to σ lying between 3 and 4; i.e. the moments v of the central 68% out of the n having this distribution should not range over more than 2.5 - 3.5 orders of magnitude. Hence, if the magnetic moment of a rock chip is roughly proportional to its volume, the dimensions of the chips in the central 68% - range should not span more than one order of magnitude.

CHAPTER 6 SUMMARY AND MAIN CONCLUSIONS

1. On Disko Island, West Greenland, oriented samples were collected from 45 flat-lying flows of felsparphyric basalt lava (110 samples) and from seven sites in an underlying breccia and seven intrusive bodies (37 samples). Various magnetic properties of these rocks were measured in the laboratory.

2. Alternating-field (AF) demagnetization showed that all samples possess a stable to very stable component of primary magnetic remanence. A mean paleomagnetic direction, computed from 37 lava flows in two profiles after treatment to 200 Oersteds, corresponds to a mean pole position at 62°N, 169°W, with a 95% error oval of mean radius 9°. This pole position is similar to that of most Lower Tertiary formations from Europe and North America reported in the literature.

3. The age of the basalt flows was found to be 70 ± 4 million years, by a commercial K-Ar analysis of one fresh sample. This value is broadly consistent with local geologic evidence and with datings from other formations in the area.

4. The primary remanence is reverse, i.e. of opposite polarity to the earth's present field. The between-flow dispersion of magnetic directions is 19°, a value similar to the present amplitude of geomagnetic secular variation. On the plausible assumption that this observed dispersion between flows represents mainly the amplitude of secular variation at the time the rocks were formed, it is concluded that the amplitude of secular variation about 70 m.y. ago was similar to that of today. The time span covered by the two profiles may

have been less than 10^5 years, judging from the lack of sedimentation between flows.

5. The primary remanence component is thermal or chemical remanence acquired on cooling (from a molten state) through a blocking temperature interval below 580°C. The large variation found in oxidation state, grain size and other relevant parameters both between and within the rock units seems to rule out self-reversal of the magnetization during cooling.

6. In Disko, no regional heating or metamorphism has taken place to introduce stable secondary components of remanence. However, it is likely that the intensity of the original magnetization has decayed considerably in some samples since their origin.

7. In all samples a magnetically unstable component of remanence occurs. It is of normal polarity and was shown to be viscous remanence (VRM) built up during the present (Brunhes) geomagnetic epoch. In the "class N" samples, which comprise about one-third of those collected in Disko lava profiles, this unstable component predominates, causing the resultant natural remanence (NRM) to be of normal polarity. Tests on pilot samples showed that significant magnetization of this kind may be built up in a constant weak field in times as short as one week, following AF demagnetization.

8. The magnetic properties of the Disko basalts reside in titanomagnetite. Microscope observation showed roughly equidimensional grains of that mineral, of average size 20-50μ, amounting to about 6% of the rock volume. Thermomagnetic curves obtained from these basalts are compatible with the microscope observations, which show

that exsolution has commonly taken place in this mineral, causing the formation of magnetite with less than 10 mole percent of titanium mineral, plus ilmenite. The intensity and stability of the present remanence of the samples is positively correlated with the extent of this exsolution. These magnetic properties also are negatively correlated with susceptibility, possibly due to the limited amount of oxygen available within a flow. However, because demagnetization curve shapes above 200 Oe are similar in all pilot samples, the stable component of remanence probably resides in roughly the same portions of the grain size spectrum in all samples.

9. In some rapidly cooled lavas, breccia units and intrusives, there occur relatively fine-grained, often skeletal, unexsolved titanomagnetites. These rocks are magnetically stable in direction but not intensity; also, they tend to have high Koenigsberger (Q-) ratios and to display characteristic VRM properties. These features are probably controlled by the small grain size and other effects associated with the rapid cooling of these rocks.

10. On average, the intensity of primary remanence in the Disko lava flows is $3 \cdot 10^{-3}$Gauss, that of secondary remanence in situ is inferred to be $1.7 \cdot 10^{-3}$Gauss, and their average susceptibility is 3.10^{-3}Gauss/Oe. These figures exclude the mostly rapidly cooled rock units in one profile and the breccia and intrusive sites, for which the average values are $7 \cdot 10^{-3}$, $0.5 \cdot 10^{-3}$ and $2.0 \cdot 10^{-3}$ c.g.s. units respectively.

11. The remanence of 36 oriented samples from six flat-lying olivine basalt flows at Cape Dyer, Baffin Island, was measured, along

with several other magnetic properties of these samples. Except for three samples, they were all normally magnetized and very stable to AF and thermal treatment. The mean remanence direction obtained from five of these flows after 400 Oe treatment corresponds to a paleomagnetic pole at 83°N, 55°W, with an error oval of mean radius 12°.

12. From published evidence, the Cape Dyer flows appear to be of Lowest Tertiary age, and the above pole position is consistent with that age. More sampling in the Tertiary area of Baffin Island is needed before significant conclusions on local paleogeography and continental drift can be drawn from paleomagnetic measurements on these.

13. The major (∿95%) component of the natural remanence of the normal Cape Dyer samples appears to be primary. In some of the flows it resides in highly oxidized titanomagnetite grains; in others the grains are less oxidized and there is evidence of rapid cooling. The titanomagnetite concentration is of the order of 1% and the size of grains visible under the microscope is of order 15μ.

14. The reverse remanence found in three samples from one flow in Cape Dyer is less stable to AF and thermal demagnetization than is the remanence of the normal samples. The reverse remanence also shows relatively large within-sample variations. The most likely explanation for its presence is that some parts of that flow suffered secondary remagnetization *in situ*, at a time when the polarity of the earth's field was reversed.

15. The remanence intensity of the six Cape Dyer flows averages

$4 \cdot 10^{-3}$ Gauss, and their mean susceptibility is $0.6 \cdot 10^{-3}$ Gauss/Oe. Hence the remanence exceeds the induced magnetization by an order of magnitude. From this and aeromagnetic anomaly maps it is therefore concluded that the remanence of most or all of the exposed Tertiary rock in Baffin Island is of normal polarity.

16. The magnetism of about 50 samples of gneiss from the basement on both sides of Baffin Bay and the Labrador Sea was investigated. Their magnetic properties were found to reside in grains of pure magnetite; their Q-ratios are low ($\sim$0.2) and their mean susceptibility is about $1 \cdot 10^{-3}$ Gauss/Oe. From these data it is concluded that gneiss from the localities concerned would generally produce much smaller anomalies than would Tertiary basalt formations, so that it may be possible to distinguish between the two types of rock, where unexposed, from magnetic anomaly maps. However, it was also found that samples from Precambrian basic rock units and some gneisses may yield total magnetization values similar to those of Tertiary basalt, and that the net magnetization of reversely magnetic Tertiary basalt may be quite small due to the opposing influence of secondary and induced magnetization components. This possibility imposes a need for additional caution in interpreting aeromagnetic maps.

17. The remanence intensity of Tertiary submarine basalts in Baffin Bay has been estimated to be similar to that in the Mid-Atlantic and much higher than the inferred remanence intensity of rocks underlying the magnetic "smooth zones" of the Atlantic Ocean.

18. The remanence of over 20 samples of Tertiary gabbro was shown to be stable and having a higher intensity ($\sim 6 \cdot 10^{-3}$G) than that

of the average basalt in North Atlantic coastal areas. The remanence intensity of a similar number of rhyolite samples was found to be very low, and such rocks are therefore not likely to contribute significantly to magnetic anomalies. In both cases, magnetite is the chief carrier of remanence.

19. The effect of seven dyke intrusions on the magnetic properties of the adjacent rock was investigated. It is found that this effect is very small or negligible beyond a distance of one-fifth dyke thickness on either side of the dyke, when the ambient temperature before the intrusion is less than 100°C.

20. By studies on various magnetic properties of rock chips and cores recovered during deep drilling in Iceland, it was found that the thickness of the crustal layer responsible for the production of magnetic anomalies there is at least 2 km. Geothermal activity appears to affect the amount and composition of titanomagnetites in solid basalt only slightly, as these parameters were found to be similar to those in surface outcrops.

21. Instruments were designed and constructed for the measurement of (i) temperature dependence of magnetic moment and Curie point in rocks, and (ii) their room-temperature saturation magnetization. Apart from aiding in the work described above, these instruments were used to demonstrate a proportional relationship between the room-temperature susceptibility of various rock types and their content of pure magnetite.

REFERENCES

Ade-Hall, J. M. Geophys. Jour. 18, p. 93-107 (1969)

Ade-Hall, J. M., T. P. Hubbard, and H. C. Palmer. EOS 51, p. 277 (1970)

Ade-Hall, J. M., M. A. Khan, P. Dagley, and R. L. Wilson. Geophys. Jour. 16, p. 389-399 (1968a)

Ade-Hall, J. M., M. A. Khan, P. Dagley, and R. L. Wilson. Geophys. Jour. 16, p. 401-415 (1968b)

Ade-Hall, J. M., and E. A. Lawley. Geol. Jour. special issue No. 2 p. 217-230 (1970)

Ade-Hall, J. M., H. C. Palmer, and T. P. Hubbard. Geophys. Jour. 24, p. 137-174 (1971)

Ade-Hall, J. M., P. Ryall, and R. E. Gerstein. EOS 53, p. 355 (1972)

Ade-Hall, J. M., R. L. Wilson, and P. J. Smith. Geophys. Jour. 9, p. 323-336 (1965)

Allaart, J. H., D. Bridgewater, and N. Henricksen. Am. Assoc. Petroleum Geol. Memoir 12, p. 859-882 (1969)

Aumento, F., B. Loncarevic, and D. I. Ross. Phil. Trans. Roy. Soc. A268, p. 623-650 (1970)

Banerjee, S. K. Jour. Appl. Phys. 41, p. 966-973 (1970)

Barrett, D. L., C. E. Keen, K. S. Manchester, and D. Ross. Nature 229, p. 551-553 (1971)

Björnsson, S. (Ed.) Iceland and mid-ocean ridges. Soc. Sci. Isl. 38, 209 p (1967)

Bullard, E. C., J. E. Everett, and A. G. Smith. Phil. Trans. Roy. Soc. A258, p. 41-51 (1965)

Bullard, E. C., and H. Gellman. Trans. Roy. Soc. A247, p. 213-278 (1954)

Bullock, P. W. Palaeomagnetism and its application to geological problems in South-West Greenland. M.Sc. thesis, University of Newcastle Upon Tyne, 91 p. (1967)

Burlatskaya, S. P., T. Nechayeva, and G. N. Petrova. Izvestiya (Geophysics) No. 12 p. 754-759 (1968)

Carmichael, C. M. Can. Jour. Earth Sci. 7, p. 239-257 (1970)

Chemical Rubber Company. Handbook of Chemistry and Physics. Cleveland, 3604 p. (1962)

Clarke, D. B. The Tertiary basalts of Baffin Bay. Ph.D. thesis, University of Edinburgh, 122 p. (1968)

Clarke, D. B. Contr. Mineral. Petrol. 25, p. 203-224 (1970)

Clarke, D. B., and B. G. J. Upton. Can. Jour. Earth Sci. 8, p. 248-258 (1971)

Collinson, D. W., K. Creer, and S. K. Runcorn (eds.) Methods in Palaeomagnetism; Amsterdam, Elsevier, 690 p. (1967)

Cox, A. Nature 179, p. 685-686 (1967)

Cox, A. Science 163, p. 237-245 (1969)

Cox, A. Jour. Geophys. Res. 75, p. 7501-7503 (1970)

Creer, K. M., J. Ibbetson, and W. Drew. Geophys. Jour. 19, p. 93-101 (1970)

Creer, K. M. and N. Petersen. Zeits. Geophys. 35, p. 501-515 (1969)

Creer, K. M. and M. Sanver. Palaeogeophysics (ed. Runcorn, S. K.) p. 91-100. London; Academic Press (1970)

Dagley, P. Earth Planet. Sci. Lett. 6, p. 349-354 (1969)

Dagley, P., and J. M. Ade-Hall. Palaeogeophysics (ed. Runcorn, S. K.) p. 165-170. New York, Academic Press (1970)

Dagley, P., and R. L. Wilson. Nature Physical Science 26, p. 16-18 (1971)

Dagley, P., R. L. Wilson, J. M. Ade-Hall, G. P. L. Walker, S. E. Haggerty, T. Sigurgeirsson, N. D. Watkins, P. J. Smith, J. Edwards, and R. L. Grasty. Nature 216, p. 25-29 (1967)

De Boer, J., J. Schilling, and D. C. Krause. Earth Planet. Sci. Lett. 9, p. 55-60 (1970)

Deutsch, E. R. Am. Assoc. Petroleum Geol. Memoir 12, p. 931-954 (1969)

Deutsch, E. R., and C. R. Somayajulu. Earth Planet. Sci. Lett. 7, p. 337-345 (1970)

Drever, H. Arctic 11, p. 199-210 (1958)

Duckworth, H. E. Electricity and Magnetism. New York, Holt, Rinehart and Winston 424 p. (1960)

Dunlop, D. and G. F. West. Revs. Geophys. 7, p. 709-759 (1969)

Elsasser, W. M. Revs. Mod. Phys. 28, p. 135-163 (1956)

Evans, M. and M. L. Wayman. EOS 52, p. 193 (1971)

Eyles, V. A. The composition and origin of the Antrim laterites and bauxites. Belfast H.M.S.O. 90 p. (1952)

Fahrig, W. F., E. Irving, and G. D. Jackson. Sci. 8, p. 455-467 (1971)

Fisher, R. A. Proc. Roy. Soc. A117, p. 295-306 (1953)

Gaucher, E. H. S. Geophysics 30, p. 762-782 (1965)

Geological Survey of Canada. Geophysics Papers 5434-5450, series G (1970)

Ghisler, M., and P. V. Sharma. Grönl. Geol. Unders. Report no. 20, 25 p. (1969)

Gilliland, M. W., H. C. Clark, and J. F. Sutter. EOS, 50, p. 131 (1969)

Girdler, R. Geophys. Jour., 5, p. 197-206 (1961)

Grant, A. C. EOS, 53, p. 407 (1972)

Grommé, C. S. Jour. Geomag. Geoel., 17, p. 879-882 (1965)

Grommé, C. S. and E. H. McKee. EOS, 52, p. 187 (1971)

Grommé, C. S., D. L. Peck, and T. L. Wright. Jour. Geophys. Res., 74, p. 5277-5293 (1969)

Guja, N. and S. A. Vincenz. EOS, 52, p. 188 (1971)

Haines, G. V., W. Hannaford, and P. H. Serson. Publ. Dominion Obs., 39, p. 123-149 (1970)

Hanna, W. F. Jour. Geophys. Res., 72, p. 595-610 (1967)

Harrison, C. G. A. Jour. Geophys. Res., 73, p. 2137-2142 (1968)

Heirtzler, J. R., G. O. Dickson, E. M. Herron, W. C. Pitman, and X. Le Pichon. Jour. Geophys. Res., 73, p. 2119-2136 (1968)

Henderson, G. Grönl. Geol. Unders. Report no. 22, 64 p. (1969)

Hide, R. Science, 157, p. 55-56 (1967)

Hood, P. and M. E. Bower. Geol Surv. Canada paper 71-23 (in press 1972)

Hood, P., P. Sawatzky, and M. E. Bower. Geol. Surv. Canada paper 66-58 11 p. (1967)

Hospers, J. Nature, 173, p. 1183-1184 (1954)

Hyndman, R. D., D. B. Clarke, H. Hume, J. Johnson, M. J. Keen, I. Park, and G. Pyé. Geol. Surv. Canada paper 71-23 (in press 1972)

Irving, E. Paleomagnetism and its application to geological and geophysical problems. New York, Wiley, 399 p. (1964)

Irving, E. Can. Jour. Earth Sci., 7, p. 1528-1538 (1970)

Irving, E., J. Park, S. E. Haggerty, F. Aumento, and B. Loncarevic. Nature, 228, p. 974-976 (1970)

Irving, E., W. A. Robertson, P. M. Stott, D. H. Tarling, and M. A. Ward. Jour. Geophys. Res., 66, p. 1927-1933 (1961)

Irving, E., P. M. Stott, and M. A. Ward. Phil. Mag., 6, p. 225-241 (1961)

Jaeger, J. C. Am. Jour. Science, 255, p. 306-318 (1957)

Jenkins, G. M., and D. G. Watts. Spectral analysis and its applications. San Francisco, Holden-Day, 525 p. (1968)

Johnson, G. L., A. Closuit, and J. A. Pew. Arctic, 22, p. 56-68 (1969)

Keen, M. J., B. D. Loncarevic, and G. N. Ewing. The Sea (ed. Maxwell, A. E.) vol. 4, part II, p. 251-292 (New York, Wiley) (1971)

Kidd, D. J. Arctic, 6, p. 227-251 (1953)

Kilbourne, D. Geol. Soc. Am. Bull., 80, p. 2069-2075 (1969)

Kristjansson, L. G. On the palaeomagnetism and geology of North Western Iceland. M.Sc. thesis, University of Newcastle upon Tyne, 59 p. (1967)

Kristjansson, L. G. Earth Planet. Sci. Lett., 4, p. 448-450 (1968)

Kristjansson, L. G. Earth Planet. Sci. Lett., 8, p. 101-108 (1970)

Kristjansson, L. and T. Buason. EOS, 51, p. 275 (1970)

Larochelle, A. Geol. Surv. of Canada, paper 62-2 p. 44-47 (1964)

Larochelle, A. Jour. Geophys. Res., 74, p. 2571-2575 (1969)

Larson, E., F. Mutschler, and G. Brinkworth. Earth Planet. Sci. Lett., 7, p. 29-32 (1969a)

Larson, E., M. Ozima, T. Nagata, and D. Strangway. Geophys. Jour., 17, p. 263-292 (1969b)

Larson, E. and D. Strangway. Jour. Geophys. Res., 74, p. 1505-1515 (1969)

Laughton, A. S. Nature, 232, p. 612-617 (1971)

Lawley, E. A. Earth Planet. Sci. Lett., 10, p. 145-149 (1970)

Lawley, E. and J. M. Ade-Hall. Earth Planet. Sci. Lett., 11, p. 113-120 (1971)

Le Pichon, X., R. D. Hyndman, and G. Pautot. Jour. Geophys. Res., 76, p. 4724-4743 (1971)

Marcley, R. G. Am. Jour. Phys., 29, p. 86-89 (1961)

Marshall, M. and A. Cox. Geol. Soc. Am. Bull., 82, p. 537-552 (1971)

Mayhew, M. A., C. Drake, and J. Nafe. Can. Jour. Earth Sci., 7, p.199-214 (1970)

McMahon, B. E. and D. Strangway. Geophys. Jour., 15, p. 265-285 (1968)

McMurry, E. EOS, 52, p. 188 (1971)

Melson, W. G. and G. Switzer. Am. Mineral., 51, p. 664-676 (1966)

Mooney, H. M. and R. Bleifuss. Geophysics, 18, p. 383-393 (1953)

Moorbath, S., H. Sigurdsson, and R. Goodwin. Earth Planet. Sci. Lett., 4, p. 197-205 (1968)

Mundry, E. Geol. Jahrb., 85, p. 755-766 (1968)

Murthy, G. S. Paleomagnetic studies in the Canadian Shield. Ph.D. thesis, University of Alberta, 170 p. (1969)

Nagata, T. Rock Magnetism. Tokyo; Maruzen, 350 p. (1961)

Naidu, P. S. Jour. Geophys. Res., 75, p. 2649-2662 (1971)

Nairn, A. E. M. (ed.) Descriptive Palaeoclimatology. New York, Wiley 401 p. (1961)

Nairn, A. and H. Vollstadt. Geol. Rundschau, 57, p. 385-400 (1967)

National Energy Authority.Reykjanes. (Report on investigation of the geothermal area). Reykjavik, 122 p. (1971)

Néel, L. Ann. Geophys., 5, p. 99-136 (1949)

Néel, L. Adv. Phys., 4, p. 191-243 (1955)

O'Reilly, W. and S. K. Banerjee. Nature, 211, p. 265-285 (1966)

Ostenso, N. and R. J. Wold. Mar. Geophys. Res., 1, p. 178-219 (1971)

Ozima, M. and E. Larson. Jour. Geophys. Res., 75, p. 1003-1018 (1970)

Ozima, M. and M. Ozima. Jour. Geophys. Res., 76, p. 2051-2056 (1971)

Ozima, M., M. Ozima, and I. Kaneoka. Jour. Geophys. Res., 73, p. 711-723 (1968)

Palmason, G. Crustal structure of Iceland from explosion seismology. Doctoral thesis, University of Iceland, 239 p. (1970)

Park, I., D. B. Clarke, J. Johnson, and M. J. Keen. Earth Planet. Sci. Lett., 10, p. 235-238 (1971)

Parry, L. G. Phil. Mag., 11, p. 303-312 (1965)

Pauly, H. Medd. Dansk Geol. Foren., 19, p. 8-26 (1969)

Pearce, G. W. Design and calibration of apparatus for the alternating field demagnetization of rocks. M.Sc. thesis, Memorial University of Newfoundland, 134 p. (1967)

Pitman, W. EOS, 52, p. IUGG 130-135 (1971)

Pitman, W. EOS, 53, p. 351 (1972)

Pitman, W. C. and M. Talwani. Geol. Soc. Amer. Bull., 83, p. 619-646 (1972)

Pomonarev, V. N. and I. I. Glukhikh. Izvestiya (Geophysics), 7, p. 742-745 (1963)

Pulvertaft, T. C. R. and D. B. Clarke. Grönl. Geol. Unders. Report No. 11, p. 15-17 (1967)

Puranen, M., V. Marmo, and U. Hamalainen. Geoexploration, 6, p. 163-184 (1968)

Pye, G. D. and R. D. Hyndman. Jour. Geophys. Res., 77, 938-944 (1972)

Rao, K. V. Paleomagnetism of the Ordovician Redbeds of Bell Island, Newfoundland. M.Sc. thesis, Memorial University of Newfoundland, 201 p. (1970)

Rosenkrantz, A. and T. C. R. Pulvertaft. Am. Assoc. Petroleum Geol. Memoir 12, p. 883-898 (1969)

Ross, D. I. and K. S. Manchester. EOS, 53, p. 406 (1972)

Sakamoto, N., P. Ince, and W. O'Reilly. Geophys. Jour., 15, p. 509-515 (1968)

Sanver, M. Phys. Earth Planet. Interiors., 1, p. 403-421 (1968)

Schaeffer, R. M. and E. Schwarz. Can. Jour. Earth Sci., 7, p. 268-273 (1970)

Schönharting, G. Vermessung des erdmagnetischen Feldes längs einiger Profile in Nord-Island, deren Auswertung und Interpretation. Ph.D. thesis, Ludwig-Maximilian University, München, 121 p. (1969)

Schult, A. Beitr. Mineral. Petrogr., 11, p. 196-216 (1965)

Serson, P. H., W. Hannaford, and G. V. Haines. Science, 162, p. 355-357 (1968)

Shapiro, V. A. and N. A. Ivanov. Doklady (Geophysics), no. 173, p. 6-8 (1967)

Sigurgeirsson, T. Science in Iceland, 2, p. 13-20 (1970)

Smith, P. J. Jour. Geophys. Res., 72, p. 5087-5100 (1967a)

Smith, P. J. Geophys. Jour., 12, p. 239-258 (1967b)

Soffel, H. Zeits. Geophys., 37, p. 451-470 (1971)

Somayajulu, C. R. Paleomagnetic studies of volcanic rocks in Ireland, Newfoundland and Labrador. M.Sc. thesis, Memorial University of Newfoundland, 197 p. (1969)

Stacey, F. D. Adv. Phys., 7, p. 1887-1900 (1962)

Stacey, F. D. Earth Planet. Sci. Lett., 2, p. 67-68 (1967)

Stacey, F. D. Physics of the earth. New York, Wiley, 324 p. (1969)

Strangway, D. Mining Geophysics, vol. II, Soc. Explor. Geophys., p. 454-473 (1967)

Strangway, D., E. E. Larson, and M. Goldstein. Jour. Geophys. Res., 73, p. 3787-3795 (1968)

Talwani, M. and O. Eldholm. EOS, 53, p. 406 (1972)

Talwani, M., C. C. Windisch, and M. Langseth. Jour. Geophys. Res. 76, p. 473-517 (1971)

Tarling, D. H. Geophys. Jour., 11, p. 423-432 (1966)

Tarling, D. H. Earth Planet. Sci. Lett., 3, p. 81-88 (1967)

Tarling, D. H. Palaeogeophysics (ed. Runcorn, S. K.). Academic Press, New York, p. 193-208 (1970)

Thellier, E. and F. Rimbert. Comptes Rend. Acad. Sci. Paris, 239, p. 1404-1406 (1954)

Torreson, O. W., T. Murphy, and J. Graham. Jour. Geophys. Res., 54, p. 111-129 (1949)

Vekua, L. V. Izvestiya (Geophysics), p. 1088-1091 (1961)

Verhoogen, J. Jour. Geol., 70, p. 168-181 (1962)

Vine, F. and D. H. Matthews. Nature, 199, p. 947-949 (1963)

Vogt, P. Nature, 226, p. 43-44 (1970)

Walker, G. P. L. Quart. Jour. Geol. Soc., 114, p. 367-393 (1959)

Walker, G. P. L. Bull. Volc., 29, p. 375-406 (1966)

Wasilewski, P. J. Jour. Geomag. Geoel., 20, p. 129-153 (1968)

Wasilewski, P. J. Jour. Geomag. Geoel., 21, p. 655-667 (1969)

Watkins, N. D. Nature, 206, p. 879-882 (1966)

Watkins, N. D., W. Cambray, and A. Richardson. EOS, 51, p. 270 (1970)

Watkins, N. D. and S. E. Haggerty. Geophys. Jour., 15, p. 305-315 (1968)

Watkins, N. D., T. Paster, and J. Ade-Hall. Earth Planet. Sci. Lett., 8, p. 322-328 (1970)

Watkins, N. D. and A. Richardson. Geophys. Jour., 16, p. 79-96 (1968)

Wegener, A. Die Entstehung der Kontinente und Ozeane, 4th revised ed. (1929). (English transl. by J. Biram, The origin of continents and Oceans. New York, Dover Publications, 246 p. (1966)

Wensink, H. Geol. en Mijnb., 43, p. 403-413 (1964)

Wilson, J. T. and D. B. Clarke. Nature, 205, p. 349-350 (1965)

Wilson, R. L. Geophys. Jour., 20, p. 1-9 (1970)

Wilson, R. L. Geophys. Jour., 22, p. 491-504 (1971)

Wilson, R. L., S. E. Haggerty, and N. D. Watkins. Geophys. Jour., 16, p. 79-96 (1968)

Wilson, R. L. and P. J. Smith. Jour. Geomag. Geoel., 20, p. 367-380 (1968)

Yukutake, T. Jour. Geomag. Geoel., 19, p. 103-117 (1967)

TABLE 3.1a

Remanence intensity of one sample from each flow of profile GL, Disko

Flow	$\overline{J}_o$ 10^{-3}G	J_{max} 10^{-3}G	AF (Oe)	$\overline{\Delta}$ 10^{-3}G	*In situ* VRM, 10^{-3}G
GL 20	3.55	4.25	50-100	-0.7	-0.9
19	-1.5	0.5	100	-2.0	-5.4
18	3.5	3.55	50	-0.05	-0.1
17	-1.7	1.0	100	-2.7	-4.0
16	4.65	4.7	100-150	-0.1	-0.1
15	-1.95	1.0	100	-2.95	-3.2
14	2.7	2.8	100	-0.1	-0.1
13	3.4	4.3	100	-0.9	-0.9
12	1.6	2.7	100	-1.05	-1.1
11	3.65	4.35	50	-0.7	-0.85
10	3.65	4.0	50-100	-0.35	-0.45
9	2.5	2.5	50-100	-0.05	-0.1
8	-1.8	0.45	50	-2.25	-3.2
7	-1.05	1.85	100	-2.9	-3.1
6	2.05	2.65	100	-0.6	-0.6
5	-1.0	0.7	50	-1.7	-2.35
4	-1.45	0.5	100	-1.95	-2.35
3	5.15	5.5	50	-0.35	-0.35
2	3.9	4.15	50-100	-0.25	-0.25
1	4.9	5.0	50	-0.1	-0.1
arithm.av.	1.7	2.8		-1.1	-1.5

... Cont.

TABLE 3.1b

Remanence intensity of one sample from each flow of profile GM, Disko

Flow	$\overline{J}_o$ 10^{-3}G	J_{max} 10^{-3}G	AF (Oe)	$\overline{\Delta}$ 10^{-3}G	*In situ* VRM, 10^{-3}G
GM 16	-1.1	1.2	100	-2.3	-2.7
15	9.2	9.2	50	0.0	0.0
14	-1.9	1.7	50-100	-3.6	-4.3
13	4.3	4.4	50	-0.1	-0.1
12	1.6	2.3	100	-0.7	-0.7
11	2.4	2.8	100-150	-0.4	-0.4
10	5.0	5.0	50	0.0	0.0
9	4.1	5.6	100-150	-1.5	-1.6
8	-1.15	1.3	50	-2.4	-3.0
7	-0.9	0.55	50	-1.5	-3.0
6A	3.4	3.6	50	-0.2	-0.5
6	4.3	4.3	50	0.0	-0.1
5	-0.8	0.9	100	-1.7	-2.8
4	0.6	1.2	50	-0.6	-3.0
3	-1.8	0.3	150-200	-2.1	-3.7
2	9.55	9.8	50	-0.25	-0.4
1	-1.95	1.4	100	-3.35	-3.6
arithm.av.	2.05	3.3		-1.2	-1.8

... Cont.

TABLE 3.1c

Remanence intensity of one sample from each of the flows of profile GK, the intrusives (GD) and the breccia (GR) sites in Disko

Unit	J_o 10^{-3}G	J_{max} 10^{-3}G	AF (Oe)	Rock type
GK 10	-1.4	1.1	50	
9	5.1	5.1	0	
8	4.0	4.0	0	
7	12.3	12.3	0	flows
6	26.6	26.6	0	
5	9.5(a)	9.5	0-50	
4	5.9(a)	5.9	0-50	
3	10.2(a)	10.2	0	
GK 2	4.2	4.9	50	
1	6.6	6.6	0	
GD 3A	2.4	3.15	50	sills
3	6.2	6.2	0	
2	1.7	1.9	150	
GD 1	7.0	7.4	50	dykes
4	33.0	33.0	0	
GR 7	6.0	(6.0)	?(b)	
6	8.9	(8.9)	?(b)	
5	4.3	4.3	0-50	
4	1.3(a)	2.5	50	breccia
3	5.7	5.75	0-50	
2	5.9	6.0	0-50	
1	22.0	22.2	0-50	

... Cont.

(a) Low inclinations

(b) Only demagnetized at 200 Oe

TABLE 3.1 (Continued)

This table shows the remanence intensity of one sample (the -1 sample) from each rock unit sampled in Disko.

$\overline{J}_o$ = the NRM intensity of each sample (usually one specimen per sample), positive for reverse magnetic polarity. The tabulated value is the average of two measurements, 4-6 weeks apart, during which interval the specimens were stored upside down in the earth's field (0.54 Oe)

J_{max} = the maximum reverse remanence intensity recorded during AF demagnetization in steps of 50 Oe. Slightly higher values of this variable would have been obtained by reading J_{max} off smoothed graphs such as those of Figs. 3-6 and 3-7

AF (Oe) = the peak field applied in the treatment after which J_{max} was recorded

$\overline{\Delta}$ = $\overline{J}_o - J_{max}$, the approximate intensity of the secondary (viscous) remanence component, assuming for simplicity that J_{max} and $\overline{\Delta}$ are antiparallel (as in Fig. 3-21), and that the VRM has been completely erased at the fields recorded in the previous column

In situ VRM = *in situ* viscous remanence intensity obtained by exponential extrapolation of the two measured values of $\overline{\Delta}$ back to the date of collecting. Note that $\overline{\Delta}$ could not be obtained for most of the class R' samples, where $J_{max} = J_o$

TABLE 3.2a

Remanence intensity (natural remanence and remanence after 200 Oe treatment) and susceptibility for all samples from profile GL, Disko

Sample	$\|J_o\|$ 10^{-3}G	J_{200} 10^{-3}G	K 10^{-3}G/Oe	C	Sample	$\|J_o\|$ 10^{-3}G	J_{200} 10^{-3}G	K 10^{-3}G/Oe	C
GL 1-1	4.9	3.2	1.8	R	GL 11-1	3.6	1.6	2.4	R
2	7.5	3.6	1.9	R	2	3.4	1.9	1.7	R?
3	4.2	0.9	1.7	R'	3	2.0	1.6	2.3	R
GL 2-1	3.9	3.6	2.9	R	GL 12-1	1.6	2.1	5.2	R
2	3.1	3.0	2.8	R	2	1.0	1.6	4.4	R?
3	4.0	3.5	3.7	R	3	3.4	3.3	2.9	R
GL 3-1	5.1	3.6	3.9	R	GL 13-1	3.4	3.8	2.8	R
2	5.7	3.7	3.4	R	2	1.3	1.6	3.0	R
3	5.3	4.2	4.0	R	3	4.4	4.6	3.0	R
GL 4-1	1.4	0.2	6.5	N	GL 14-1	2.7	2.7	3.4	R
2	0.9	1.4	5.7	R?	2	2.7	2.5	3.6	R
3	3.2	3.0	4.6	R	3	1.7	1.7	2.8	R
GL 5-1	1.0	0.3	6.6	N	GL 15-1	1.9	1.0	3.5	N
2	5.5	4.4	3.4	R	2	3.9	3.0	3.3	R
3	0.8	0.2	5.5	N	3	2.8	3.2	2.7	R
GL 6-1	2.0	1.9	4.2	R	GL 16-1	4.6	4.1	2.4	R
2	1.5	1.1	5.1	N	2	3.2	2.5	1.0	R
3	0.8	0.4	5.5	N	3	4.0	3.1	2.7	R
GL 7-1	1.0	1.5	2.9	N	GL 17-1	1.7	0.7	5.5	N
2	0.7	0.7	2.1	N	2	1.3	1.2	3.9	R?
3	5.0	4.1	2.3	R	3	1.1	0.5	4.9	N
GL 8-1	1.8	0.3	3.8	N	GL 18-1	3.5	3.2	1.8	R
2	0.5	0.9	2.9	N	2	3.3	2.7	2.1	R
3	1.0	1.1	2.7	R	3	2.7	2.3	0.9	R
GL 9-1	2.5	2.3	1.6	R	GL 19-1	1.5	0.3	7.6	N
2	2.9	2.4	1.7	R	2	1.5	0.7	8.0	N
3	3.8	3.2	1.5	R	3	3.4	2.5	3.2	R
GL 10-1	3.6	3.0	3.3	R	GL 20-1	3.6	3.0	4.8	R
2	5.0	4.1	2.3	R	2	4.5	4.1	2.2	R
3	1.2	0.4	3.6	N	3	5.3	4.5	2.1	R

... Cont.

TABLE 3.2b

Remanence intensity (natural remanence and remanence after 200 Oe treatment) and susceptibility for all samples from profile GM, Disko

Sample	$\|J_o\|$ 10^{-3}G	J_{200} 10^{-3}G	K 10^{-3}G/Oe	C	Sample	$\|J_o\|$ 10^{-3}G	J_{200} 10^{-3}G	K 10^{-3}G/Oe	C
GM 1-1	1.9	1.0	4.2	N	GM 9-1	4.1	5.0	3.6	R
2	5.2	3.8	2.6	R	2	6.1	5.2	2.2	R
GM 2-1	9.5	8.2	4.2	R	GM 10-1	5.0	4.0	1.6	R
2	6.3	5.6	3.1	R	2	5.6	5.0	3.4	R
GM 3-1	1.8	0.3	3.8	N	GM 11-1	2.4	2.7	2.8	R
2	5.2	3.4	2.4	R	2	2.3	2.2	3.1	R
GM 4-1	0.6	0.4	6.0	N	GM 12-1	1.6	1.8	3.5	R
2	1.6	0.3	5.7	N	2	3.4	3.1	1.3	R
GM 5-1	0.8	0.7	4.3	N	GM 13-1	4.3	3.3	1.7	R
2	2.4	0.1	3.4	N	2	4.5	3.5	1.4	R
GM 6-1	4.3	2.7	2.6	R	GM 14-1	1.9	1.2	3.7	N
2	2.5	1.6	2.5	R	2	7.2	5.9	3.7	R
GM 6A-1	3.4	2.8	3.0	R	GM 15-1	9.2	7.8	1.9	R
2	2.0	1.4	0.3	R	2	0.2	0.8	1.8	N
GM 7-1	0.9	0.2	4.2	N	GM 16-1	1.1	0.8	5.4	N
2	0.7	0.4	4.2	N	2	1.9	1.4	3.3	R
GM 8-1	1.1	0.6	3.1	N					
2	6.9	5.0	3.0	R					

... Cont.

TABLE 3.2c

Remanence intensity (natural remanence and remanence after 200 Oe treatment) and susceptibility for all samples from profile GK, from intrusives (GD) and breccia (GR) in Disko

Sample	$\|J_o\|$ 10^{-3}G	J_{200} 10^{-3}G	K 10^{-3}G/Oe	C	Sample	$\|J_o\|$ 10^{-3}G	J_{200} 10^{-3}G	K 10^{-3}G/Oe	C
GK 3-1	10.2	2.9	0.8	R'	GK 7-1	12.3	2.3	2.2	R'
2	9.1	2.8	0.8	R'	2	10.8	1.8	2.6	R'
GK 4-1	5.9	4.6	1.2	R'	GK 8-1	3.9	1.0	3.0	R'
2	5.8	5.1	3.2	R	2	3.2	0.8	2.9	R'
GK 5-1	9.5	7.3	2.8	R'	GK 9-1	5.1	0.6	2.0	R'
3	5.4	4.2	2.6	R	2	5.6	0.8	3.3	R'
GK 6-1	26.6	4.1	2.8	R'	GK10-1	1.4	0.4	2.3	N
2	20.6	5.1	3.0	R'	2	2.3	2.0	3.5	R
GK 1-1[a]	6.6	2.5	2.9	R	GK 2-1[a]	4.1	2.3	3.0	R
2	6.3	2.3	2.8	R	2	5.0	1.6	1.3	R'
GD 1-1	7.0	1.8	0.9	R'	GD 3-1	6.2	0.4	2.7	R'
2	7.1	2.1	0.8	R'	2	4.2	0.6	2.4	R'
GD 2-1	1.7	1.8	1.9	R	GD3A-1	2.4	1.6	3.5	R
2	1.4	1.8	2.7	R	2	4.1	0.9	3.9	R'
GD2A-1[b]	16.8	15.7	2.0	?	GD 4-1	23.3	3.3	2.8	R'
					2	12.3	0.4	2.9	R'
GR 1-1	22.1	4.7	0.9	R'	GR 4-1	1.3	1.1	2.1	N
2	9.8	2.0	1.1	R'					
3	13.8	6.7	0.7	R'?	GR 5-1	3.7	3.4	1.5	R
GR 2-1	5.9	1.8	0.9	R'	GR 6-1	8.9	2.1	0.9	R'
2	5.0	1.6	1.1	R'					
					GR 7-1	6.0	3.8	1.9	R'?
GR 3-1	5.7	2.6	0.8	R'	2	5.6	2.3	4.1	R'?
2	3.9	1.8	1.1	R'	3	3.6	2.9	2.6	R'?
AP 1[c]	1.7	1.2	4.3	R	LGK 3[c]	5.8	1.8	2.5	R'
GKS 1[c]	7.3	5.4	3.1	R					

TABLE 3.2 (Continued)

$|J_o|$ = measured NRM intensity, without regard to sign. In the case of -1 samples, this is the same as $|\overline{J}_o|$ of Table 3.1

J_{200} = intensity of remanence after 200 Oe AF treatment

K = volume susceptibility

C = inferred magnetic class (N for *in situ* normal polarity, R and R' for reverse polarity; see Sect. 3.4)

(a) = GK 1 and GK 2 are sills occurring at the base of profile GK

(b) = GD 2A is probably the same intrusive as GD 2, and this sample has not been used in the average of Table 3.3

(c) = Up-down oriented handsamples from isolated outcrops; see Sect. 3.2

TABLE 3.3

Some magnetic properties of igneous rocks on Disko

Rock group	N	n	$\lvert\overline{J}_o\rvert$ 10^{-3}G	$\overline{J}_{200}$ 10^{-3}G	$\overline{K}$ 10^{-3} G/Oe
GL flows	20	3	2.9	2.3	3.4
GM flows	17	2	3.5	2.7	3.1
GK flows	8	2	8.6	3.0	2.4
Breccia sites	7	1-3	6.5	2.7	1.5
2 dykes and 5 sills	7	2	6.6	1.7	2.4

Arithmetic averages of site-mean values are shown

N = no. of sites averaged

n = no. of samples measured per site (usually one specimen per sample)

$\lvert\overline{J}_o\rvert$ = NRM intensity (averaged without regard to sign); note a slightly different usage in Table 3.1

$\overline{J}_{200}$ = remanence intensity after 200 Oe demagnetization (all directions have reverse polarity)

$\overline{K}$ = volume susceptibility

TABLE 3.4

Mean remanence directions for two lava profiles on Disko

Profile	N	n	$\overline{D}$	$\overline{I}$	α_{95}	δ_k
GL	20	3	133	-64.4	7.0	16.6
GM	17	2	150	-69.2	9.6	20.5
Both	37	-	140	-66.7	5.7	19.0

All samples measured after AF treatment at 200 peak Oersteds

N = no. of flow-mean directions averaged

n = no. of samples measured per flow (usually one specimen per sample)

$\overline{D}$ = declination, degrees east of north

$\overline{I}$ = inclination, degrees positive down

α_{95} = radius of 95% confidence circle, degrees

δ_k = observed between-flow dispersion angle, degrees (Sanver, 1968)

The statistical parameter k (Sect. 2.9.2) for GL and GM together has the value 18.0.

TABLE 3.5

Remanence directions and intensities obtained by progressive AF demagnetization of Disko pilot samples

GL 5-2 (R) AF peak Oe	D	I	$\|J\|$ 10^{-3}G
NRM	92.2	-59.2	5.5
50	94.0	-62.0	5.9
100	94.7	-62.4	5.75
150	95.1	-62.8	5.1
200	94.5	-61.7	4.4
300	91.6	-63.9	3.0
400	89.8	-64.4	2.2
500	90.3	-63.9	1.72
600	90.6	-64.1	1.35
700	89.5	-64.1	1.14
800	88	-64	1.02
GL 8-2 (N) AF peak Oe	D	I	$\|J\|$ 10^{-3}G
NRM	148.9	+44.1	0.5
50	176.5	-42.8	0.5
100	178.8	-64.9	0.9
150	184.6	-69.9	0.92
200	181.8	-71.7	0.88
300	184.3	-69.6	0.61
400	179.3	-73.5	0.43
500	208.0	-67.2	0.26
600	217	-58.7	0.12
700	215	-69	0.16

... Cont.

TABLE 3.5 (Continued)

GL 10-1 (R) AF peak Oe	D	I	$\|J\|\ 10^{-3}G$
NRM	101.6	-51.2	3.65
50	101.2	-55.7	4.00
100	100.7	-57.7	3.98
200	104.1	-58.0	3.02
300	102.1	-58.4	2.0
400	101.7	-57.5	1.3
500	103.1	-57.6	0.9
600	102.9	-58.3	0.66
700	100.2	-58.1	0.51
800	104	-56	0.52
GL 15-1 (N) AF peak Oe	D	I	$\|J\|\ 10^{-3}G$
NRM	115.1	+63.6	1.95
50	121.6	+37.5	1.2
100	122.2	-14.3	1.0
150	122.4	-30.1	1.01
200	122.6	-36.4	0.97
250	122.8	-37.8	0.89
300	124.7	-37.8	0.75
400	130.1	-39.3	0.49
500	129.4	-38.5	0.26
600	122	-39	0.18

... Cont.

TABLE 3.5 (Continued)

GR 2-1 (R') AF peak Oe	D	I	$\|J\|$ 10^{-3}G
NRM	103.8	-59.2	5.9
50	100.6	-60.9	6.0
100	98.4	-59.1	4.5
150	98.3	-59.2	2.7
200	101.2	-57.7	1.8
300	103.9	-53.5	1.15
400	102.5	-55.0	0.80
500	95.4	-51.2	0.56
600	110.8	-54.7	0.38
700	72	-70	0.4
GK 9-1 (R') AF peak Oe	D	I	$\|J\|$ 10^{-3}G
NRM	172.1	-56.6	5.1
50	175.0	-57.4	3.2
100	179.4	-55.7	1.4
200	181.1	-55.0	0.6
300	180.5	-55.3	0.45
400	179.4	-53.6	0.32
500	184.5	-53.6	0.18
600	166	-73	0.17

D = declination, degrees east of north

I = inclination, degrees positive down

$|J|$ = remanence intensity (without regard to sign)

See figures 3-6 and 3-7

TABLE 3.6

Thermal demagnetization of Disko pilot samples

GL 5-4 (R) Temp. °C.	D	I	$\|J\|$ 10^{-3}G
NRM	111.6	-63.0	4.2
150	109.4	-64.1	4.4
250	111.4	-64.6	4.5
350	112.3	-66.0	3.6
430	110.8	-64.8	2.5
490	109.7	-67.1	2.1
540	108.6	-66.7	1.7
590	109	-68	0.5

GM 4-1x (N)	D	I	$\|J\|$ 10^{-3}G
	320	-25	0.54
	103	-86.3	0.54
	109	-82.5	1.05
	109	-84.7	0.95
	90	-84.8	0.58
	128	-79	0.36
	118	-73	0.17
	spurious		0.04

GD 1-3 (R') Temp. °C.	D	I	$\|J\|$ 10^{-3}G
NRM	106.3	-49.9	13.0
150	108.0	-50.9	12.2
250	104.6	-51.8	9.4
350	93	-50	0.23
430	90	-47	0.22
490	65	-56	0.18
540	62	-49	0.10
590	spurious		0.06

Legend: see Table 3.5

see also Figure 3-8

TABLE 3.7a

Paleomagnetic field directions obtained from samples of the flows of profile GL, Disko after 200 Oe AF treatment

Sample	D	I	Sample	D	I
GL 1-1	103.7	-59.9	GL 11-1	157.4	-49.5
2	103.5	-65.7	2	157.8	-47.7
3	103.9	-63.7	3	161.4	-50.0
GL 2-1	153.7	-82.6	GL 12-1	178.3	-61.9
2	170.9	-77.4	2	175.7	-59.7
3	164.0	-70.5	3	172.8	-68.4
GL 3-1	146.7	-78.9	GL 13-1	187.9	-70.7
2	164.0	-76.1	2	181.1	-67.6
3	216.3	-85.8	3	161.4	-69.9
GL 4-1	116.9	-70.3	GL 14-1	109.1	-47.1
2	122.9	-68.5	2	109.3	-48.7
3	133.1	-68.5	3	141.6	-60.3
GL 5-1	115.0	-57.9	GL 15-1	122.6	-36.4
2	94.5	-61.7	2	117.8	-46.4
3	108.6	-65.5	3	119.9	-43.1
GL 6-1	96.7	-61.9	GL 16-1	196.5	-65.9
2	102.1	-54.4	2	195.3	-71.8
3	101.2	-60.0	3	192.2	-74.4
GL 7-1	183.7	-60.7	GL 17-1	123.3	-40.2
2	174.7	-77.6	2	128.6	-47.3
3	164.9	-70.6	3	120.0	-45.0
GL 8-1	184.4	-65.9	GL 18-1	139.6	-59.5
2	181.8	-71.7	2	119.4	-59.3
3	184.7	-69.8	3	140.2	-56.4
GL 9-1	103.9	-57.5	GL 19-1	130.1	-44.2
2	99.1	-61.2	2	130.0	-49.6
3	94.3	-62.8	3	125.4	-53.9
GL 10-1	104.1	-58.0	GL 20-1	122.4	-62.4
2	103.6	-58.1	2	137.2	-63.3
3	105.4	-42.5	3	128.0	-64.0

... Cont.

TABLE 3.7b

Paleomagnetic field directions obtained from samples of the flows of profile GM, Disko, after 200 Oe AF treatment

Sample	D	I	Sample	D	I
GM 1-1	100.9	-50.1	GM 9-1	217.4	-70.0
2	97.9	-58.2	2	214.5	-62.3
GM 2-1	140.7	-71.5	GM 10-1	112.5	-41.8
2	145.1	-71.7	2	122.5	-48.3
GM 3-1	234.7	-63.8[a]	GM 11-1	117.4	-48.4
2	209.6	-72.4	2	113.9	-50.3
GM 4-1	108.8	-82.0	GM 12-1	195.5	-58.5
2	-105.6	-89.5	2	185.6	-68.8
GM 5-1	201.0	-68.7	GM 13-1	184.2	-69.3
2	182.2	-60.4	2	194.0	-69.1
GM 6-1	209.6	-79.5	GM 14-1	131.6	-47.5
2	228.0	-82.7	2	135.4	-57.5
GM 6A-1	97.8	-66.2	GM 15-1	199.2	-66.0
2	100.5	-55.6	2	185.3	-48.3[a]
GM 7-1	89.4	-54.2	GM 16-1	157.0	-65.9[a]
2	104.7	-57.1	2	150.6	-65.9
GM 8-1	174.2	-57.8			
2	175.6	-56.3			

(a) In these rather poorly stable samples, two specimens were averaged.

TABLE 3.7c

Paleomagnetic field directions obtained from samples of lava flows of profile GK, intrusives and breccia in Disko, after 200 Oe AF treatment

Sample	D	I	Sample	D	I
GK 3-1	183.3	-32.8	GK 7-1	120.2	-70.0
2	177.0	-33.0	2	132.4	-71.0
GK 4-1	160.9	-21.4	GK 8-1	156.8	-58.8
2	155.0	-32.0	2	171.5	-61.3
GK 5-1	158.0	- 7.1	GK 9-1	181.1	-55.0
3	154.4	- 8.4	2	179.0	-60.8
GK 6-1	146.7	-66.0	GK 10-1	172.7	-67.9
2	155.7	-65.3	2	181.6	-77.1
GK 1-1	357.0	-49.2	GK 2-1	316.5	-82.4
2	13.5	-51.6	2	332.0	-81.2
GR 1-1	98.2	-63.9	GR 3-1	101.8	-67.4
2	142.8	-64.2	2	107.1	-52.7
3	86.8	-52.5			
			GR 4-1	80.3	-69.4
GR 2-1	101.2	-57.7			
2	97.9	-57.2	GR 5-1	113.2	-80.8
GD 1-1	99.4	-49.3	GD 3-1	43.1	-64.1
2	109.6	-52.8	2	53.6	-57.3
GD 2-1	144.2	-59.1	GD 3A-1	74.0	-71.7
2	146.5	-55.5	2	54.0	-67.2

D = declination, degrees east of north

I = inclination, positive down

TABLE 3.8a

Flow-mean paleo-field directions after 200 Oe demagnetization, profiles GL and GM, Disko

Flow	D	I	δ_w	Flow	D	I	δ_w
GL 1	103.7	-63.1	2.4	GM 1	99.5	-54.2	4.1
2	164.3	-76.9	5.1	2	142.9	-71.6	0.6
3	164.1	-81.0	5.5	3	224.5	-68.6	6.3
4	124.4	-69.4	2.5	4	110.9	-86.2	4.2
5	106.3	-62.0	5.1	5	190.2	-64.8	5.7
6	100.2	-58.8	3.4	6	217.2	-81.2	2.1
7	175.8	-69.8	7.4	6A	99.4	-60.9	5.3
8	183.7	-69.1	2.5	7	96.8	-55.9	4.5
9	99.4	-60.6	3.0	8	174.9	-57.1	0.8
10	104.5	-52.9	7.3	9	215.7	-66.2	3.9
11	158.8	-49.1	1.6	10	117.2	-45.2	4.8
12	175.8	-63.3	3.8	11	115.7	-49.3	1.5
13	176.8	-69.8	4.1	12	191.5	-63.7	5.6
14	117.8	-52.9	10.5	13	189.1	-69.3	1.7
15	120.2	-42.1	4.5	14	133.3	-52.5	5.1
16	195.0	-70.7	3.6	15	190.6	-57.3	9.6
17	123.9	-44.2	3.9	16	153.8	-65.9	1.3
18	133.3	-58.8	5.2				
19	128.7	-49.3	4.2				
20	129.1	-63.4	2.8				

D = declination, degrees east of north

I = inclination, degrees positive down

δ_w = dispersion angle = $\cos^{-1}(R/N)$, degrees (Section 2.9)

Three samples were averaged per flow in profile GL, and two samples per flow in profile GM.

TABLE 3.8b

Site-mean paleo-field directions for GK-flows, intrusives and breccia, (where oriented samples were collected) after 200 Oe demagnetization.

flow		D	I	δ_w	n
GK	3	180.2	-32.9	6.4	2
	4	158.1	-26.6	14.7	2
	5	156.2	- 7.8	4.6	2
	6	151.3	-65.7	4.5	2
	7	126.2	-70.0	5.0	2
	8	163.8	-60.3	9.3	2
	9	180.1	-57.9	7.1	2
	10	176.0	-72.5	11.5	2
intrusive		D	I	δ_w	n
GK	1	5.1	-50.7	13.0	2
	2	324.8	-81.9	3.0	2
GD	1	104.3	-51.2	8.8	2
	2	145.4	-57.3	4.6	2
	3	48.9	-60.8	10.2	2
	3A	62.9	-69.7	9.9	2
breccia		D	I	δ_w	n
GR	1	106.0	-62.3	13.1	3
	2	99.5	-57.5	2.2	2
	3	105.0	-60.1	7.5	2
	4	80.3	-69.4	-	1
	5	113.2	-80.8	-	1

n = number of samples averaged

See legend to Table 3.8a

TABLE 3.9a

Thermomagnetic data for selected Disko basalt samples having high Curie points ($T_c > 500^oC$)

Sample	origin	C	Curie point (T_c, °C)		M'_o/M_o
			heating	cooling	
GL 8-2	flow	N	520	510	1.2
GL 15-1	"	N	260+510	510 (a)	1.5
GM 3-1	"	N	290+530	540	1.3
GM 4-1	"	N	530	?	1.1
GM 15-2	"	N	520	510	1.4
GL 5-2	"	R	560	560	1.2
GL 10-1A	"	R	550	550	1.3
GM 1-2	"	R	550	550	1.3
GM 12-2	"	R	570	565	~1 (b)
GK 5-1	"	R	560	560	1.4
GD 2A-1	sill	R	500	510	0.8

M_o,M'_o = sample moment at room temperature before and after heating; the maximum temperature reached was usually 20-40° above the T_c, and the applied field was in the range 400-600 Oe

C = magnetic class (Section 3.4)

The thermomagnetic curves generally have a small tail beyond the Curie temperature defined in Appendix 2.2; see Table 3.12 for data on two class R samples with T_c above 600°C

(a) This sample was also heated to a higher temperature (Sect. 3.9.6)

(b) A low-temperature hump occurred in the heating curve (Fig. 3-13)

TABLE 3.9b

Thermomagnetic data for selected Disko basalt samples having low Curie points ($T_c \leq 400^oC$)

Sample	origin	C	Curie point (T_c, ^oC) heating	Curie point (T_c, ^oC) cooling	M'_o/M_o
GD 1-2	dyke	R'	290	545	2.6 (a)(b)
GD 3-1	sill	R'	190	distributed	0.8
GD 4-2	dyke	R'	200	220	1.0
GR 2-1	breccia	R'	280	?	3.0 (a)
GR 7-3	"	R' or R	250	525	2.3 (b)
GK 6-1	flow	R'	265	500	1.0
GK 9-2	"	R'	405	520	1.3

M_o, M'_o: see Table 3.9a; the maximum temperature reached was usually about 600^oC, and the applied field in the electromagnet was in the range 500-1000 Oe

C = magnetic class (Section 3.4)

? = this quantity was not measured

(a) Measured with the ballistic magnetometer (saturation moment)

(b) Rapid chemical changes were taking place at T_c on heating

TABLE 3.10

Results from ballistic magnetometer measurements on Disko basalt specimens

Sample	T_c, °C	C	D_s, cm	atn.	length, cm	vol., cc	eq.% mt.	H', Oe
GL 4-2	520?	N	18.3	4	2.0	7.3	(2.41)	780
GM 3-1	300+530	N	11.7	4	1.95	7.8	(1.44)	700
GM 15-2	520	N	26.4	1	2.02	8.0	(0.82)	840
GL 2-2	560?	R	26.8	2	2.1	8.0	(1.52)	1210
GL 12-3	560?	R	17.9	4	2.4	9.1	(1.90)	980
GM 1-2	550	R	20.7	2	1.92	6.8	(1.38)	830
GK 6-1	265	R'	16	2	1.8	6.9	(1.06)	∿600
GR 2-1	280	R'	8	2	1.9	6.6	(0.56)	∿700
-"-	heated to 600°C		25	2	"	"	1.35	∿1000
GR 7-3	250	R or R'	14.5	1	2.1	8.4	(0.43)	∿700
GD 1-2	290	R'	12.5	1	1.75	6.7	(0.46)	∿600
-"-	heated to 600°C		18.0	2	"	"	1.22	720
-"-	do.700°C		17	2	"	"	1.17	∿1000

T_c = Curie point (on heating), with a question mark at those which were not measured but inferred from results on magnetically similar samples

C = magnetic class (Sect. 3.4)

D_s = saturation deflection, estimated graphically from measurements of ballistic magnetometer deflections at seven values of applied field intensity, using equation (2.2)

atn. = attenuation setting of the magnetometer (Appendix 2.1)

length = length of the specimen, used in obtaining a correction factor for the deflection (Appendix 2.1)

vol. = volume of the specimen

... Cont.

TABLE 3.10 (Continued)

eq.% mt. = that content of pure magnetite in the specimen, in volume per cent, which would have given the same saturation deflection of the magnetometer as the actual specimen. Values in brackets correspond to specimens from samples which are not known to contain pure magnetite as the only magnetic constituent (cf. Sect. 2.7)

H' = the characteristic field at which 63% of the specimen saturation magnetization is reached (eq. 2.2)

TABLE 3.11

The remanence intensity and susceptibility of samples from partial vertical sections through two Disko lavas

Flow GL 5	position	$\lvert J_o \rvert$ 10^{-3}G	K 10^{-3}G/Oe	C
(top of flow)	perhaps 5 m above 5-4 E			
GL 5-4 E	1.5 m above GL 5-4 D	1.6	7.4	N
GL 5-4 D	0.9 " C	1.9	3.3	N
GL 5-4 C	1.1 " B	4.7	2.1	R
GL 5-4 B	0.9 " A	1.2	3.9	N
GL 5-4 A	0.8 " 5-4	0.7	4.1	N
GL 5-4	about 2 m above contact	3.9	3.3	R
Flow GM 13				
(top of flow)	perhaps 10 m above 13-3 F			
GM 13-3 F	2.2 m above GM 13-3 E	5.1	1.3	R
GM 13-3 E	2.2 " D	8.5	2.5	R
GM 13-3 D	2.2 " C	0.4	1.4	N
GM 13-3 C	2.2 " B	0.1	3.6	N
GM 13-3 B	1.5 " A	3.0	3.1	N
GM 13-3 A	1.4 " 13-3	5.2	1.5	R
GM 13-3	1.5 m above contact	5.1	3.2	R

J_o = NRM intensity, without regard to sign

K = volume susceptibility

C = magnetic class (in-situ NRM polarity)

TABLE 3.12

Thermomagnetic data for interbasaltic red sediments and highly reddened flow tops, Disko and Iceland

Sample	origin	locality	Curie point (T_c, °C)		M'_o/M_o
			heating	cooling	
GL 9 - GL 10	red sed.	Disko	600	600	0.8
GM 6A-2	flow top	Disko	615	590	0.9
GM 14-3	flow top	Disko	605	585	0.7
Hamar	red sed.	Iceland	600	600	0.8
N BRC[(a)]	red sed.	Iceland	~600	620	0.9
IS BRC[(a)]	red sed.	Iceland	620	615	0.9

M'_o, M_o: see legend to Table 3.9

(a) Measured by Kristjansson (1967)

TABLE 3.13

Summary of differences in various magnetic properties for three classes of magnetic behaviour in 147 basalt samples from Disko Island

(a) Number of samples whose remanence was measured:

	N samples	R samples	R' samples
Profile GL:	15	44[a]	1
GM:	12	32	0
GK:	1	5	10
Intrusives	0	6	8
Breccia	1	2	10[a]

(b) Average magnetic properties:

	Profiles GL and GM only			Number of samples
NRM polarity	Normal	Reverse	Reverse	
Susceptibility	$4.7 \cdot 10^{-3}$	$3.0 \cdot 10^{-3}$	$2.1 \cdot 10^{-3}$	all (147)
Primary remanence	$1.0 \cdot 10^{-3}$	$4.5 \cdot 10^{-3}$	$9.6 \cdot 10^{-3}$	-1 samples (59)
In-situ VRM	$3.3 \cdot 10^{-3}$	$0.4 \cdot 10^{-3}$	$\tilde{<} .1 \cdot 10^{-3}$	-1 samples (59)
Opaque content	6-7%	6-7%	4-5%	14
Oxidation index	4	1-2	1	16
Curie point	560°C	low+520°C	200-300°C	16
Q_t-ratio	9	7	<10	14
J_{200}/J_o	< 0	always > 0.4	0-0.4	all (147)
Parameter H'	800 Oe	1000 Oe	$\leq$ 700 Oe	10

(a) Includes a few samples of uncertain class.

The remanence and susceptibility values are given in units of Gauss and Gauss/Oe respectively. A diagram, showing the relative magnitudes of the primary remanence, the viscous remanence and the induced magnetization in the average sample of each class, is given in Fig. 3-21.

TABLE 4.1a

Remanence directions and intensities obtained by progressive AF demagnetization of pilot specimens from Cape Dyer lava flows (C. R. Somayajulu).

Specimen 1-2-1				Specimen 2-1-5		
AF peak Oe	D	I	J/J_o	D	I	J/J_o
NRM	320.1	+76.1	(J_o=3.4.10^{-3}G)	99.0	+85.7	(J_o=2.14.10^{-3}G)
25	319.9	+76.1	1.00	97.0	+85.7	0.95
50	319.9	+76.1	0.99	91.0	+85.7	0.92
100	319.5	+76.3	0.96	75.9	+85.2	0.79
150	319.9	+76.3	0.91	69.4	+84.7	0.62
200	319.2	+76.3	0.80	66.2	+85.0	0.50
300	318.3	+76.2	0.73	68.8	+84.6	0.33
400	320.9	+76.8	0.60	73.5	+85.0	0.23
500	321.8	+75.5	0.52	54.0	+83.6	0.15
600	307.7	+78.9	0.41	63.4	+83.6	0.12
700	301.2	+70.0	0.30	55.7	+83.5	0.08
800	237.9	+77.1	0.22	152	+82.3	0.06
900	208.2	+72.3	0.18	67	+81.9	0.05
Specimen 4-3-2				Specimen 5-3-1		
NRM	52.0	+81.5	(J_o=5.5.10^{-3}G)	22.3	+78.2	(J_o=7.6.10^{-3}G)
25	52.2	+81.6	1.01	21.4	+78.6	1.01
50	52.0	+81.2	0.92	22.5	+78.3	1.00
100	51.1	+81.2	0.66	22.7	+78.3	0.95
150	51.5	+81.3	0.45	21.8	+78.3	0.85
200	51.3	+81.4	0.31	21.6	+78.1	0.72
300	50.8	+81.1	0.18	22.5	+78.5	0.49
400	51.9	+80.3	0.12	21.7	+78.1	0.39
500	45.2	+80.5	0.09	19.0	+78.3	0.31
600	69.6	+80.4	0.07	22.5	+77.8	0.27
700	44.3	+81.3	0.05	20.6	+78.8	0.23
800	52.0	+76.4	0.04	23.2	+76.7	0.19
900	47.5	+72.6	0.03	22.4	+76.7	0.17

... Cont.

TABLE 4.1a (Continued)

Specimen 6-1-1 (orientation uncertain)					Specimen 3-4-3 (3^{-})		
AF peak Oe	D	I	J/J_o		D	I	J/J_o
NRM	250.1	+66.7	(J_o=5.7.10^{-3}G)		208.0	-82.4	(J_o=3.1.10^{-3}G)
25	250.2	+66.8	0.99		213.1	-81.5	1.02
50	249.8	+66.7	0.96		212.9	-81.5	0.99
100	248.9	+66.4	0.90		212.3	-81.4	0.82
150	248.9	+66.4	0.85		211.0	-81.4	0.65
200	248.3	+66.7	0.77		211.8	-81.0	0.51
300	248.0	+68.2	0.63		212.1	-81.8	0.31
400	247.0	+71.1	0.51		197.0	-77.4	0.21
500	244.3	+71.8	0.42		229.5	-74.5	0.14
600	244.2	+74.4	0.34		229.5	-69.1	0.10
700	243.2	+72.9	0.28		110.3	-68.1	0.07
800	256.8	+74.2	0.19		193.8	-47.0	0.05
900	257.7	+74.5	0.15		110.2	-56.2	0.03
Specimen 3-2-1, cooled in the earth's field from 600°C. (LK)							
TRM	87.6	+70.7	(J_o=15.3.10^{-3}G)				
100	87.8	+70.3	0.96				
200	88.1	+70.4	0.85				
350	88.3	+70.6	0.63				
500	88.1	+71.2	0.45				
700	95.5	+70.6	0.28				

... Cont.

TABLE 4.1b

Supplementary AF demagnetization results to 400 Oe peak field (LK).

Specimen 1-5-2a				Specimen 2-4-2		
AF peak Oe	D	I	J/J_o	D	I	J/J_o
NRM	313.4	+74.4	($J_o = 3.4.10^{-3}$G)	16.0	+76.0	($J_o = 1.9.10^{-3}$G)
50	313.4	+74.3	0.97	20.3	+74.7	0.88
100	313.4	+74.5	0.91	21.2	+74.2	0.72
200	313.8	+74.9	0.80	22.2	+72.3	0.53
300	313.8	+75.0	0.56	22.4	+74.4	0.41
400	319.0	+74.5	0.39	19.6	+74.3	0.33
Specimen 3-6-3				Specimen 4-6-X(unoriented)		
NRM	71.7	+84.1	($J_o = 2.6.10^{-3}$G)	63.1	+80.0	($J_o = 2.4.10^{-3}$G)
50	74.7	+83.9	0.97	62.8	+79.9	0.99
100	77.3	+84.2	0.84	62.1	+79.9	0.97
200	80.3	+83.8	0.73	61.2	+79.7	0.88
300	79.6	+83.9	0.49	64.5	+80.0	0.74
400	64.5	+84.3	0.36	63.4	+80.3	0.64
Specimen 5-6-2				Specimen 6-5-1 (orientation uncertain)		
NRM	34.8	+79.5	($J_o = 9.4.10^{-3}$G)	40.5	+61.7	($J_o = 3.3.10^{-3}$G)
50	32.6	+79.3	0.99	40.4	+60.8	0.94
100	32.2	+79.3	0.96	40.8	+60.7	0.90
200	31.2	+79.3	0.76	40.1	+60.7	0.74
300	34.6	+79.7	0.48	37.3	+62.7	0.55
400	39.8	+79.8	0.30	40.1	+64.6	0.42

D = declination, degrees (east of north in oriented samples)

I = inclination, degrees positive down

Fig. 4-1 plots J as a function of demagnetizing field for the first six specimens of Table 4.1

NRM values are the average of two measurements.

TABLE 4.2

Magnetic remanence results - Cape Dyer sample averages

Sample	NRM			after 400 Oe treatment			
	J_o	D	I	J_{400}	D	I	δ_s
DY 1-1	3.0	342.7	+75.2	1.6	323.4	+75.2	1.5
2	3.1	317.5	+76.3	1.8	318.5	+76.7	1.1
3	2.5	306.7	+75.4	1.5	305.6	+75.7	2.0
4	2.2	286.4	+78.5	1.2	287.4	+78.4	2.1
5	3.2	300.6	+75.3	1.3	299.8	+76.0	4.3
6	3.5	possibly error in orientation in field					
DY 2-1	2.1	116.4	+85.6	0.5	82.3	+84.2	2.2
2	4.0	341.1	+87.2	1.0	348.8	+82.3	0.9
3	3.0	15.6	+78.0	0.7	16.1	+74.6	7.3
4	2.6	24.5	+76.3	0.7	20.2	+74.9	1.2
5	(1.0)	intensity low and variable in sample					
6	1.4	31.2	+82.5	0.4	31.2	+80.6	0.7
DY 3-1	1.0	30.6	+85.2	0.5	33.9	+80.4	5.4
2	3.6	352.2	-70.0	1.2	359.8	-69.9	6.3
3	3.0	219.0	-79.6	0.8	202.0	-74.2	4.8
4	2.1	218.0	-78.9	opposite specimen polarities			
5	1.7	314.9	+86.7	1.0	341.1	+86.3	9.2
6	3.0	78.1	+83.5	1.0	72.0	+83.0	3.4

TABLE 4.2 (Continued)

Sample	NRM			after 400 Oe treatment			
	J_o	D	I	J_{400}	D	I	δ
DY 4-1	2.2	possibly error in orientation in field[a]					
2	2.1	16.5	+81.5	0.2	357.1	+81.5	0.7
3	5.6	49.9	+81.6	0.7	48.5	+80.7	1.4
4	1.4	0.0	+72.8	0.7	10.8	+73.4	4.1
5	4.2	0.8	+77.5	2.5	354.7	+77.5	4.2
6	2.4	21.3	+79.3	1.5	16.1	+78.9	3.3
DY 5-1	59	339.3	+85.4	16	339.3	+84.1	0.9
2	6.7	small, crumbly sample - omitted					
3	7.7	21.9	+77.8	3.0	21.0	+77.9	0.5
4	4.7	24.8	+80.3	1.9	19.3	+80.2	0.4
5	10.5	12.6	+81.3	2.0	9.7	+81.3	3.8
6	10.7	37.8	+79.1	3.9	39.9	+79.0	1.7
DY 6-1	5.7			2.9			
2	6.6	inclinations		3.3			
3	6.4	about +70°		3.2			
4	6.0	declinations		2.9			
5	3.3	scattered		1.4			
8	2.7			1.3			

J_o = natural remanence intensity, in 10^{-3} Gauss

J_{400} = remanence intensity after 400 peak Oe

D = declination, degrees east of north

I = inclination, degrees positive down

δ_s = half-angle between specimen directions, degrees

Two specimens were measured per sample and averaged

(a) J_{400} in one specimen = $0.18.10^{-3}$Gauss

TABLE 4.3

Some magnetic properties of Cape Dyer basalts - summary

Flow	N	J_o 10^{-3}G	direction of NRM			direction after 400 Oe treatment				J_{400}/J_0	K 10^{-3} G/Oe	VRM
			D	I	k	D	I	k	δ_w			
1	5	2.9	308	+77	480	308	+77	528	3.1	0.54	0.4	no
2	5	2.3	27	+83	154	22	+80	158	5.8	0.25	0.2	yes
$3^{+(a)}$	3	1.9	40	+87	313	39	+84	244	4.2	0.50	0.2	yes
$3^{-(a)}$	3	2.9	(— ∿ -75			Poor stability				—)	0.1	yes
4	6	3.0	14	+79	242	12	+79	263	4.4	0.36[b]	0.5	no
5	5	7.9	20	+81	425	18	+81	415	3.6	0.34	1.0	no
6	5	5.1	(— ∿ +70		—	—	—	—[c]		0.48	1.3	no

... Continued

TABLE 4.3 (Continued)

N = number of samples (usually two specimens measured per sample)

J_0 = intensity of natural remanence (NRM)

D = declination, degrees east of north

I = inclination, degrees positive downward

k = Fisher's precision parameter

δ_w = dispersion angle, degrees (Sanver, 1968)

J_{400} = intensity of remanence after AF demagnetization to 400 peak Oersteds

K = initial volume susceptibility

VRM = viscous remanence; "yes" if VRM is found to build up in specimens on storage

(a) 3^+, 3^- = flow 3, the sign denoting samples having positive or negative NRM inclinations

(b) two distinct stability groups were found, one averaging $J_{400}/J_0 = 0.11$, the other 0.60

(c) not used in the paleomagnetic analysis

TABLE 4.4

Thermal demagnetization results - Cape Dyer.

Specimen 1-3-7 (unoriented)			
Temp. °C.	D	I	J/J_o
NRM	57.0	+75.0	(J_o=2.64.10^{-3}G)
210	53.4	+75.3	0.96
365	55.1	+75.1	0.80
440	54.5	+75.1	0.54
515	55.0	+74.9	0.35
600	56.4	+74.4	0.17
610	55.9	+72.7	0.12
630	64.6	+73.2	0.08

Specimen 2-5-X (unoriented)		
D	I	J/J_o
27.1	+80.8	(J_o=0.7.10^{-3}G)
25.4	+79.2	0.71
44.1	+79.4	0.52
29.6	+78.6	0.42
34.6	+78.2	0.14
unstable		<0.05

Specimen 4-6-X (unoriented)			
NRM	2.3	+80.0	(J_o=2.3.10^{-3}G)
210	1.7	+80.4	0.97
365	1.5	+80.3	0.83
440	1.8	+80.4	0.70
515	7.3	+80.4	0.51
600	6.5	+80.8	0.19
610	6.5	+79.1	0.14
630	35.8	+81.2	0.08

For specimens from flow 3, refer to Table 4.5

Specimen 5-3-X (unoriented)			
NRM	62.8	+80.6	(J_o=7.6.10^{-3}G)
210	59.4	+80.6	0.94
365	60.0	+80.6	0.83
440	57.6	+80.9	0.72
515	57.8	+80.8	0.56
600	50.4	+81.5	0.15
610	44.3	+81.7	0.06
630	71.2	+81.5	0.03

Specimen 6-3-2 (unoriented)		
47.3	+73.7	(J_o=1.5.10^{-3}G)
47.3	+73.7	0.81
29.4	+81.2	0.76
50.0	+73.0	0.74
48.0	+66.5	0.20
unstable		

TABLE 4.5

Thermal demagnetization results for Cape Dyer specimens from flow 3

Temperature °C	Specimen 3-1-2a			Specimen 3-2-4			Specimen 3-4-4			Specimen 3-6-3a		
	D	I	J	D	I	J	D	I	J	D	I	J
NRM	123	+87	0.9	336	-70	3.9	225	-80	3.1	65	+82	2.7
160	47	+87	0.9	332	-71	3.2	222	-80	3.0	62	+81	2.5
230	76	+86	0.5	329	-73	0.74	220	-80	2.6	60	+81	1.9
300	11	+83	0.6	332	-70	0.55	147	+71	0.04	56	+80	1.2
300 (repeat)				161 (decreasing Z later)	+68	0.18						
360	343	+84	0.55				41	+83	0.3	68	+81	1.0
540	?	?	0.2							VRM?		0.3

J = remanence intensity, 10^{-3} Gauss

D = declination, degrees east of north

I = inclination, degrees positive down

TABLE 4.6

Susceptibility of Cape Dyer samples

Flow\sample	1	2	3	4	5	6
1	(0.51)	(0.43)	(0.36)	0.31	0.56	(0.38)
2	(0.17)	0.34	0.26	(0.16)	(0.14)	(0.13)
3	0.15	0.17[a]	(0.10)	(0.10)	0.13	0.42
4	(0.33)	0.41	1.1	0.18	(0.81)	(0.32)
5	(2.2)	(0.82)	1.0	0.74	1.1	0.98
6	(1.4)	(1.5)	irregular cores			(1.2)[b]

All susceptibility values are in units of 10^{-3}G/Oe

Values in brackets were measured on single specimens and are less accurate than the others; see Sect. 2.6.1

The susceptibility of the specimens 6-1, 2, 3, 4 together was $1.5 \cdot 10^{-3}$G/Oe, and that of 6-5, 8 was $0.95 \cdot 10^{-3}$G/Oe

(a) On heating of two specimens from sample 3-2 to 600°C in air, their susceptibility increased to $1.2 \cdot 10^{-3}$G/Oe

(b) This is specimen 6-8, which was measured instead of 6-6

TABLE 4.7

Artificial thermal remanence of Cape Dyer basalt

Specimen	J_o	J_{th}	H_p	r	H_{pc}
1-4-1	2.18	2.02	0.45	0.75	0.34
1-5-2a	3.38	3.7	0.39	0.95	0.37
4-3-3	5.68	9.48	0.26	1.1	0.29
4-4-2	1.36	1.04	0.56	0.8	0.45
5-4-1	4.89	2.42	0.87	1.1	0.96
5-5-2	9.92	0.83	5.1	discarded	
6-4-1	5.97	6.33	0.41	1.0 (a)	0.41
6-8-1	2.7	3.8	0.31	1.0 (b)	0.31

J_o = NRM intensity, 10^{-3} Gauss

J_{th} = TRM intensity after cooling in 0.43 Oe field from 580°C, 10^{-3}G

H_p = paleofield inferred by direct proportions, Oe

r = M'_o/M_o (Table 4.8)

$H_{pc} = r \cdot H_p$ = paleofield intensity corrected for changes in magnetic mineral on heating, Oe

(a) Material for thermomagnetic work was not available; result from the thermomagnetic curve of 6-5 was used

(b) The thermomagnetic curve is not reversible (cf. Fig. 4-7) and the susceptibility of the specimen dropped by 13% on heating

Note: as J_o in DY 4-3 is much softer to AF than that in DY 4-4, the lower H_p values obtained from the former could be due to NRM decay in time

TABLE 4.8

Thermomagnetic data on selected Cape Dyer basalt samples

Sample	type of curve	Curie point (T_c, °C)		M'_o/M_o
		heating	cooling	
1-4	7 rl	555	550	0.75
1-5	7 rl	570	560	0.95
2-2	8 r	290	550	2.4
2-3	9 r	250	505	2
2-6	8 l	305+ tail	545	1.6
3-1	9 l	265	560	3.8
3-2	9 r	315	550	5 (a)
3-3	9 r	270	540	6
3-4	9 r	260	?	?
3-5	9 l	235	?	?
3-6	8,9 l	260+ tail	560	> 2
4-1	7 l	540	540	1.1
4-3	7 l	555	565	1.1
4-4	7 lr	$\geq$580	$\geq$580	0.8
4-6	7 lr	595	585	0.8
5-1	7 l	555	555	1.0
5-3	7 l	575	565	1.0
6-5	7 r	565	distr. to 590	1.0
6-8	7 r	530	530	1.0

For legend, see Table 3-9

(a) Moment change M'_o/M_o also measured with the ballistic magnetometer, giving a 5.5 fold increase in saturation moment

"Type of curve" refers to Fig. 4-7 (7), 4-8 (8) or 4-9 (9), right-hand (r) or left-hand (l) side

TABLE 4.9

Results from ballistic magnetometer measurements
on Cape Dyer lava samples

Sample	T_c, °C	D_s cm	length, cm	vol., cm^3	eq.% mt.	H', Oe
1-4	555	4.5	1.95	7.8	0.14	1100
1-5	570	9.0	1.95	7.8	0.28	1000
3-2	315	3.1	2.1	8.5	(0.09)	~1200
"	heated to 600°C	17	"	"	0.50 (a)	~ 750
3-6	260+560	5.2	1.9	7.6	(0.17)	600
4-1	540	5.2	2.0	8.1	0.16	950
4-6	590	6.3	2.05	8.2	0.19	~1500
5-6	560?	15	1.7	6.8	0.55	1350
6-8	530	18.7	2.2	8.3	0.56	900

Legend: See Table 3.10

(a) Another specimen from the same sample was also heated to 600°C and measured, giving 0.44% magnetite content, and H'=850 Oe

TABLE 4.10

(a) The magnetic properties of olivine basalt samples from Baffin Island, collected by D. B. Clarke

Sample	locality	weight gm	est. dens. g/cc	vol. cc	J_o 10^{-3}G	K 10^{-3}G/Oe	J_{100/J_o}
PP 11	?	17.3	2.7	6.4	0.53	0.06	0.64
5	?	18.6	2.7	7.0	0.02	0.02	0.70
G10	?	13.8	2.9	4.8	2.8	0.29	0.51
GB 15	Durban Is.	16.7	2.7	6.2	3.4	0.38	0.80
DX 9	Padloping	12.2	2.7	4.5	6.7	0.64	0.87
ROR	?	19.2	2.7	7.1	0.52	0.08	0.89
R 77	Reid's Bay	12.5	2.8	4.5	3.4	1.8	0.99
NN	?	7.0	2.7	2.6	2.0	0.40	0.74
	Average of eight samples				2.3	0.46	

(b) Magnetic properties of rock samples from Svartenhuk

		J_o	K	J_{100/J_o}
508	felsparph. sill	8.0	2.5	0.69
529	thick picrite flow	0.7	0.20	0.98
593	thin " "	2.9	0.40	0.95
581	felsparph. flow	4.4	1.1	0.95
671	picrite sill	1.6	2.7	0.36

Legend: see Table 3.2

est. dens. = estimated density

vol. = volume, calculated from the weight and density

TABLE 4.11

Some Lower Tertiary paleomagnetic studies in North America

(a) North America Oligocene

	no. of units	no. of samples	age m.y.	treat-ment	pole position: north lat.	pole position: east long.	polarity
Mary's Peak sill (Clark 1971)	1	200	30	400 Oe	63°	196°	N
Buck Hill volc. (Gilliland et al. 1969)	22	140	27-36	AF	82°	80°	N+R
Arizona volc. (Grommé and McKee 1970)	67	?	22-37	AF	78°	146°	?
(b) North American Eocene-Paleocene (Fig. 4-4)							
Green River sed.	1	7		?	78°	202°	N
Siletz River flows	8	57		225°C	37°	311°	N+R
Beaverhead flows	4	?		100-450 Oe	66°	239°	N
Flagstaff intrus.	1	15		AF	72°	194°	R
Spanish Peaks dykes	6	39		AF	81°	211°	N
Golden flows	3	15		250 Oe	76°	63°	R
Cape Dyer flows	5	24		400 Oe	83°	305°	N

TABLE 5.1

Estimated *in-situ* intensity of magnetization of two Disko lava profiles

Component	Intensity, 10^{-3} G		Net sense
	GL	GM	
Observed NRM, J_o	1.7	2.1	reverse
Primary remanence, J_p	2.8	3.3	reverse
In-situ VRM, J_v	1.5	1.8	normal
In-situ NRM, J_n	1.3	1.5	reverse
In-situ induced magnetization, J_i	2.2	2.0	normal
Total *in-situ* magnetization, J_t	0.9	0.5	normal

The arithmetic average of N flow intensity values in each profile (Table 3.3) is shown; one sample was measured per flow.

J_o is the mean of two measurements (Table 3.1).

J_p is the maximum J in the AF curve (Fig. 3.6).

J_v was obtained by extrapolation in time.

$J_n = J_p + J_v$

$J_i = KF$, where K is the volume susceptibility and F the present field at Disko (0.560e).

$J_t = J_n + J_i$

TABLE 5.2

Estimated average *in-situ* magnetization of some igneous rocks on Disko

Component	Intensity 10^{-3} G	Net sense
Primary remanence, J_p	7.3	reverse
In-situ VRM, J_v estimated	0.5	normal
In-situ induced magnetization, J_i	1.2	normal
Total *in-situ* magnetization, J_t	5.6	reverse

The arithmetic average of 22 site-mean intensity values (lava profile GK, breccia and intrusives; Table 3.3) is shown. For most sites, 2 samples were averaged. See also explanatory notes, Table 5.1. Of the 22 samples from these sites, 2 are class N, 8 class R and 12 are R´.

TABLE 5.3a

Magnetic properties of gneiss samples collected at Baffin Bay sites

No.	Description	Type of site	Locality	K_3 10^{-3} G /Oe	J_8, 10^{-3} G
GG 0	Granodiorite	glacial drift	Narssarssuaq	<0.01	0.003
1	granitic	road cut	Narssarssuaq	0.07	0.02
3	anorthositic rock	road cut	Narssarssuaq harbour	5.7	7.4
4	pyroxenite, fine-grained	road cut	Narssarssuaq harbour	7.0	0.40
5	granite (supracrustal)	sea cliffs	Julianehåb	0.10	0.02
6	basic (?) dark	blasting	Julianehåb	1.4	0.21↑
7	granitic gneiss	blasting	Julianehåb	2.0	0.35↑
8	horneblende schist	blasting	Julianehåb	0.10	0.015↑
9	epidiorite	blasting	Julianehåb	0.6	0.03↑
10	granodiorite	blasting	Julianehåb	1.9	0.15↑
11	hornblende schist	construction	Frederikshåb	0.09	0.05↑
12	dioritic	construction	Frederikshåb	0.40	0.03↑
13	dioritic	road cut	Godthåb	0.27	0.10↑
14	gneiss	blasting	Söndre Ström.	0.46	0.07↑
15	biotite gneiss	glacial drift	Söndre Ström.	0.83	0.04↑
17	biotite gneiss	road cut	Egedesminde	<0.01	0.01↑
18	granodiorite gneiss (with aplite)	road cut	Egedesminde	0.20	0.09↑
21	granodiorite with biotite	blasting	Jakobshavn	0.58	0.03↑
20	granite gneiss	construction	Jakobshavn	0.26	0.04↑

TABLE 5.3a (cont.)

No.	Description	Type of site	Locality	K 10^{-3}G /Oe	J_o 10^{-3} G
22	granodiorite with biotite	road cut	Godhavn	0.36	0.04
23	hornblende granite gneiss	hills	Godhavn	0.03	0.01
24	granodiorite with biotite	road cut	Godhavn	0.93	0.05↑
25	dioritic	hills	Godhavn	0.03	0.01
26	foliated granodiorite	construction	Godhavn	0.31	0.01
30	igneous (anorthositic?)	hills	Cape Dyer	2.1	1.1
31	schistose biotite-feldspar	glacial drift	Cape Dyer	0.02	0.00
32	granodiorite-gneiss	hills	Cape Dyer	0.26	0.03
34	not determined	shore line	Broughton Island	0.05	0.01↑

The rocks were collected in 1970 in west Greenland (samples GG 0-26) and Baffin Island (GG 30-34). Descriptions are by Dr. J. S. Sutton, Geology Department, Memorial University, from the hand samples. K (volume susceptibility) and J_o (NRM intensity) were measured on 2.2 cm. diameter cylinders 1.5-2.8 cm. long. Arrows indicate rocks that were oriented in the field; they were all normally magnetized. The two Narssaq samples are classed as anorthosite/ultrabasic in Fig. 5.1b.

TABLE 5.3b

Magnetic properties of rock samples from Labrador, Baffin Island and West Greenland

Sample No.	Description	K, 10^{-3} Gauss/Oe	J_o, 10^{-3} Gauss/Oe	density, gm/cc
Labrador coast[a]				
BN 4	Metavolcanic or mafic	9.1	3.6	
F 2	gneiss, coarse-grained	0.09	0.16	
F 92A	gneiss, coarse-grained	2.9	0.65	
F 115	gneiss, coarse-grained	<0.01	0.002	
F 145A	gneiss, coarse-grained, foliated	0.02	0.003	
K 37	gneiss, coarse-grained	0.04	0.002	
K 37A	gneiss, coarse-grained	0.04	0.001	
K 138	gneiss, coarse-grained	0.04	0.004	
K 143A	gneiss, coarse-grained	0.04	0.002	
K 220	metasediment, pale fine-grained	0.42	0.02	
Frobisher Bay, Baffin Island[b]				
FB 1-1	granitic gneiss, foliated	4.5	0.8 ↑	2.72
FB 1-3	epidote-amphibolite	6.8	1.2 ↑	2.72
FB 2-1	biotite-epidote quartzite	7.2	2.0 ↑	3.1
FB 2-2	biotite-epidote quartzite	0.04	0.006↑	2.72
FB 2-4	biotite-epidote quartzite	2.0	0.16 ↑	2.98
Baffin Bay coast[c]				
GG 2 G	glacial drift, Narssarssuaq	1.7		1.85
GG 16 G	glacial river, Söndre Ström	0.6		1.82
GG 19 G	roadside in town, Egedesminde	0.15		1.8
GG 33 G	periglacial drift, Cape Dyer	0.10		1.62

TABLE 5.3b (continued)

Sample No.	Description	K, 10^{-3} Gauss/Oe	J_o, 10^{-3} Gauss/Oe	density, gm/cc
GG 35 G	periglacial drift, Broughton Island	0.11		1.4
GG 36 G	1 km. away from GG 53 G, drift	0.02		1.3
GG 37 G	river gravel, Frobisher Bay	1.6		1.3

K = volume susceptibility

J_o = NRM intensity

(a) Unoriented rock samples collected in Kaipokok area north of Makkovik on the Labrador coast by Dr. J. S. Sutton and described by him. These rocks are from the Hopedale series of gneiss.

(b) Oriented samples collected by Dr. B. T. May and Mr. W. J. Drodge at Frobisher Bay in the summer of 1968. The arrows indicate that all samples were normally magnetized. Sample descriptions by Dr. J. S. Sutton.

(c) Gravel samples from the Baffin Bay coast, collected by the author. The density values are those of the gravel as obtained from the dimensions and weight of the susceptibility bridge sample holder. The K-values listed are those for the solid rock, assuming a solid-rock density of 2.8-2.85 gm/cc.

TABLE 5.4

Microscopically estimated magnetite content and magnetic susceptibility for samples of Precambrian rocks from Baffin Bay

Sample	Location	Squares counted	Vol. % magnetite	K, 10^{-3} gauss/Oe
GG 0	Narssarssuaq	6000	0.03	0.01
GG 4	Narssaq	too fine-grained		
GG 7	Julianehab	6000	0.67	2.0
GG 10	Julianehab	6000	0.60	1.9
GG 15	Sondre Strom	6000	0.12	0.83
GG 24	Godhavn	6000	0.5	0.93
F 92A	Labrador coast	8000	0.98	2.9
FB 1-1	Frobisher Bay	12000*	1.8	4.5
FB 1-3	Frobisher Bay	8000	2.7	6.7
FB 2-1	Frobisher Bay	6000	2.3	7.2
FB 2-4	Frobisher Bay	6000	0.95	2.0
74480	Fiskenaesset**	3500 to 10000 points	0.7	1.8
74519	Fiskenaesset		1.3	4.3
68638	Fiskenaesset		0.5	1.5
68635	Fiskenaesset		0.2	0.92
68548	Fiskenaesset		$\lesssim$ 0.05	0.08

K = volume susceptibility, measured on 9 cm. long cores in the case of the Frobisher Bay samples, and 2 cm. long specimens in others.

* This sample was very inhomogenous, so two polished sections were made, one from a light-coloured part of the sample and another one from a dark part. 6000 squares were counted in each slide. See also data and footnote in Table 5.5.

** Data from Ghisler and Sharma (1969). These authors counted points in thin sections, and measured susceptibilities with a fluxgate magnetometer arrangement around short core specimens.

TABLE 5.5

Results from ballistic magnetometer; Precambrian rocks, Baffin Bay Coast

Sample No.	T_c °C.	D_s, centim.	atn.	length, cm.	volume, cc.	volume % magnetite	H',Oe
FB 1-1a	560?	20.2	4	2.0	8.0	2.43	860
FB 1-1b	560	10.3	4	2.1	8.4	1.18	980
FB 1-1d	560	18.7	4	2.3	9.2	1.98	920
FB 2-1	560?	26.7	4	1.8	7.2	3.56	1380
GG 10	560?	29.9	1	2.1	8.3	0.89	1430
GG 24	560	13.6	1	2.05	8.2	0.4	∿1800
GG 0	?	<.0.05	1	2.8	11	0.00	-
F 92A	565	23.2	2	1.85	7.4	1.42	1120

Legend: See Table 3.10. FB refers to samples from Frobisher Bay, GG to samples from West Greenland, and F 92 A is a sample from the Labrador coast. The specimens FB 1-1a, b, d are all from the same hand sample, but the susceptibilities of the first two were not measured separately and only FB 1-1d was used in Fig. 3-16.

TABLE 5.6

Thermomagnetic curves for Precambrian rocks, Baffin Bay Coast

Sample No.	Locality	Curie point (T_c, °C.)		M'_o / M_o
		Heating	Cooling	
GG 10	Julianehåb	570	565	0.9
GG 15	Söndre Ström.	575	575	1.0
GG 24	Godhavn, Disko	560	560	1.0
GG 30 (a)	Cape Dyer	530	545	0.6
FB 1-3	Frobisher Bay	560	560	1.0
F 92A	Labrador Coast	565	565	1.0

M'_o / M_o : see Table 3.9

(a) Weathered, brownish sample.

TABLE 5.7

Thermomagnetic results for various basic rocks from Iceland having high Curie points (T_c < 500°C.)

Sample	Type	Locality	Curie point (T_c, °C.)		M'_o/M_o
			Heating	Cooling	
Arn 2	gabbro	NW Iceland	570	?	?
Kol. KL	gabbro	W Iceland	570	570	0.75
Lýsuhóll	gabbro	W Iceland	560	560	1.0
Lón K.O.	gabbro	SE Iceland	565	565	1.0
Músarnes 2	gabbro	SW Iceland	545	545	0.95
Leidh B6	diabase	SW Iceland	570	560	∿1.0
Stardalur 60 m basalt (Fig.5-9)			620[a]	615	∿0.4
Stardalur 73 m basalt			560	560	1.0
Stardalur 96.5m basalt			585	585	0.4
Stardalur 105.4m basalt			615	∿610	0.2
Stardalur 119.6m basalt			570	570	0.7
R22 1230m drill chips (Fig.5-10)			590	590	0.6
R4 6304' drill chips			585	585	0.6
H3 900 m drill chips			600	595	0.7
H8 1752 m drill chips			570[b]	?	0.6
Surtsey beach sand			510	530	∿1.3
Bolungarvik			560	560	1.1

Legend: See Table 3.9

(a) A hump occurred in the heating curve.

(b) 560°C. for a specimen mounted in plaster.

TABLE 5.8

Thermomagnetic curves for various Icelandic rocks having low Curie points (T_c < 400°C.)

Sample	Origin	Part of Iceland	C	Curie point (T_c, °C)		M'_o/M_o
				Heating	Cooling	
HG 11	dyke	NW	R'	190	510	1.5
MG 10	dyke	NW	R'	200 (a)	535	1.6
A 6-5	dyke	NW	R'	230 (b)	530	3
SG 7	dyke	NW	R or R'	265 (c)	?	?
JG 3	dyke	SW	R'	255	?	?
RG 0	dyke	SW	R	260	530	1.4
KY St.	column	SW	R'	165	545	∿2
M 6	dyke	SW	R' (d)	180	510	1.7
Ne 4	flow	S	R'	350	505	1.2
B 3-3	flow	NW	N or R'	170	?	?

Not included in this table are results on flows that may have been heated by dykes, and results on flows with distinctly two Curie points on heating. Legend: See Table 3.9.

(a) Another sample (MG 6) from the same dyke had T_c = 245°C.

(b) Another sample (A6-1) from the same dyke had T_c = 225°C.

(c) A large hump occurred in the heating curve.

(d) This sample contains minor amount of pyrite and is vesicular.

TABLE 5.9

Magnetic properties of samples of acid rocks from Iceland

Sample No.	Type	Collection	Locality	J_o, $10^{-3}Gcm^3/g$	K $10^{-3}\frac{Gcm^3}{Oe.g}$	Pol.
HV 1	acid tuff	1	Bláskeggsá Hvalfjördur	0.02	0.06	N?
HV 2	acid tuff	1	Blaskeggsa Hvalfjördur	<0.01	0.05	
HV 2A	pitchstone	2	Blaskeggsa Hvalfjördur	0.07	0.4	
HV 3	acid tuff	1	Skroppugil Hvalfjördur	1.6	0.6	N
HV 4	acid tuff	2	Skroppugil Hvalfjördur	0.55	0.6	
HV 5	acid tuff	2	Skroppugil Hvalfjördur	0.6	0.6	
HV 6	dark rhyol. dyke	1	Saurbæ r Hvalfjördur	0.01	<0.02	
HV 7	light rhyol.	2	Saurbæ r Hvalfjördur	0.17	0.45	
HV10	granophyre	3	Flydrur Borgarfj.	0.13	0.7	
SJ	granophyre	3	Flydrur Borgarfj.	0.6	0.8	
Fró	granophyre	3	Fródá Snæ f. nes	0.2	0.6	
Ó.Á.	obsidian	3	Hrafntinnusker, Rang.	0.03	?	
Ak.	light rhyolite	3	Akureyri (glacial dr.)	0.04	<0.02	
HL 1	dark rhyolite	3	Hlídarfjall Eyjafjördur	0.3	0.3	
HL 2	dark rhyolite	3	Hlídarfjall Eyjafjördur	0.3	0.24	
MÓ 1	pitchstone	2	Móskardshnúkar Kjós	0.06	0.2	
MÓ 3	light rhyolite	1	Móskardshnúkar Kjós	<0.01	<0.02	
MÓ 4	dark rhyolite	1	Móskardshnúkar Kjós	0.3	0.2	N

TABLE 5.9 (Continued)

Sample No.	Type	Collection	Locality	J_o, $10^{-3}Gcm^3/g$	K $10^{-3}\frac{Gcm^3}{Oe.g}$	Pol.
MÓ 4A	light rhyolite	1	Móskarjshnúkar Kjós	0.06	0.04	
MÓ 5	flow-band rhyol.	2	Móskarjshnúkar Kjós	0.6	0.04	
MÓ 7	altered rhyolite	2	Móskarjshnúkar Kjós	<0.01	<0.02	
IBFL	rhyolite dyke	2	Skeggjastadir Kjós	0.1	0.2	
LV 4	pitchstone	2	Þverdalur, Esju, Kjós	0.01	<0.02	
LV 5	light rhyolite	1	Þverdalur, Esju, Kjós	0.01	0.02	
LV 6	brown rhyolite	1	Þverdalur, Esju, Kjós	0.06	0.15	S
LV 7	altered rhyol.	1	Þverdalur, Esju, Kjós	<0.01	<0.02	
GR 1	dark rhyolite	1	Grímmannsfell Mosf. sv.	0.24	0.15	NS
GR 2	dark rhyolite	1	Grímmannsfell Mosf. sv.	0.18	0.1	N
GR 3	dark rhyolite	2	Grímmannsfell Mosf. sv.	0.21	0.06	
Hofn	light rhyolite	3	Heppa Hornafjördur	0.02	<0.02	

Collection: 1, collected by the writer from solid outcrop; 2, collected by the writer in beach or scree, presumably near outcrop; 3, donated by friends; pol., polarity (shown where measured); s, shallow inclinations.

TABLE 5.10

Results from ballistic magnetometer measurements on Icelandic samples

Sample No.	T_c, °C.	Type	D_s, cm.	atn.	Weight gm.	Vol. cc.	eq.%mt.	H', Oe
Stardalur 73	560	from	17.5	4	(a)	7.0	2.4	1000
Stardalur 96.5	585	drill	20.7	4	(a)	8.6	2.3	950
Stardalur119.6	570	core	4.1	1	1.9	0.70	1.45	850
R22 1230 m	590	chips	6.6	1	3.0	1.2	1.4	1000
R 4 6304'	585	chips	1.7	1	0.6	0.24	1.7	~ 800
- 2100 m	?	chips	31	1	7.4	2.8	2.7	1100
H 3 900 m	?	chips	0.4	1	1.7	0.7	~0.15	?
H 8 1752 m	570	chips	2.8	1	1.1	0.44	1.6	800
Bolungarvik	560	beach sand	3.8	1	2.1	0.7	1.3	850
Hvalfjördur	620?	red sediment	0.9	1	1.5	0.7	0.32	400
Ha 3 gabbro	560?	crushed rock	5.8	1	4.1	1.35	1.05	1100
E 10-2 lava	525	crushed rock	5.3	1	1.35	0.47	2.8	800
A 4-6 lava	550	crushed rock	3.9	1	9.0	3.12	0.31	~ 850
17-12 gabbro	560?	crushed rock	23	2	9.0	3.04	3.4	950
Leidh. diabase	570	crushed rock	11.5	1	8.4	3.01	0.95	1050
Arnarfj. Tjáldanes	?	beach sand	11.8	1	8.2	2.7	1.08	950

Legend: See Table 3.10

(a) Cores, respectively 1.75 and 2.15 cm. long; the other samples are crushed rock.

TABLE 5.11

Samples used in magnetic measurements on drill chips and cores from deep drill holes in Iceland

Reykjavik				Reykjanes			
Depth m	Hole	Chief material	Mean density g/cc	Depth m	Hole	Chief material	Mean density g/cc
801	R22	basalt		420	H3	sediment	2.7
815	R 4	breccia		570	H6	tuff (core)	
,840	R32	diabase (core)	3.05	610	H3	palagonite breccia	
961	R22	basalt + sediment + tuff		756	H3	sediment	
1100	R 4	breccia		900	H3	palagonite breccia	2.8
1141	R22	basalt		1150	H3	basalt	
1230	R22	basalt	2.8	1302	H8	basalt	
1375	R 4	tuff		1374	H8	tuff (core)	2.7
1555	R22	basalt		1500	H8	palagonite breccia	2.8
1650	R 4	basalt + tuff	2.85	1650	H8	basalt	
1923	R 4	basalt	2.9	1752	H8	basalt	2.8
2100	R 4	basalt	2.9				
2200	R 4	basalt					

Fig. 1-1

(a) Orientation of a vector $\vec{V}$ in geographic coordinates.
D = declination. I = inclination (positive down).

(b) Coordinates of a magnetic vector (not shown) with respect to axes fixed in a drill core. See text.
d = declination. i = inclination relative to the XY - plane.

Fig. 1-2

(a) Compositional diagram of the iron-titanium oxides (after Nagata 1961). Titanomagnetites occupy the thick line drawn between magnetite (mt.) and ulvöspinel, (ulv.), the compositional parameter x increasing from 0 to 1 in the direction of the arrow. ilm., ilmenite; ps., pseudobrookite.

(b) Curie point T_c of the titanomagnetites plotted as a function of x (after Ozima and Larson 1970).

(c) Saturation moment (in Bohr magnetons, μ_B, per molecule) at 0°K, plotted as a function of x (after Banerjee 1970). Solid curve, experimental results for solid solutions of titanomagnetites. Broken line, average moment for a heterogeneous mixture of magnetite and ulvöspinel.

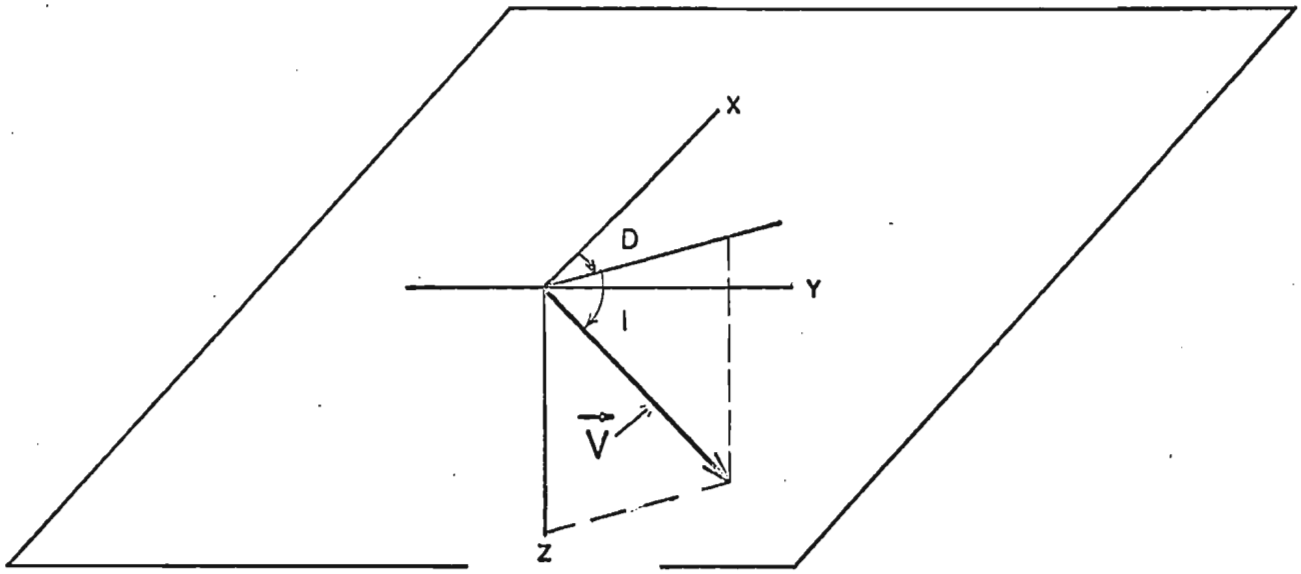

a)

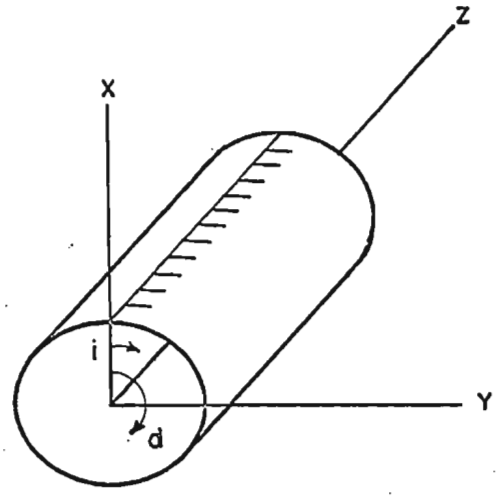

b)

FIG. 1 - 1

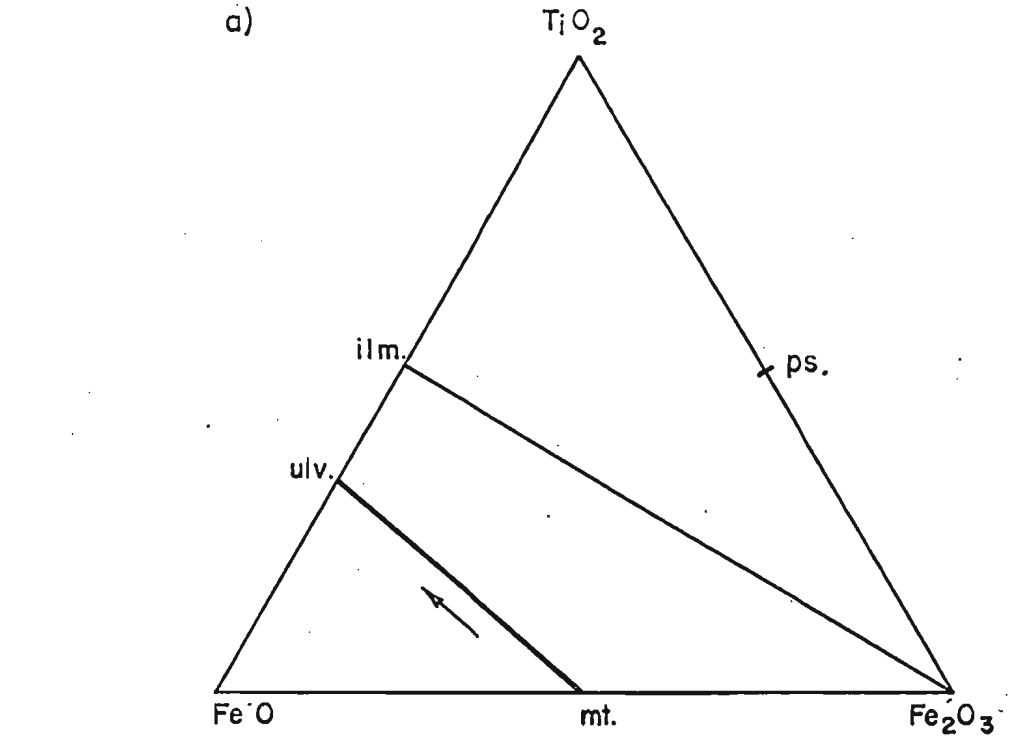
a)
TiO_2
ilm.
ps.
ulv.
FeO
mt.
Fe_2O_3

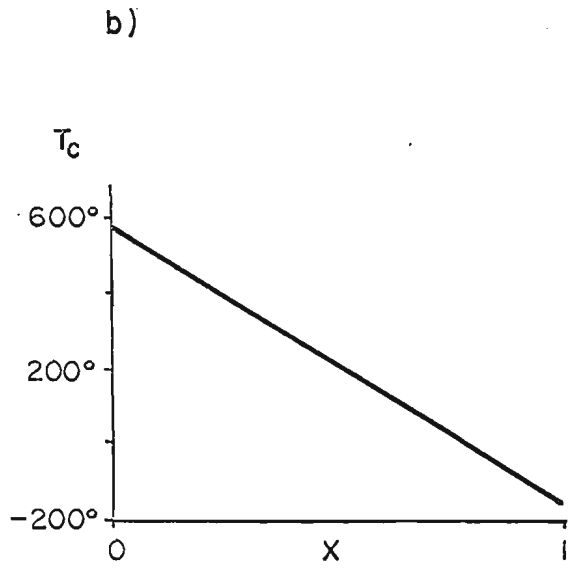
b)
T_C
600°
200°
−200°
0
X
1

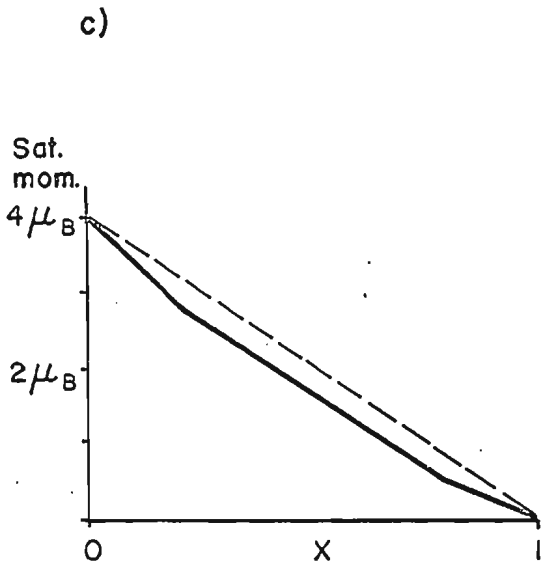
c)
Sat.
mom.
$4\mu_B$
$2\mu_B$
0
X
1

FIG. 1 - 2

Fig. 2-1

(a) Wiring diagram for the ballistic magnetometer.
M, microswitch operated by the sample;
S, shorting switch; R_c, damping resistor;
R_a, attenuating resistors; Galv., galvanometer.

(b) Diagram of the cylindrical tube for the ballistic magnetometer, in cross-section. Actual size. P, square magnet poles; M, microswitch; S, stopper. The sample is blown back and forth by air coming through a conduit (not shown) in the stopper S.

Fig. 2-2

Typical results from ballistic magnetometer measurements on rock samples from the Baffin Bay coast.

Fig. 2-3

Sectional views of thermomagnetic balance. a, quartz rod and cross bar; b, mirror; c, detachable quartz sample cup; d, ferrite magnets; e, brass counter-weight; f, oil damping pot; g, conical glass support; h, electromagnet; i, pole piece. j-n, furnace: j, alumel heating wire wound on quartz tube; k, asbestos lining; l, asbestos lid; m, thin brass tube; n, sheathed thermocouple. o, compensating coil; p, from lamp; q, to vertical scale.

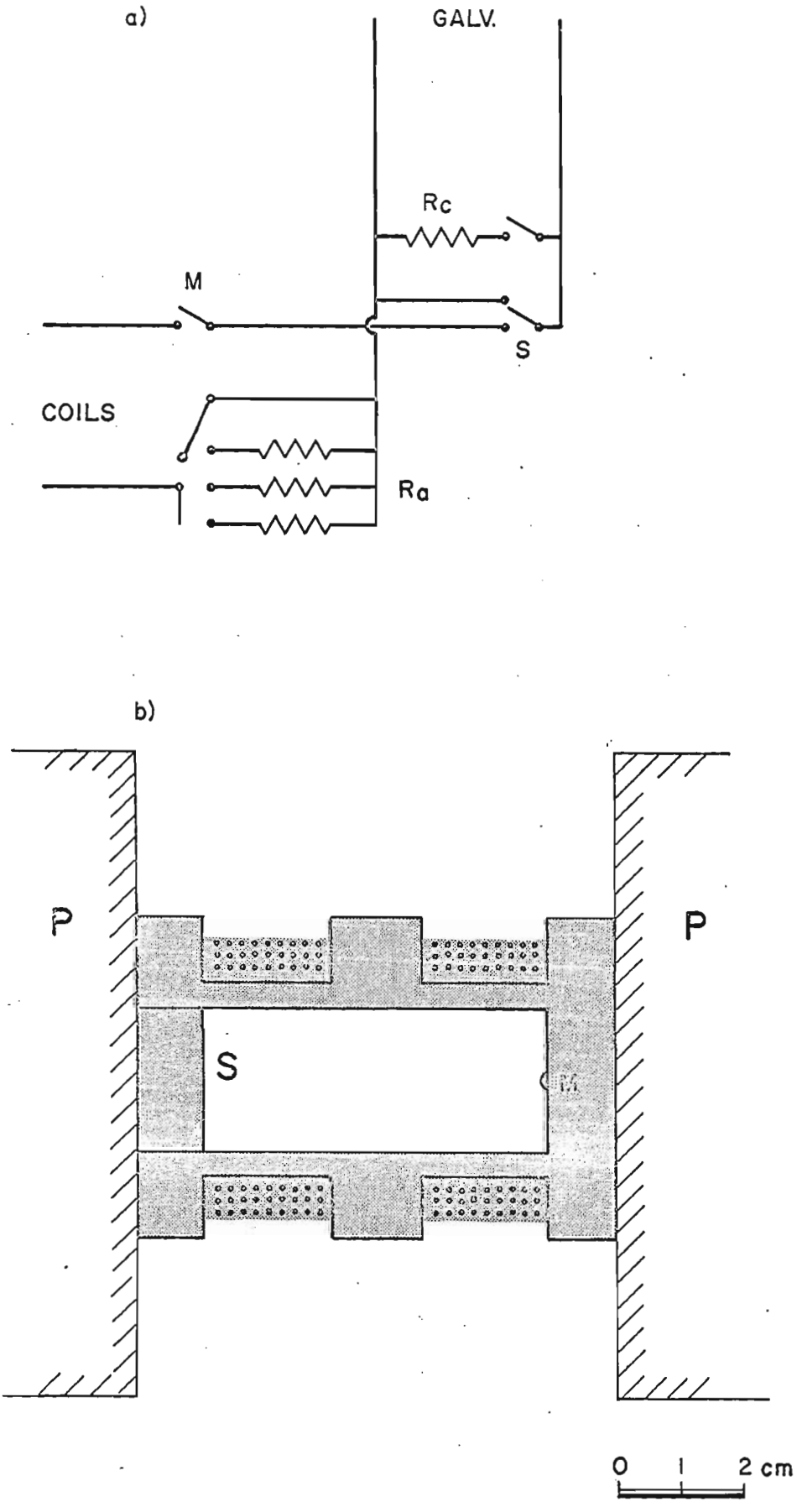

FIG. 2 - 1

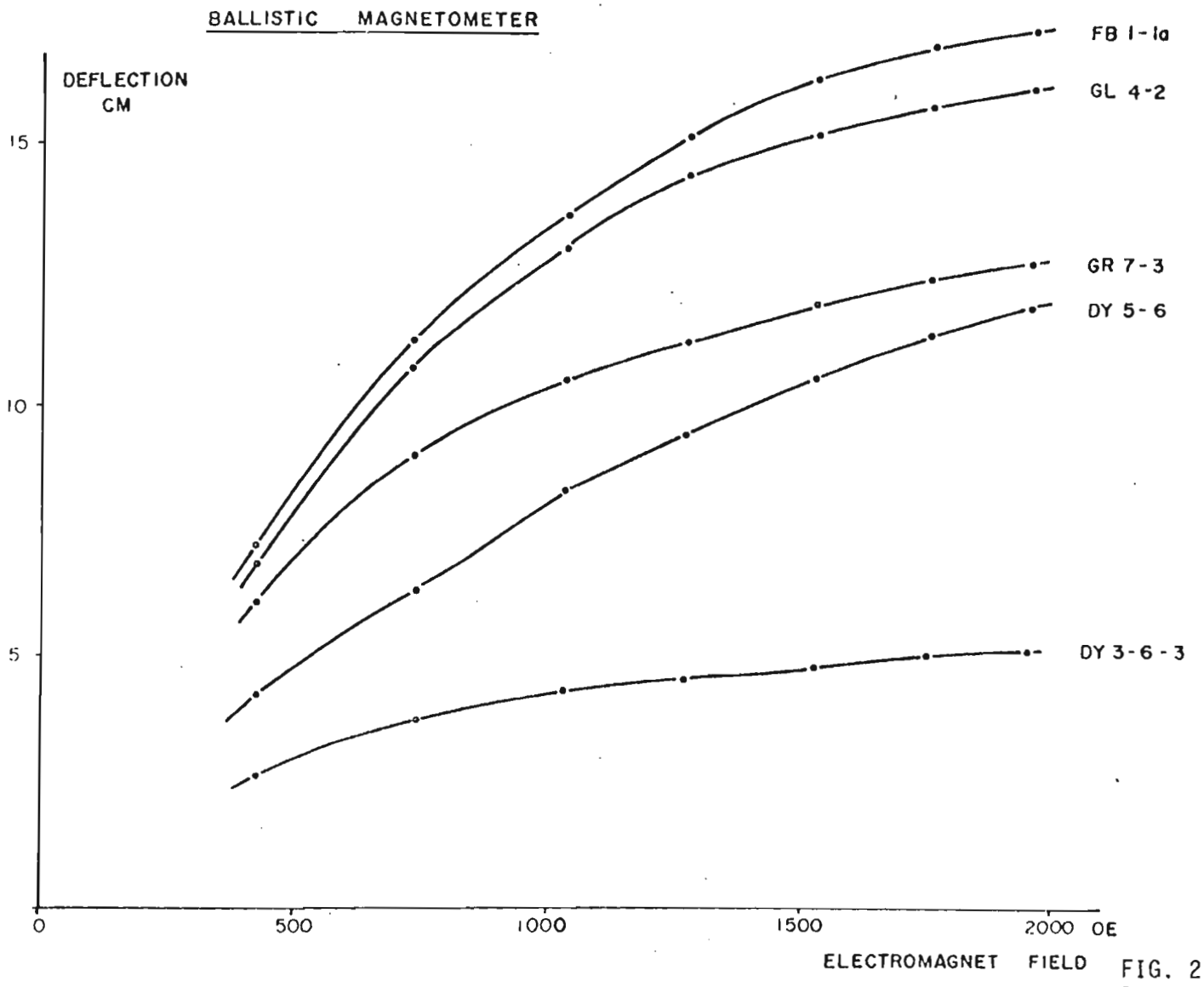
BALLISTIC MAGNETOMETER
DEFLECTION
CM
15
10
5
0
500
1000
1500
2000 OE
ELECTROMAGNET FIELD
FB 1-1a
GL 4-2
GR 7-3
DY 5-6
DY 3-6-3

FIG. 2 - 2

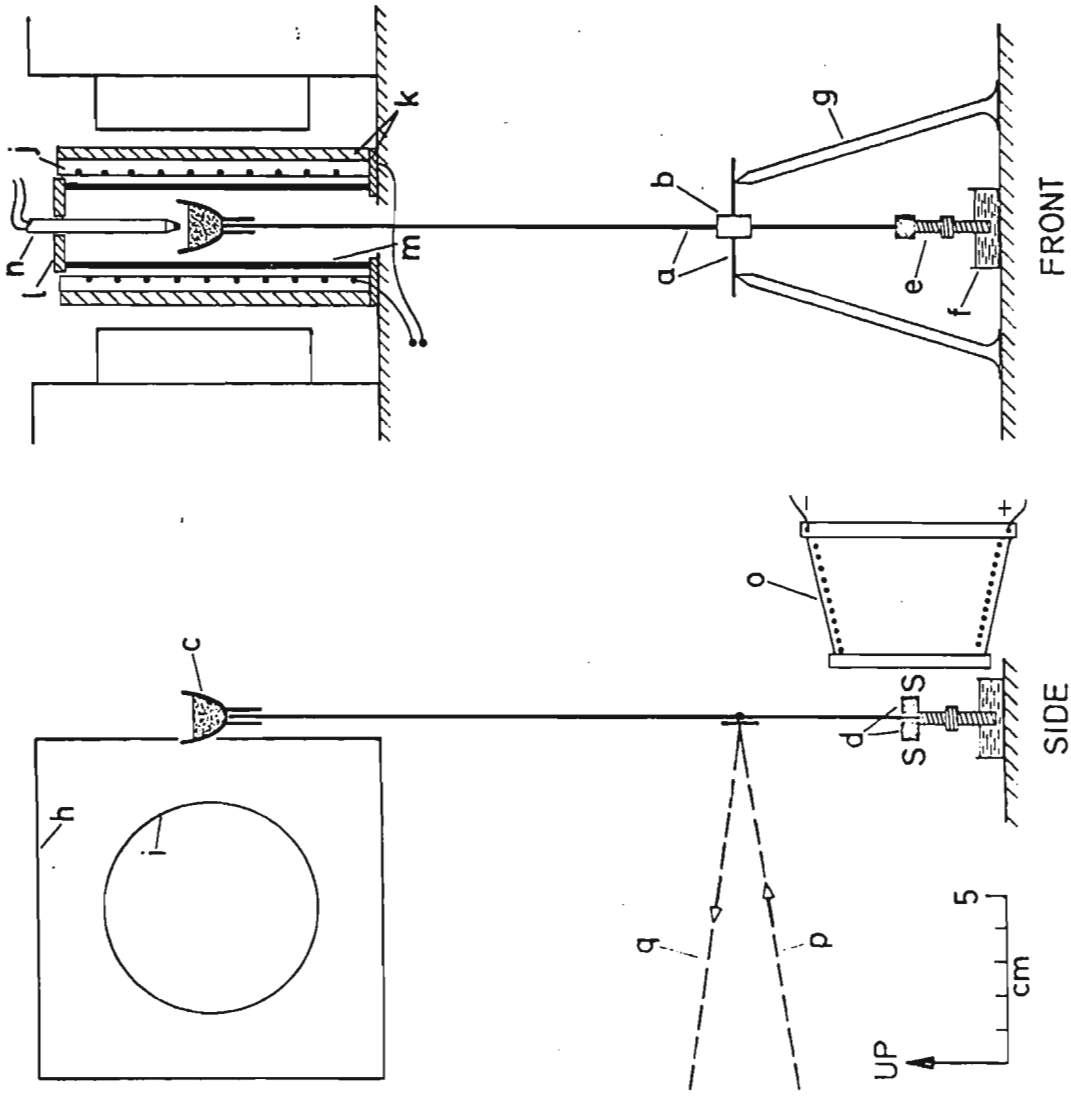

FIG. 2 - 3

Fig. 3-1

Index map of Baffin Bay and nearby regions.

Fig. 3-2

Map and schematic cross-section of paleomagnetic sampling localities on the south coast of Disko Island. In the lower part of the figure, the vertical scale is about three times the horizontal scale.

Fig. 3-3

Results from AF demagnetization of one sample from each flow in profiles GL and GM in Disko. J_{max} is the inferred primary remanence intensity, and $J_{max} - J_o$ the inferred secondary remanence intensity. Class R samples are those above the broken line, class N are those below it; note the different scales on the axes.

Fig. 3-4

(a) The secondary part of the measured NRM intensity of samples from Disko (same as in Fig. 3-3) plotted against sample susceptibility.

(b) The primary part of the NRM intensity of the same samples, plotted against sample susceptibility.

Fig. 3-5

The primary part, J_{max} (Table 3.1), of the measured NRM intensity of samples from the breccia, the GK- flows and the intrusives in Disko, plotted against sample susceptibility. One sample per site.

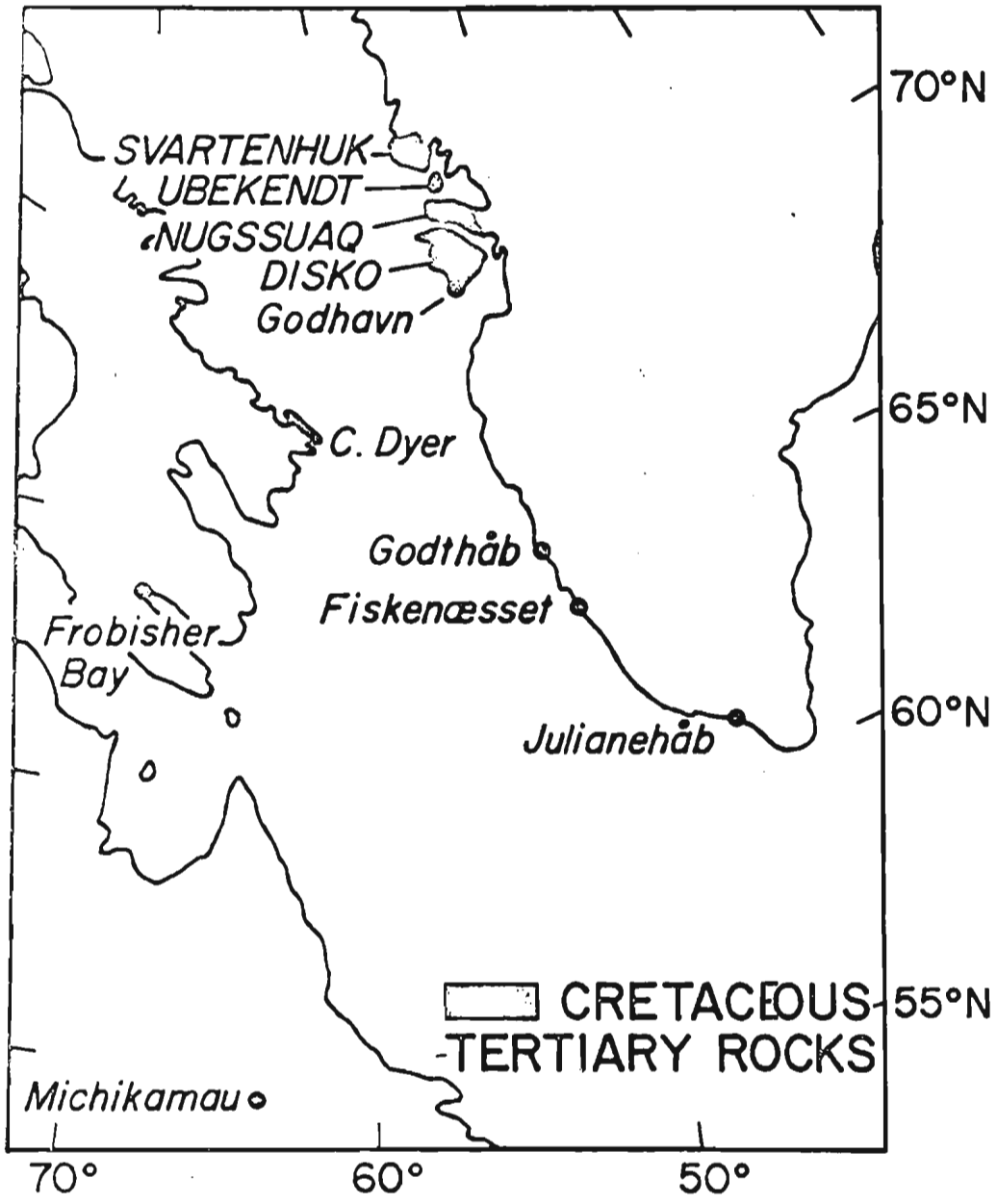
70°N
65°N
60°N
55°N
SVARTENHUK
UBEKENDT
NUGSSUAQ
DISKO
Godhavn
C. Dyer
Godthåb
Fiskenæsset
Frobisher Bay
Julianehåb
Michikamau
CRETACEOUS-TERTIARY ROCKS
70°
60°
50°

FIG. 3 - 1

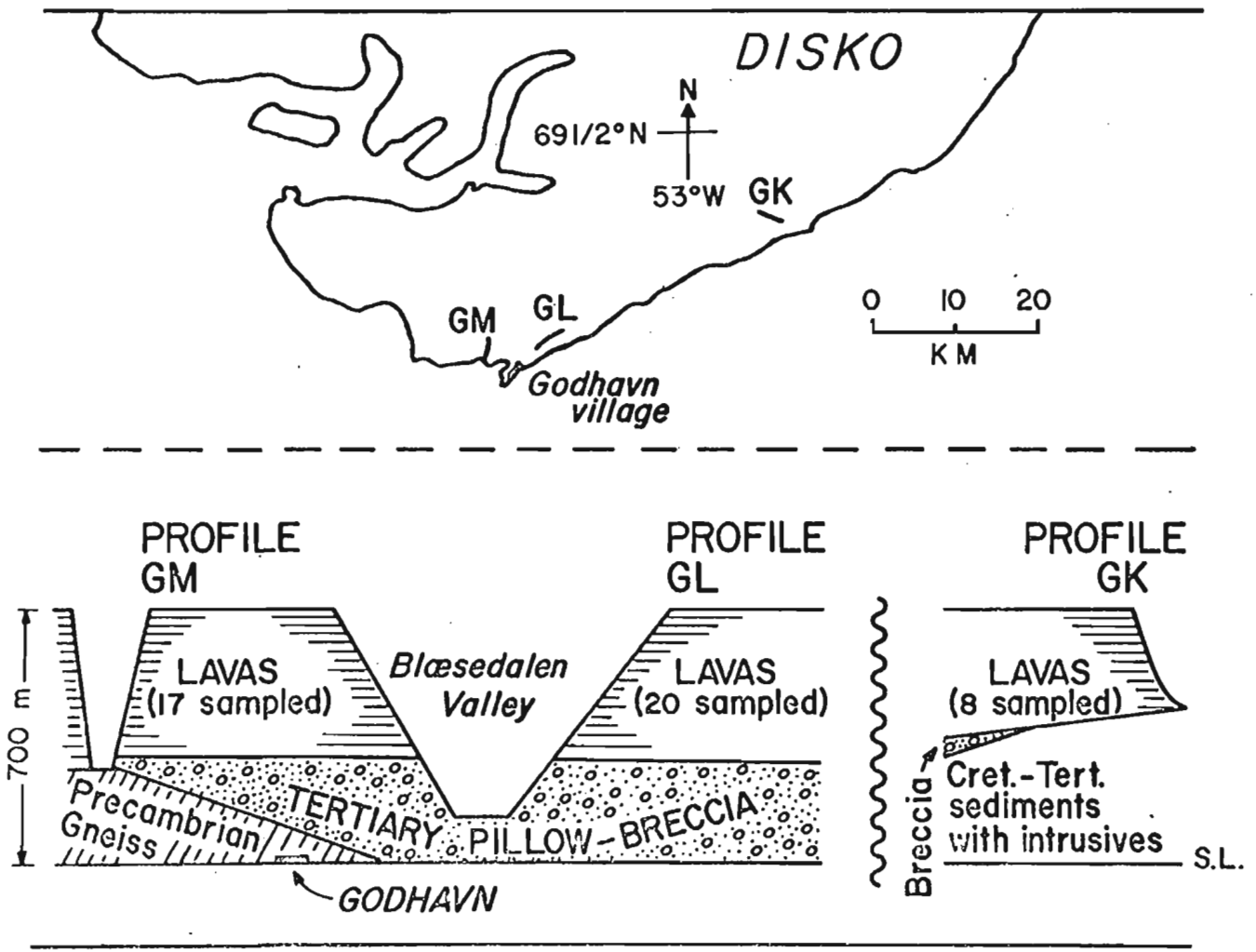
DISKO
N
69 1/2°N
53°W
GK
GM
GL
0 10 20
K M
Godhavn
village
PROFILE
GM
PROFILE
GL
PROFILE
GK
700 m
LAVAS
(17 sampled)
Blæsedalen
Valley
LAVAS
(20 sampled)
LAVAS
(8 sampled)
Precambrian
Gneiss
TERTIARY PILLOW-BRECCIA
Breccia
Cret.-Tert.
sediments
with intrusives
S.L.
GODHAVN

FIG. 3 - 2

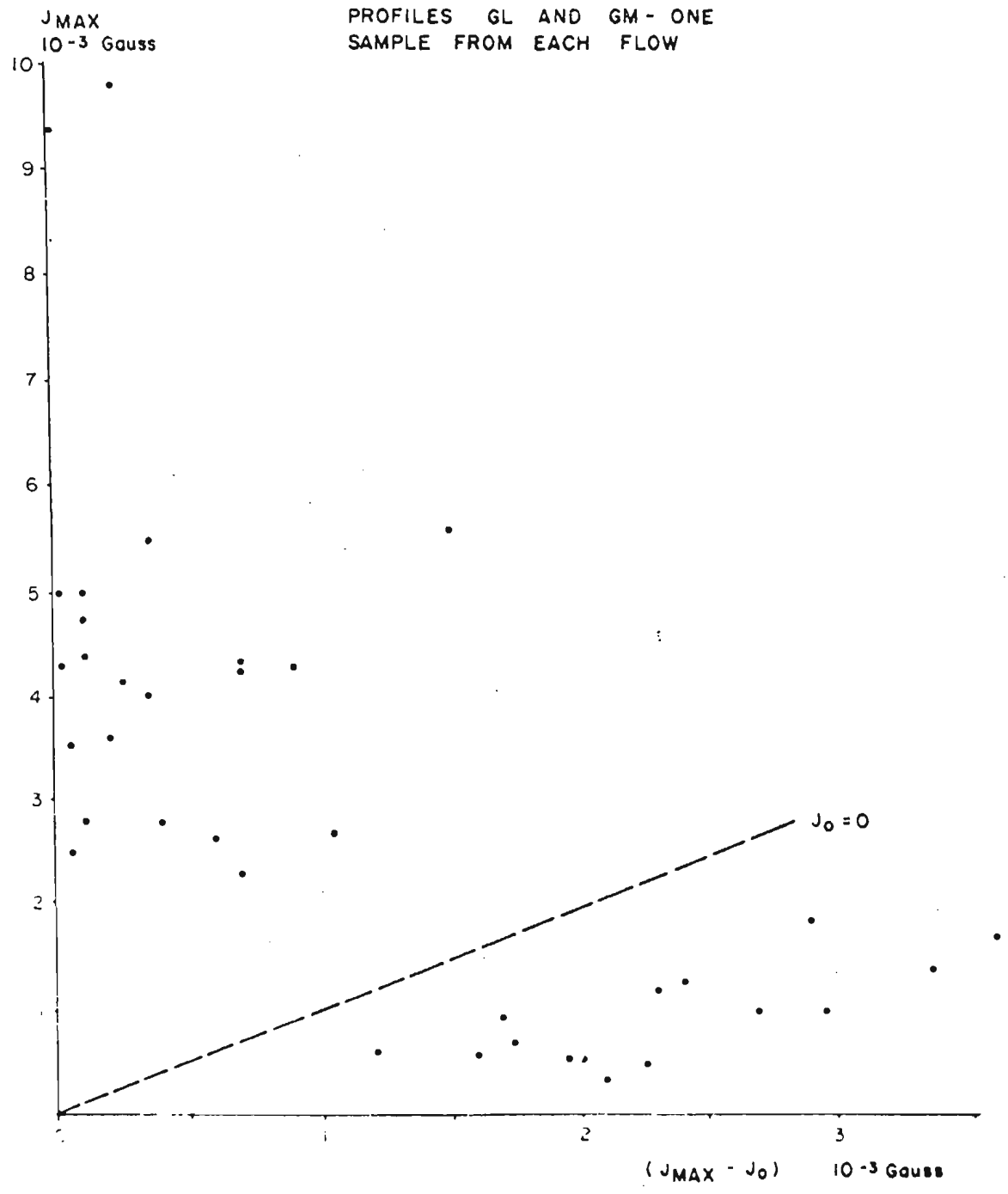
PROFILES GL AND GM - ONE
SAMPLE FROM EACH FLOW
JMAX
10-3 Gauss
10
9
8
7
6
5
4
3
2
1
2
3
Jo = 0
(JMAX - Jo) 10-3 Gauss

FIG. 3 - 3

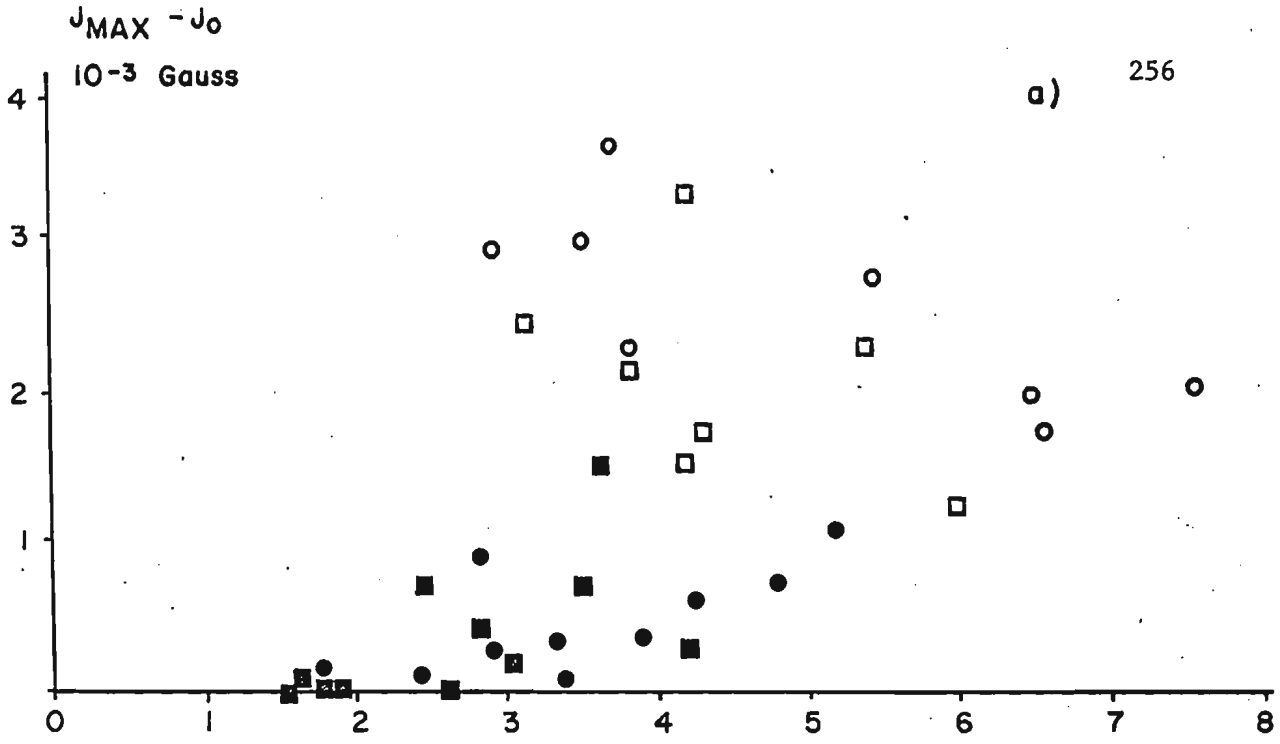
$J_{MAX} - J_o$
10^{-3} Gauss
a)
0
1
2
3
4
5
6
7
8

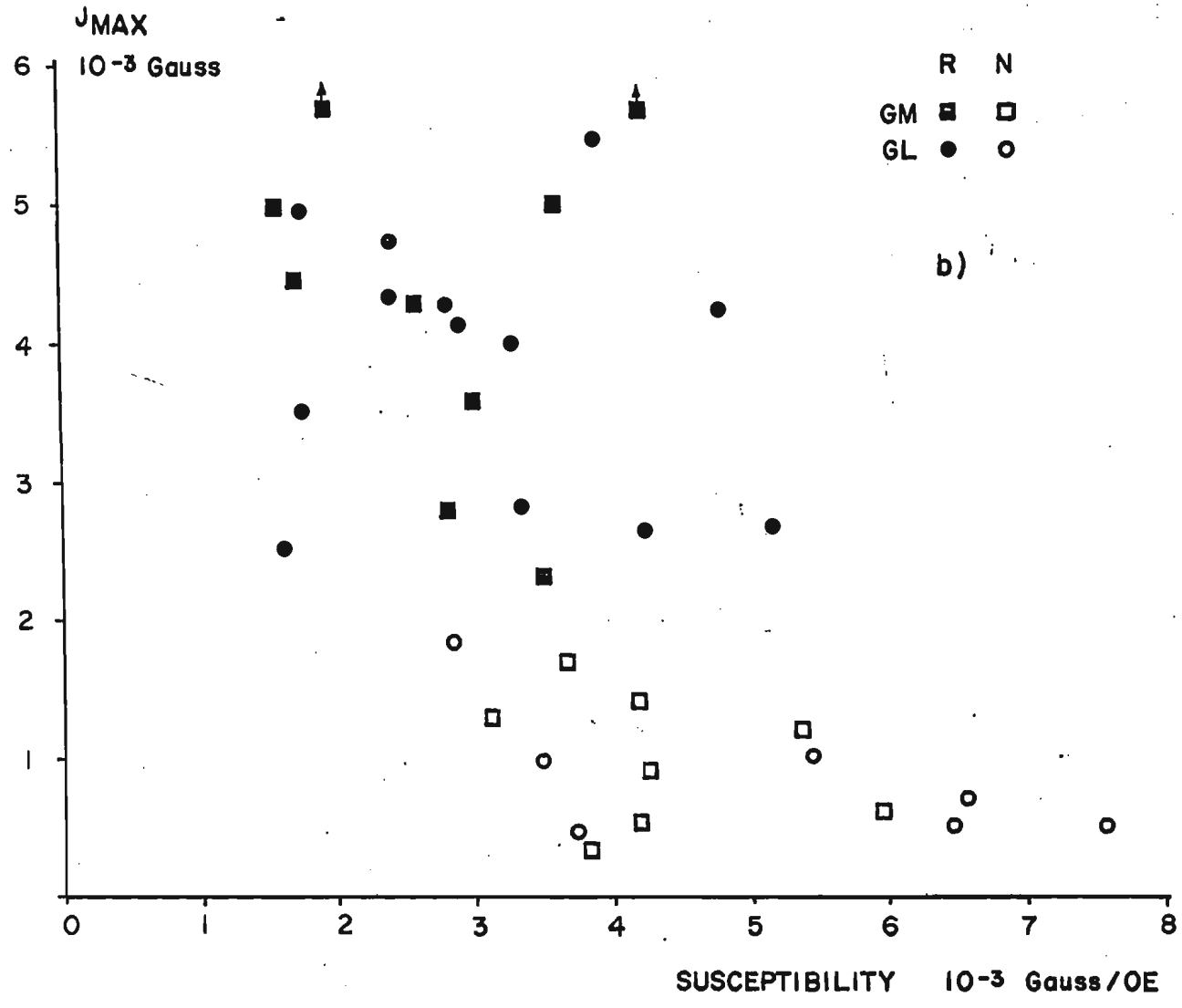
J_{MAX}
10^{-3} Gauss
R N
GM
GL
b)
0
1
2
3
4
5
6
7
8
SUSCEPTIBILITY 10^{-3} Gauss/OE

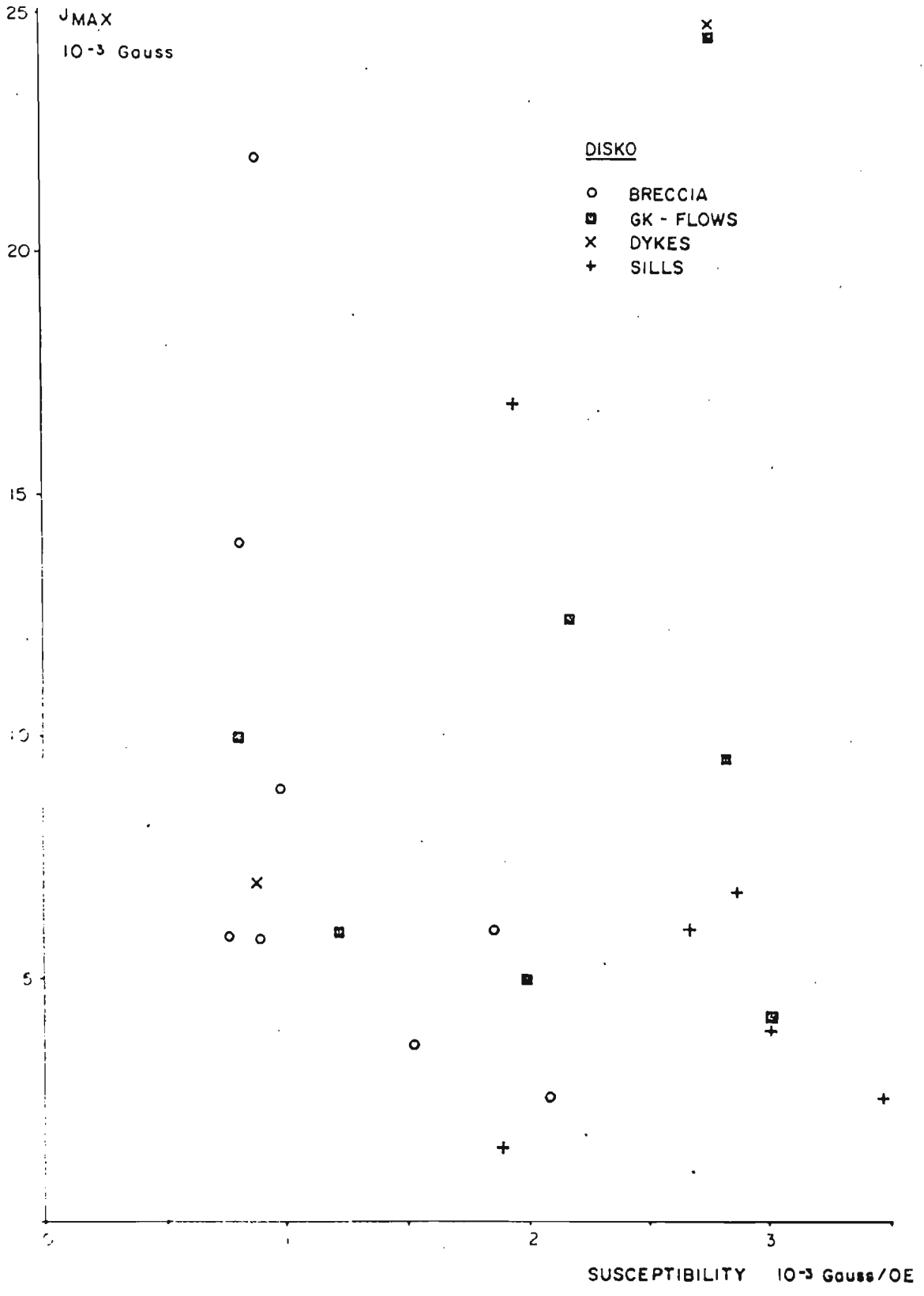
25
20
15
10
5
0
1
2
3
JMAX
10-3 Gauss
DISKO
BRECCIA
GK - FLOWS
DYKES
SILLS
SUSCEPTIBILITY 10-3 Gauss/OE

FIG. 3 - 5

Fig. 3-6

Left: Remanent intensity J as a function of AF demagnetizing field for three typical South Disko basalts; GL 8-2 (class N); GL 10-1 (class R); and GK 9-1 (class R´). Reverse polarity is plotted above the zero line.

Right: Polar equal-angle projection of remanence directions for the same samples. The declination of GK 9-1 has been altered by 180° to avoid overlap. Numbers refer to demagnetizing fields. In both parts of the figure, open (filled) circles refer to reverse (normal) magnetization directions. Broken lines indicate that in the last step of each demagnetization, spurious components appeared in J. In the last step, the treatment was repeated and the results averaged. Note the difference in stability between the three classes.

Fig. 3-7

As fig. 3-6, with different samples. GL 5-2 is class R, GL 15-1 is class N, and GR 2-1 (whose declination has been altered by 180° on the right to avoid overlap) is class R´.

Fig. 3-8

Thermal demagnetization results on Disko basalt samples.

Left: remanence intensity at room temperature as a function of temperature of maximum heating. Note that the scale for dyke sample GD 1-3 has been compressed by a factor of two relative to the other samples.

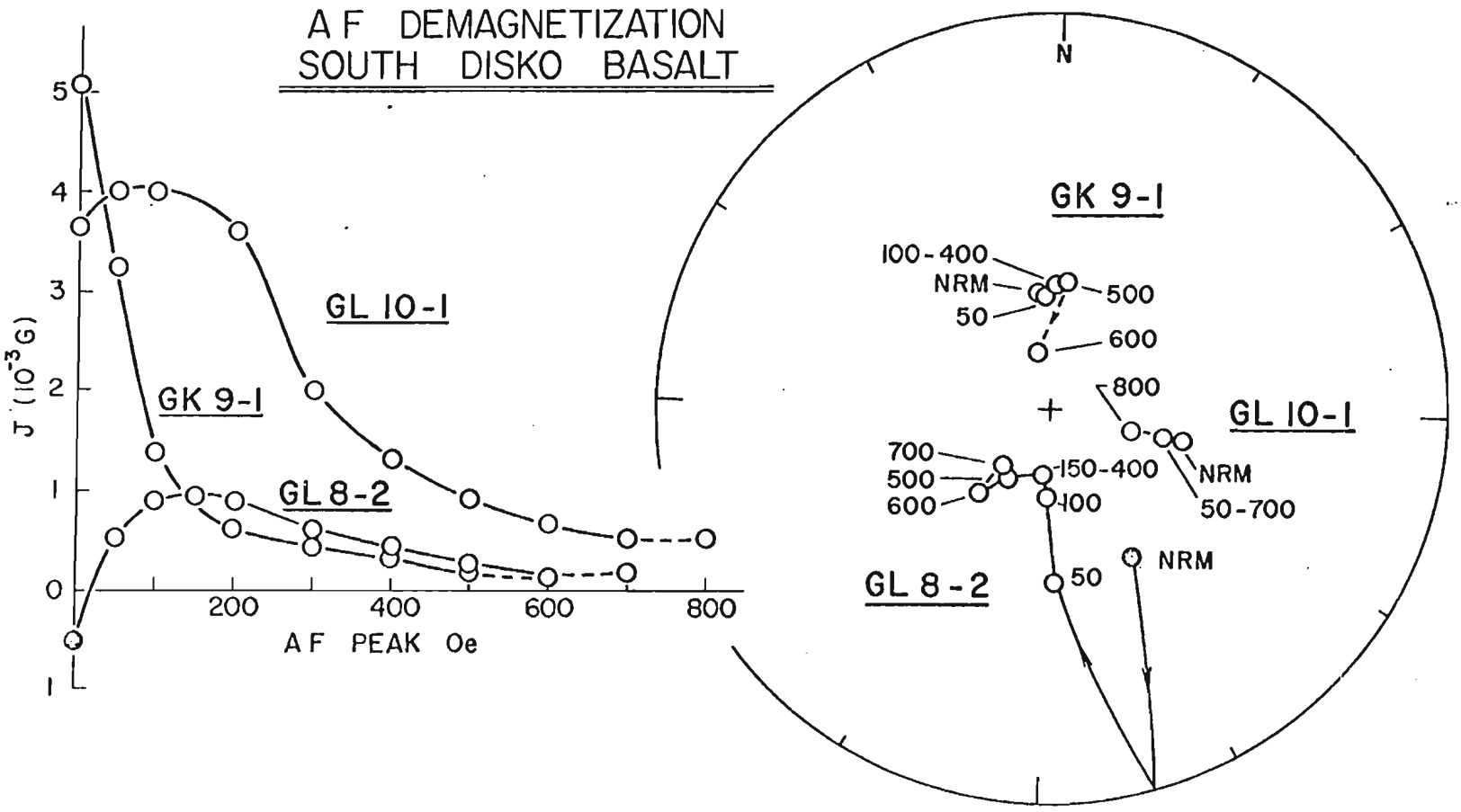
A F DEMAGNETIZATION
SOUTH DISKO BASALT
J (10⁻³G)
5
4
3
2
1
0
1
200
400
600
800
A F PEAK Oe
GL 10-1
GK 9-1
GL 8-2
N
GK 9-1
100-400
NRM
50
500
600
800
GL 10-1
700
500
600
150-400
100
NRM
50-700
GL 8-2
50
NRM

FIG. 3 - 6

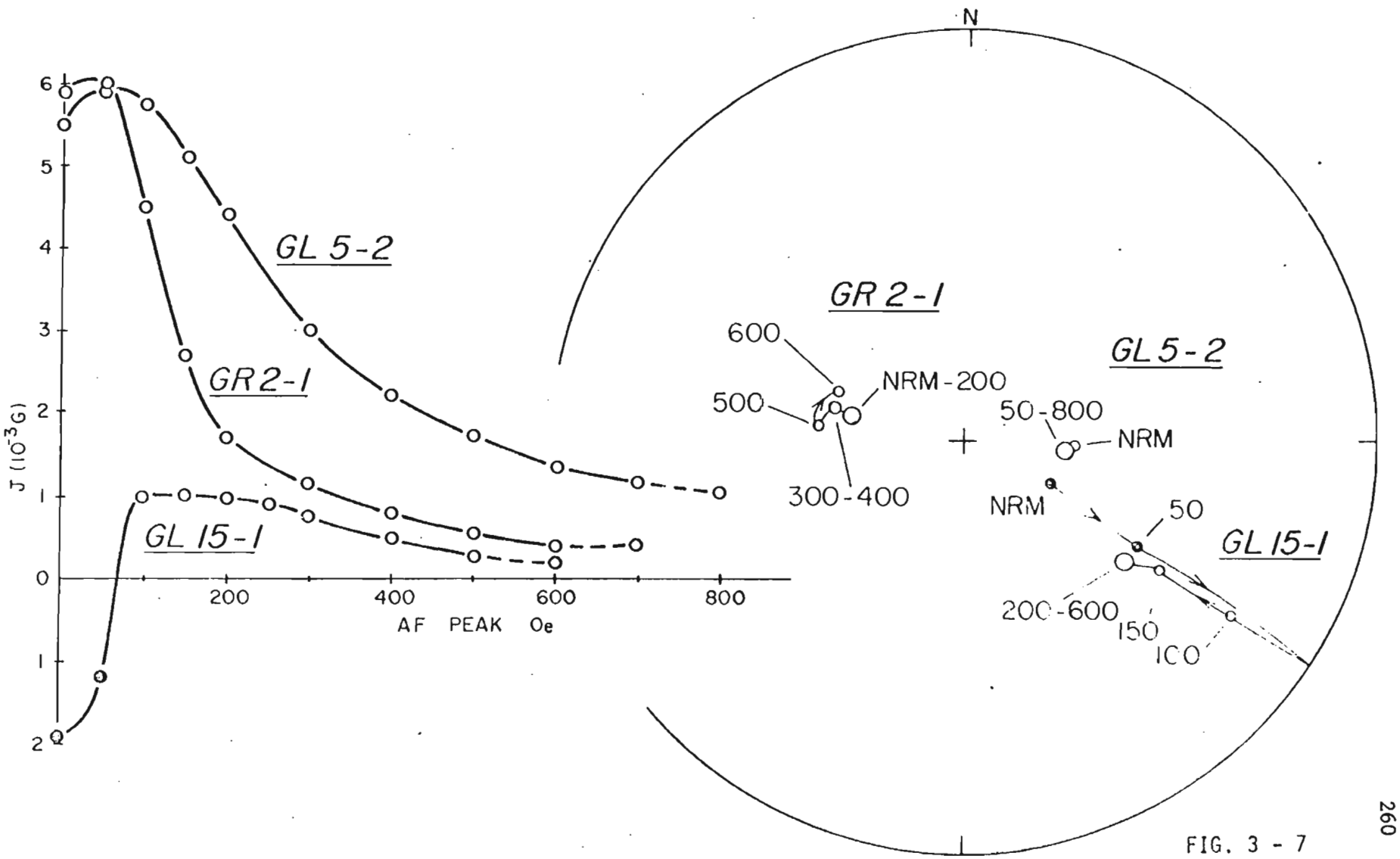
GL 5-2
GR2-1
GL 15-1
J (10^{-3}G)
AF PEAK Oe
N
GR 2-1
600
500
NRM-200
300-400
GL 5-2
50-800
NRM
NRM
50
GL 15-1
200-600
150
ICO

FIG. 3 - 7

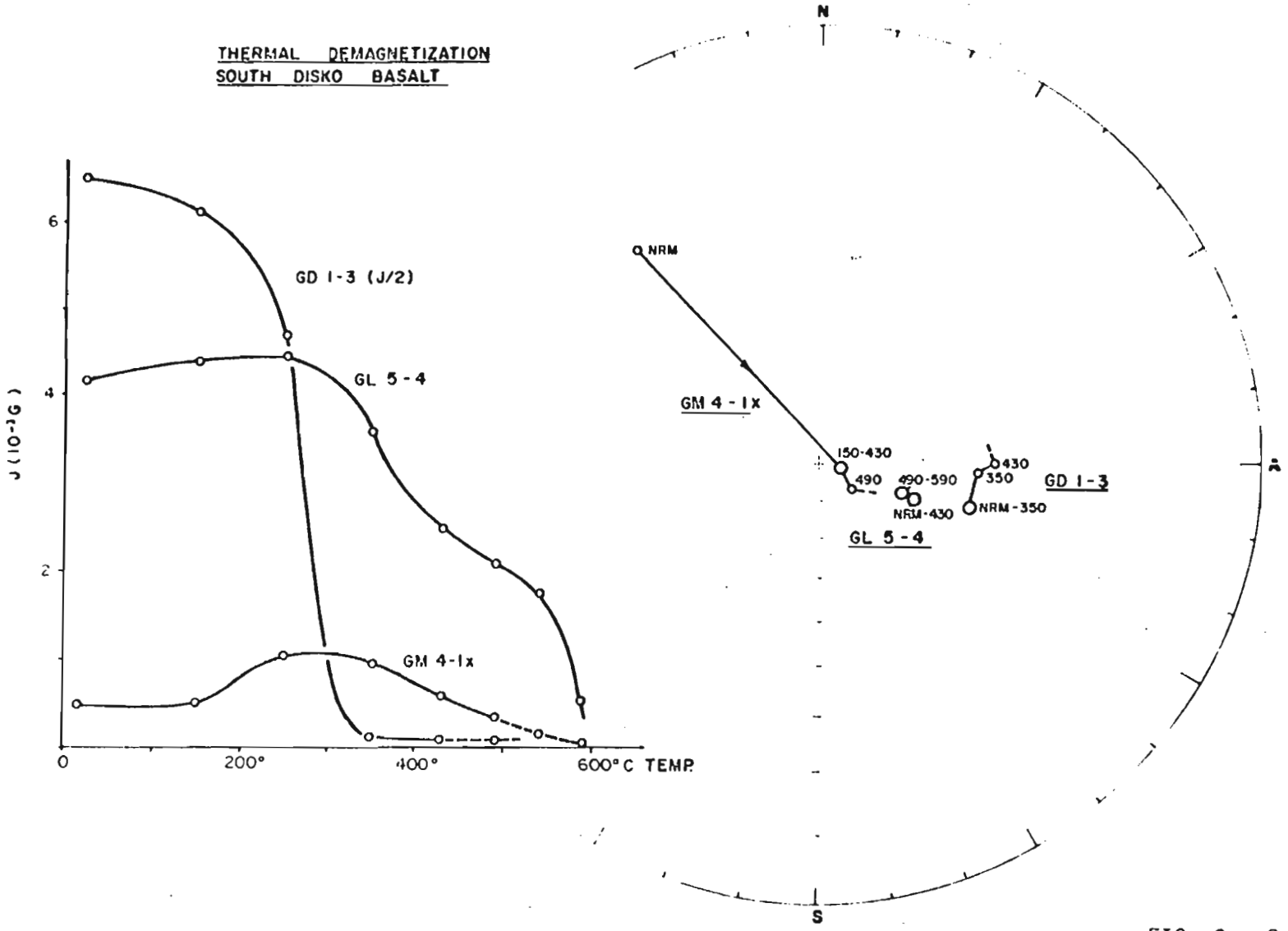
THERMAL DEMAGNETIZATION
SOUTH DISKO BASALT
J (10⁻³G)
6
4
2
0
200°
400°
600°C TEMP.
GD 1-3 (J/2)
GL 5-4
GM 4-1x
N
S
NRM
GM 4-1x
150-430
490
490-590
430
350
GD 1-3
NRM-430
NRM-350
GL 5-4

FIG. 3 - 8

Right: Directional changes of remanence during thermal demagnetization, on a polar equal-angle projection. In both parts of the figure, broken lines indicate the presence of spurious components in J.

The measurements were carried out one year after collection of the samples, so that the NRM direction of the class N sample GM 4-1 had had time to change to a reverse polarity (see text).

Fig. 3-9

Mean paleomagnetic field directions for individual flows (as numbered) in Disko profiles GL and GM, after demagnetization at 200 Oe peak field. Polar azimuthal projection of one quadrant, with the vertical (Z) and inclination values given on the East axis. Directions for successive flows are connected by straight lines.

Fig. 3-10

Left: Paleomagnetic pole position for Disko, calculated from the overall flow-mean remanence direction of profiles GL and GM (Table 3.4), with 95% confidence oval. Also shown are pole positions and 95% confidence ovals from 28 Tertiary flows in East Greenland (Tarling, 1967) and from 253 flows in the Faeroe Islands (Tarling, 1970).

Middle: Individual flow directions for profiles GL and GM, after 200 Oe treatment. Right: Individual site directions for profile GK, breccia and intrusives after 200 Oe treatment. Polar equal-angle projection.

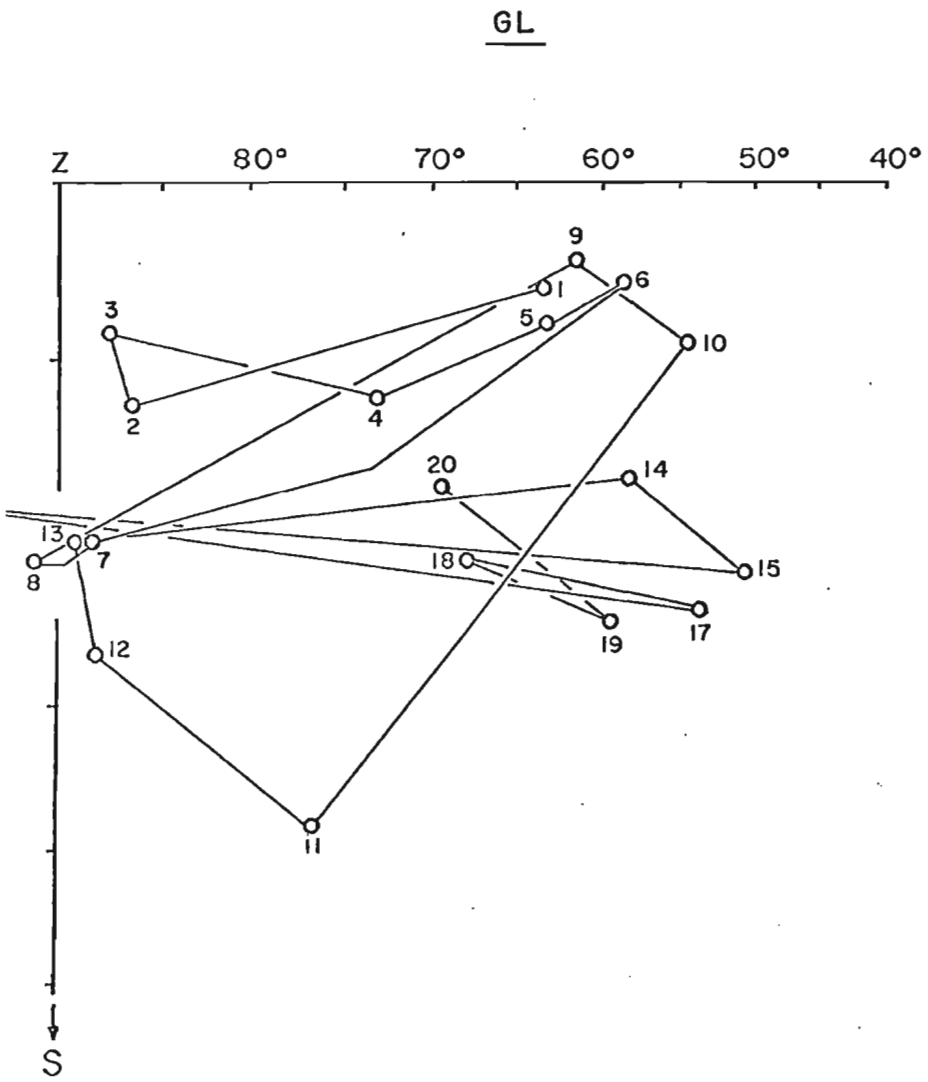
GL
Z
80°
70°
60°
50°
40°
9
1
6
3
5
10
2
4
20
14
13
7
8
18
15
19
17
12
11
S

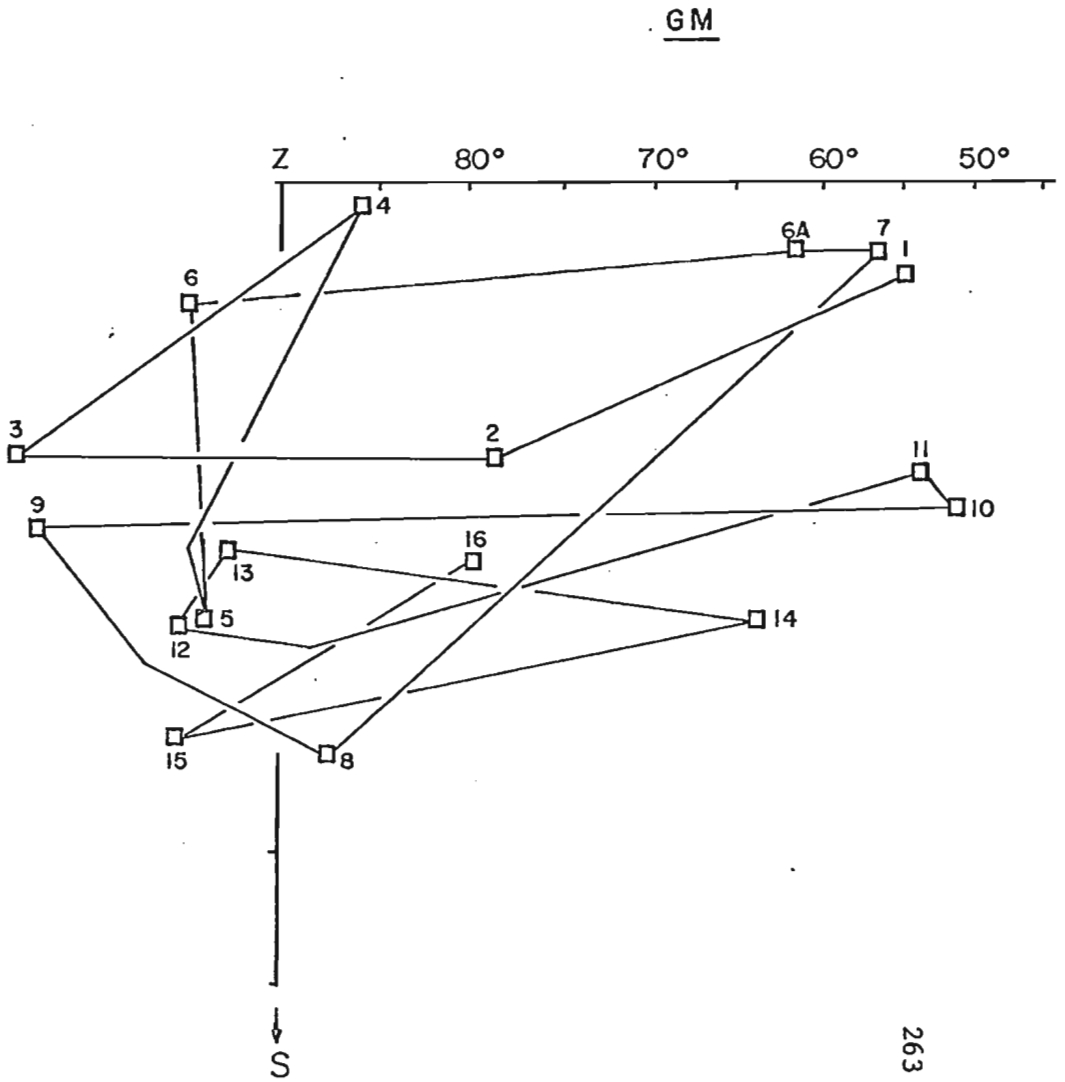
GM
Z
80°
70°
60°
50°
4
6A
7
1
6
3
2
11
10
9
16
13
5
12
14
15
8
S

FIG. 3 - 9

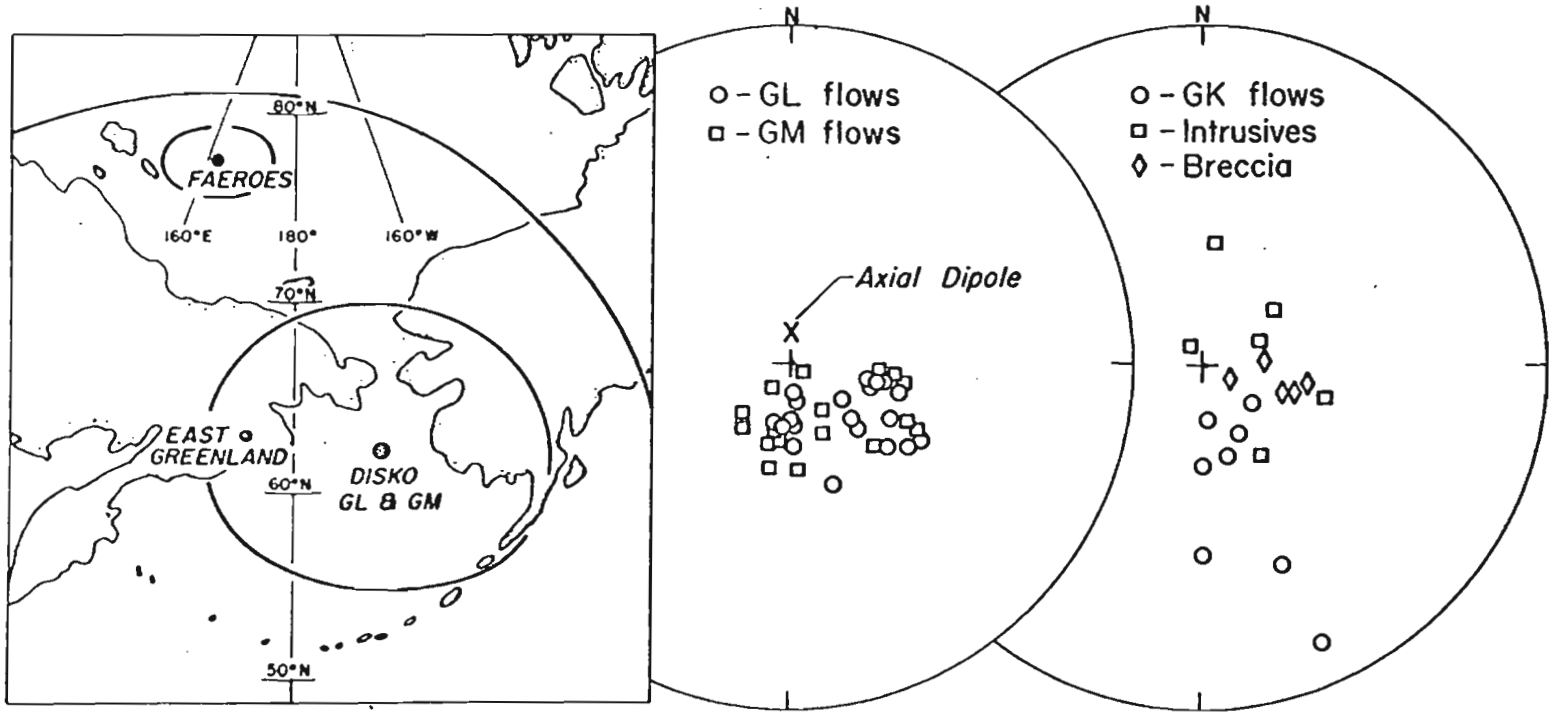
80°N
FAEROES
160°E
180°
160°W
70°N
EAST GREENLAND
60°N
DISKO GL & GM
50°N
N
o - GL flows
□ - GM flows
Axial Dipole
N
o - GK flows
□ - Intrusives
◊ - Breccia

FIG. 3 - 10

Fig. 3-11

Polar projection, showing schematically the movement of the paleomagnetic pole (M) relative to Disko (D), when Disko and Greenland rotate from an original (O) position to a new (N) position. The pivot of Bullard et al. (1965) is at the center of projection. H is the Greenwich meridian. The angles R and p are explained in the text.

Fig. 3-12

Typical strong-field thermomagnetic curves for Disko class N lava samples. T_c = Curie point using the definition of Appendix 2.2, but note the presence of a low-Curie-point component. H_{ex} = external field during measurement.

Fig. 3-13

Strong-field thermomagnetic curves for Disko class R lava samples. Of five curves obtained, four resembled that of GL 5-2. See legend to Fig. 3-12.

Fig. 3-14

(a) Artificial TRM intensity, acquired by Disko and Cape Dyer samples on cooling from 600°C in air, plotted against susceptibility. Open (filled) circles represent Disko class N (R) samples, and crosses represent high-Curie-point Cape Dyer samples. Lines corresponding to Q-ratios for certain magnetite grain sizes (Q=7.2 for 1.5μ; Q=2.0 for 6μ; and Q= 0.5 for multi-domain grains, as obtained by Parry 1965) are drawn. Double circles are average

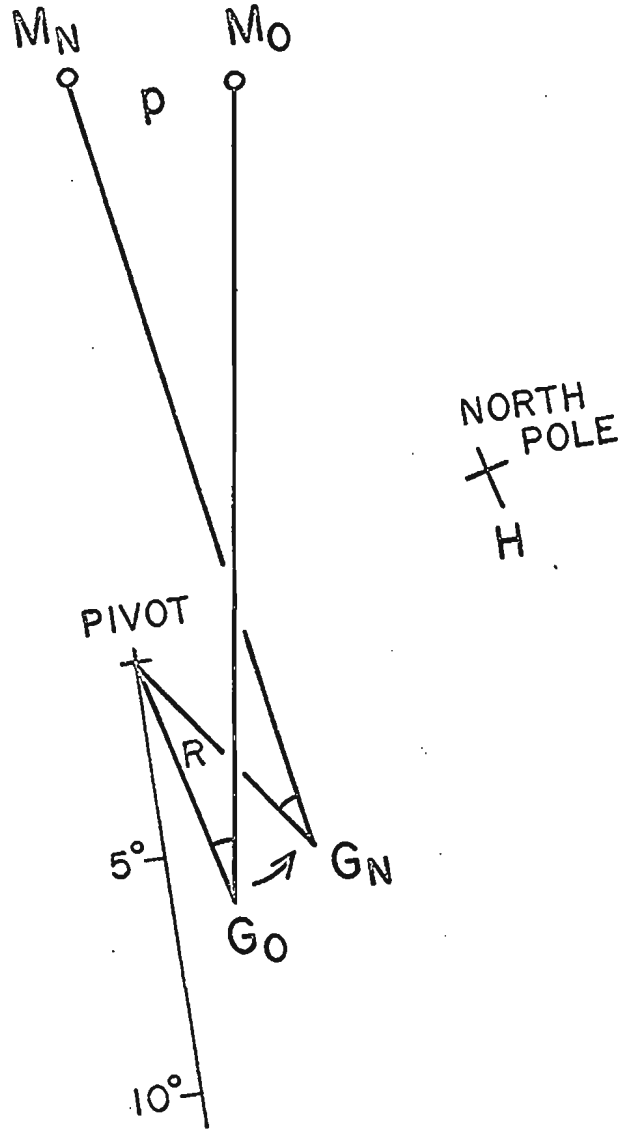

FIG. 3 - 11

THERMOMAGNETIC CURVES
DISKO CLASS N SAMPLES

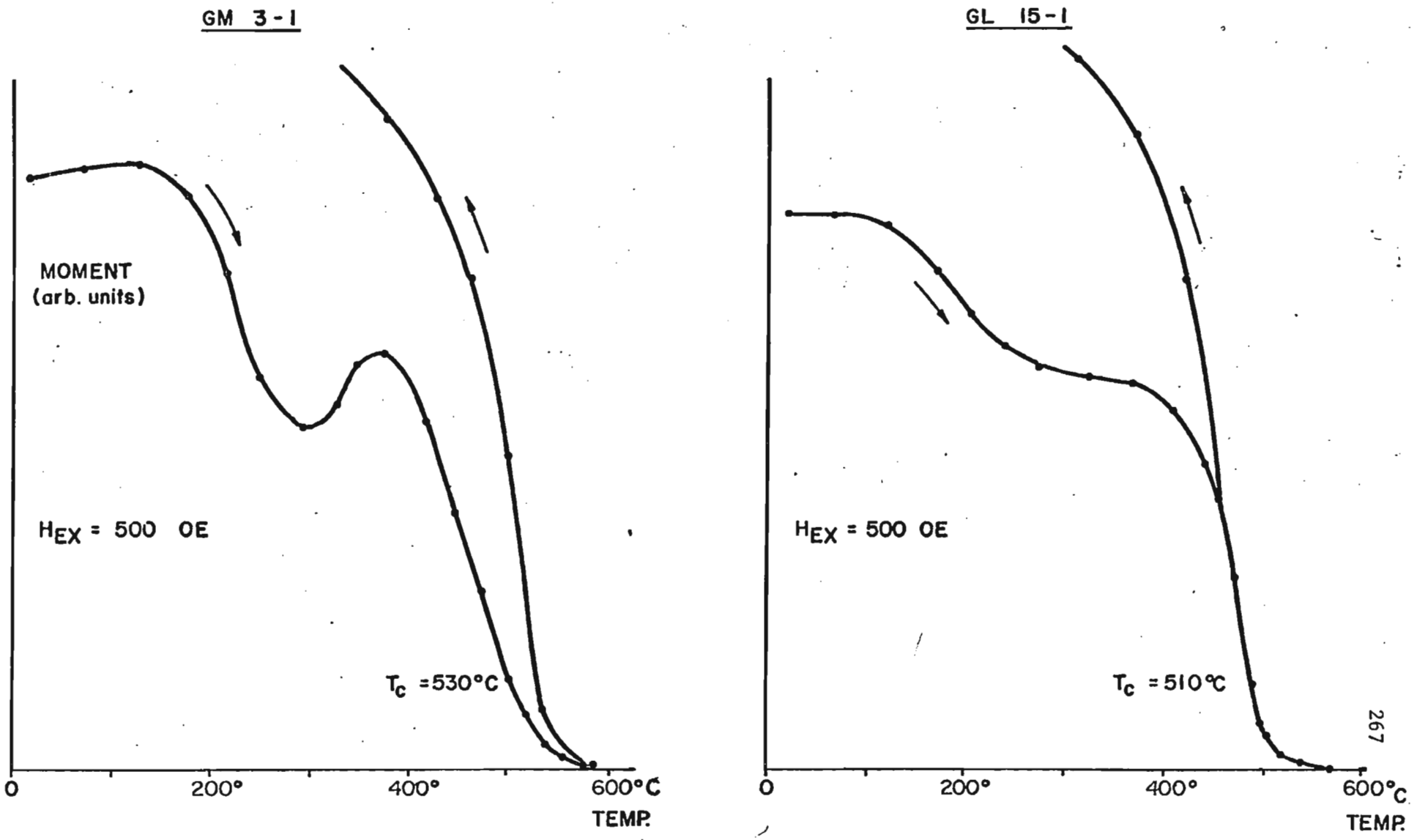

FIG. 3 - 12

THERMOMAGNETIC CURVES
DISKO CLASS R SAMPLES

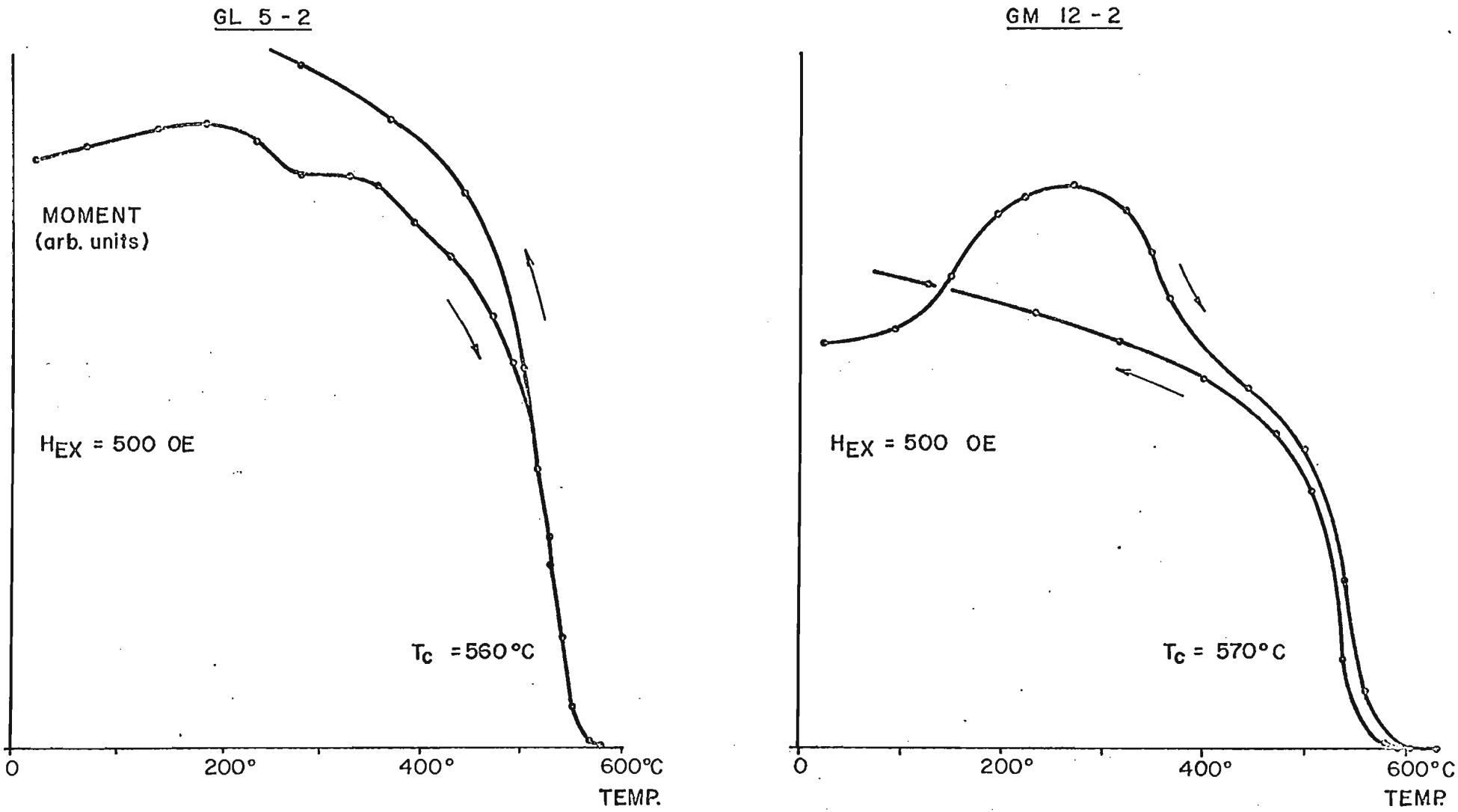

FIG. 3 - 13

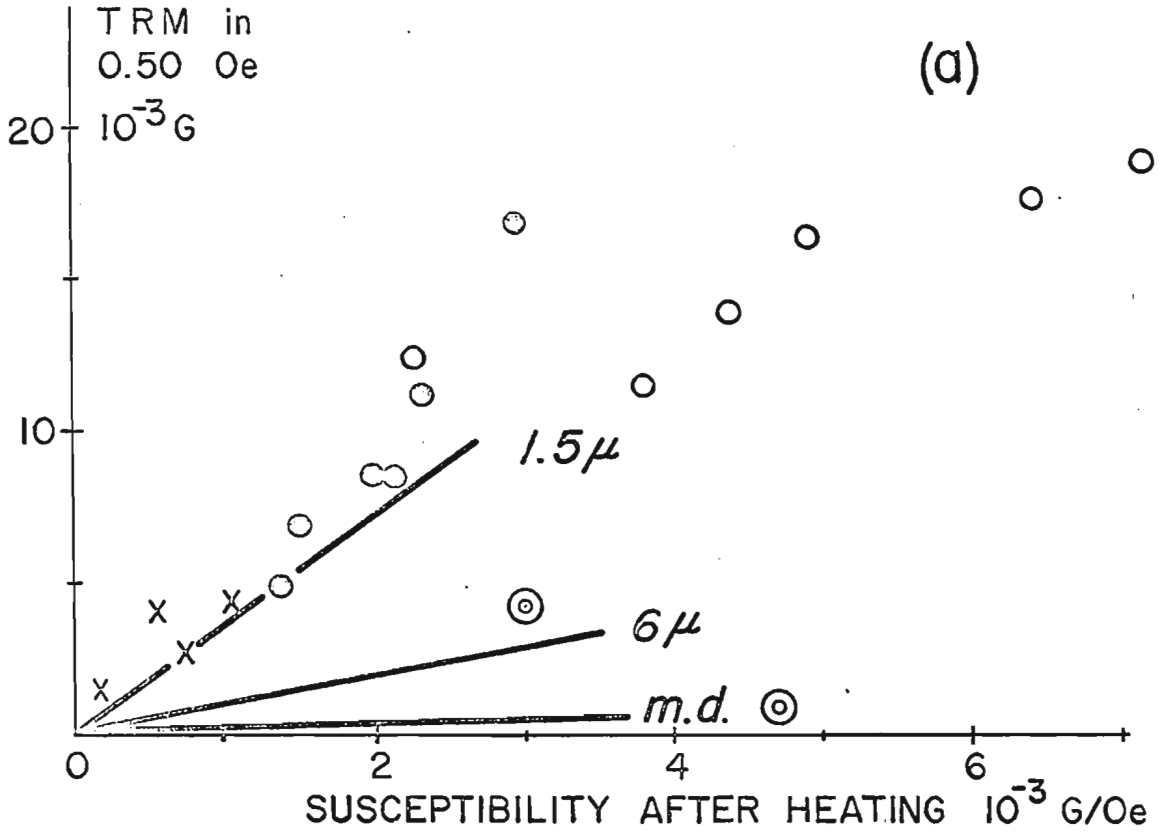
TRM in
0.50 Oe
10^{-3} G
(a)
20
10
1.5μ
6μ
m.d.
0
2
4
6
SUSCEPTIBILITY AFTER HEATING 10^{-3} G/Oe

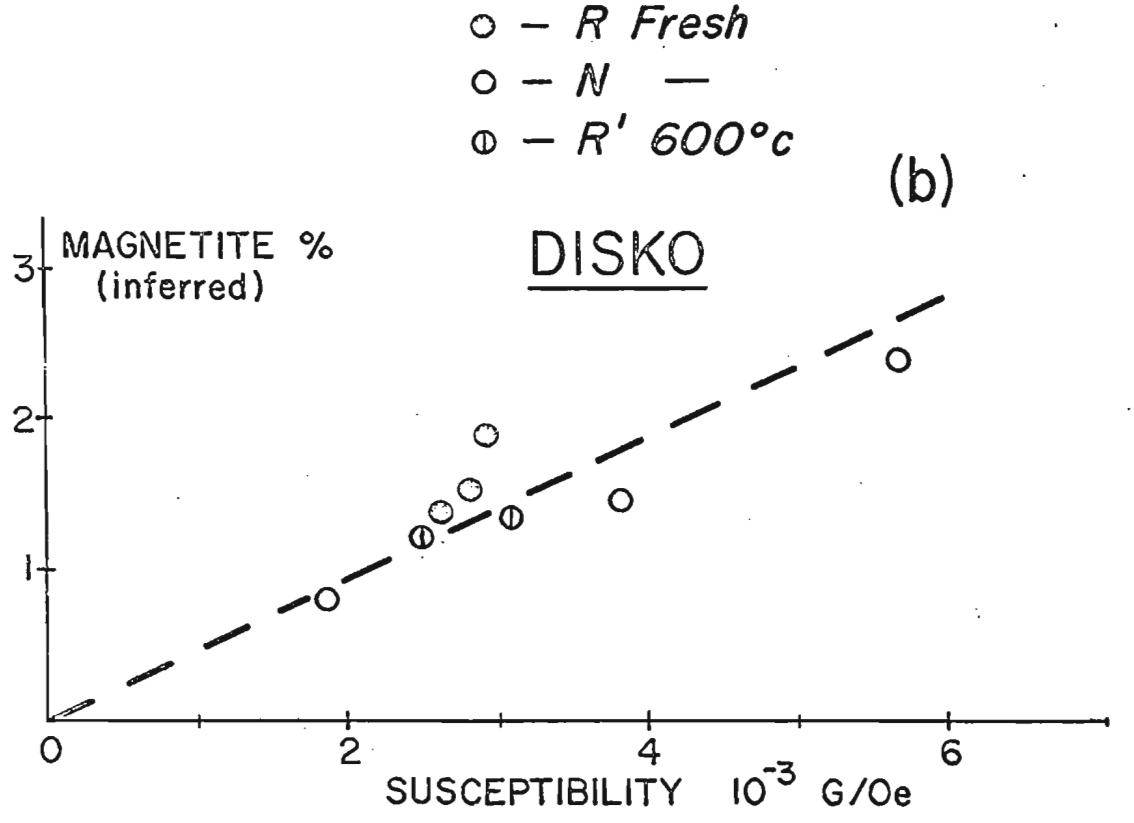
○ – R Fresh
○ – N —
◐ – R' 600°c
(b)
DISKO
MAGNETITE %
(inferred)
3
2
1
0
2
4
6
SUSCEPTIBILITY 10^{-3} G/Oe

FIG. 3 - 14

values of J_{max} and susceptibility before heating, as obtained from the data of Section 3.11.8.

(b) Magnetite percentage (by volume) in Disko rocks, as inferred from ballistic magnetometer measurements, plotted against susceptibility. Note that in the fresh class N and R rocks this is not the true percentage, because of the presence of low-Curie-point titanomagnetites (Fig. 3-12; Sect. 2.7). Reciprocal slope of broken line: $2.1 \cdot 10^{-3}$ G/Oe per percent.

Fig. 3-15

Changes in room-temperature susceptibility K during stepwise thermal demagnetization of Disko basalt samples.
Top to bottom: Class N, R and R´. The temperatures are those reached during each heating.

Fig. 3-16

Magnetite percentage in various rock types, inferred from saturation magnetization measurements, plotted against sample susceptibility. All rocks have a single high (>500°C) Curie point only. Solid circles represent fresh gneiss from the Baffin Bay coast; solid squares, fresh basalt from Baffin Island; open circles, low-Curie-point basalt from Baffin Bay that had been heated to 600°C in air; solid triangles, fresh basalt, diabase and gabbro from Iceland; and open triangles, fresh drill chips from geothermal drill holes in Iceland. B,G are the average susceptibilities of collections of basalt lavas and of gabbros from Iceland (Kristjansson 1970).

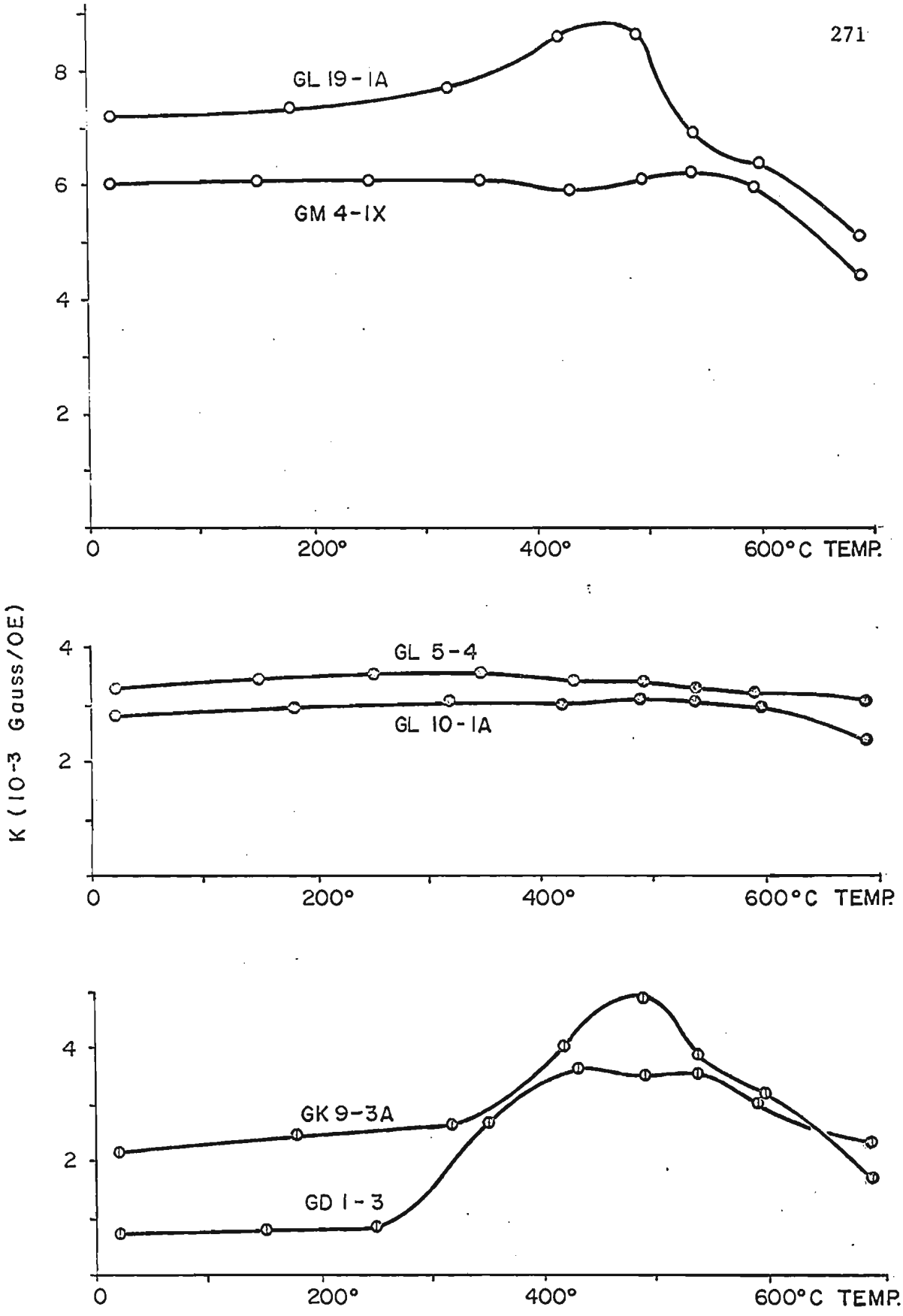
GL 19-1A
GM 4-1X
8
6
4
2
0
200°
400°
600°C TEMP.
K (10-3 Gauss/OE)
GL 5-4
GL 10-1A
4
2
0
200°
400°
600°C TEMP.
GK 9-3A
GD 1-3
4
2
0
200°
400°
600°C TEMP.

FIG. 3 - 15

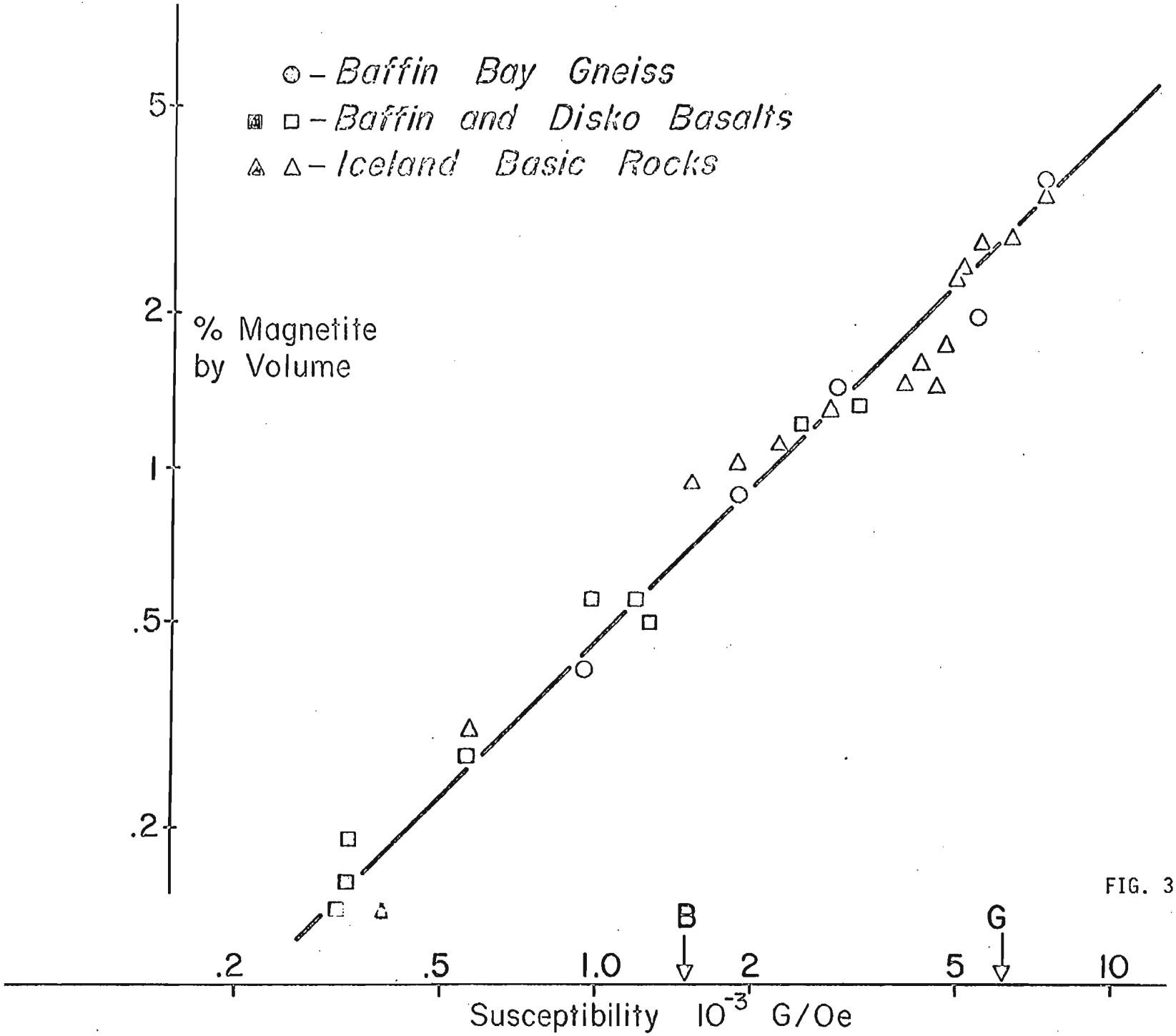
○ – Baffin Bay Gneiss
□ – Baffin and Disko Basalts
△ – Iceland Basic Rocks
% Magnetite by Volume
5
2
1
.5
.2
B
G
.2
.5
1.0
2
5
10
Susceptibility 10^{-3} G/Oe

FIG. 3 - 16

Fig. 3-17

Strong-field thermomagnetic curves for two class R′ samples from flows in profile GK, Disko. See legend to Fig. 3-12.

Fig. 3-18

Thermomagnetic curves for class R′ samples from an intrusive and from the breccia in Disko. See legend to Fig. 3-12.

Fig. 3-19

Viscous magnetization built up in Disko basalt specimens over a period of ten weeks, on standing in the earth's field (0.5 Oe).

Fig. 3-20

(a) Typical strong-field thermomagnetic curve for a sample of interbasaltic red sediment. Note the linearity of the curve, and the Curie point of 620°C.

(b) Normalized remanence intensities of four samples of interbasaltic red sediment.

Samples marked GL are from Disko, the others from Iceland.

Fig. 3-21

Average intensity values of primary (P), secondary (S) and induced (KF) magnetization components of Disko rocks in situ. In this schematic drawing, the vectors are projected onto the YZ-plane; the actual vectors $\vec{P}$ and $\overrightarrow{KF}$ make angles of 67° and 82° with the horizontal plane (Table 3.4) and $\vec{S}$ is parallel to $\overrightarrow{KF}$ for a short VRM time constant (Sect. 1.4), but has an inclination of 79° and zero declination for a long time constant. The average intensities are taken from Table 3.13.

THERMOMAGNETIC CURVES
DISKO GK FLOWS

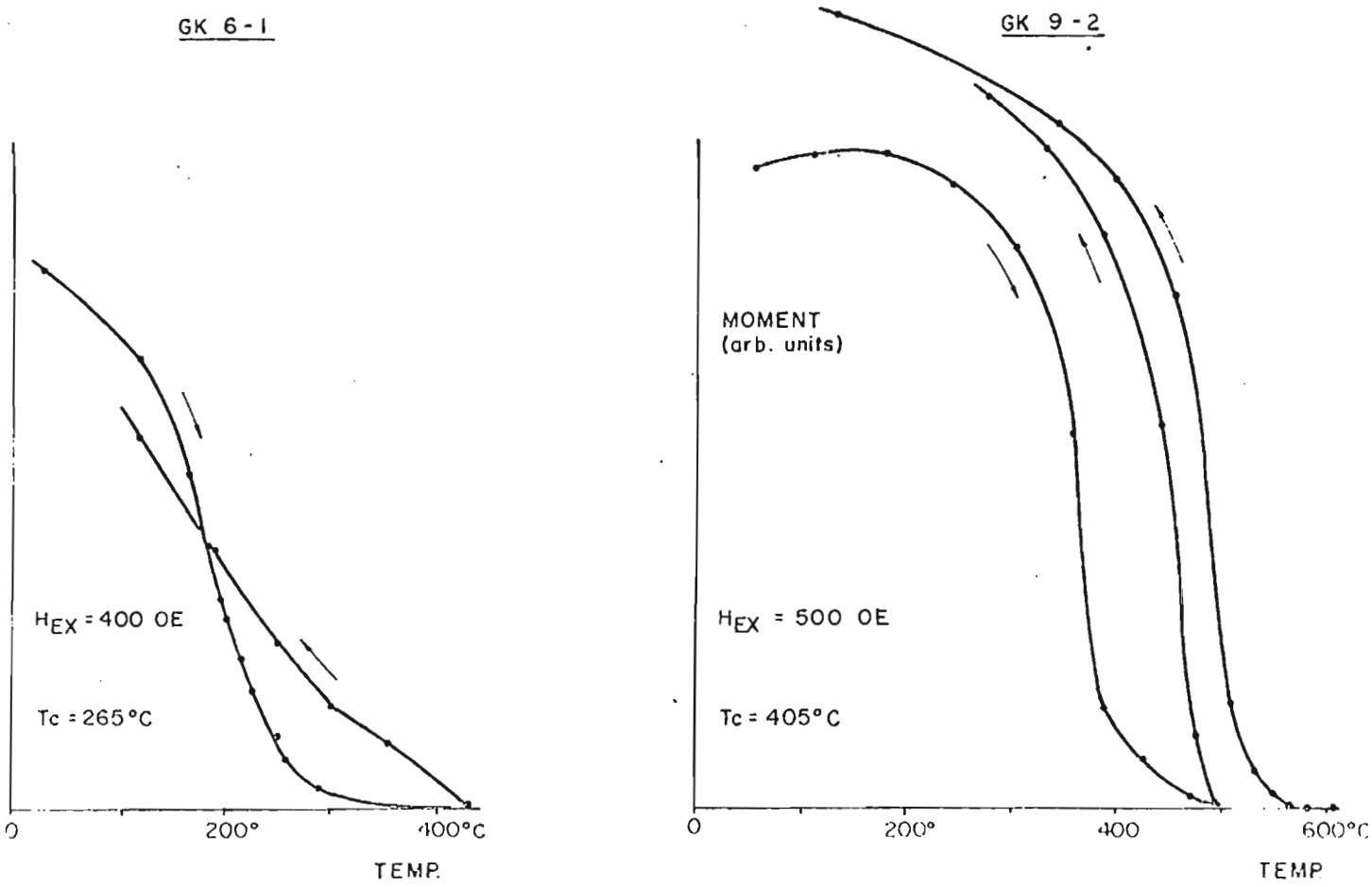

FIG. 3 - 17

THERMOMAGNETIC CURVES
DISKO DYKE AND BRECCIA

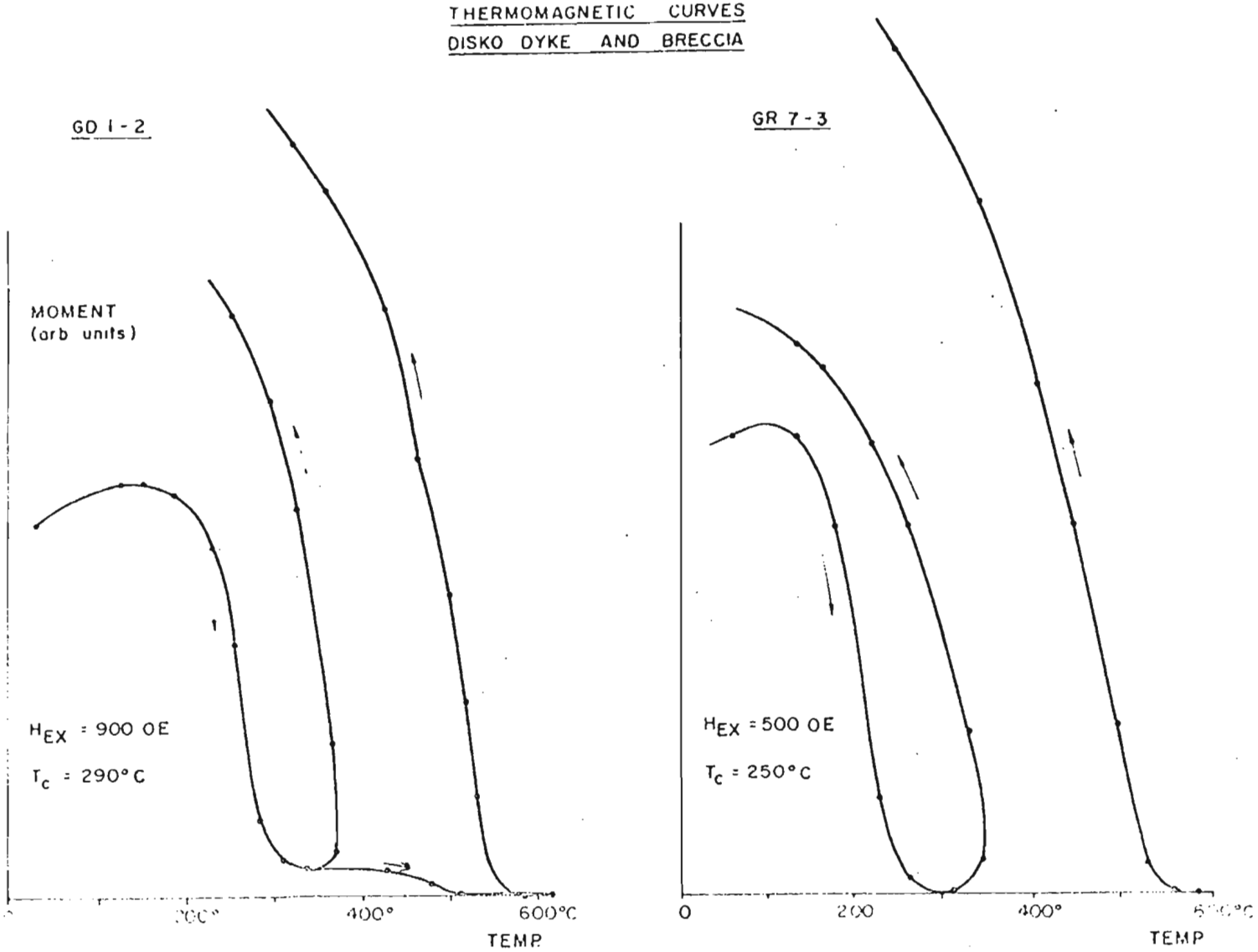

FIG. 3 - 18

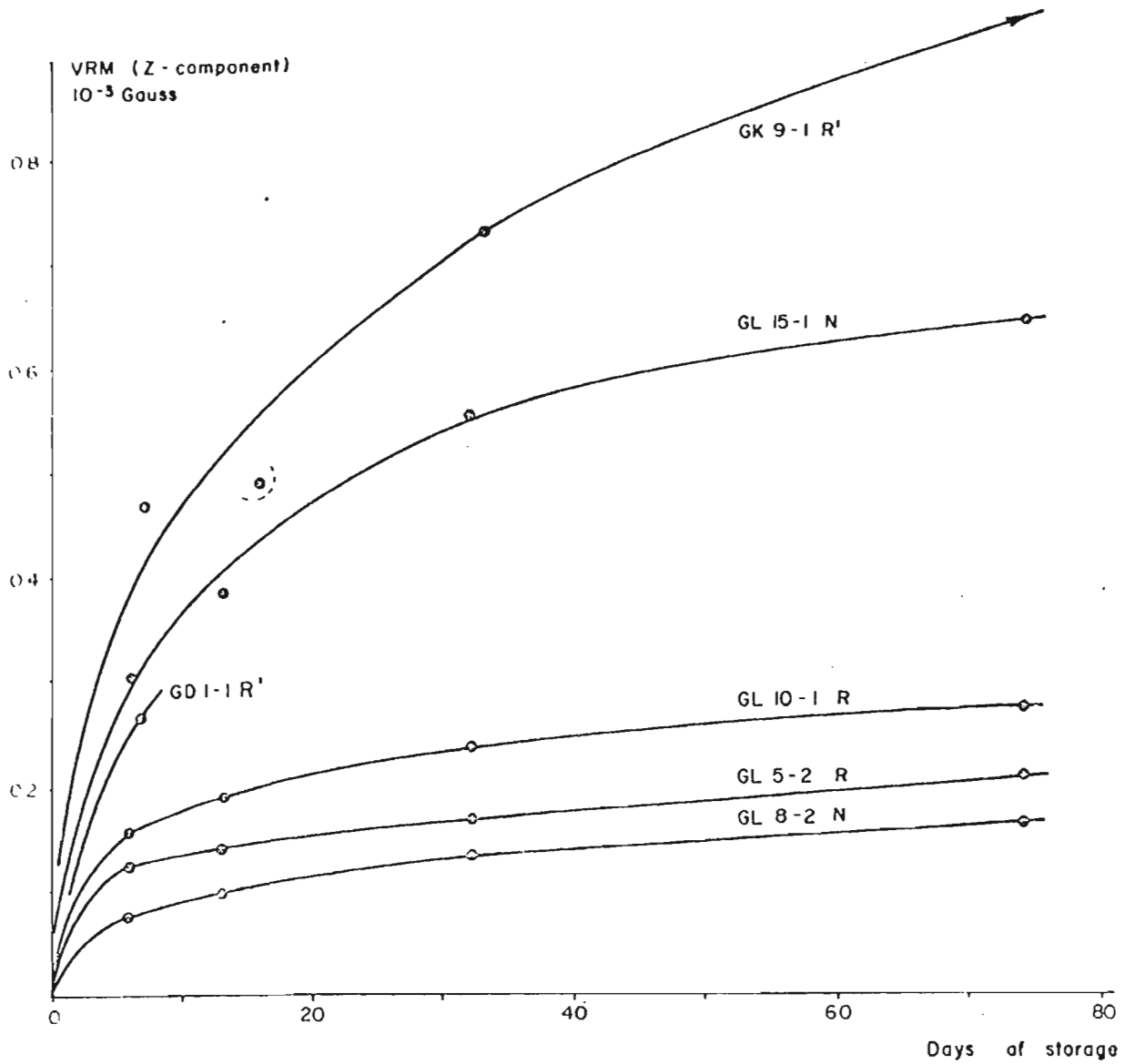
VRM (Z - component)
10⁻³ Gauss
0.8
0.6
0.4
0.2
0
20
40
60
80
Days of storage
GK 9-1 R'
GL 15-1 N
GD 1-1 R'
GL 10-1 R
GL 5-2 R
GL 8-2 N

FIG. 3 - 19

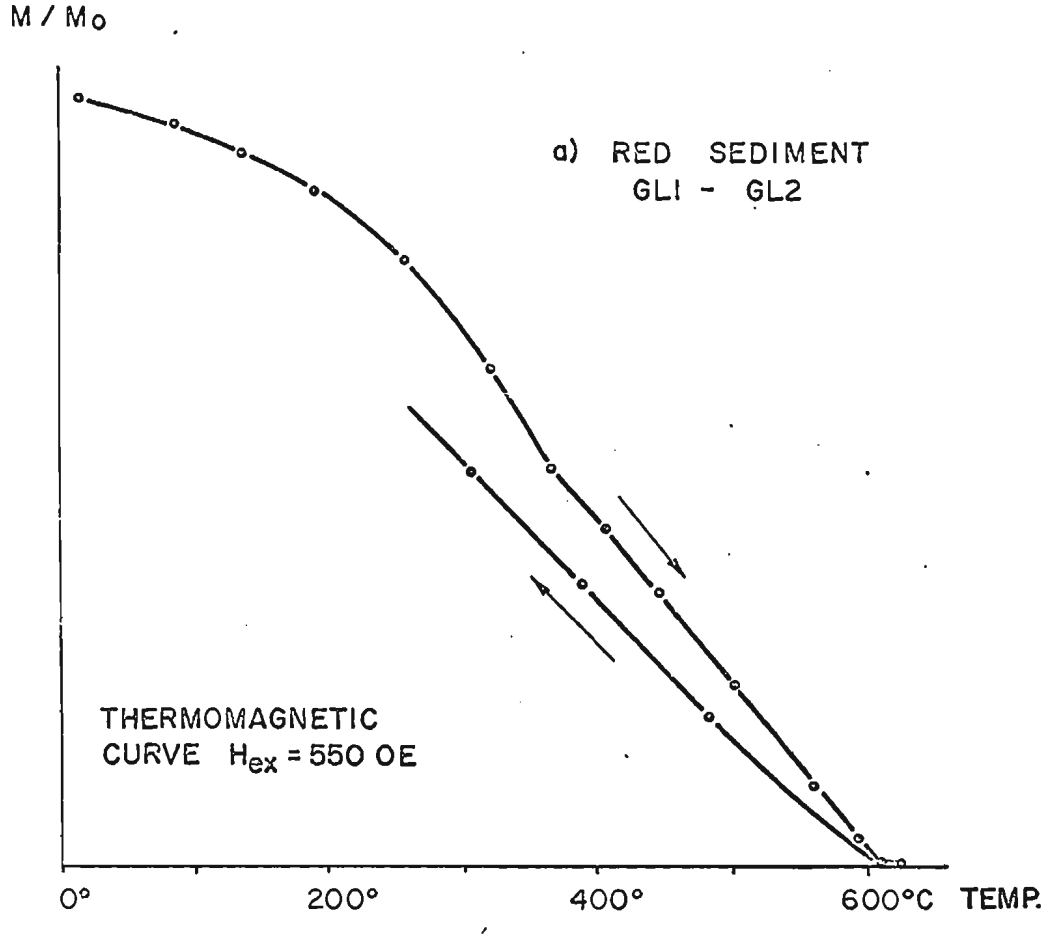
M / Mo
a) RED SEDIMENT
GL1 - GL2
THERMOMAGNETIC
CURVE Hex = 550 OE
0°
200°
400°
600°C TEMP.

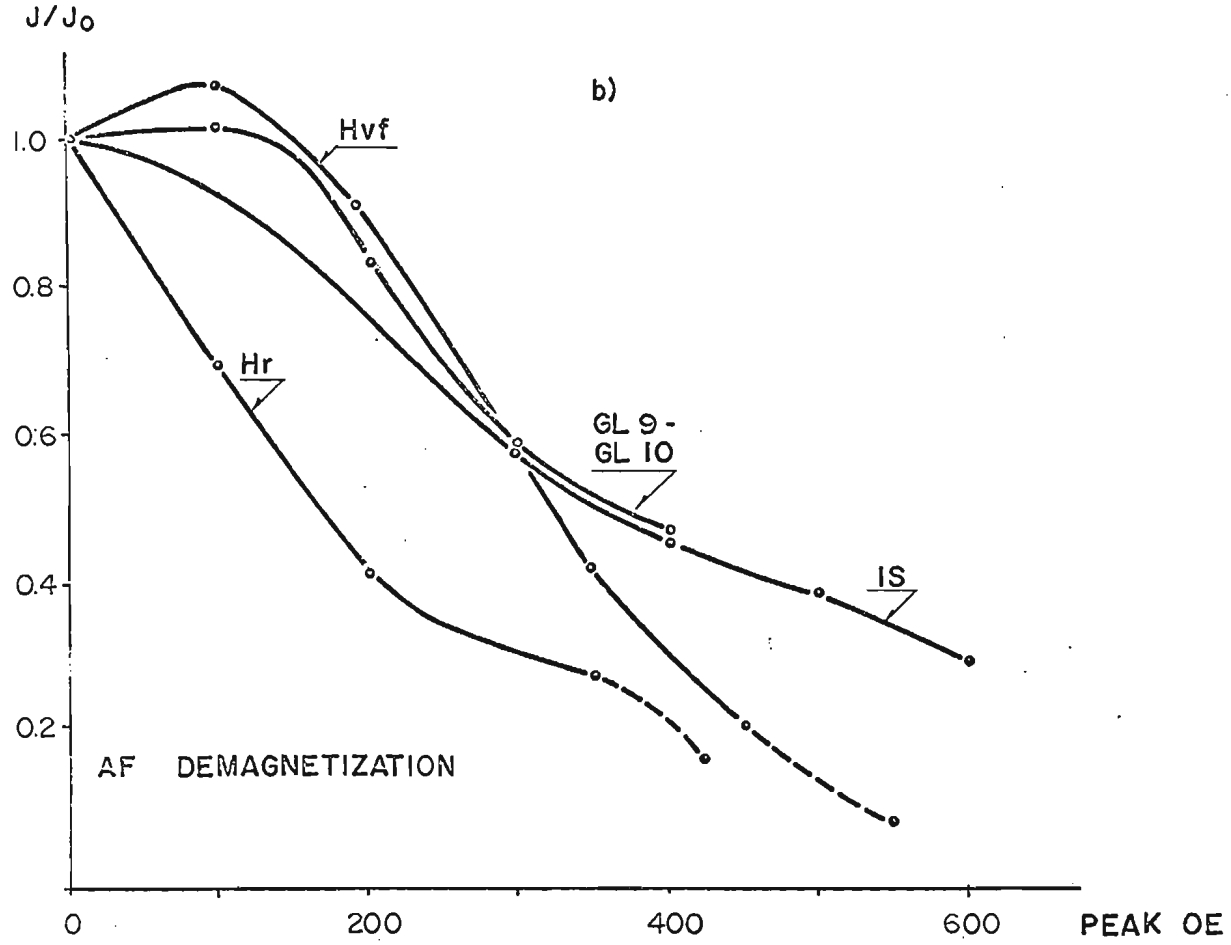
J/Jo
b)
1.0
0.8
0.6
0.4
0.2
Hvf
Hr
GL 9 -
GL 10
IS
AF DEMAGNETIZATION
0
200
400
600
PEAK OE

FIG. 3 - 20

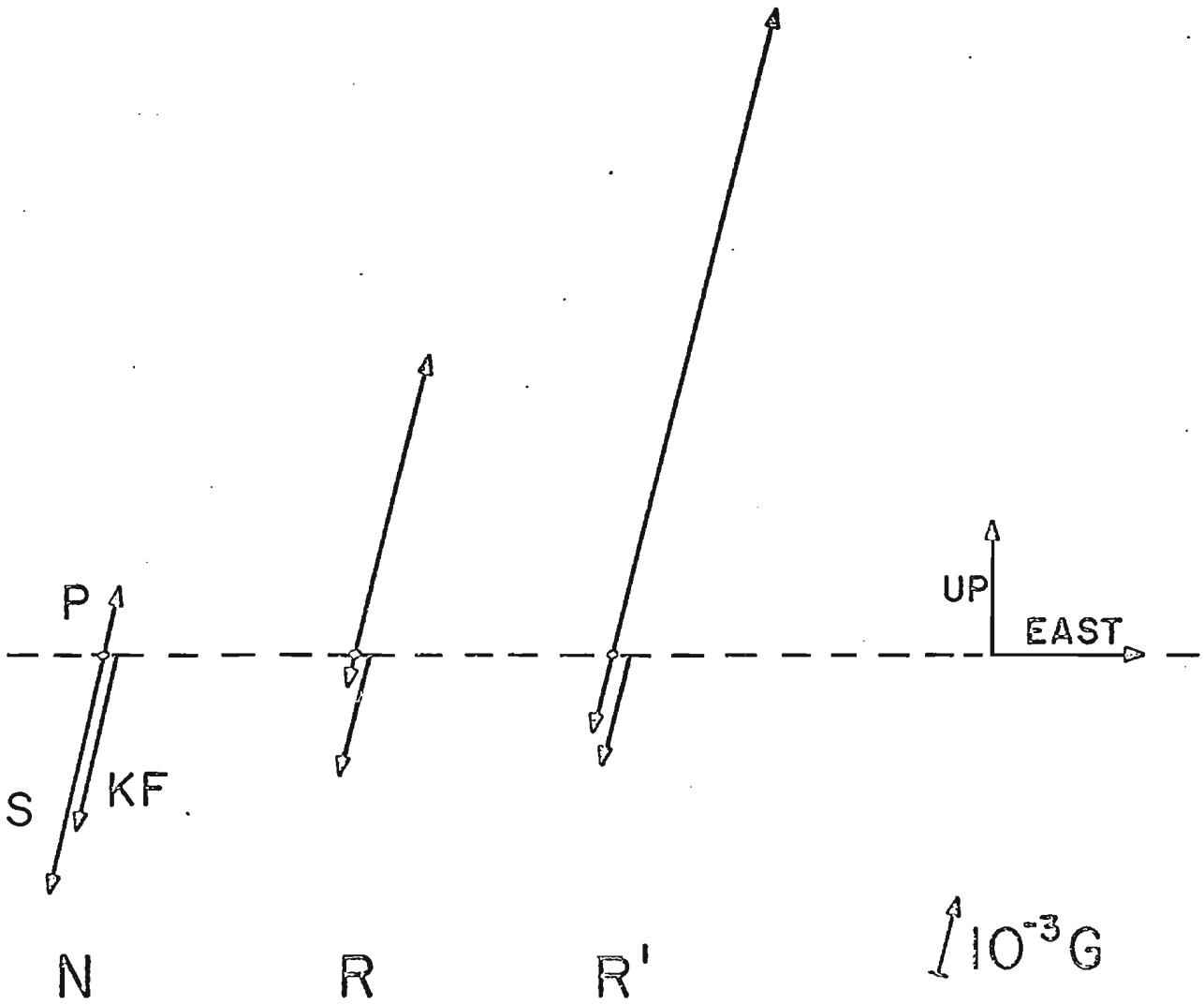

FIG. 3 - 21

Fig. 4-1

Remanence intensity of one pilot specimen from each of the six Cape Dyer flows, during stepwise AF demagnetization. Numbers denote flows; the flow 3 specimen ($\bar{3}$) had reverse NRM polarity.

Fig. 4-2

NRM intensity (J_o) vs. initial volume susceptibility (K) for some Cape Dyer samples. In a few cases, single data points correspond to the average of two or more samples from a particular flow. Flow 3 samples here are all normally magnetized (+).

Fig. 4-3

Cape Dyer flow mean directions and 95% confidence circles after AF treatment to 400 peak Oe. N samples were averaged per flow (Table 4.3). Flow 3 samples here are all normally magnetized (+). + Mean direction, flows 1 to 5; X axial dipole field; + 1968 field. Polar azimuthal projection.

Fig. 4-4

Paleomagnetic poles from early Tertiary rocks in North America. Matching numbers refer to: $|\bar{\cdot}|$ sampling sites; O pole positions. 1. Green River sediments, Colorado (Torreson et al. 1949); 2. Siletz River basalts, Oregon (Cox 1957); 3. Beaverhead volcanics, Montana (Hanna 1967); 4. Flagstaff intrusives, Colorado (McMahon and Strangway 1968); 5. Spanish Peaks dike swarm, Colorado (Larson and Strangway 1969); 6. Basalts, Golden, Colorado

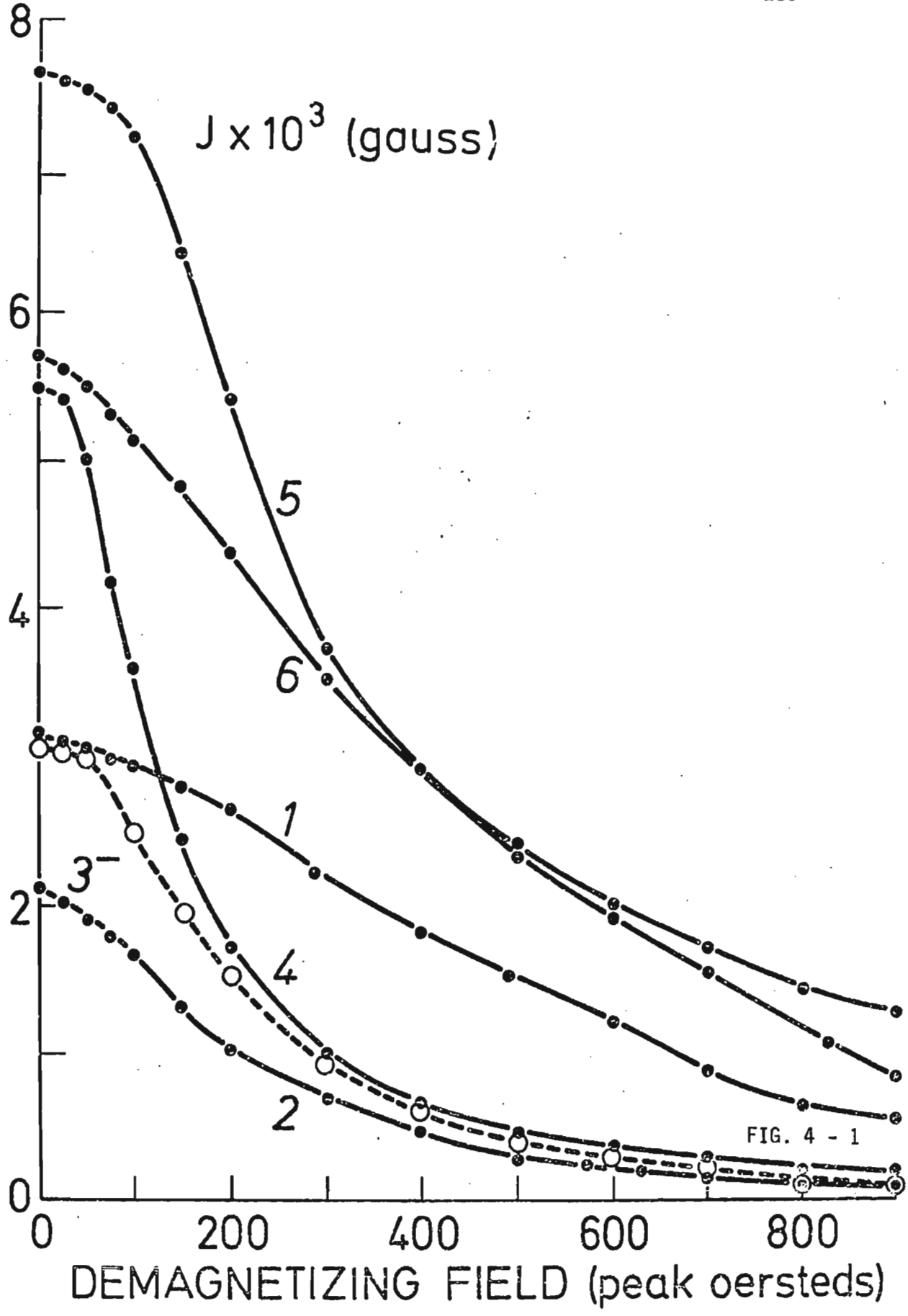
8
6
4
2
0
J x 10³ (gauss)
5
6
1
3
4
2
0
200
400
600
800
DEMAGNETIZING FIELD (peak oersteds)

FIG. 4 - 1

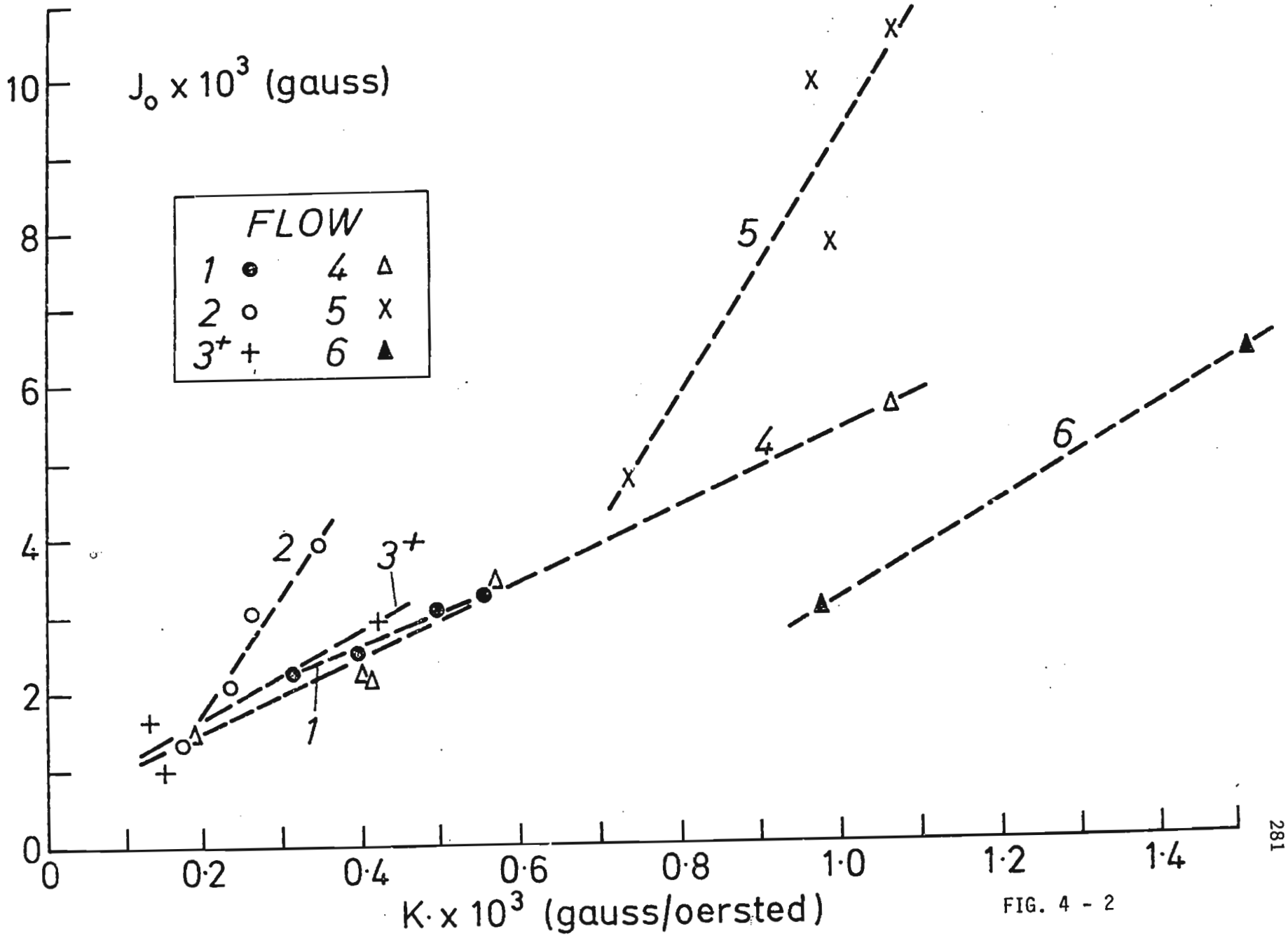
$J_o \times 10^3$ (gauss)
FLOW
1 ●
2 ○
3+ +
4 Δ
5 X
6 ▲
10
8
6
4
2
0
0
0·2
0·4
0·6
0·8
1·0
1·2
1·4
$K \cdot \times 10^3$ (gauss/oersted)
1
2
3+
4
5
6

FIG. 4 - 2

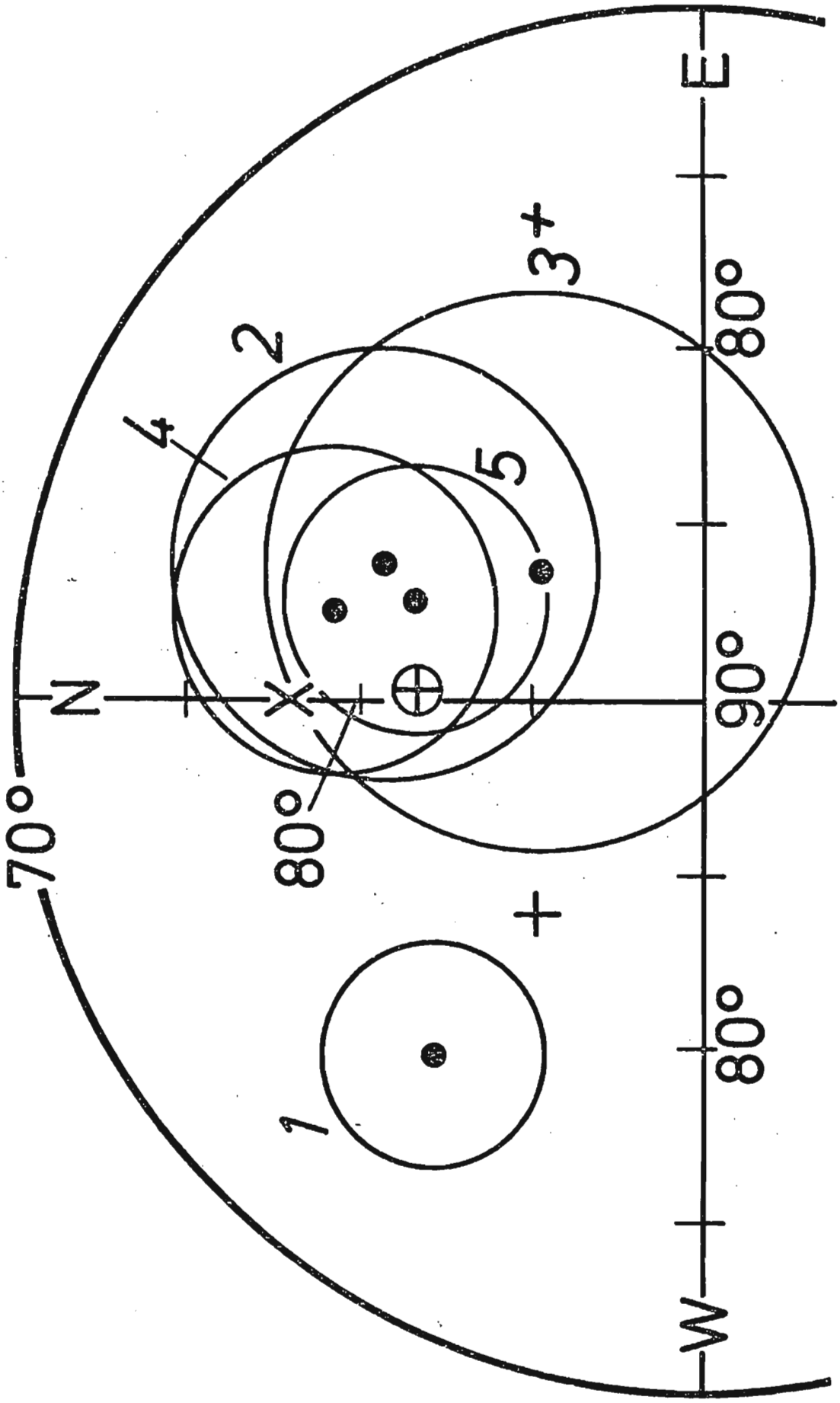

FIG. 4 - 3

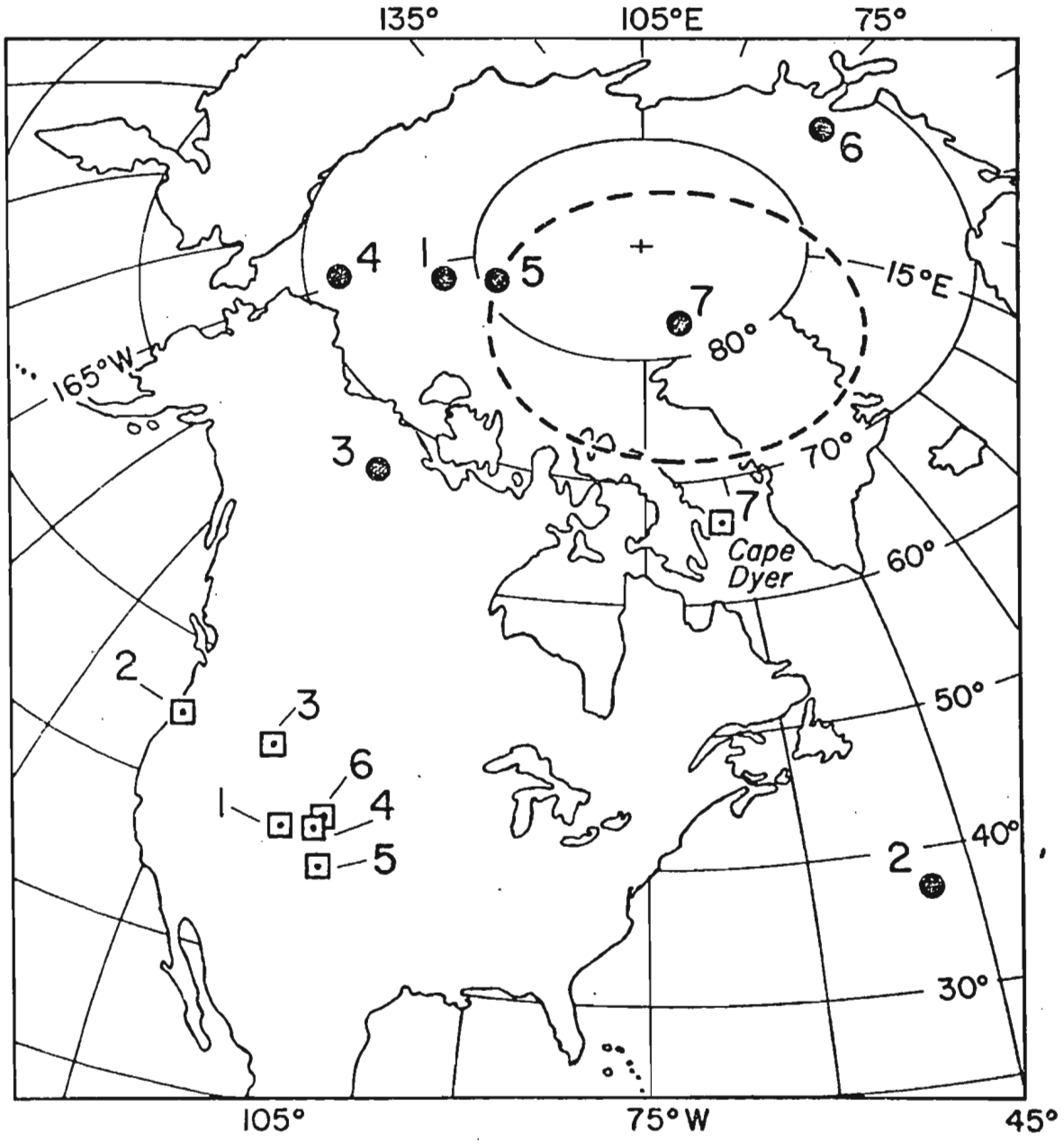
135°
105°E
75°
6
4
1
5
7
15°E
80°
165°W
3
70°
7
Cape
Dyer
60°
2
3
50°
6
1
4
40°
5
2
30°
105°
75°W
45°

FIG. 4 - 4

(Larson et al. 1970): the pole shown is a weighted mean of poles quoted for the two "upper" flows and the "lowest" flow. 7. This study, shown with 95% confidence oval.

Fig. 4-5

Normalized remanence intensity of single specimens from Cape Dyer flows 1,2,5,6, after stepwise thermal demagnetization in air. Data from Table 4.4.

Fig. 4-6

Remanence intensity of single specimens from Cape Dyer flow 3, after stepwise thermal demagnetization in air. Sample numbers are shown. Solid (open) circled denote normal (reversed) NRM polarity. Data from Table 4.5.

Fig. 4-7

Thermomagnetic curves for Cape Dyer basalt samples from flows 1 and 6: the curves for samples from flows 4 and 5 are similar to these, or intermediate between them.

Fig. 4-8

Thermomagnetic curves for samples from Cape Dyer flow 2.

Fig. 4-9

Thermomagnetic curves for samples from Cape Dyer flow 3. Note the difference between the curve for 3-1 (+NRM polarity) and 3-3 (-NRM polarity) at low temperatures.

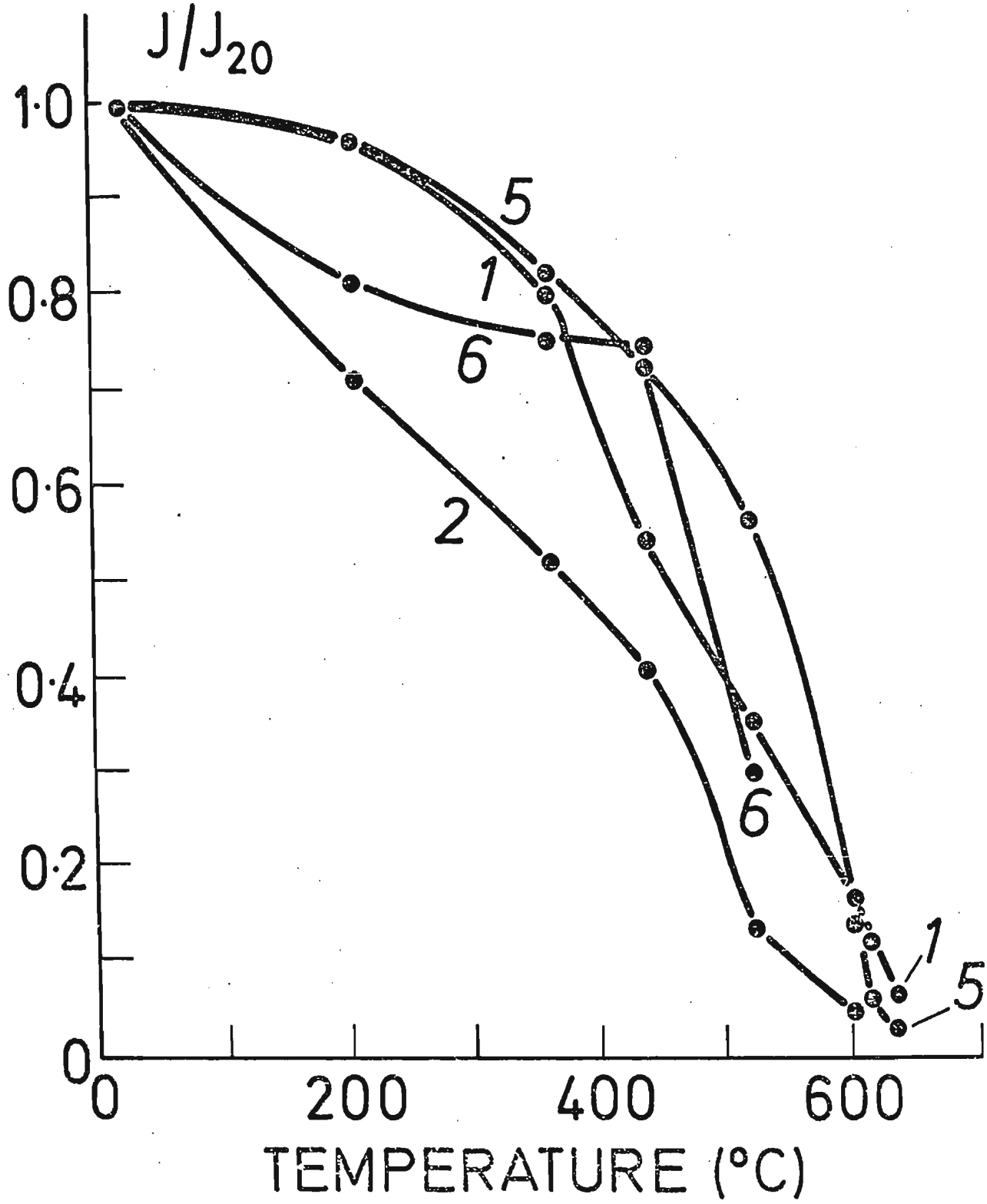

FIG. 4 - 5

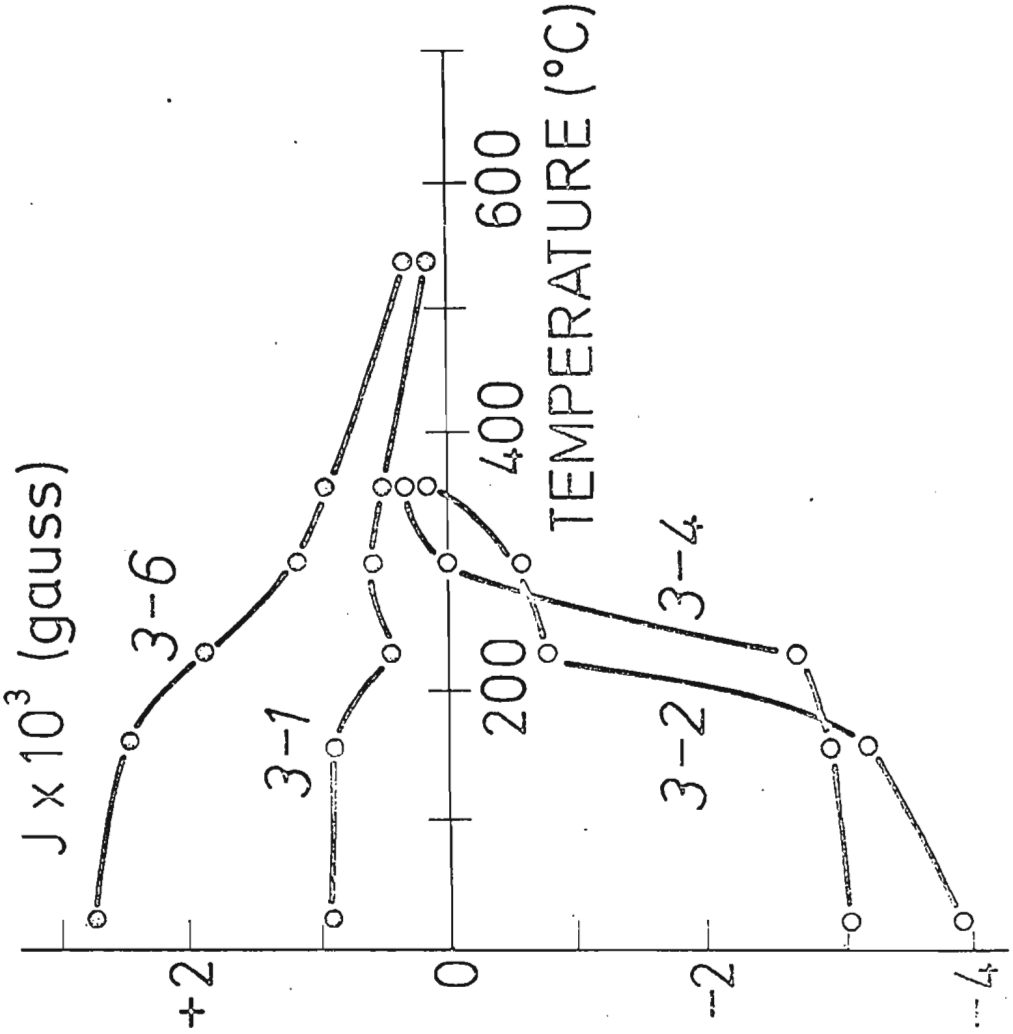

FIG. 4 - 6

THERMOMAGNETIC CURVES
CAPE DYER

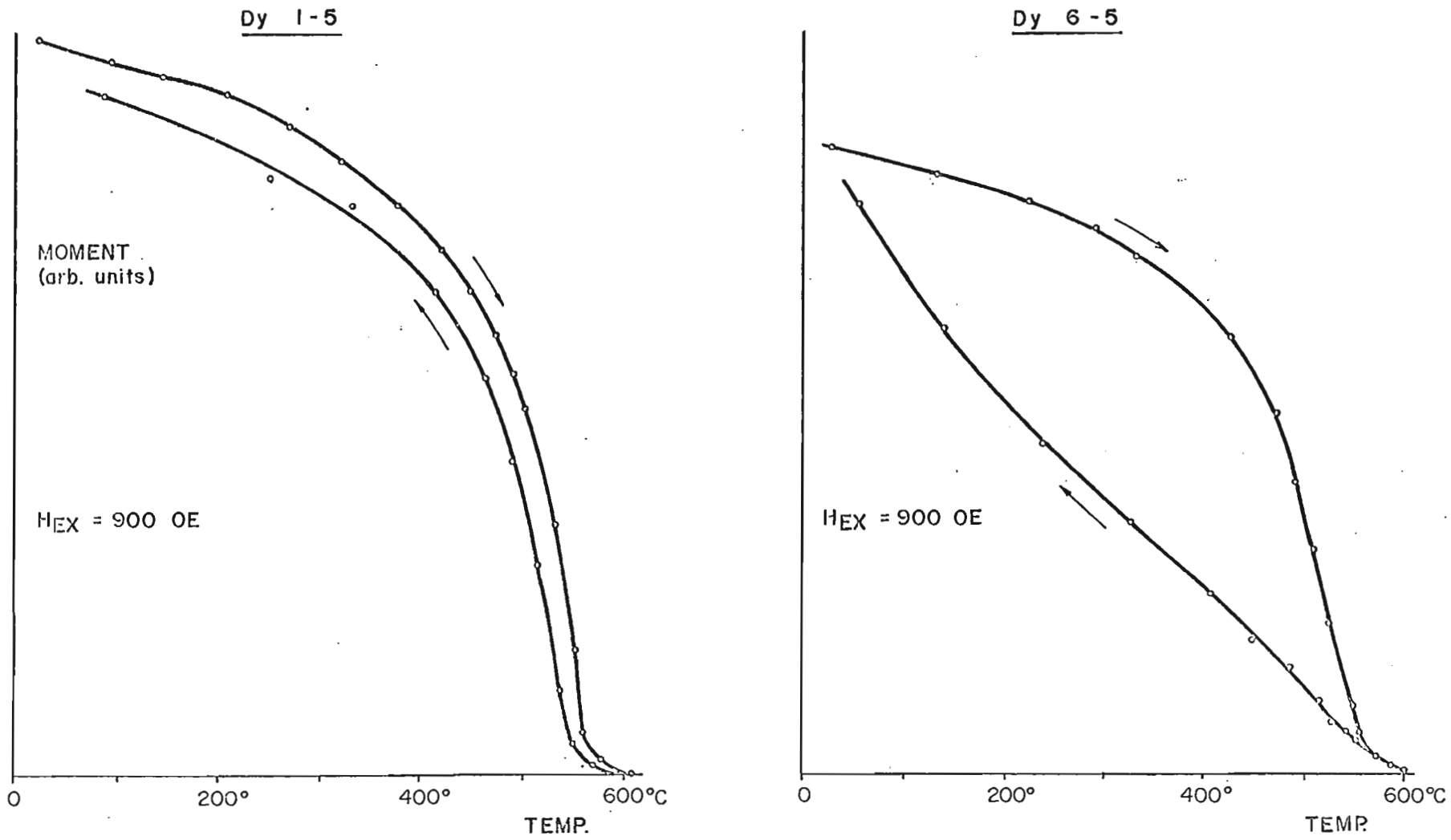

FIG. 3 - 7

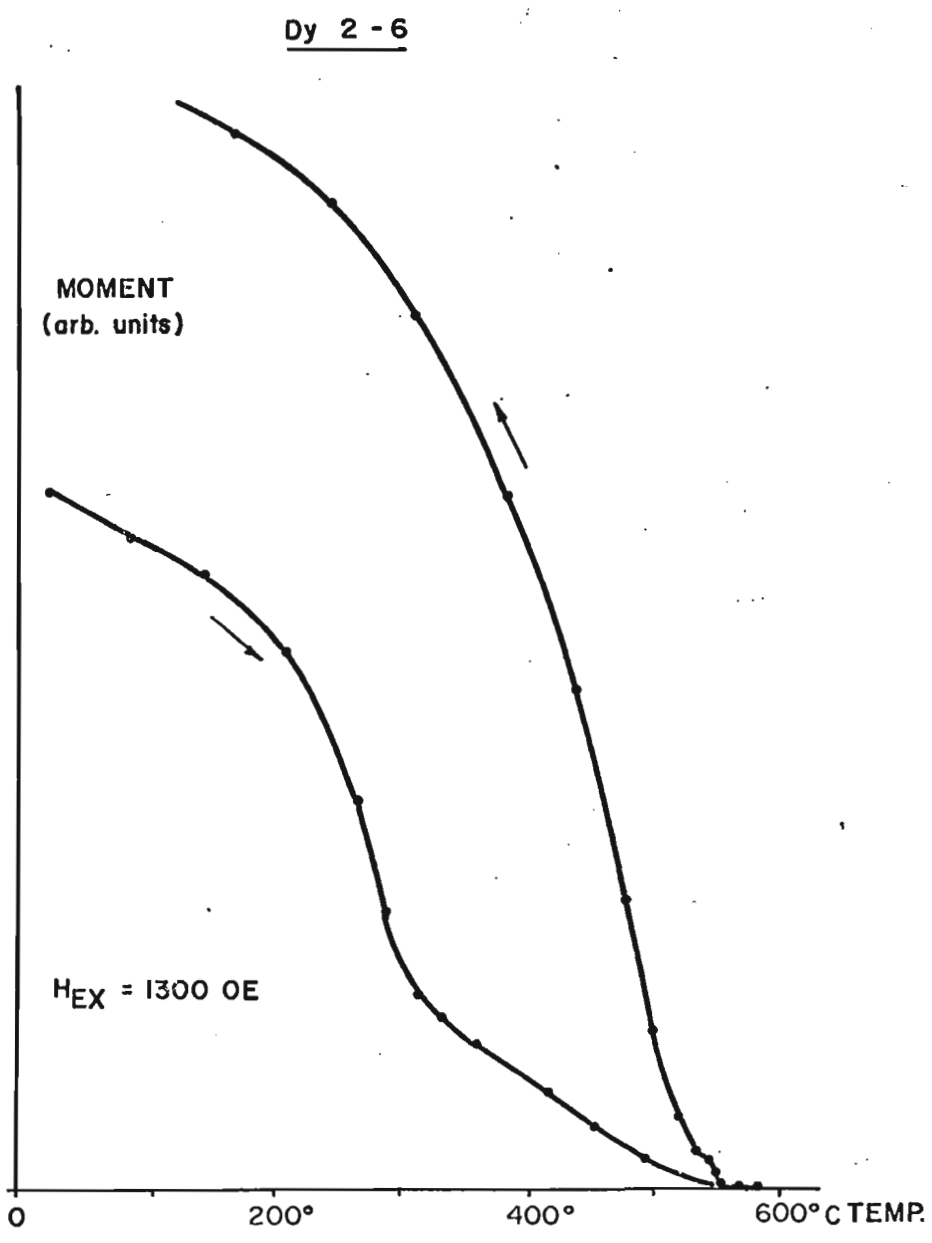
Dy 2 - 6
MOMENT
(arb. units)
H_{EX} = 1300 OE
0
200°
400°
600°C TEMP.

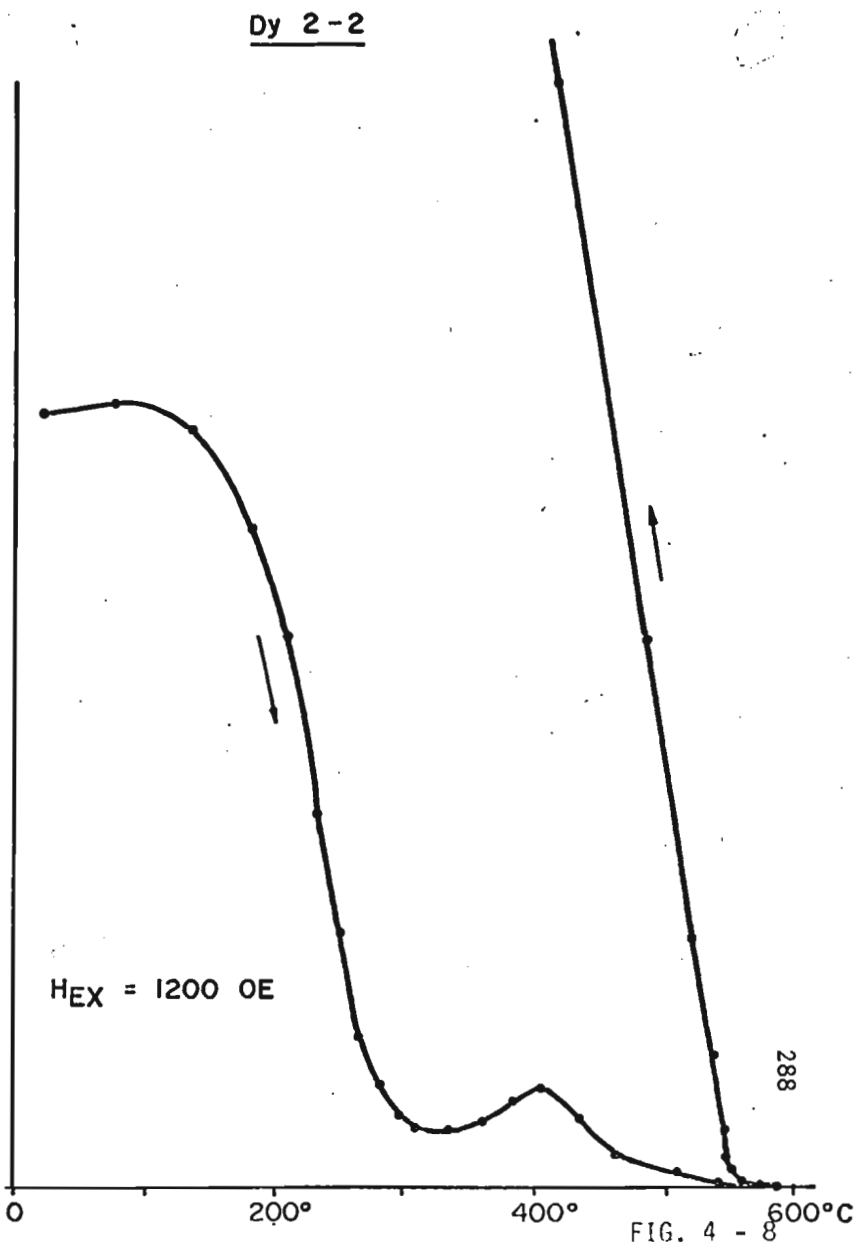
Dy 2 - 2
H_{EX} = 1200 OE
0
200°
400°
600°C

FIG. 4 - 8

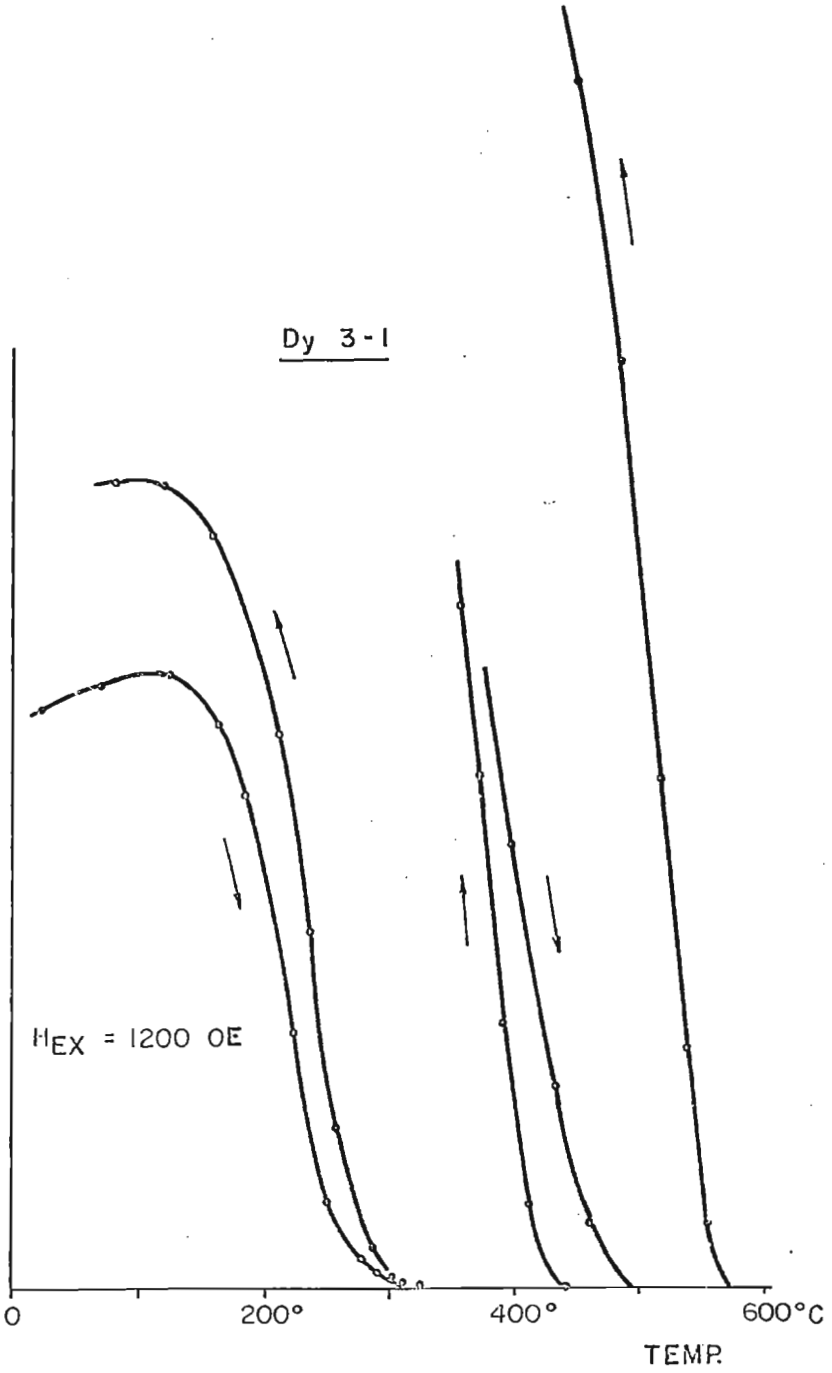
Dy 3 - 1
H_{EX} = 1200 OE
0
200°
400°
600°C
TEMP.

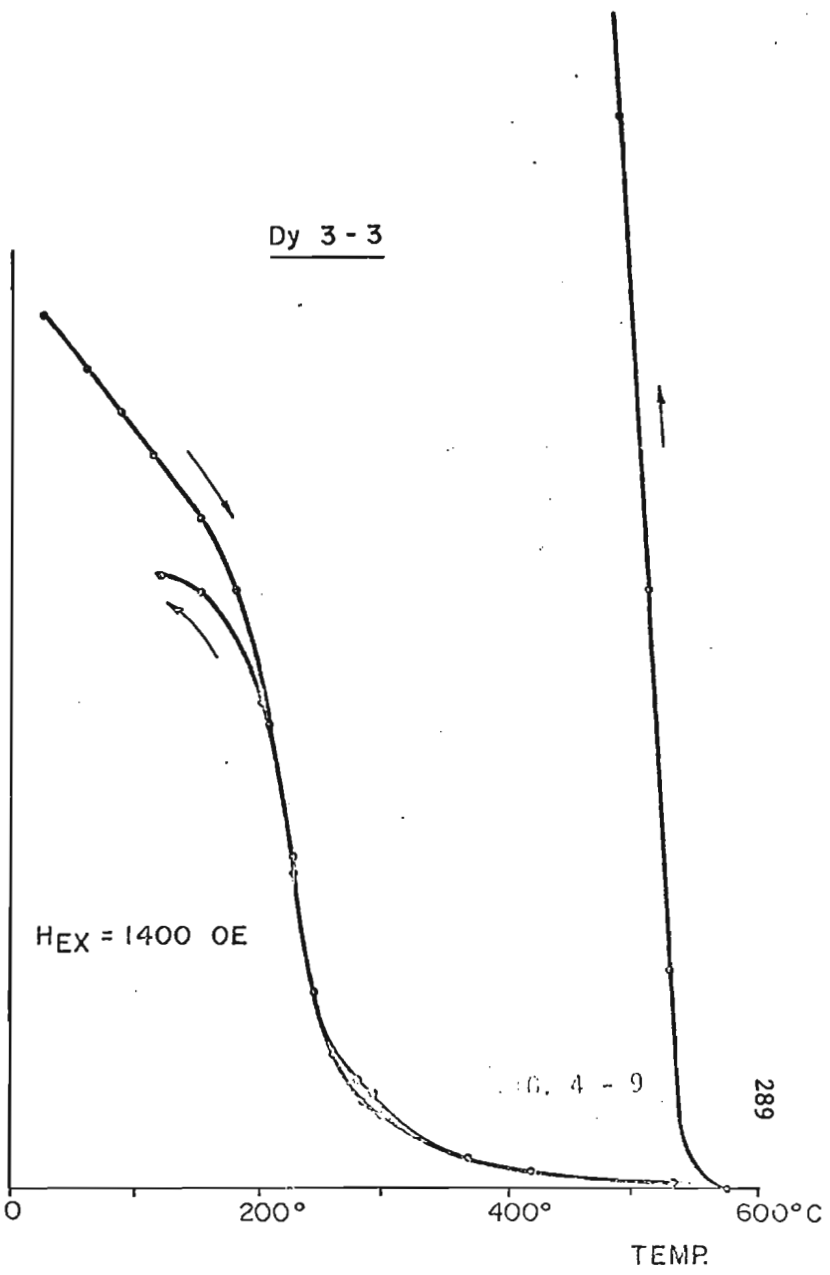
Dy 3 - 3
H_{EX} = 1400 OE
0
200°
400°
600°C
TEMP.

Fig. 4 - 9

Fig. 4-10

(a) Magnetite percentage, found by saturation magnetization measurements, versus susceptibility for specimens from fresh exsolved Cape Dyer samples (solid circles), and a specimen from flow 3 after heating to 600°C in air (circle with line). The reciprocal slope of the line is $2.1 \cdot 10^{-3}$ G/Oe/% magnetite.

(b) Strong-field magnetic moments ratio M_o'/M_o plotted against estimated mean or dominant opaque grain size for various basalt samples. Circles with line, Cape Dyer lavas; open circles, Disko basalts; crosses, Iceland dykes. Error bars for each data point are shown at top. All samples had a low Curie point ($180°C \leq T_c \leq 310°C$), with no or minor high-Curie-point component of magnetization. M_o and M_o' are the room-temperature moments respectively before and after heating in air to 600°C.

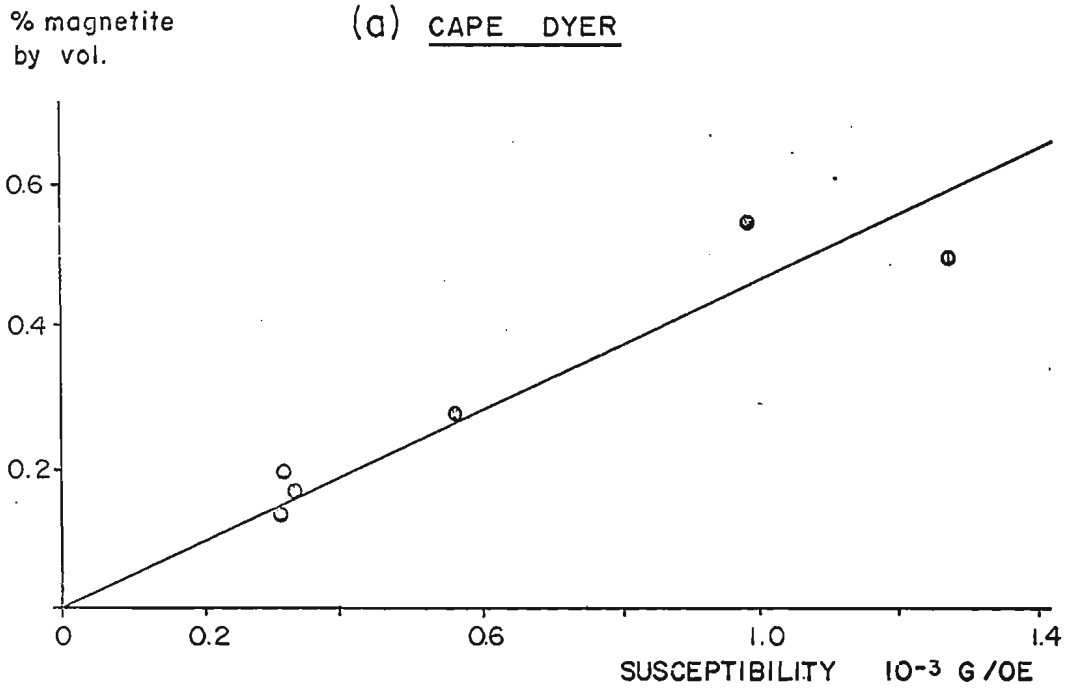
% magnetite
by vol.
(a) CAPE DYER
0.6
0.4
0.2
0
0.2
0.6
1.0
1.4
SUSCEPTIBILITY 10-3 G/OE

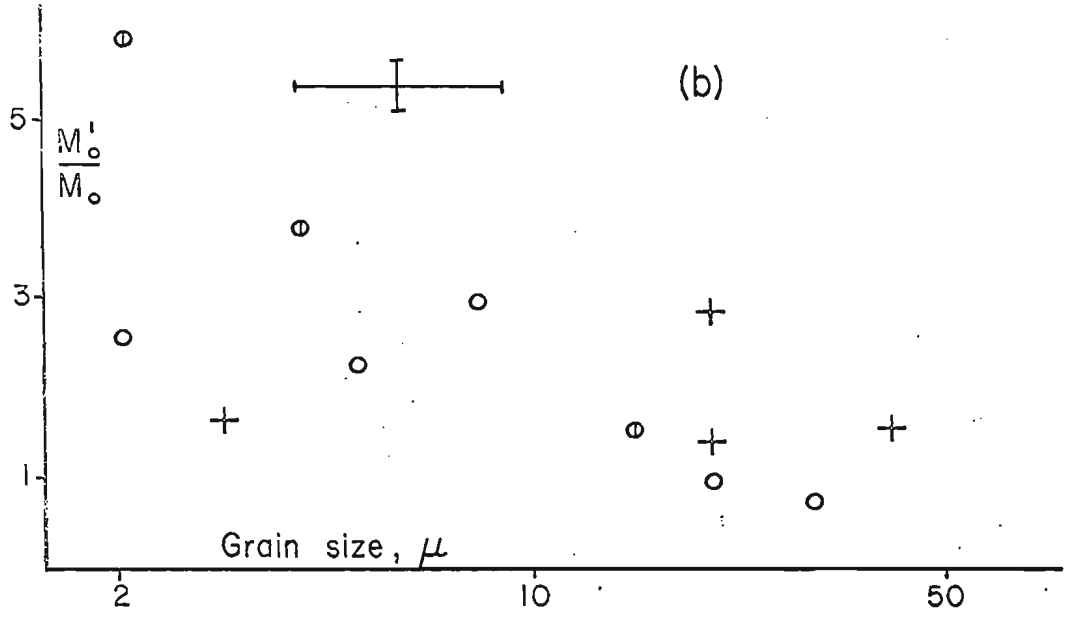
(b)
5
3
1
M'o/Mo
Grain size, μ
2
10
50

FIG. 4 - 10

Fig. 5-1

NRM intensity and volume susceptibility of Tertiary basalts and Precambrian basement rocks on Baffin Bay (Fig. 3-1).

(a) Top: Average values for 6 lava sites and 21 dike sites, Ubekendt Island (D. H. Tarling, pers. comm. 1970), plus 5 samples from Svartenhuk peninsula (collected by Dr. D. B. Clarke; Table 4.10). Middle: One sample each from all sites of lava profiles GL and GK and from 2 other lavas, 7 intrusives and 7 breccia sites, South Disko. Bottom: 35 samples from the Cape Dyer lavas, plus 8 from other Tertiary basalt exposures on Baffin Island (Table 4.10).

(b) Top: Site mean values for 44 diabase dikes between Julianehåb and Godthåb, west Greenland, possibly including a few Mesozoic (TD) dikes (Bullock 1967); plus 16 sites in north Baffin Island (Fahrig et al. 1971, and Dr. W. Fahrig, pers. comm.).
Middle: 18 anorthosite and ultrabasic samples, Fiskenaesset complex (Ghisler and Sharma 1969); 29 anorthosite samples from Michikamau (Murthy 1969), NRM only; 22 Michikamau anorthosite specimens (kindly lent by Dr. G. S. Murthy), susceptibility only; and 2 samples of basic rock near Julianehåb.
Bottom: 31 gneiss and supracrustal rock samples collected by Memorial University between Julianehåb and Godhavn, and in Frobisher Bay, Cape Dyer and Broughton, on Baffin Island; 7 gneissic gravel samples from Baffin Bay (solid-rock susceptibility only, inferred by the author from measurements on this gravel); 17 Fiskenaesset gneiss and amphibolite samples (Ghisler and Sharma 1969); and 10 gneiss samples from the Labrador coast east of

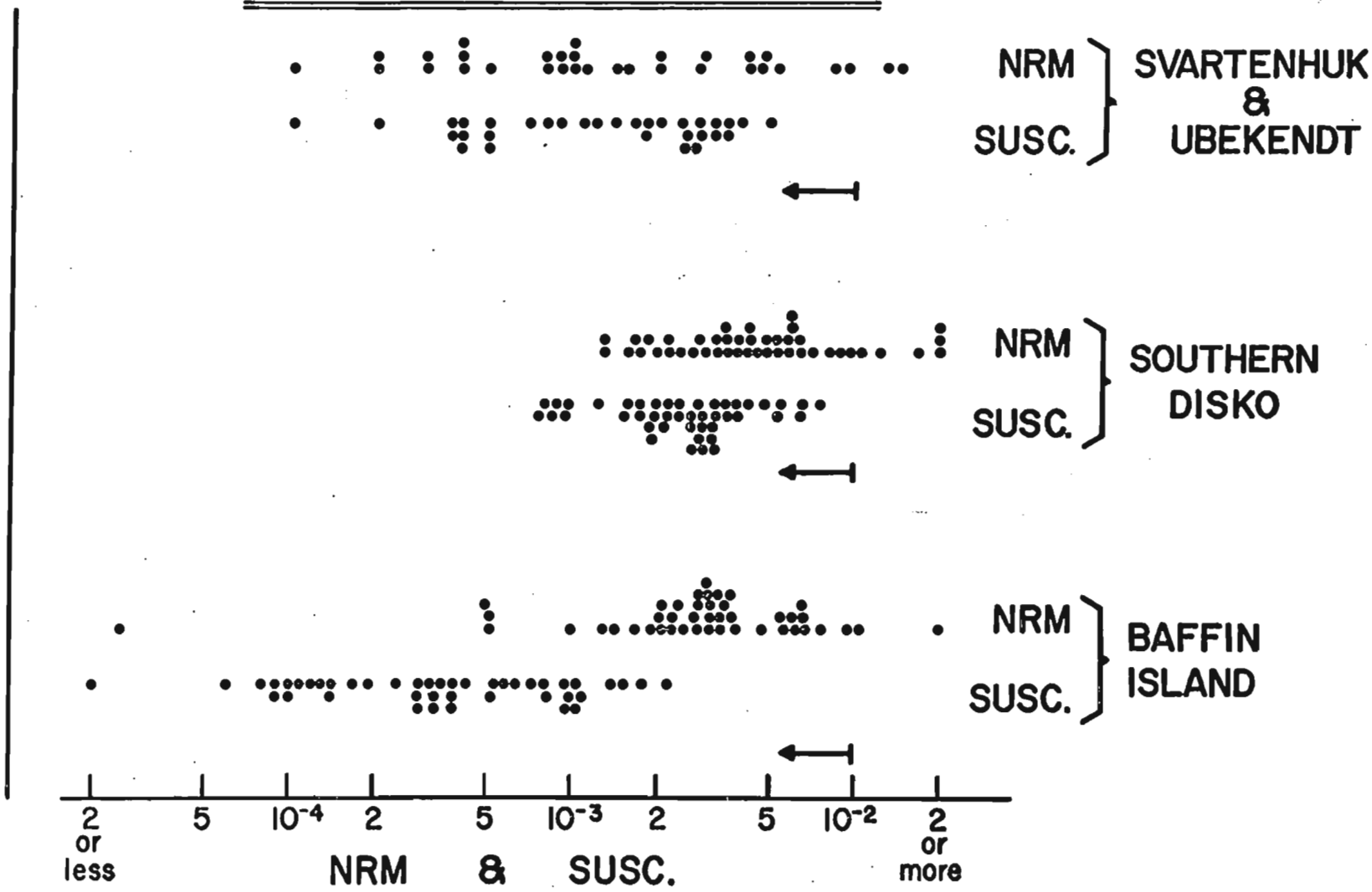
TERTIARY BASALTS
NRM
SUSC.
SVARTENHUK & UBEKENDT
NRM
SUSC.
SOUTHERN DISKO
NRM
SUSC.
BAFFIN ISLAND
2 or less
5
10-4
2
5
10-3
2
5
10-2
2 or more
NRM & SUSC.

FIG. 5 - 1a

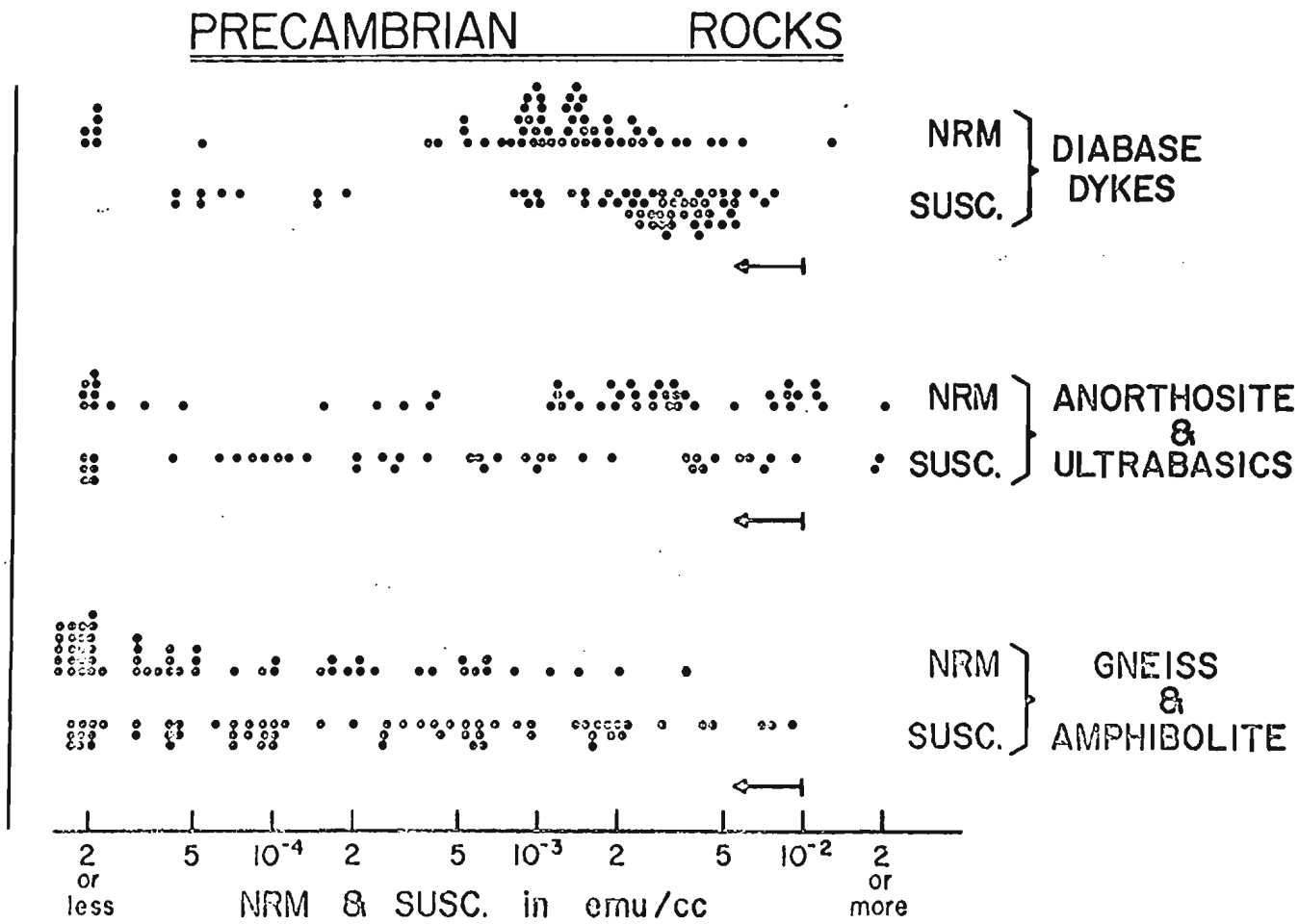
PRECAMBRIAN ROCKS
NRM
SUSC.
DIABASE DYKES
NRM
SUSC.
ANORTHOSITE & ULTRABASICS
NRM
SUSC.
GNEISS & AMPHIBOLITE
2 or less
5
10^{-4}
2
5
10^{-3}
2
5
10^{-2}
2 or more
NRM & SUSC. in emu/cc

FIG. 5 - 1b

Michikamau (collected and kindly given by Dr. J. S. Sutton).

Fig. 5-2

Normalized remanence intensity of four specimens from Tertiary lava flows in Iceland, after stepwise thermal demagnetization. Sample A7-1 showed the presence of a low-Curie-point component in its strong-field thermomagnetic curve, and its remanence direction was rather poorly stable.

Fig. 5-3

Volume percentage of magnetite, as inferred from results of microscope work, plotted against volume susceptibility of gneiss samples from the Baffin Bay coast. Each entry represents one sample, the diamond representing a sample from Labrador. The broken line is a least-squares approximation, assuming direct proportionality between the variables.

Fig. 5-4

Strong-field thermomagnetic curves for gneiss samples from Frobisher Bay and Söndre Strömfjord.

Fig. 5-5

(a) Remanence intensity after stepwise AF demagnetization of 5 gneiss samples from Greenland and Baffin Island.

(b) Magnetite content, as measured by ballistic magnetometer, plotted against susceptibility for six samples of gneiss from Greenland (circles), Frobisher Bay (squares) and Labrador (diamond).

THERMAL DEMAGNETIZATION
BASALT FLOWS - NW ICELAND

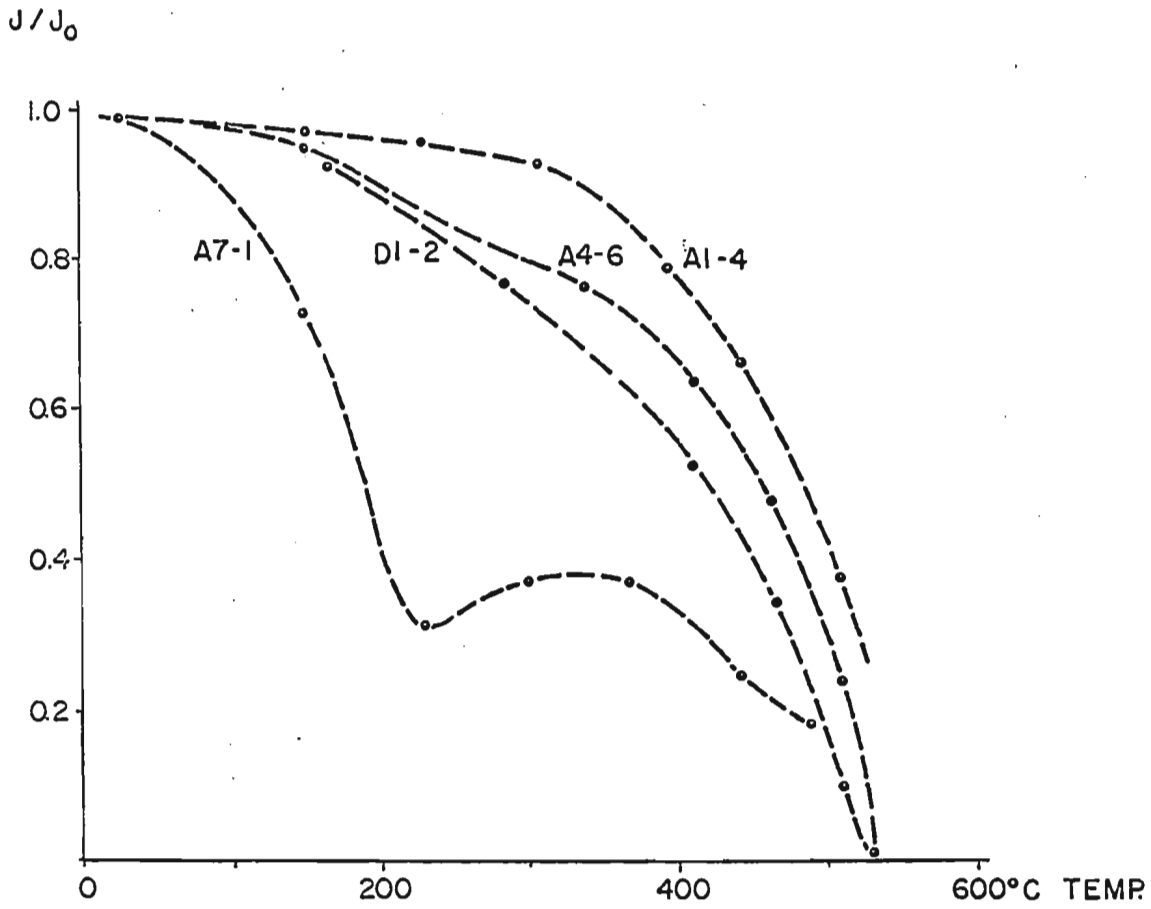

FIG. 5 - 2

SUSCEPTIBILITY–MAGNETITE % RELATION FOR BAFFIN BAY GNEISS

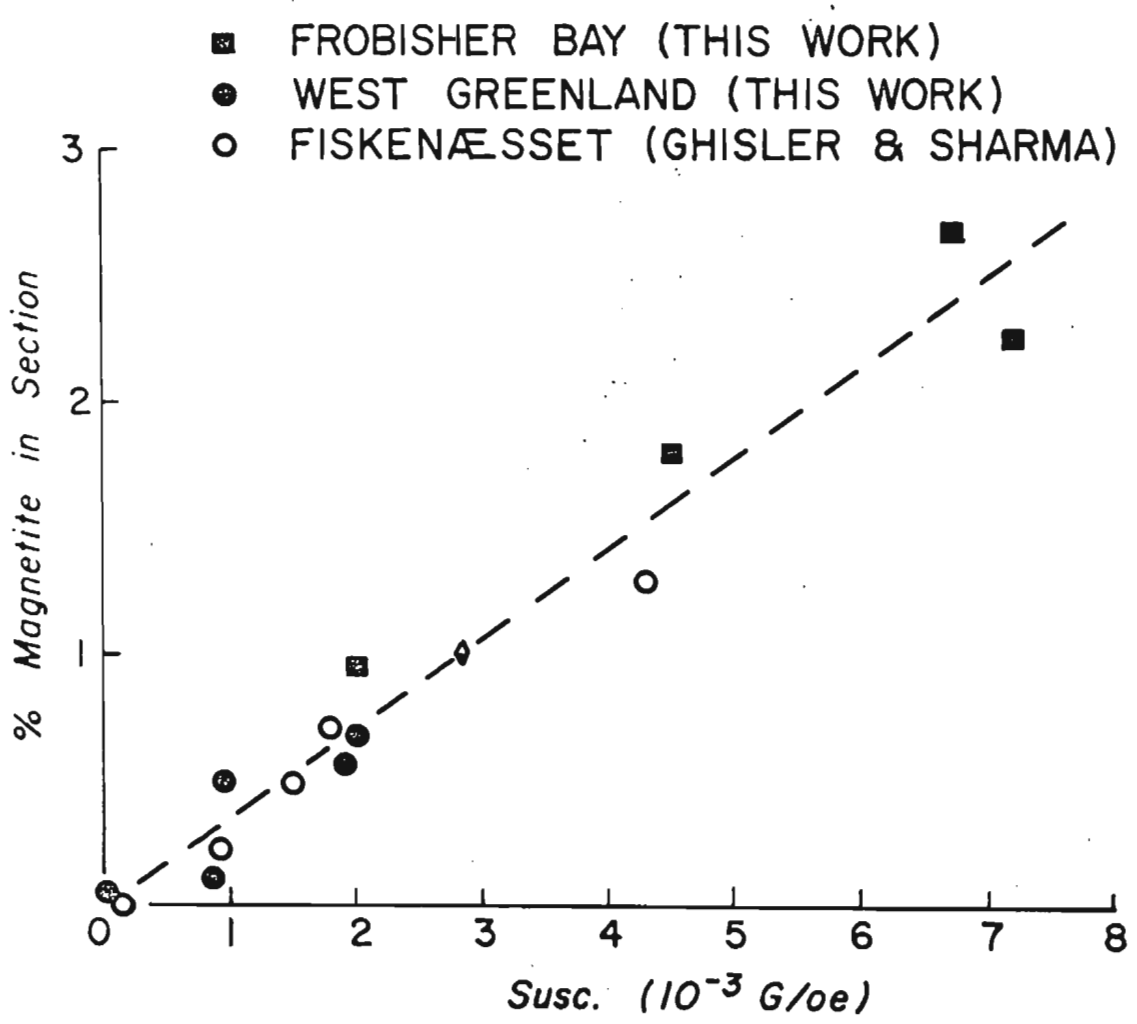

FIG. 5 - 3

THERMOMAGNETIC CURVES
BAFFIN BAY GNEISS

FB 1-3

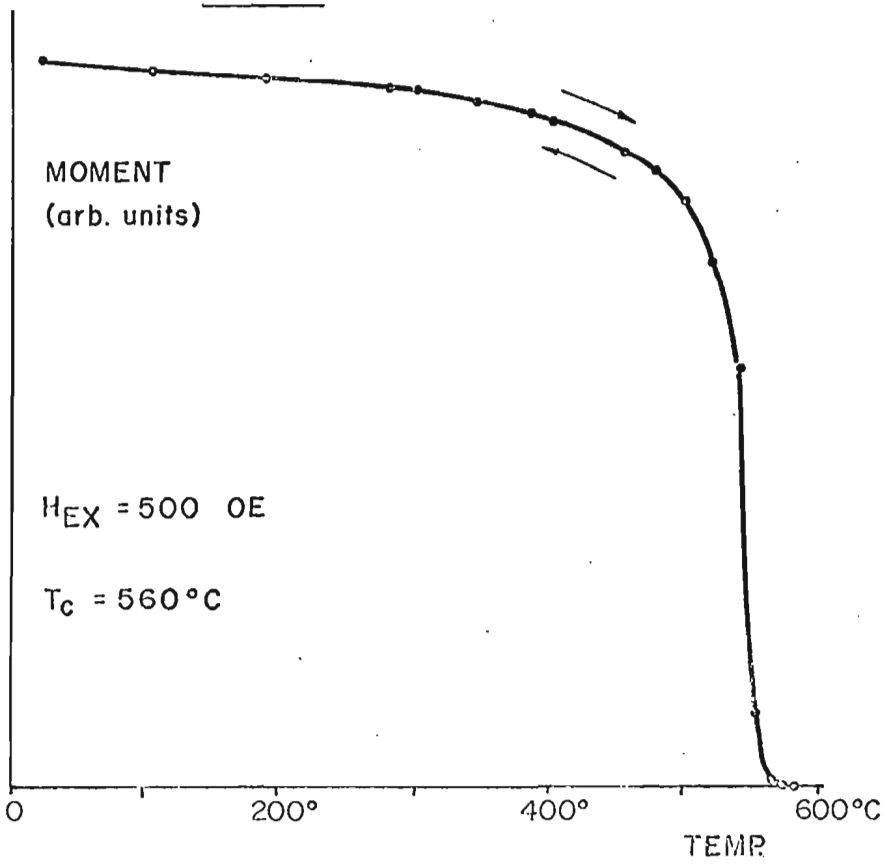

GG 15

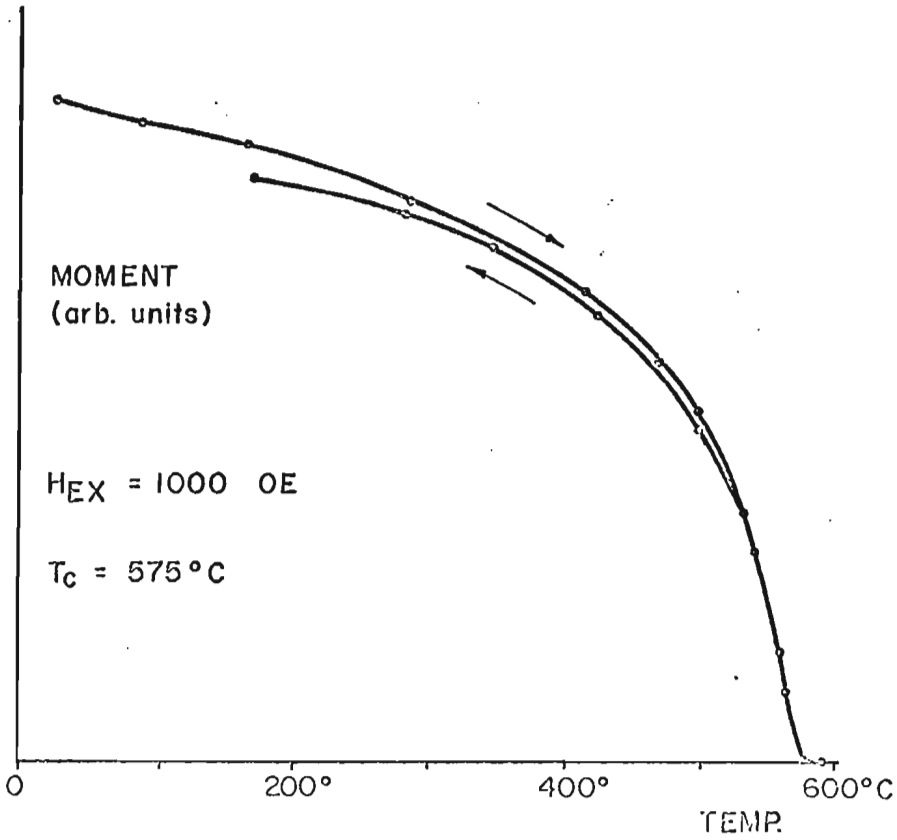

FIG. 5 - 4

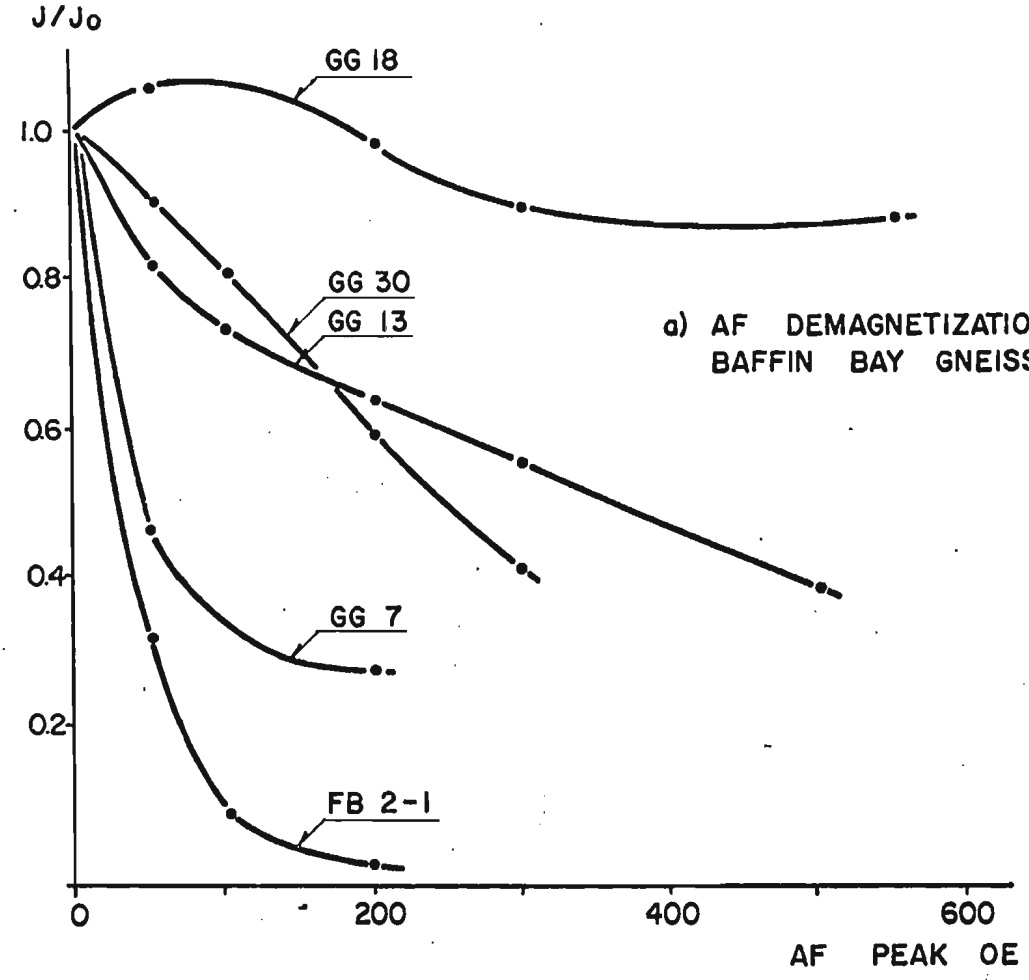

b) MAGNETITE CONTENT
(BALLISTIC METER)
IN BAFFIN BAY GNEISS

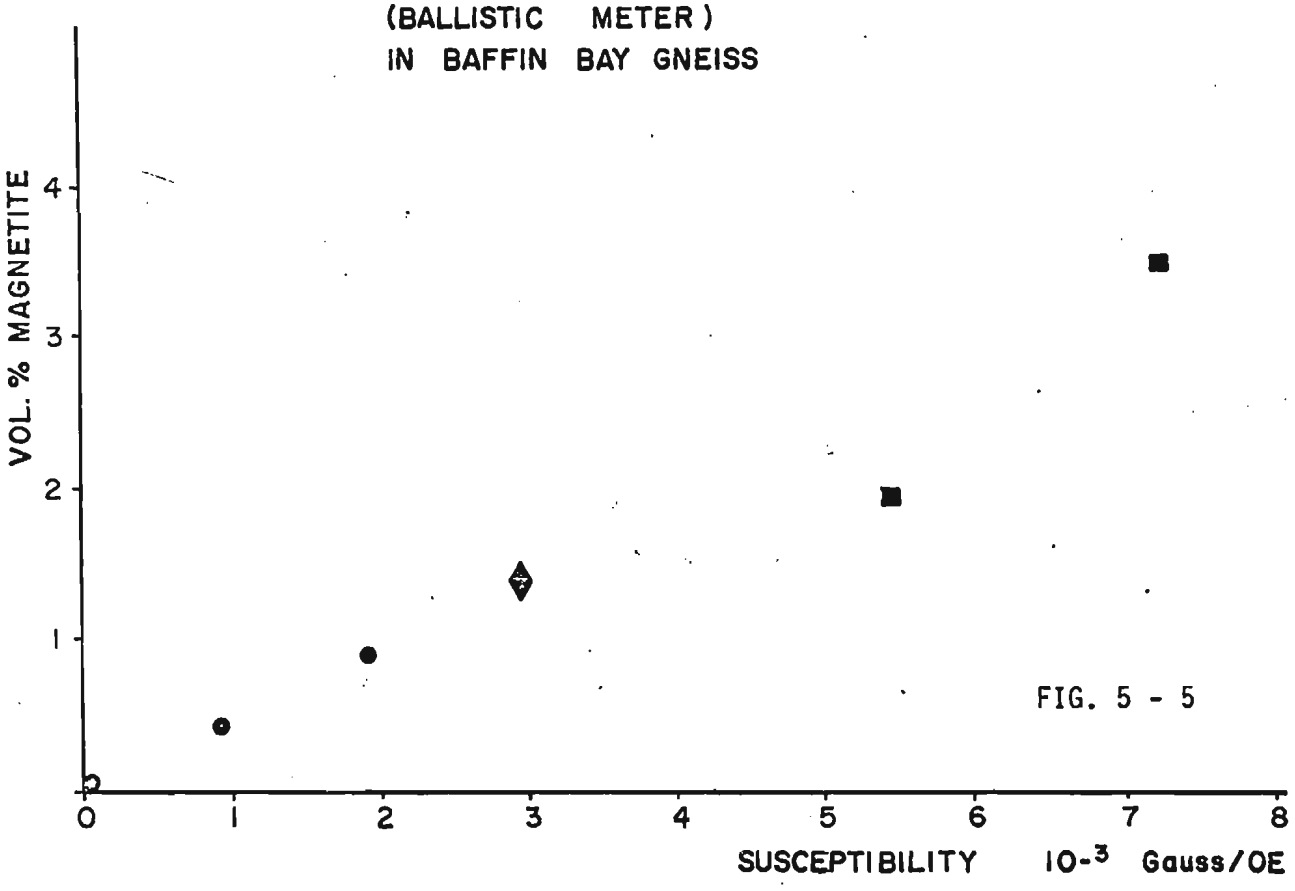

FIG. 5 - 5

Fig. 5-6

Magnetic changes brought about by heating of five Tertiary lava flows through dyke injection in Iceland. The abscissa is the distance, in meters, from the dyke contact. Rem. = remanence, referring both to polarity and AF-curve shape; K = susceptibility; TC = shape of thermomagnetic curve. - indicates no systematic change in a property as compared to samples lying further outwards; (+) indicates minor or doubtful change; + indicates major change. Dyke thicknesses are shown on the left, along with dyke and flow polarities.

Fig. 5-7

Correlation between remanence intensity (NRM) and susceptibility for samples of fresh gabbro from various localities in Iceland. The dotted lines denote logarithmic average values of magnetic properties for a collection of basalt samples from NW-Iceland (area B of Fig. 5-9).

Fig. 5-8

Results of AF demagnetization of four pilot samples of gabbro from Iceland.

Top: Remanence directions, plotted on one quadrant of an equal-angle stereographic projection, NRM to 400 Oe.

Bottom: Normalized remanence intensities. Dotted lines indicate the presence of spurious components.

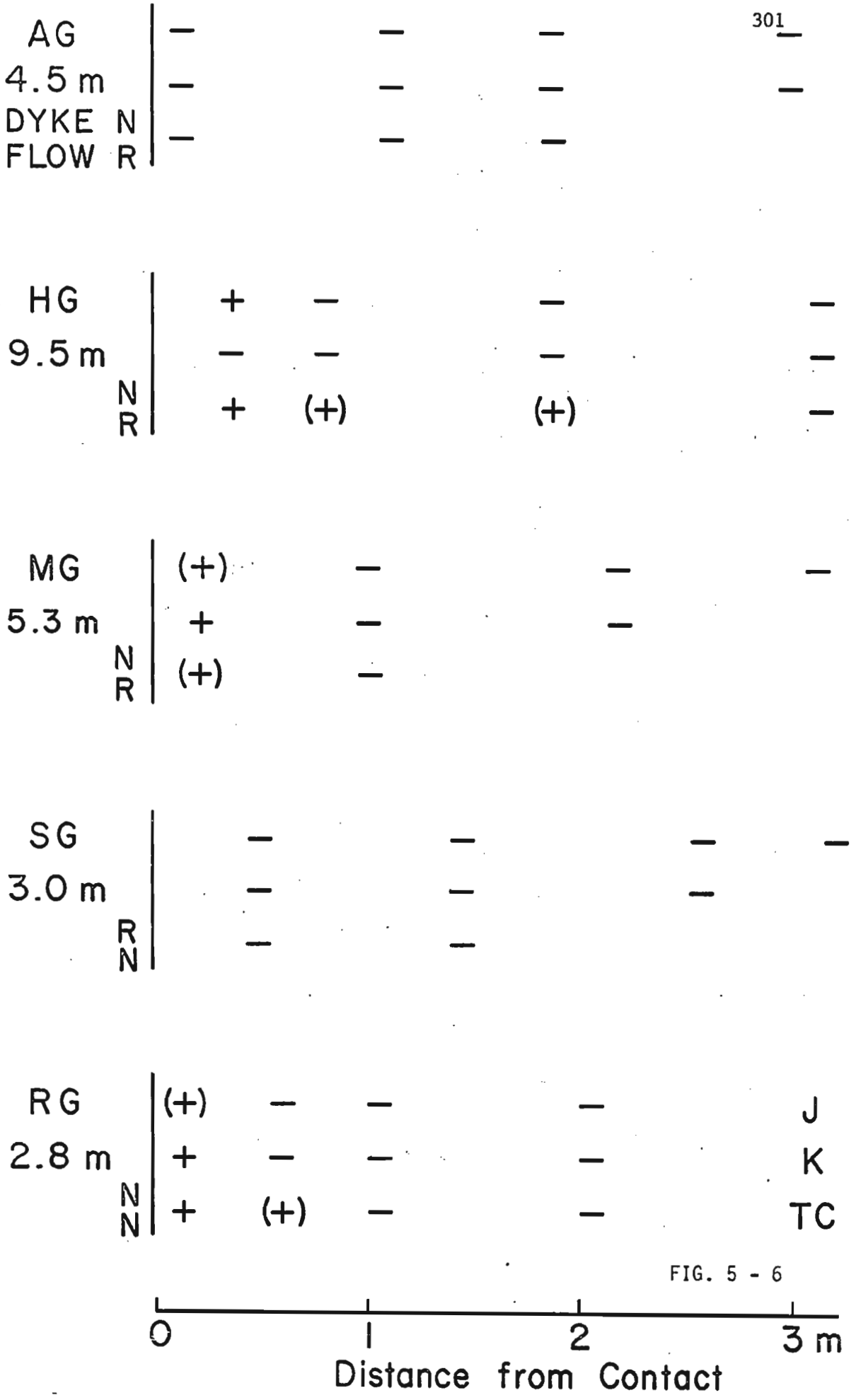
AG
4.5 m
DYKE N
FLOW R
HG
9.5 m
N
R
MG
5.3 m
N
R
SG
3.0 m
R
N
RG
2.8 m
N
N
J
K
TC
0
1
2
3 m
Distance from Contact

FIG. 5 - 6

SUSCEPTIBILITY AND REMANENT INTENSITY FOR SAMPLES OF GABBRO AND RELATED ROCKS FROM SOUTHERN AND WESTERN ICELAND.

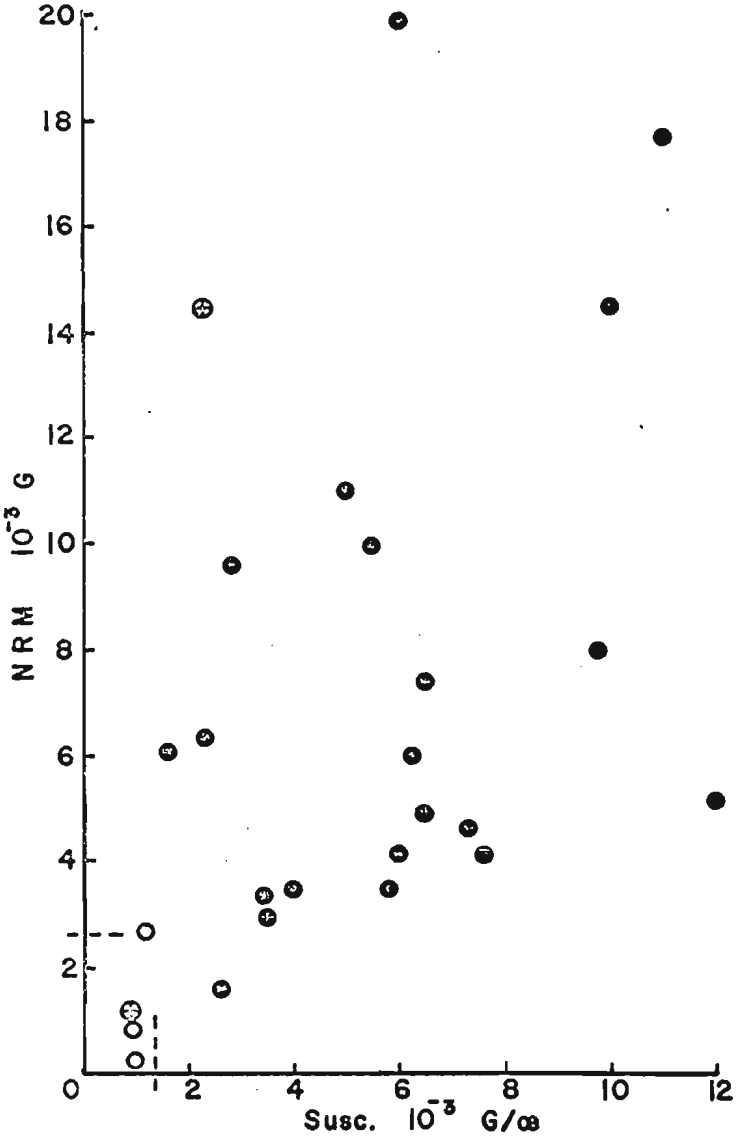

FIG. 5 - 7

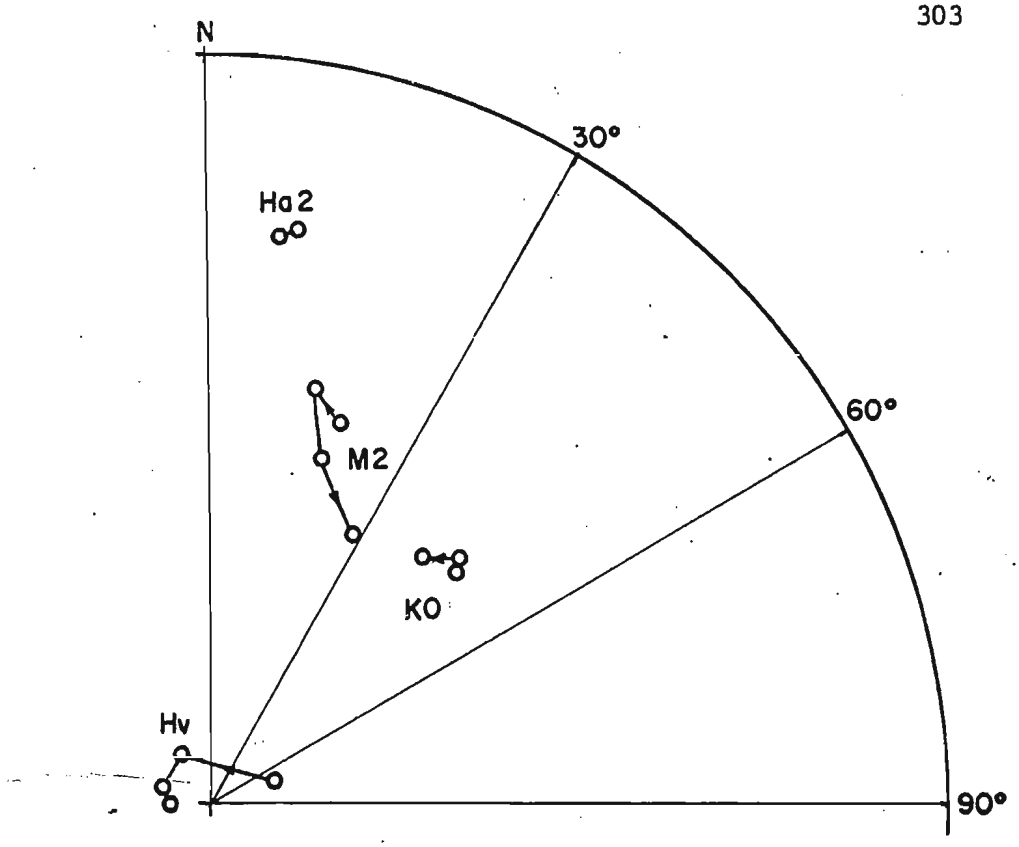

AF DEMAGNETIZATION
ICELANDIC GABBRO

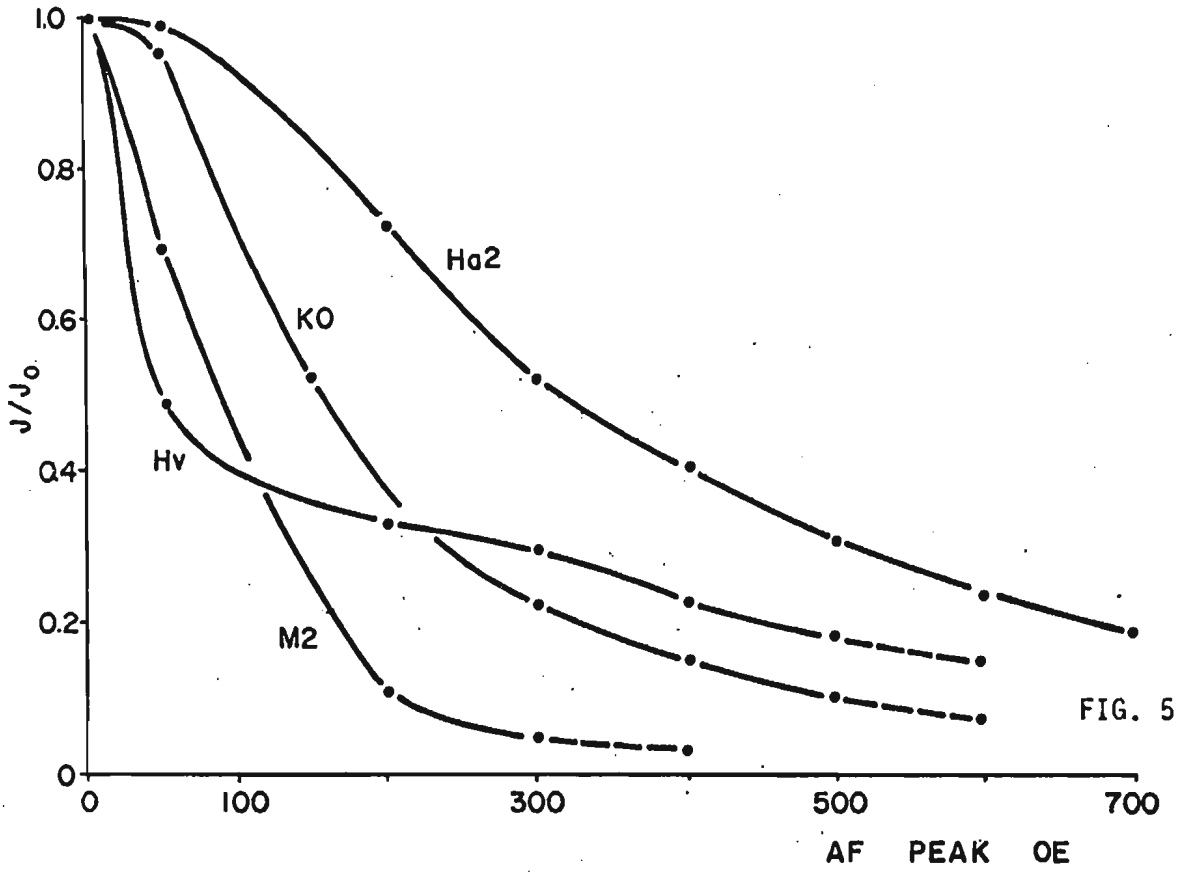

FIG. 5 - 8

Fig. 5-9

Outline map of Iceland, showing the presently active volcanic zone. Circles denote localities from which gabbro samples were obtained. B, area studied by Kristjansson (1967). R, Reykjanes peninsula.

Fig. 5-10

Map of the Reykjanes peninsula, South-West Iceland. The broken line denotes the boundary between positive and negative magnetic anomalies (Sigurgeirsson, 1970). The drill holes from which samples of drill chips were obtained for the present study were R4 and R22, about 2 km apart in the Reykjavik area, and H3 and H8, about 1 km apart in the Reykjanes area.

Fig. 5-11

Typical strong-field thermomagnetic curves for two specimens of drill chips from Iceland.

Fig. 5-12

Solid curves: Susceptibility of fresh rock (in e.m.u./gm) from drill holes in Reykjavik and Reykjanes, plotted as a function of depth in each area. Broken curves: thermal remanence (TRM) intensity (in e.m.u./gm) acquired by specimens on cooling in air from 600°C in 0.50 Oe field (except for crosses, which indicate NRM intensity values of core material in e.m.u./gm).

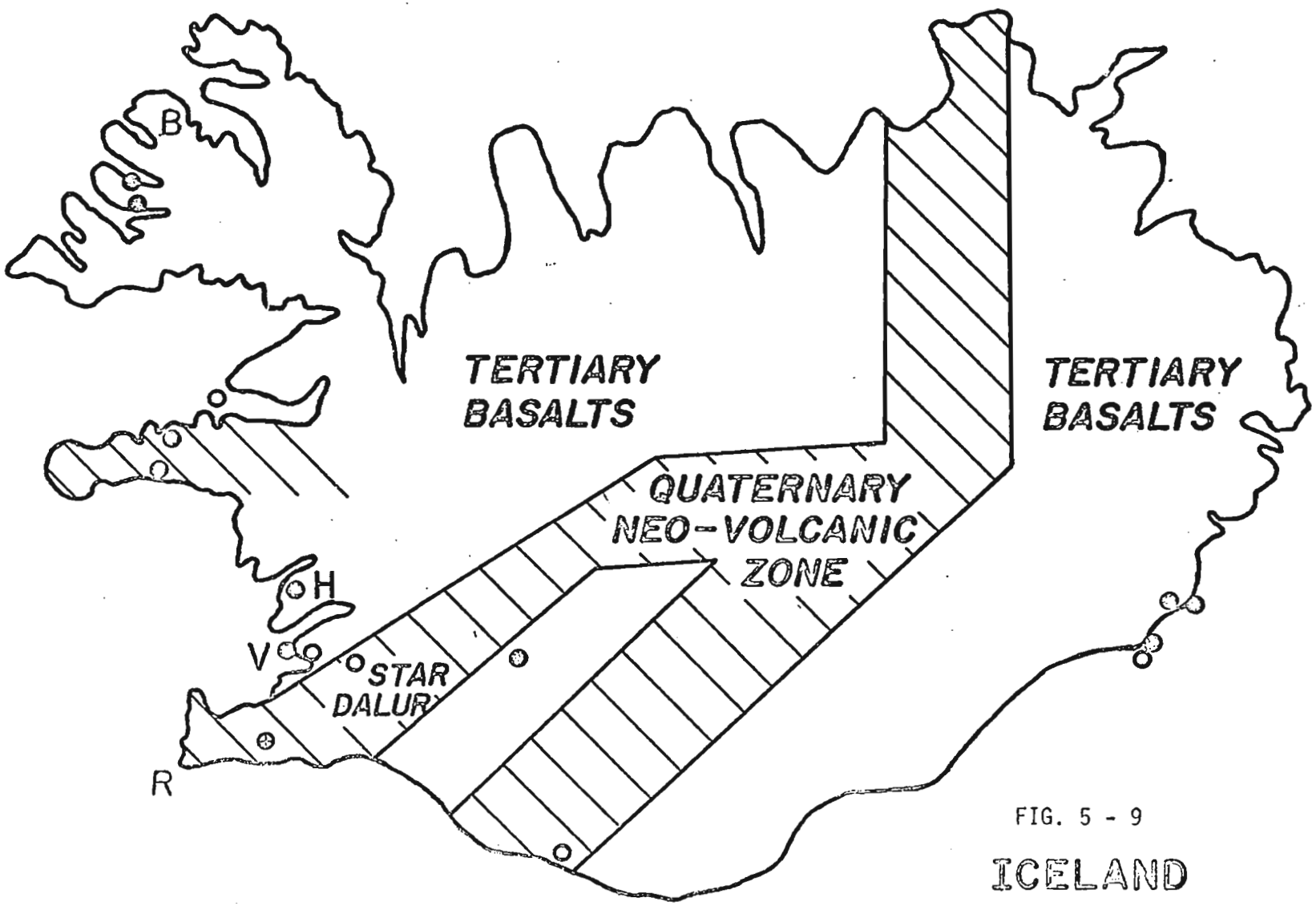

FIG. 5 - 9

ICELAND

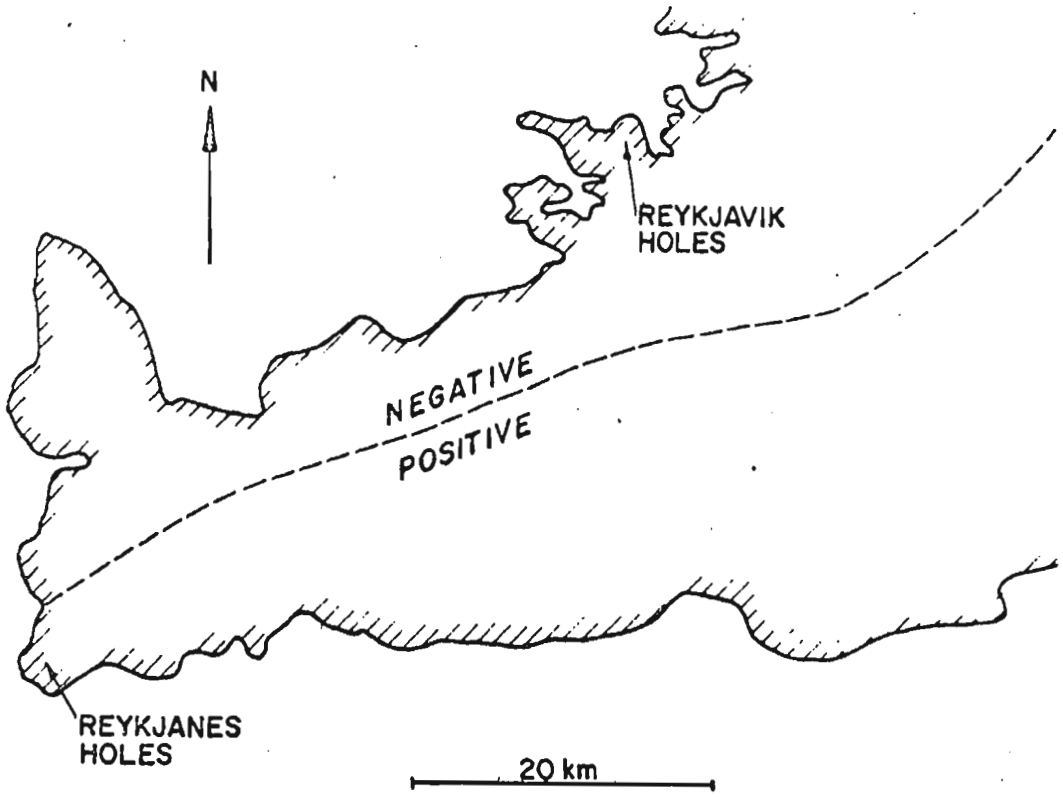

FIG. 5 - 10

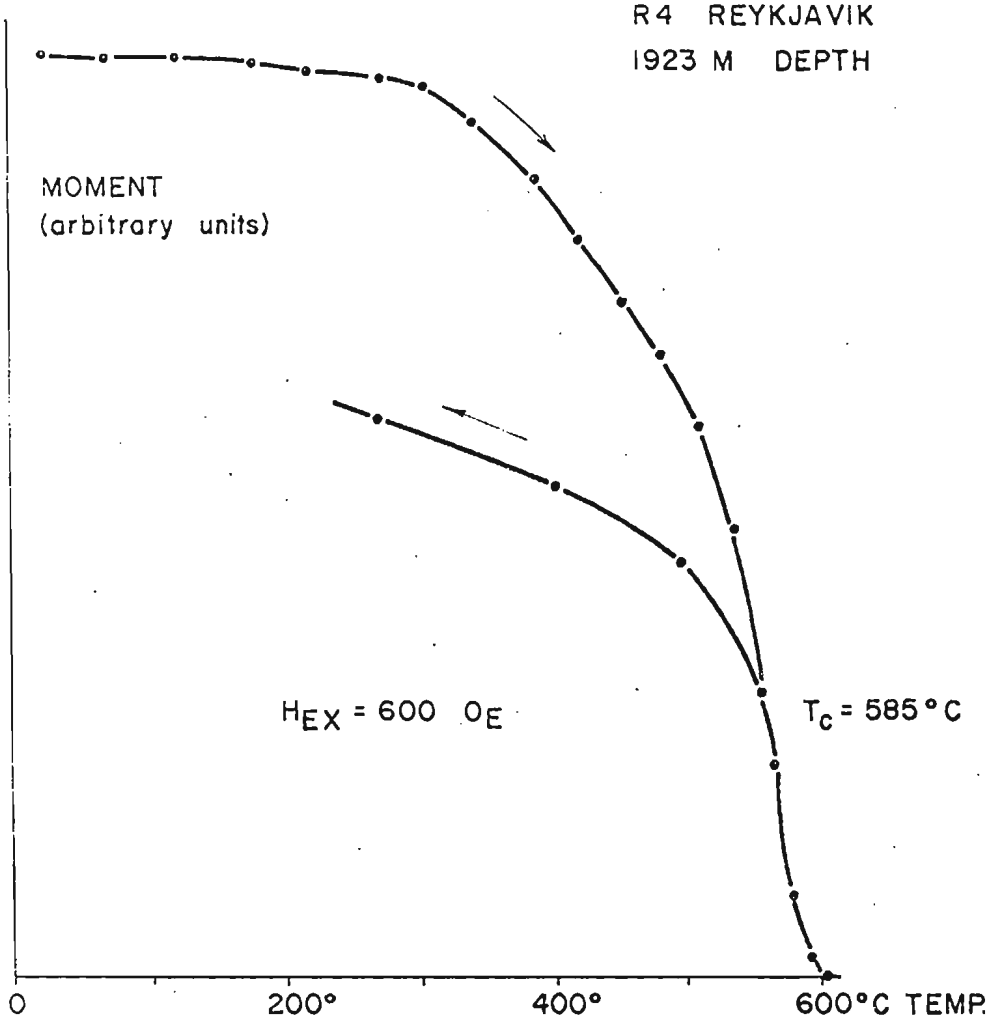
R4 REYKJAVIK
1923 M DEPTH
MOMENT
(arbitrary units)
H_{EX} = 600 O_E
T_C = 585 °C
0
200°
400°
600°C TEMP.

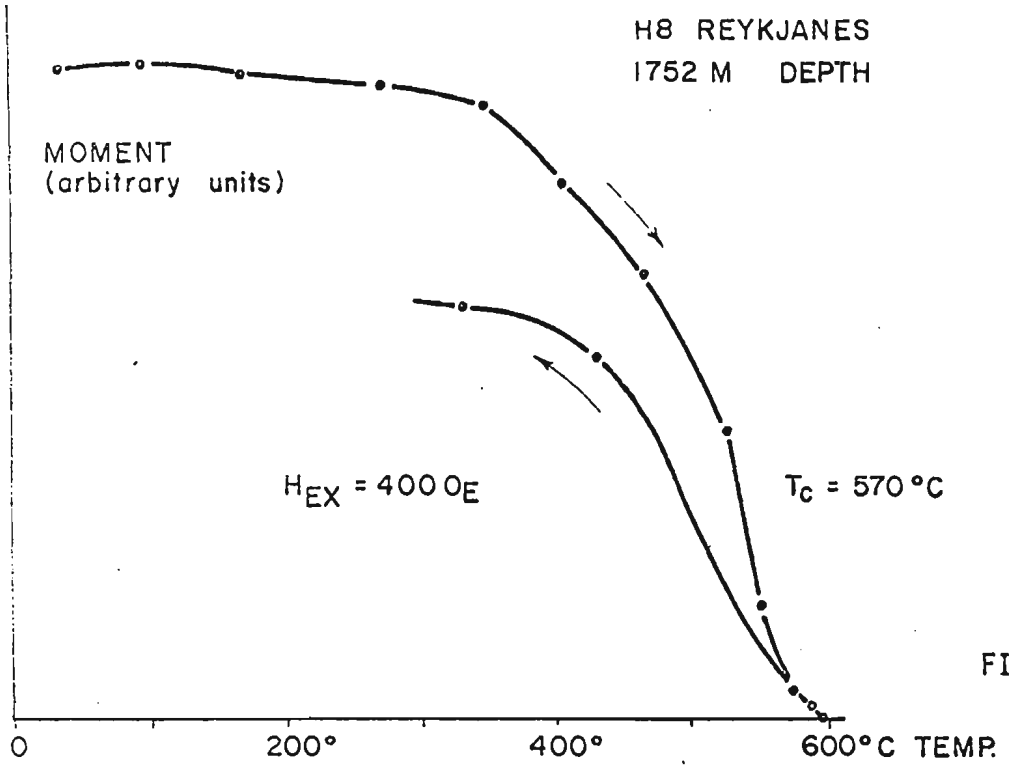
H8 REYKJANES
1752 M DEPTH
MOMENT
(arbitrary units)
H_{EX} = 400 O_E
T_C = 570 °C
0
200°
400°
600°C TEMP.

FIG. 5 - 11

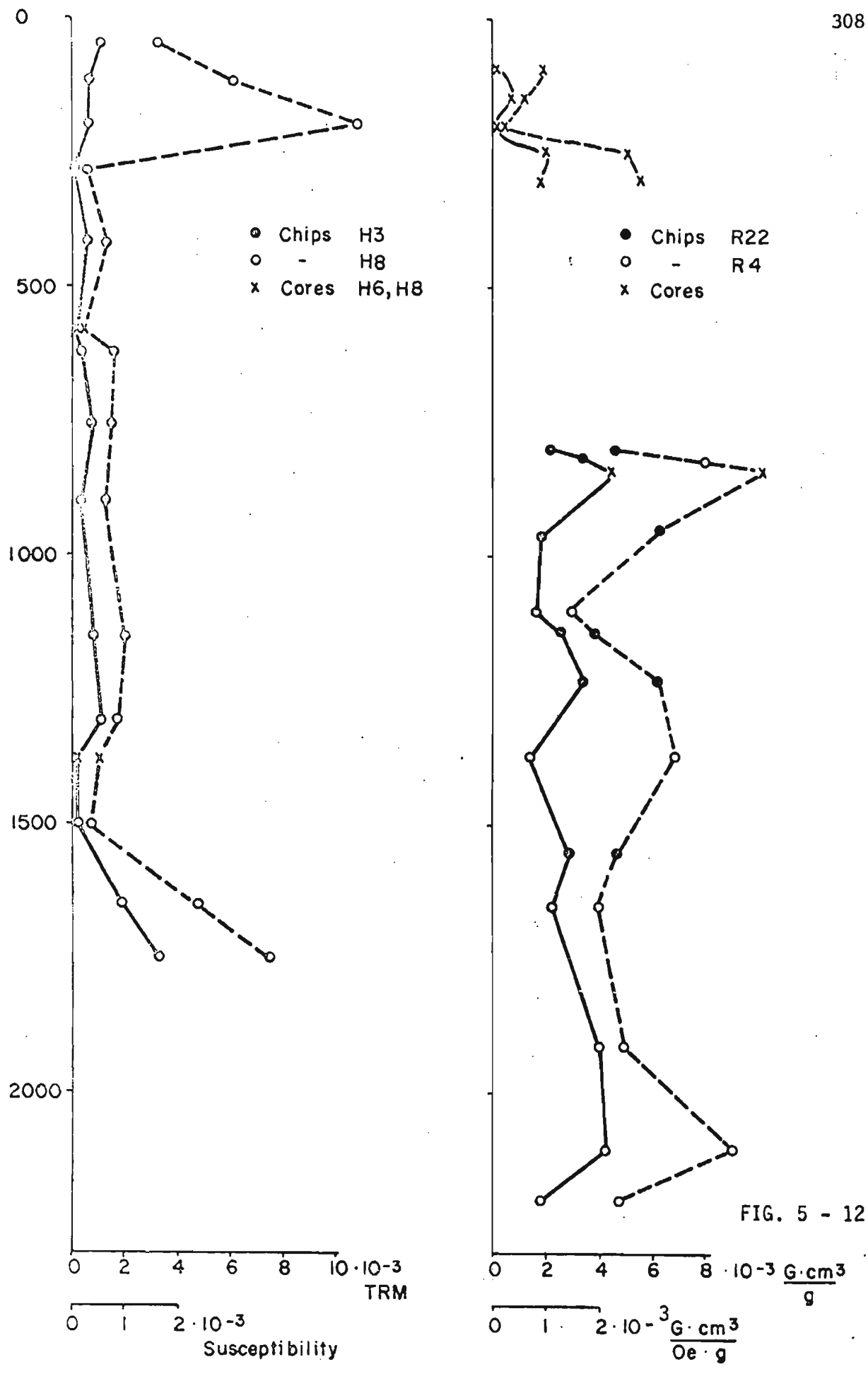
Depth M
REYKJANES
REYKJAVIK
0
500
1000
1500
2000
Chips H3
- H8
Cores H6, H8
Chips R22
- R4
Cores
0 2 4 6 8 10 · 10-3
TRM
0 1 2 · 10-3
Susceptibility
0 2 4 6 8 · 10-3 G·cm3/g
0 1 2 · 10-3 G·cm3/Oe·g

FIG. 5 - 12

Fig. 5-13

Thermal remanence intensity J_{th} acquired on cooling in 0.50 Oe from 600°C, plotted against susceptibility K_t as measured after cooling, for various basaltic samples from SW-Iceland. Two lines of constant Koenigsberger ratio Q_t as shown.

Fig. 5-14

Normalized AF demagnetization curves for mounted samples of drill chips from deep drill holes. IRM is isothermal magnetization on brief exposure to fields of the order of 100 Oe; TRM is acquired as in legend to Fig. 5-12.

Fig. 5-15

Frequency histograms of random magnetic moment magnitudes (right) and orthogonal component magnitudes for a specimen of Reykjavik drill chips, containing approximately 8000 magnetic chips. Measured with a spinner in nulled fields, the specimen being shaken or stirred thoroughly between measurements.

Fig. 5-16

Mean square component magnitude of random moment for specimens from a sample of drill chips from Reykjavik, plotted against specimen mass. Vertical bars indicate 80% confidence limits (see text). The most coarse fraction (one third by weight) of the specimens was discarded, to reduce the possible dominating effect of a few large chips on the random moment.

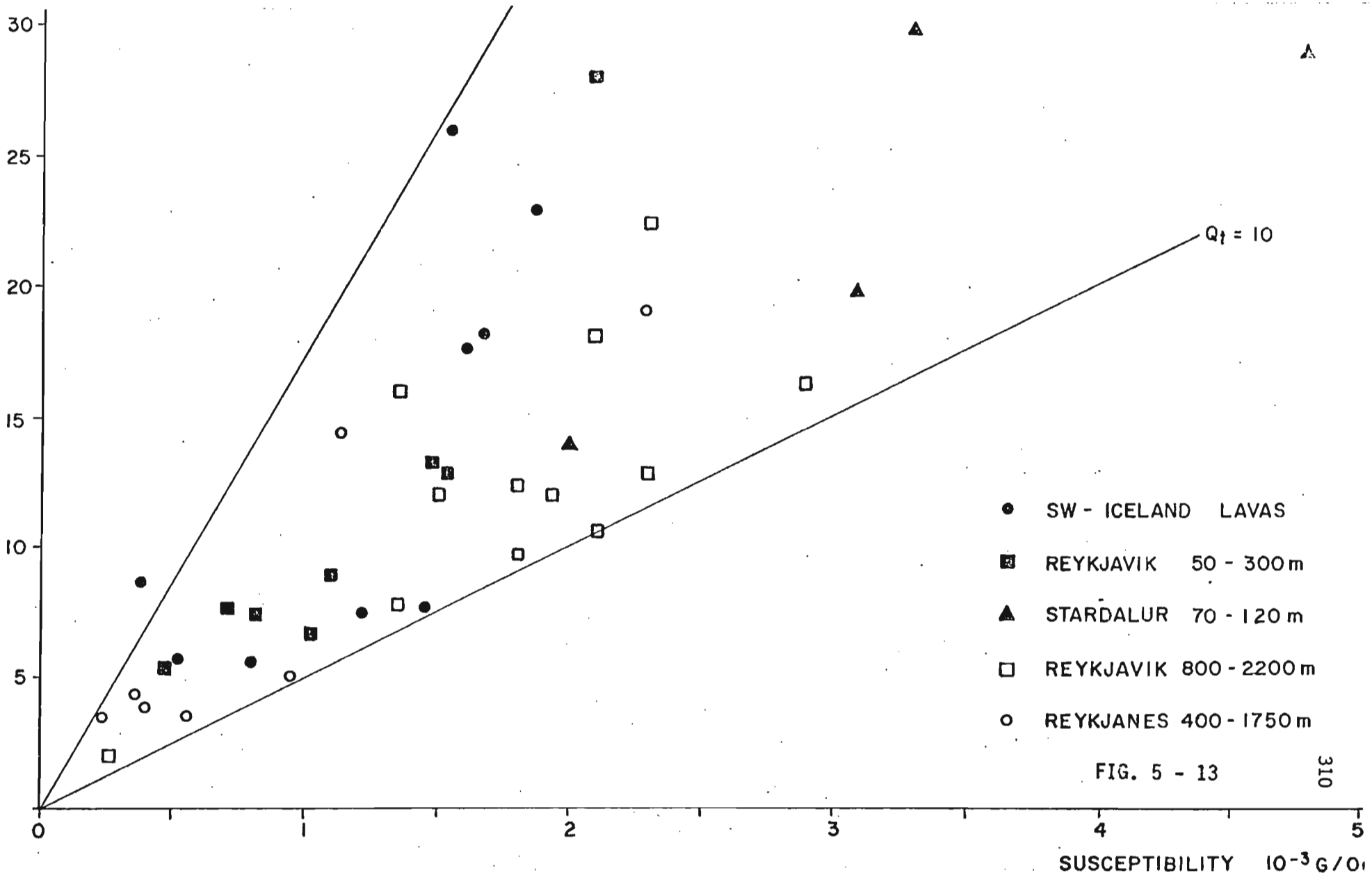
30
25
20
15
10
5
0
1
2
3
4
5
Q_t = 10
SW - ICELAND LAVAS
REYKJAVIK 50 - 300 m
STARDALUR 70 - 120 m
REYKJAVIK 800 - 2200 m
REYKJANES 400 - 1750 m
SUSCEPTIBILITY 10^{-3} G/O

FIG. 5 - 13

AF DEMAGNETIZATION

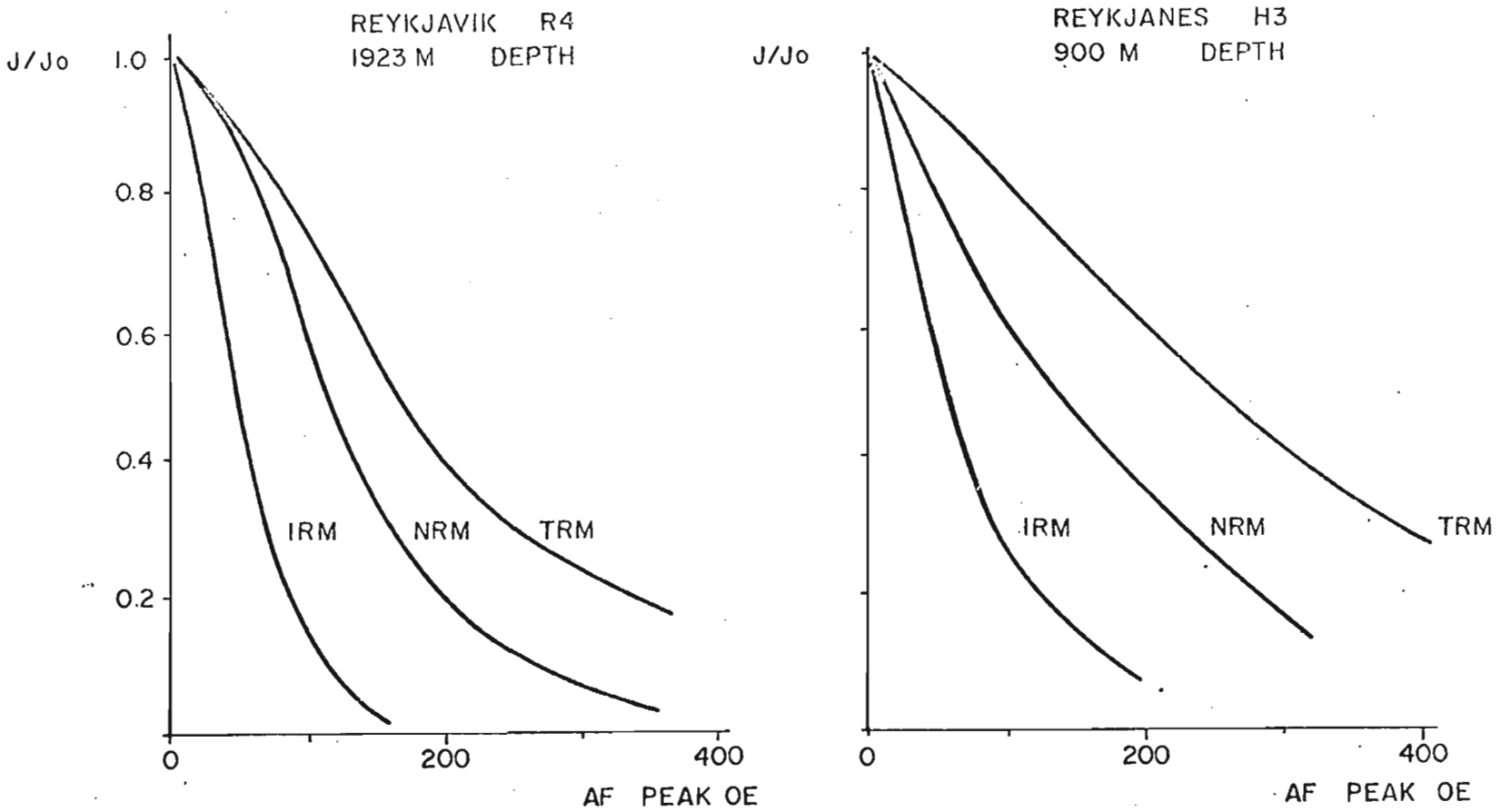

FIG. 5 - 14

RANDOM MOMENTS OF 4.6 GM OF DRILL CHIPS (R4 1923 M DEPTH).

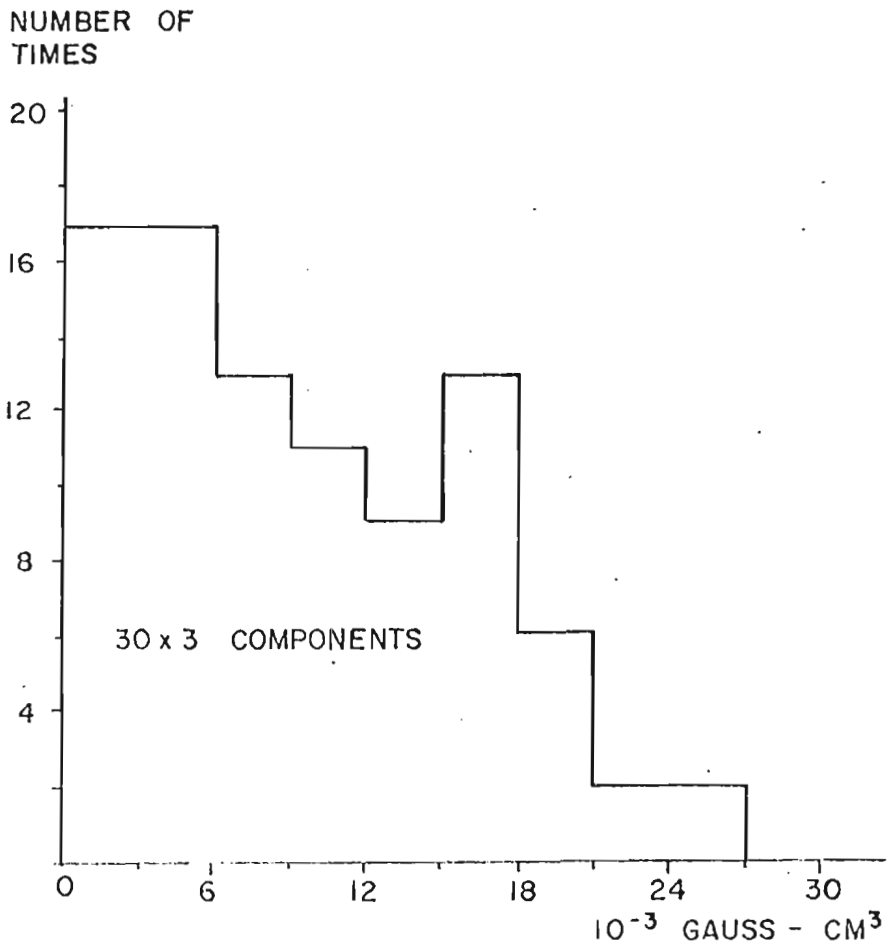

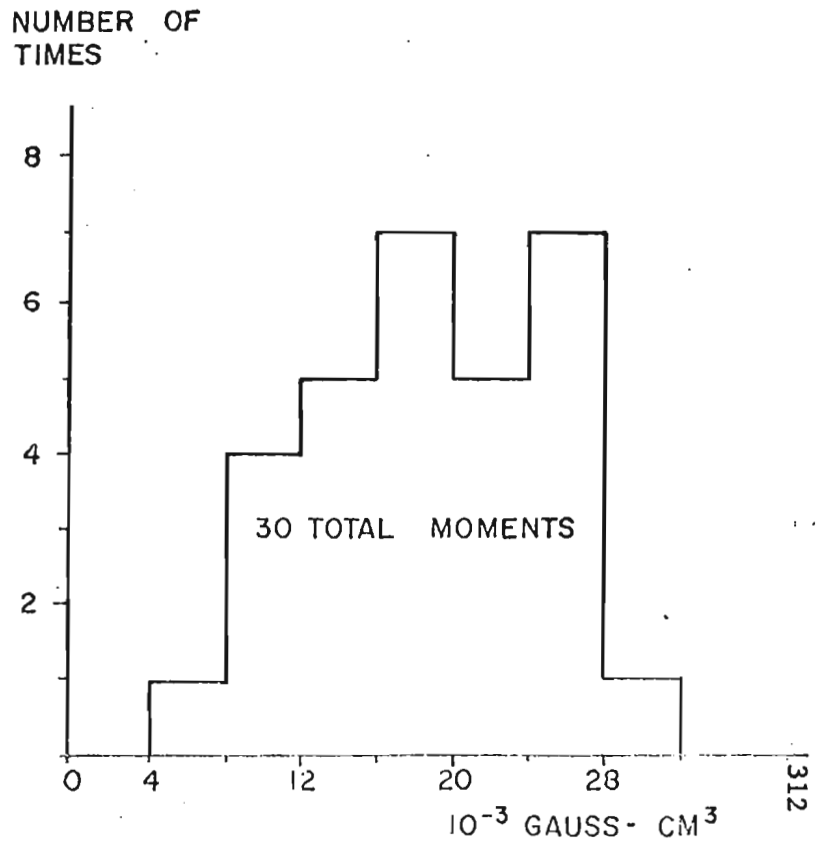

FIG. 5 - 15

DRILL CHIPS (R22 1230 M DEPTH)
PASSING 1/16" MESH. EACH POINT
REPRESENTS 12 x 3 COMPONENTS.

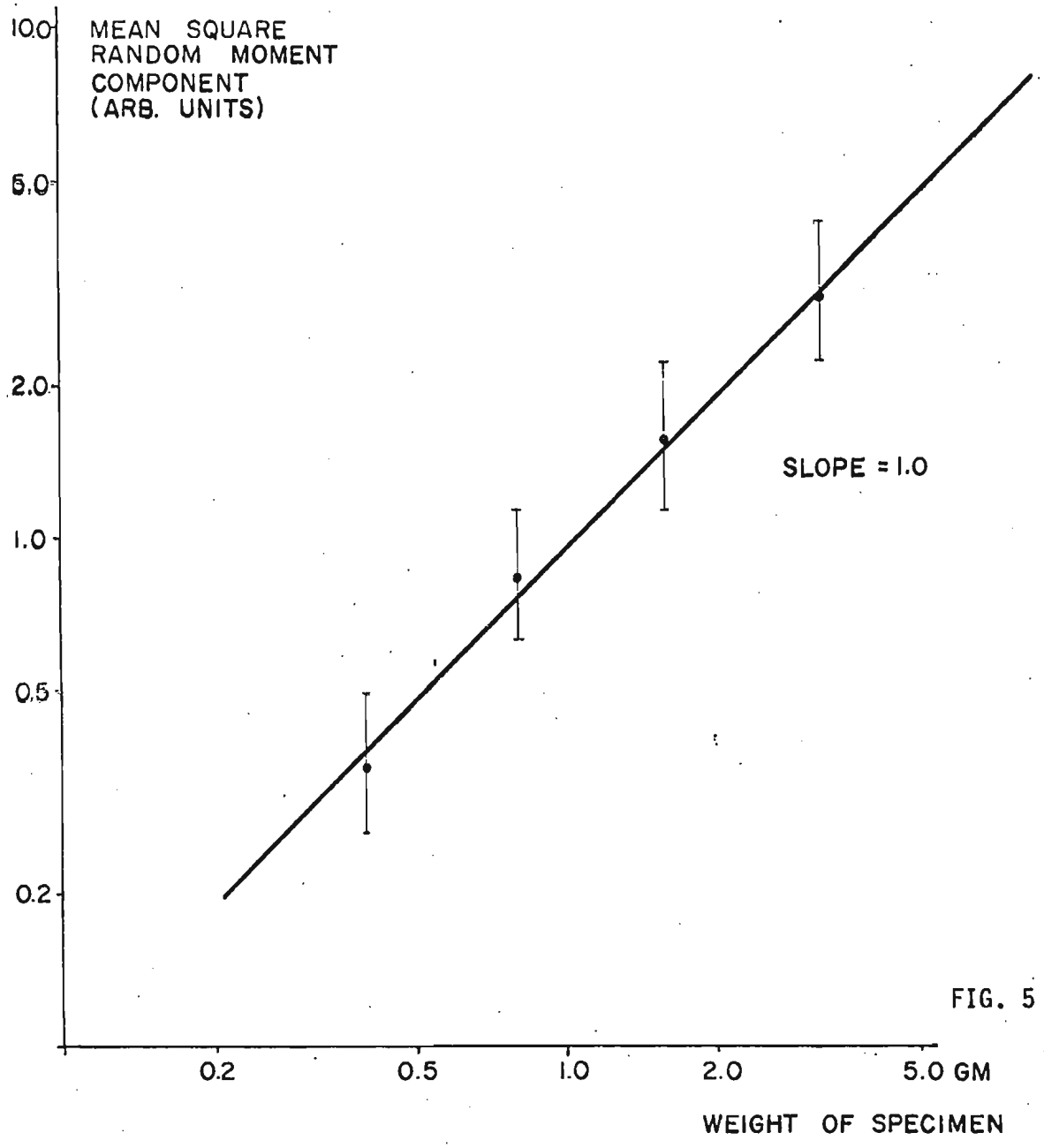

FIG. 5 - 16

Fig. 5-17

A plot of the lognormal distribution f(v) as defined in text (Appendix 5.1) with a standard deviation of $\sigma = 1$. The abscissa is normalized to the geometric mean v_m, and the area under all the curves from zero to infinity is the same. See text for an explanation of $vf(v)$, $v^2f(v)$, v_{rms} and v_h.

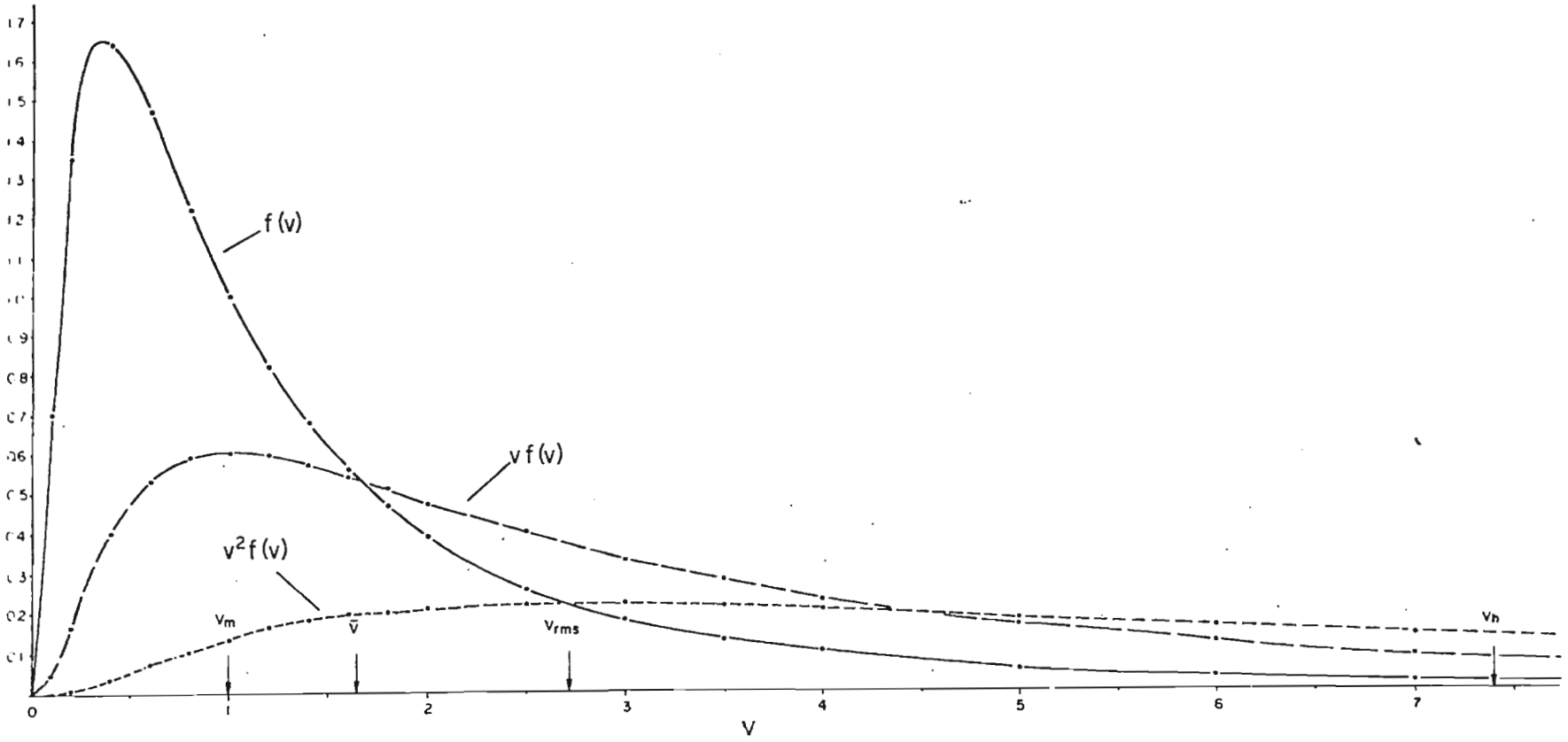

FIG. 5 - 17

PLATE 1

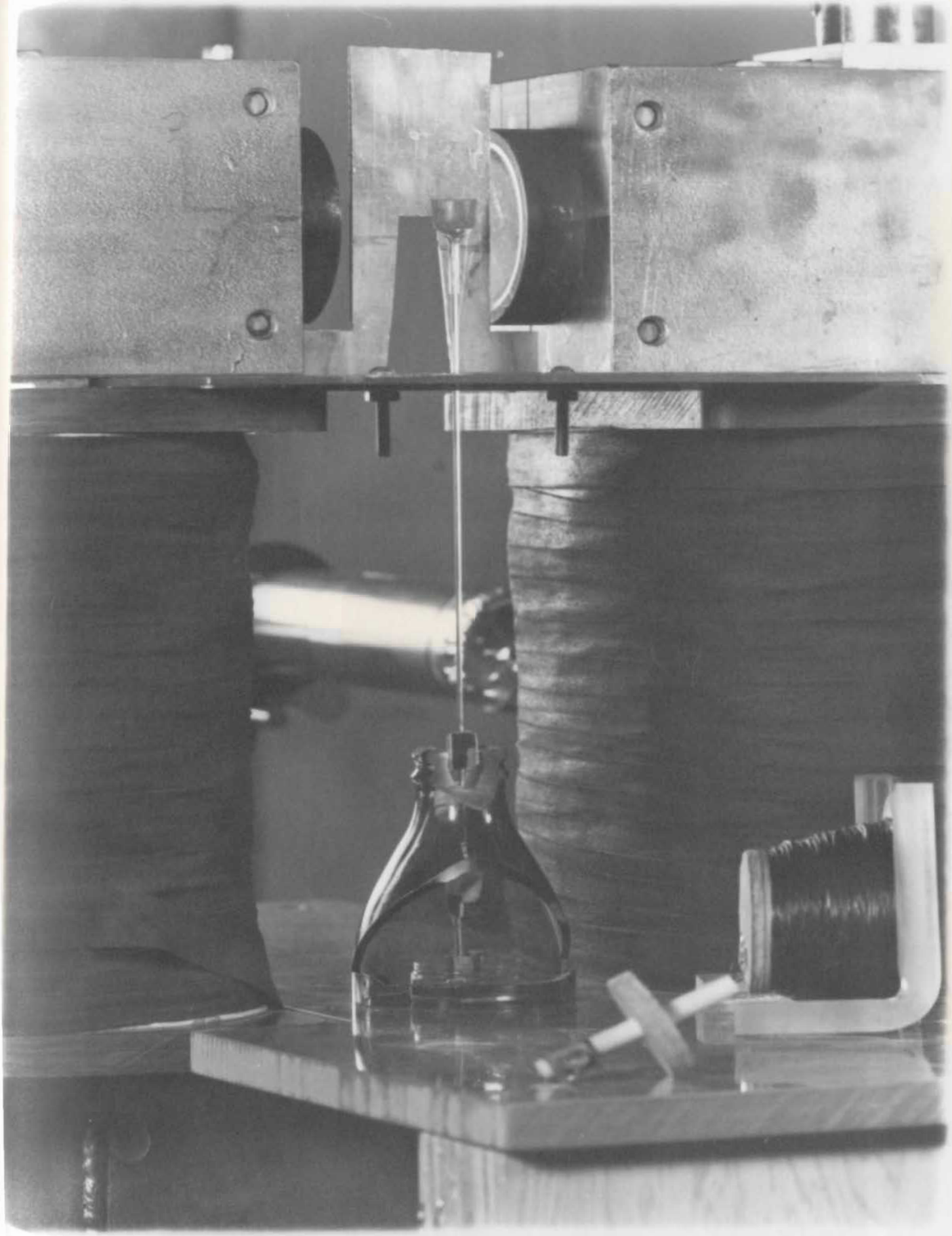

PLATE 2

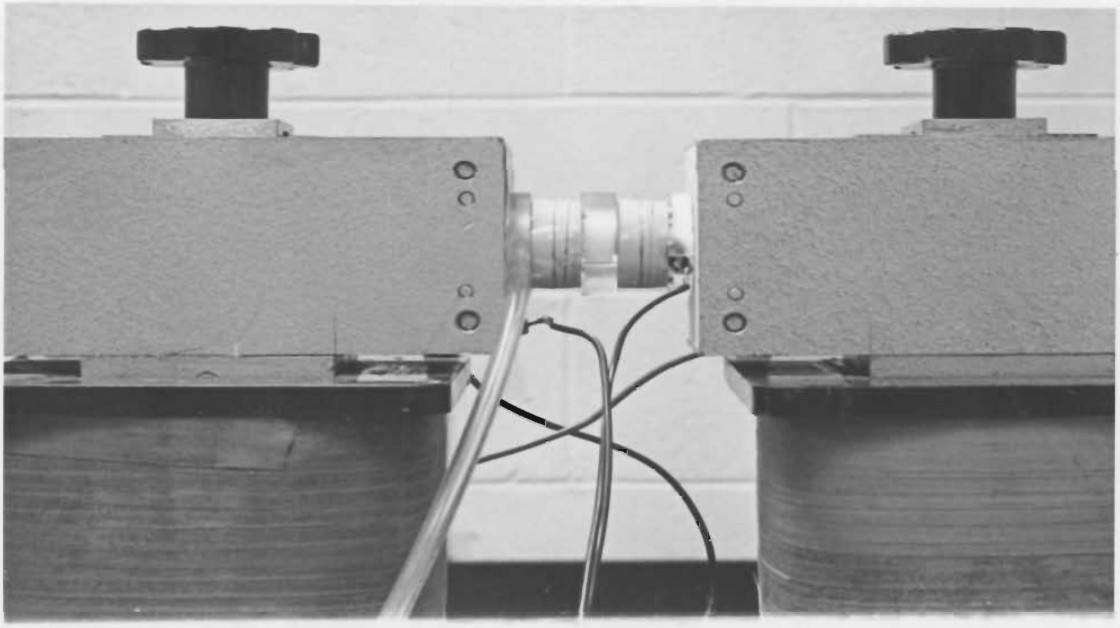

(a)

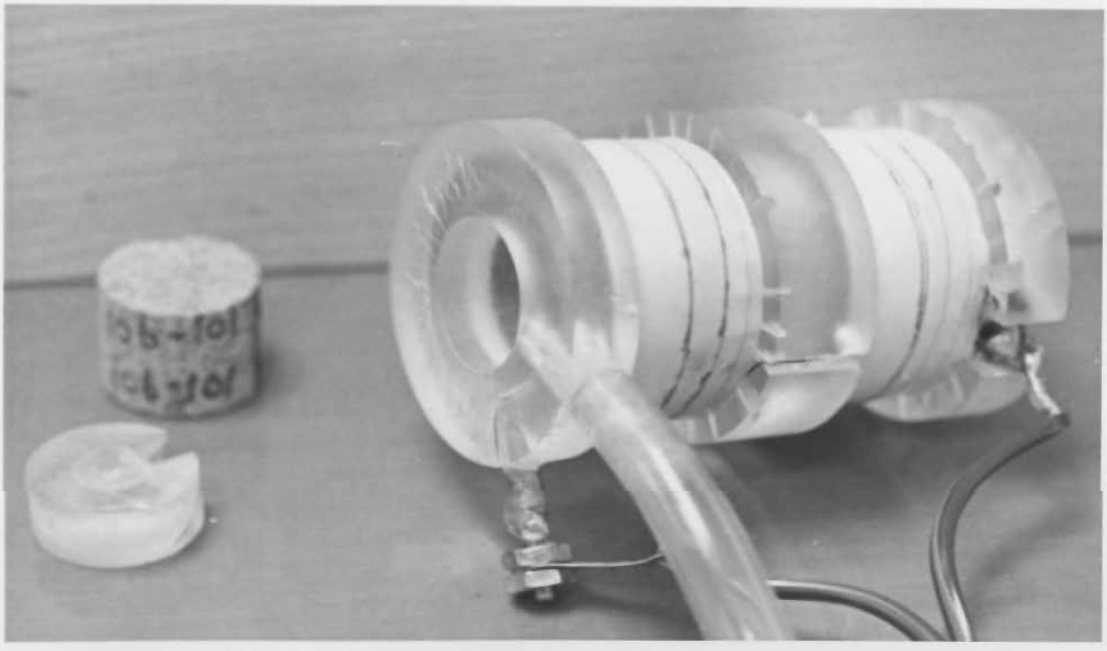

(b)

PLATE 3

(a)

(b)

PLATE 4

(a)

(b)

PLATE 5

(a)

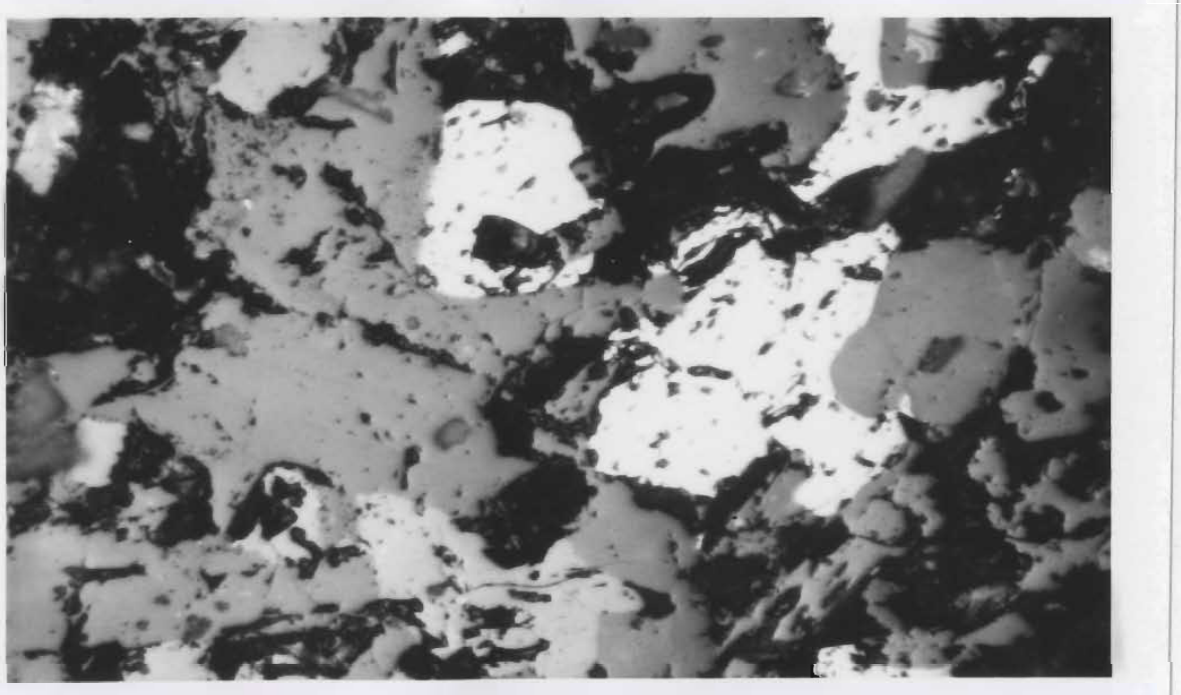

(b)

PLATE 6

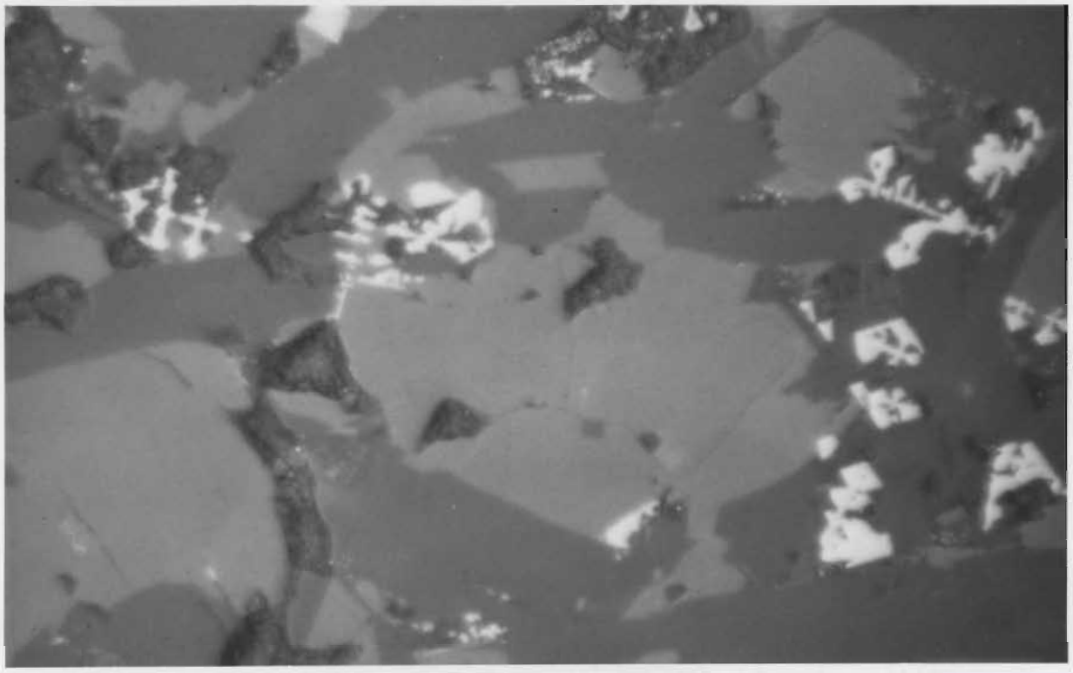

(a)

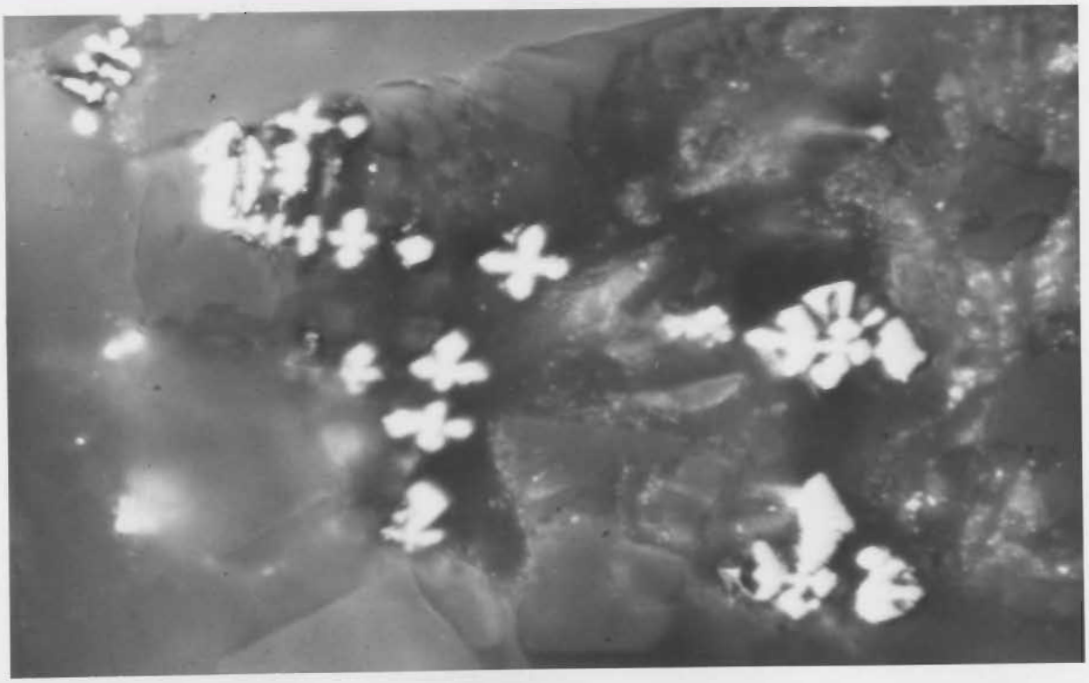

(b)

Plate 6 (a) Class R' sample (GD 1-3) from Disko, with small skeletal homogeneous titanomagnetite grains. Size of picture 160 μ.

(b) Grains from Cape Dyer, similar to (a). Sample DY 3-3. Size of picture 60 μ.

Plate 7 (a) A large titanmagnetite grain with ilmenite exsolution lamellae (white). Sample DY 6-5, Cape Dyer. Size of picture 400 μ.

(b) Part of a very large titanomagnetite grain with ilmenite exsolution lamellae (dark). Gabbro sample Arn 1, North-Western Iceland. Size of picture 1.6 mm.

Plate 8 (a) Piece of basaltic ash in interbasaltic red sediment, Disko Island. Note the concave outlines caused by air bubbles in the ash prior to solidification. Sample GL1-GL2. Size of picture 400 μ.

(b) Large magnetite grain in a gneiss sample. Note the pitting apparently characteristic of gneiss. Sample FB 1-3, Frobisher Bay. Size of picture 1.6 mm.

PLATE 7

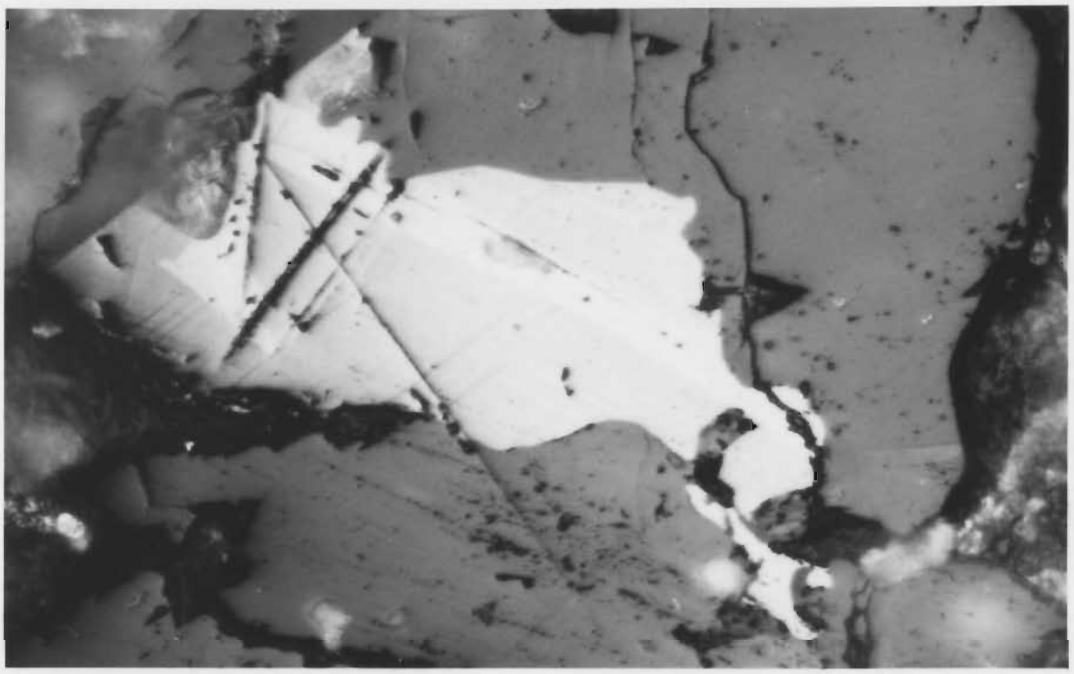

(a)

(b)

PLATE 8

(a)

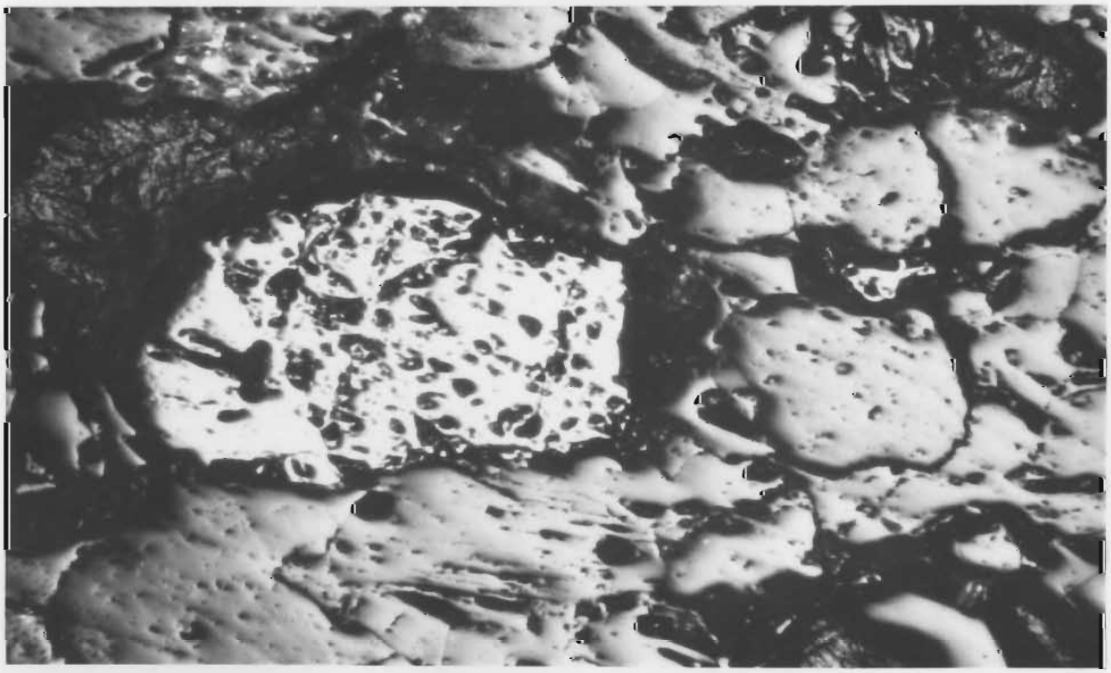

(b)